Synthesis and Functionalisation of a 3-D Spirocyclobutyl Piperidine Building Block for Medicinal Chemistry

Hannah Kemp

MSc by Research

University of York

Chemistry

December 2022

Abstract

This thesis describes the synthesis and functionalisation of a 3-D building block, cyclobutyl trifluoroborate salt **A**, for use in a modular synthetic platform that aims to elaborate fragment hits in 3-dimensions. Ni-catalysed photoredox cross-coupling and Suzuki-Miyaura cross-coupling to produce aryl cyclobutanes **B** were developed. In addition, *N*-functionalisation of aryl cyclobutanes **B** afforded five examples of lead-like compounds **C**.

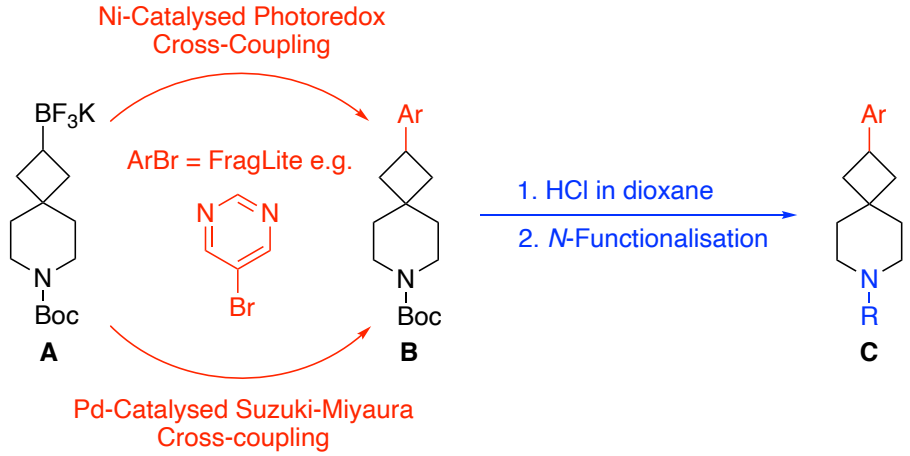

Chapter 2 describes the development of two different routes to cyclobutyl trifluoroborate salt **A**, one *via* a cyclobutene and the other *via* an enol triflate. The enol triflate route was the preferred route. In this route, the enol triflate underwent Miyaura borylation to introduce a Bpin group. Then, hydrogenation gave the cyclobutyl Bpin compound which was then converted into cyclobutyl trifluoroborate salt **A**. This gram-scale synthesis was achieved in an overall yield of 68% over four steps.

Chapter 3 describes the cross-coupling of cyclobutyl trifluoroborate salt **A** with medicinally relevant FragLites to produce aryl cyclobutanes **B**. Ni-catalysed photoredox cross-coupling and Pd-catalysed Suzuki-Miyaura cross-coupling reactions were successful in cross-coupling six aryl bromides to the building block scaffold.

N-Functionalisation of aryl cyclobutanes **B** to afford *N*-functionalised aryl cyclobutanes **C** for the synthesis of medicinally relevant lead-like compounds is described in Chapter 4. Vector analysis of *N*-functionalised aryl cyclobutane **C** (Ar = pyrimidine, R = methanesulfonamide) enabled visualisation of the vectors in chemical space that this lead-like compound accesses.

List of Contents

List of Tables

List of Figures

Acknowledgements

I would like to thank my supervisor Professor Peter O'Brien for giving me the opportunity to carry out an MSc by Research in his group on such an exciting and interesting project. His considerable help and support throughout the project has been invaluable in enabling this research and helping me to be the chemist I am today. I would also like to thank Dr Michael James and Dr Christopher Spicer for being my independent panel members.

I would like to thank the members of the POB group who have offered advice and support whenever I have needed it. These include: Giordaina, Stephen, Andres, Lucy, Stuart M, James F, James D, Will, Matthew, Jake, Ben and Stuart S. I would also like to thank Jerry, Jack and Ryan from the WPU group. Thanks to everyone for being so welcoming and a pleasure to work with.

I would also like to thank all the technical staff from the University of York department of chemistry for the support they provide. This includes Mike and Steve in stores, Heather for running the NMR service, Karl for the mass spectrometry service and Adrian for X-ray crystallography.

Lastly, I would like to thank my partner, friends and family for their love and support throughout the last year.

Author’s Declaration

I declare that this thesis is a presentation of original work and I am the sole author. This work has not previously been presented for an award at this, or any other, University. All sources are acknowledged as references.

Hannah Kemp

1. Introduction

1.1. Fragment-Based Drug Discovery

Fragment-based drug discovery (FBDD) is a technique which uses screening libraries of usually 1,000-5,000 fragments[1] to identify low molecular weight (MW ~150-250) predominantly 2-D molecules that can bind to biologically relevant active sites in proteins.[2–15] Using a small molecule for the initial stage allows each atom in the compound to potentially interact with the protein of interest. However, as the 2-D fragments have low molecular weight, the binding affinity is usually weak, in the order of mM.[16] The binding can be confirmed using a variety of sensitive biophysical techniques including NMR spectroscopy, X-ray crystallography, isothermal calorimetry, surface plasmon resonance and mass spectrometry. Once the fragment hits are established, fragment elaboration, also known as lead optimisation, can be used to improve the binding affinity of the initial fragments. Fragment elaboration can mean fragment merging, linking and growing. The process of fragment elaboration improves potency, selectivity and ADME properties (absorption, distribution, metabolism and excretion). After some iterative stages of fragment elaboration, a lead-like compound can be identified, which can be tested in clinical trials. The pipeline for FBDD is presented in Figure 1.1.

Figure 1.1 – FBDD pipeline

High-throughput screening (HTS) is an alternative to FBDD where millions of larger molecular weight compounds (MW ~400) are screened against the protein target and the identified hits are further optimised. Figure 1.2 depicts a 2-D representation comparing FBDD to HTS displaying the protein target, fragment libraries, hit identification and lead optimisation using the two techniques. HTS libraries can be considered to use combinations of fragments where some of the atoms involved are not essential to the binding of the protein of interest. Due to the larger molecular weight compounds in HTS libraries, stronger binding is achieved with the protein target (μM). A greater proportion of chemical space can be accessed using FBDD compared to HTS due to the smaller

compounds investigated. Therefore, in FBDD, higher quality interactions are achieved due to more specific binding interactions between the fragment and protein, despite the lower potency.[2] By using less complex molecules with FBDD, a 10-1000 times higher hit rate than HTS is typically observed.[4,17] HTS uses biochemical assays whereas FBDD mainly uses biophysical assays to identify its hits due to the differences in potency. Rather than potency, FBDD explores the quality of the binding between the fragment and the target compound. By comparison, HTS uses potency to identify a hit compound. The advantage of HTS is that a hit with greater potency may be found in a shorter amount of time compared to FBDD where the fragment hit requires synthetic elaboration before becoming a lead-like compound.

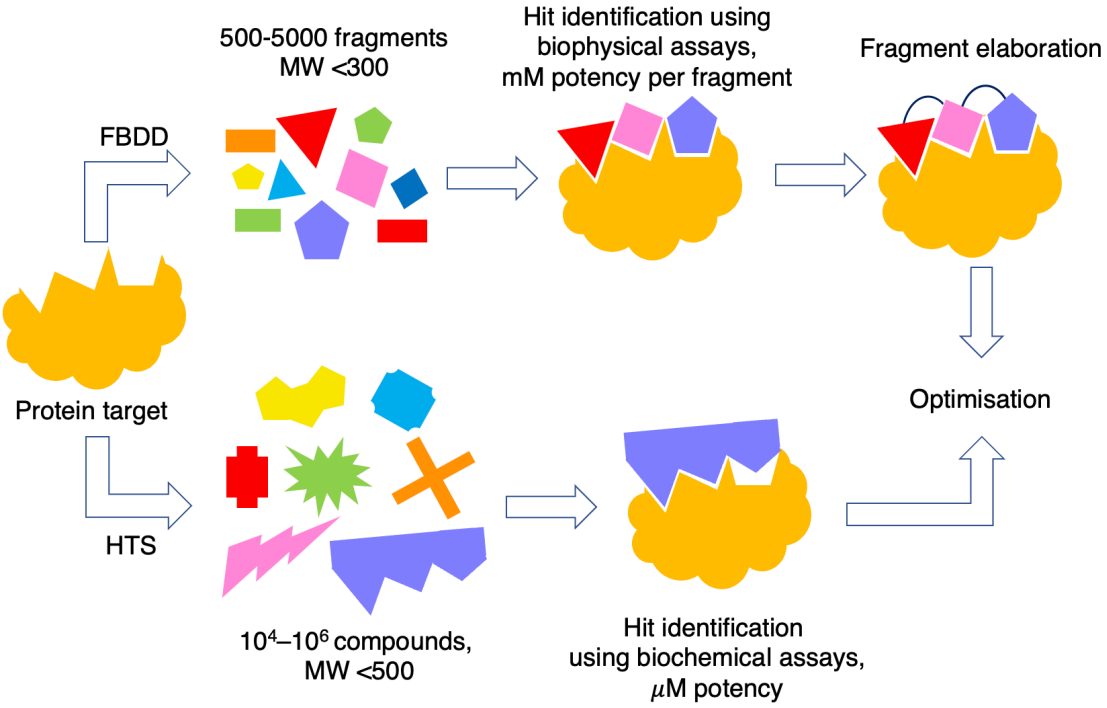

Figure 1.2 – 2-D representation of FBDD vs HTS

In 2003, researchers from Astex identified a useful fragment guideline which they called the "rule of three" (Ro3) (Table 1.1).[18] The Ro3 was based on the fact that successful fragments exhibit the following characteristics: "molecular weight ≤300 Da, the number of hydrogen bond donors ≤3, the number of hydrogen bond acceptors is ≤3 and cLogP is ≤3" where cLogP is a measure of lipophilicity by measuring the logarithm of the partition coefficient between *n*-octanol and water. These rules allow guidance as to which fragments to use in a screening library. The rules are based on Lipinski's rule of five (Ro5) which indicate the physicochemical properties that small molecule, orally bioavailable drugs usually have.[19] The Ro5 follows a molecular weight ≤500 Da; cLogP

≤5, number of hydrogen bond donors ≤5 and number of hydrogen bond acceptors ≤10. Lipinski suggested that drugs that fell out of these boundaries are less likely to be orally absorbed although there are exceptions to the rules. Nevertheless, following Lipinski's Ro5 should lead to a drug having favourable pharmacokinetic properties and an associated good ADME profile.

Table 1.1 – Rule of 3 (Ro3)[18] *and rule of 5 (Ro5)*[19]

Property	**Ro3**	**Ro5**
MW (Da)	≤300	≤500
cLogP	≤3	≤5
Number of H-bond donors	≤3	≤5
Number of H-bond acceptors	≤3	≤10

A useful set of medicinally relevant fragments for FBDD are 'FragLites' which were designed by Waring *et al.*[20] These are small compounds (≤13 heavy atoms) with two functionalities that can form either hydrogen bond donor-acceptor or acceptor-acceptor interactions in different spatial orientations, known as pharmacophore doublets. Such features increase the likelihood of FragLites to be fragment hits. The pharmacophore doublets allow potential for protein-ligand interactions, as well as an increase in the solubility of the compounds, enabling them to be used in biophysical hit identification techniques such as X-ray crystallography. FragLites contain aromatic scaffolds and this encourages lipophilic protein interactions. Lastly, a heavy bromine or iodine atom is incorporated into each FragLite due to the high visibility of these atoms in X-ray crystallography. A set of 31 FragLites was initially developed and, as of 2022, the set contains 33 FragLites[21] with the aryl bromide FragLites shown in Figure 1.3. The pharmacophore doublet donors are highlighted in red and acceptors are highlighted in blue. In Figure 1.3, the FragLites are grouped by similarities in their functionality and structure.

Pyrazoles and Isoxazole

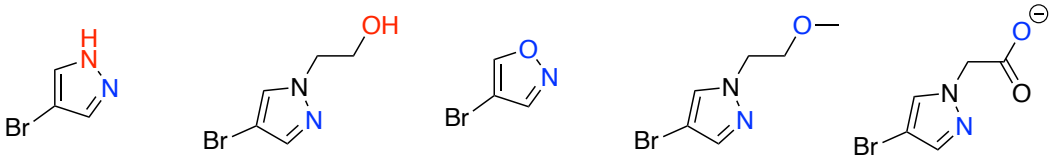

Nitriles

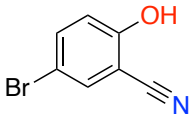

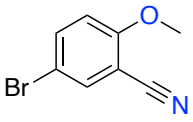

Amides

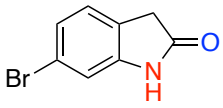

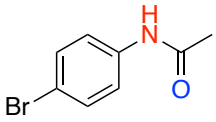

Pyridones

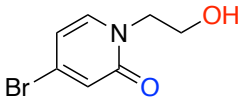

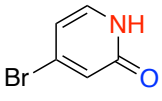

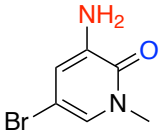

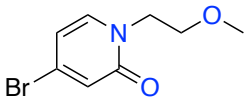

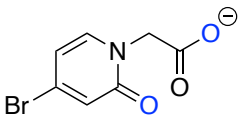

Sulfonamide and Sulfone

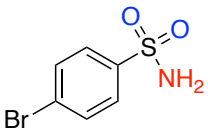

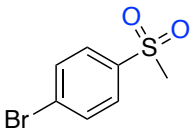

Pyrimidine/Pyrimidine like

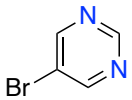

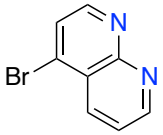

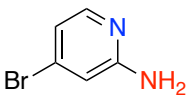

Hydroxy/Methoxy/Carboxylic Acid

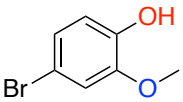

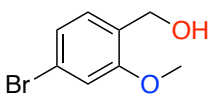

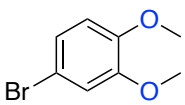

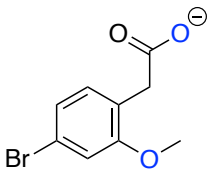

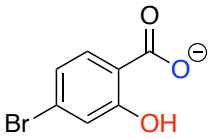

Hyroxy/Methoxy Pyridines

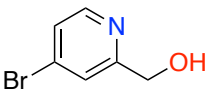

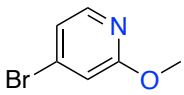

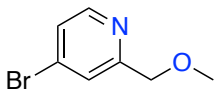

Figure 1.3 – The current aryl bromide FragLites

To demonstrate the utility of FragLites in FBDD as being potential hits in fragment screening, FragLite mapping of protein binding was demonstrated by binding the set of 33 FragLites to CDK2, BRD4 and ATAD2 proteins.[20,21] This was carried out by combining FragLites with the individual proteins and using X-ray diffraction to analyse the structure of any crystalline protein-FragLite adducts. Nine of the FragLites bound to CDK2 in six distinct sites,[20] as shown in Figure 1.4, with four of these sites being

previously unidentified. Moreover, six binding events were found across five sites for ATAD2 and twenty-one binding events across five sites for BRD4.[21] These results suggest that FragLites are likely to be fragment hits in FBDD programs, highlighting their potential as medicinally relevant fragments.

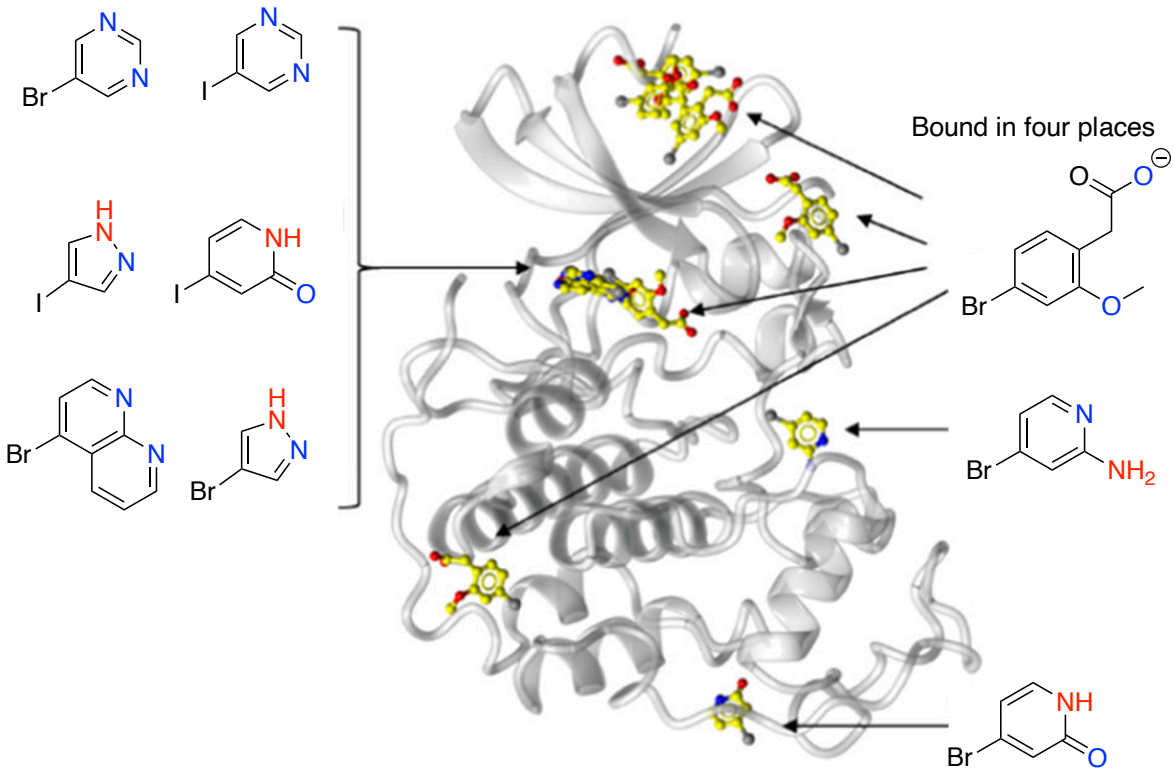

Figure 1.4 – X-ray crystal structures of FragLites bound to six binding sites of CDK2 (Figure adapted from Waring et al.[20])

1.2. Fragment Elaboration in Drug Development

To date, six FDA approved drugs have been derived from FBDD, with over 50 drugs in phase I-II trials.[22] The six approved drugs are Scemblix™ (Asciminib),[23] Balversa™ (Erdafitinib),[24] Turalio™ (Pexidartinib),[25] Lumakras™ (Sotorasib),[26] Zelboraf™ (Vemurafenib)[27] and Venclexta™ (Venetoclax)[28] (Figure 1.5). These drugs all began as initial fragment(s) which are highlighted in red and blue. These fragment(s) became drugs through fragment elaboration and/or fragment merging. All of the drugs shown in Figure 1.5 are cancer therapeutics, with three being kinase inhibitors.

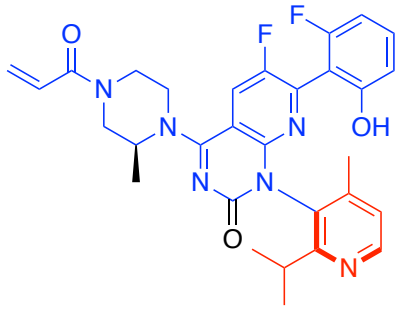

Lumakras™ (Sotorasib)

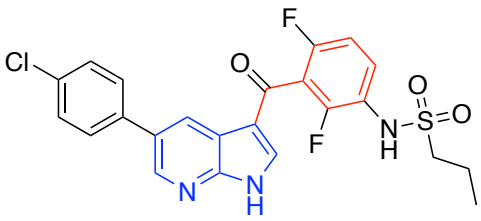

Zelboraf™ (Vemurafenib)

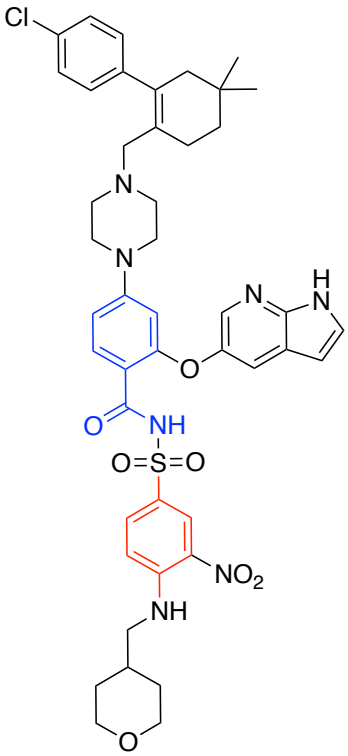

Venclexta™ (Venetoclax)

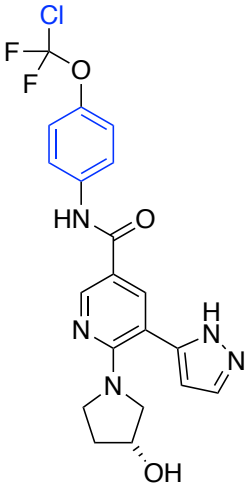

Scemblix™ (Asciminib)

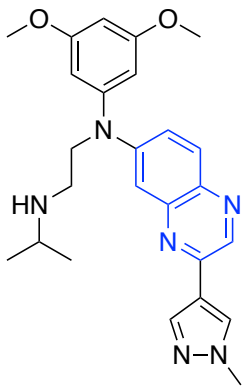

Balversa™ (Erdafitinib)

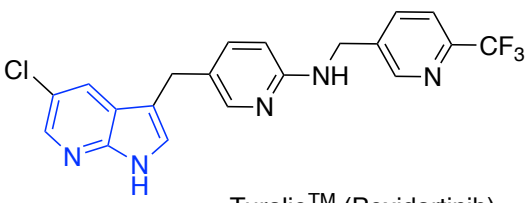

Turalio™ (Pexidartinib)

Figure 1.5 – Six approved drugs from FBDD

In 2011, the first drug derived from FBDD, Zelboraf™ (Vemurafenib), was approved for use in clinics. From its initiation by Plexxikon in 2005, only six years were required for this drug to be approved, highlighting how time-efficient FBDD can be. Although the initial fragment hit, 7-azaindole **1**, was unselective, the final drug ended up being highly selective for its target.[29] Zelboraf™ is an inhibitor of oncogenic BRAF kinase activity. BRAF kinase is a human protein involved in regulation of genes for cell replication and survival. Zelboraf™ specifically targets a mutant form of the BRAF gene. Half of metastatic melanoma cases have this BRAF mutant.[30] Zelboraf™ works as a competitive kinase inhibitor by binding to the ATP-binding domain of the mutant form of BRAF.[31] The implications of the use of Zelboraf™ are significant as patients with severe melanoma had an increased survival rate, from 64% to 84%, over a six month period compared to dacarbazine chemotherapy.[31]

The FBDD process to develop Zelboraf™ began with screening a library of 20,000 fragments with molecular weights ranging from 150-350 Da at 200 μM concentration against protein kinases. 238 Compounds inhibited the activity of three kinases: Pim-1, p38 and CSK, by at least 30%. These compounds were then co-crystallised with the kinases using X-ray crystallography. One of the co-structures revealed binding between 7-azaindole **1** and the ATP binding site of kinase Pim-1. However, multiple binding modes were observed, leading to weak affinity ($IC_{50} > 200$ μM for Pim-1). Therefore, a set of substituted 7-azaindoles were synthesised in an attempt to increase the binding affinity to Pim-1. One of these included 3-aminophenyl analogue **2** ($IC_{50} \approx 100$ μM for Pim-1). The key difference with 3-aminophenyl analogue **2** compared to 7-azaindole **1** was that 3-aminophenyl analogue **2** bound with a single unique binding mode. With further optimisation of 3-aminophenyl analogue **2**, a difluoro-phenylsulfonamide analogue **3** was discovered to exhibit high levels of potency and selectivity for an alternative kinase to Pim-1: BRAF V600E mutant ($IC_{50} = 13$ nM for mutant BRAF, $IC_{50} \approx 160$ nM for wild-type BRAF). The selectivity was seen against the wild-type BRAF and 70 other kinases.[32] Finally, addition of a phenyl group yielded Zelboraf™ (Vemurafenib), which had superior pharmacokinetic properties in both dogs and monkeys, although with slightly reduced potency ($IC_{50} = 31$ nM for mutant BRAF) compared to difluoro-phenylsulfonamide analogue **3**.[29] Zelboraf™ (Vemurafenib)

successfully passed through all phases of clinical trials and now provides a dramatically improved life expectancy for BRAF mutant late stage melanoma patients (Scheme 1.1).

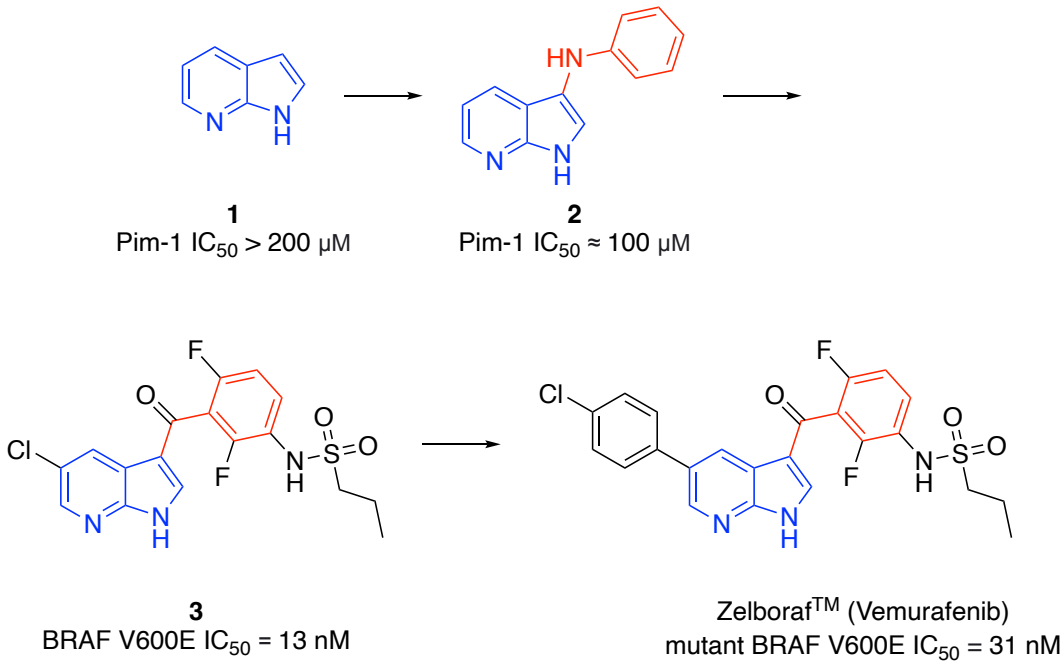

Scheme 1.1

The development of Zelboraf™ (Vemurafenib) highlights the important role that synthetic organic chemistry plays in the fragment elaboration stage, from 7-azaindole **1** to 3-aminophenyl analogue **2** to difluoro-phenylsulfonamide analogue **3** to Zelboraf™. In particular, the synthesis of 3-aminophenyl analogue **2** and difluoro-phenylsulfonamide analogue **3** will likely have required different synthetic routes. Thus, fragment elaboration relies heavily on synthetic organic chemistry.

1.3. O'Brien Group Approach to Fragment Elaboration in 3-D

In recent years, researchers at Astex have highlighted the fact that the rate-limiting step for fragment elaboration is invariably synthetic organic chemistry.[16] Often, the synthetic methodology has not been developed to elaborate the fragments from each possible vector in 3-dimensions. Ideally, fragment elaboration from each of the fragment's vectors should be established prior to X-ray screening with the target as this would increase efficiency during the fragment elaboration and optimisation stages. Therefore, research on the development of synthetic methodology for fragment elaboration is key to enable successful FBDD by removing the common barriers in fragment elaboration from lack of synthetic methodology.

To reduce the time spent on fragment elaboration in FBDD, the O'Brien group envisaged that a library of 3-D building blocks could be used for fragment elaboration. The O'Brien group is the first (to our knowledge) to make 3-D building blocks for use in fragment elaboration. There is interest in expanding 2-D fragments into 3-D space as this may improve binding properties and thus drug potency in some lead-like compounds.[33] In the O'Brien group's modular synthetic platform, a library of designed 3-D bifunctional building blocks with two distinct vectors for fragment elaboration would be used (Figure 1.6, panels A-E). The first stage of this process would be to carry out fragment screening against the protein target of interest. This screening stage will be unchanged from that currently carried out and the screening library will consist of low molecular weight, usually 2-D fragments, such as FragLites[20] (panel A). Once the hits are identified, biochemical assays and biophysical methods such as X-ray crystallography will be used to map out the binding between the fragments and the protein target (panel B). The next stage would be to virtually elaborate the fragment hits in 3-D. To do this, a library of 3-D bifunctional building blocks with distinct vectors in chemical space would be virtually combined with the fragment at one vector with structural variations at the other vector explored (panel C). Computational docking studies, guided by the X-ray crystal structures of the initial fragment hits bound to the protein of interest, can then be used to identify elaborated fragment synthetic targets (panel D). Since the library of 3-D building blocks will contain common functionality, the synthetic efforts should be minimised (panel E). Finally, after stages of iterative optimisation to elaborate the fragment, a series of lead-like compounds would be identified. A key feature of this synthetic platform is that the synthetic chemistry to attach the fragment to the building blocks and to explore

functionalisation of the other vector will be the same for all building blocks. Crucially, with a sufficient range of 3-D building blocks with different 3-D vectors, it should be possible to access a wide range of chemical space using this modular synthetic platform.

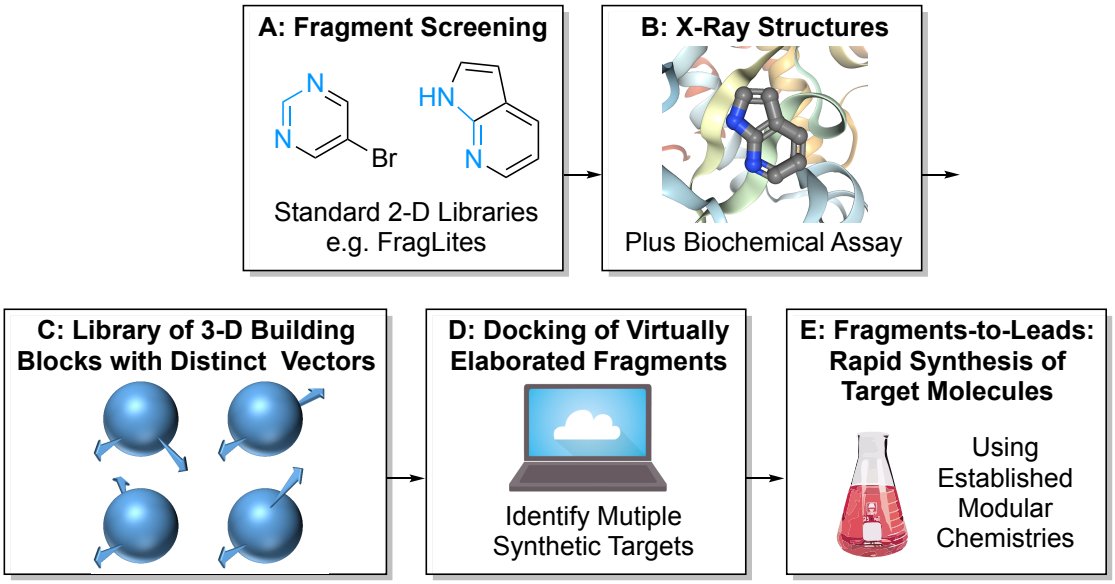

Figure 1.6 – Modular synthetic platform for fragment elaboration in 3-D

In order to build the library of 3-D building blocks, a set of design criteria were devised. One key feature of the building blocks was that they would contain *N*-protected saturated nitrogen heterocycles such as pyrrolidine[34,35] and piperidine[36,37] as these moieties are commonly found in drug candidates. The plan was that each building block would have two defined vectors in chemical space, one to attach the fragment and one to explore further protein binding interactions. Cyclopropanes were initially investigated due to their prevalence in drug molecules as well as their structural rigidity.[38–40] To functionalise from the cyclopropyl moiety, a *N*-methyliminodiacetic acid boronate (BMIDA) group was introduced to enable cross-coupling.[41] BMIDA was chosen due to its slow hydrolysis to give the boronic acid *in situ*, reducing potential side-reactions in Pd-catalysed Suzuki-Miyaura cross-coupling (SMCC) reactions. Moreover, BMIDA compounds are bench-stable, crystalline solids which allow ease of handling. It was decided that the building blocks should also satisfy the "rule of 2" for building blocks which was a concept recently introduced by AstraZeneca.[42] These rules state that reagents for drug discovery, such as building blocks, should not add more than 200 Da in molecular weight or 2 units of cLogP. Moreover, the hydrogen bond donor count should be ≤2 and the hydrogen bond acceptor count should be ≤4.

In the O'Brien group, to date, nine cyclopropyl 3-D building blocks have been successfully developed (Figure 1.7).[43–45] All building blocks have a Boc protected cyclic amine group together with a cyclopropyl BMIDA moiety. The building blocks include two fused cyclopropyl *N*-Boc pyrrolidine MIDA boronates **4** and *exo*-**5**, spirocyclic cyclopropyl *N*-Boc pyrrolidine MIDA boronates *cis*-**6** and *trans*-**7**, a spirocyclic cyclopropyl *N*-Boc azetidine MIDA boronate **8**, two fused cyclopropyl *N*-Boc piperidinyl MIDA boronates *exo*-**9** and *exo*-**10**, a spirocyclic cyclopropyl *N*-Boc piperidinyl MIDA boronate **11** and a bicyclic cyclopropyl *N*-Boc piperidinyl MIDA boronate *exo*-**12**. From these nine building blocks, the group have completed ~70 examples of Pd-catalysed SMCC reactions to attach a wide range of medicinally relevant aryl and heteroaryl groups including a number of Fraglites.[20] Some of these aryl cyclopropanes have also been subjected to Boc group removal and *N*-functionalisation (including amidation, sulfonamidation, reductive alkylation and Buchwald-Hartwig amination) to give ~30 lead-like compounds.

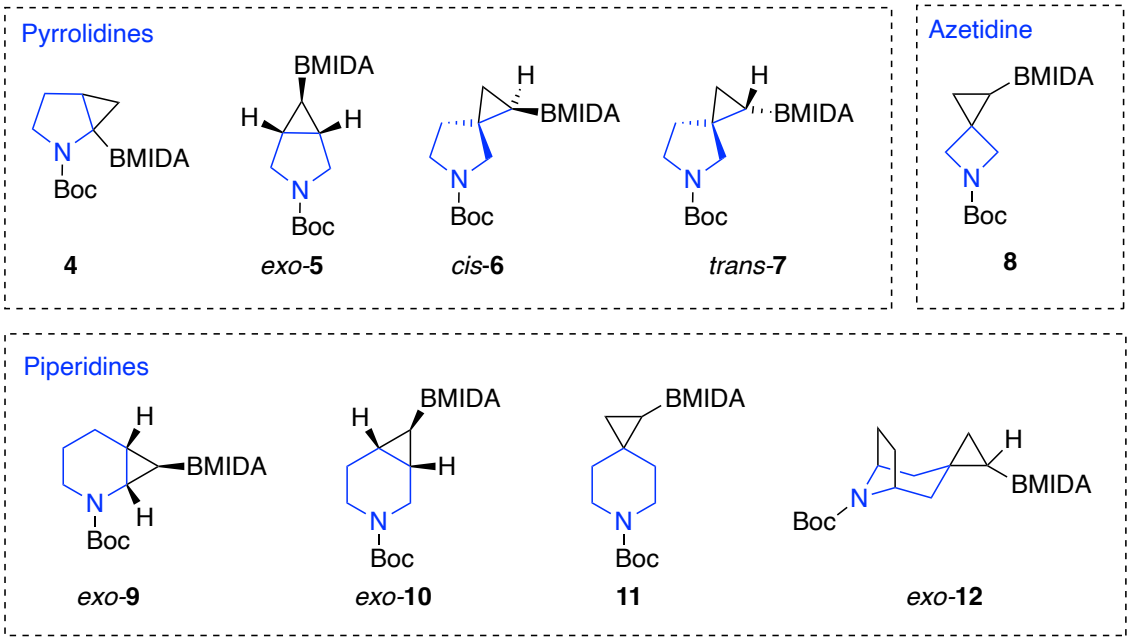

Figure 1.7 – O'Brien group's cyclopropyl building blocks

An example of fragment elaboration using one of the cyclopropyl building blocks, fused cyclopropyl *N*-Boc pyrrolidine MIDA boronate *exo*-**5**, is shown in Scheme 1.2.[44] Fused cyclopropyl *N*-Boc pyrrolidine MIDA boronate *exo*-**5** was cross-coupled with FragLite 5-bromopyrimidine (1.4 eq) using $Pd(OAc)_2$ (15 mol%), PCy_3 (30 mol%), Cs_2CO_3 (6.0 eq) in 10:1 toluene-water at 100 °C for 18 h. After purification by chromatography, pyrimidine cyclopropane **13** was produced in 83% yield. Then, Boc removal using HCl

in dioxane at room temperature for 1 h followed by mesylation using MsCl (2.2 eq) and Et_3N (4.8 eq) in CH_2Cl_2 at room temperature for 16 h gave *N*-methanesulfonamide pyrimidine cyclopropane **14** in 95% yield over the 2 steps (Scheme 1.2). Following this approach, all nine building blocks were converted into their corresponding *N*-methanesulfonamide pyrimidines. Similar functionalisation steps were carried out on all the building blocks with a variety of medicinally relevant aryl bromides as well as a variety of amine functionalisation reactions to yield the set of ~30 lead-like compounds.

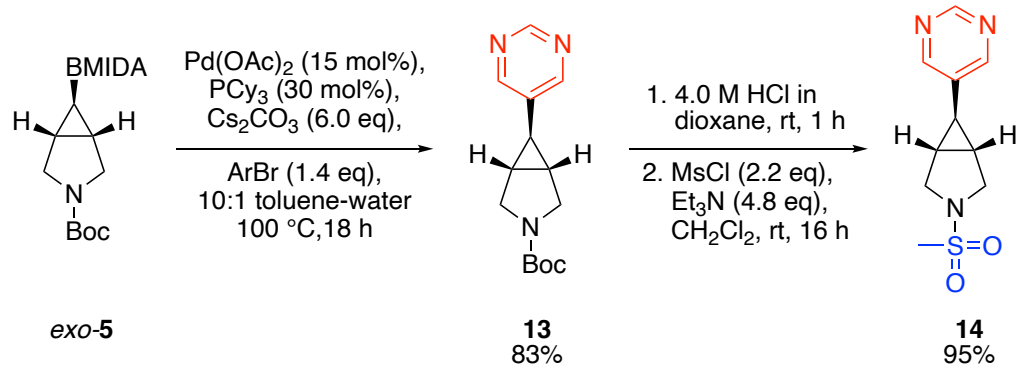

Scheme 1.2

To demonstrate that the BMIDA-functionalised and *N*-functionalised derivatives of the 3-D building blocks occupied different regions of 3-D chemical space, exit vector analysis on the nine *N*-methanesulfonamide pyrimidines was used (Figure 1.8). Exit vector analysis allows visualisation of the relative orientations of two functional groups on a bifunctional scaffold in chemical space. This technique was inspired by the CAVEAT program, introduced in 1994, which uses 3-D databases to search for molecular fragments that bind to proteins of interest. Here, Bartlett and Lauri[46] focused on the orientation of bonds in chemical space rather than the location of atoms. Komarov *et al.*[47] more recently developed the exit vector analysis idea from CAVEAT to create exit vector plots of bifunctional scaffolds. Atomic coordinates can be used to determine all the information needed to create these exit vector, Ramachandran-like, plots. The theory behind the exit vector plots is demonstrated with 1,4-disubstituted cyclohexane (Figure 1.8a). The vectors n_1 and n_2, known as the exit vectors, depict the relative orientation of two bonds extending from atoms c_1 and c_2 on a bifunctional scaffold. The distance between c_1 and c_2 is described as r (Figure 1.8b). Two planes can be determined from this: the n_1-r plane and the n_2-r plane. The angle between the n_1-r plane and n_2 is known as Φ_1. Similarly, the angle between the n_2-r plane and n_1 is known as Φ_2. Finally, the dihedral angle θ depicts the angle between the n_1-r plane and the n_2-r plane (Figure 1.8b).

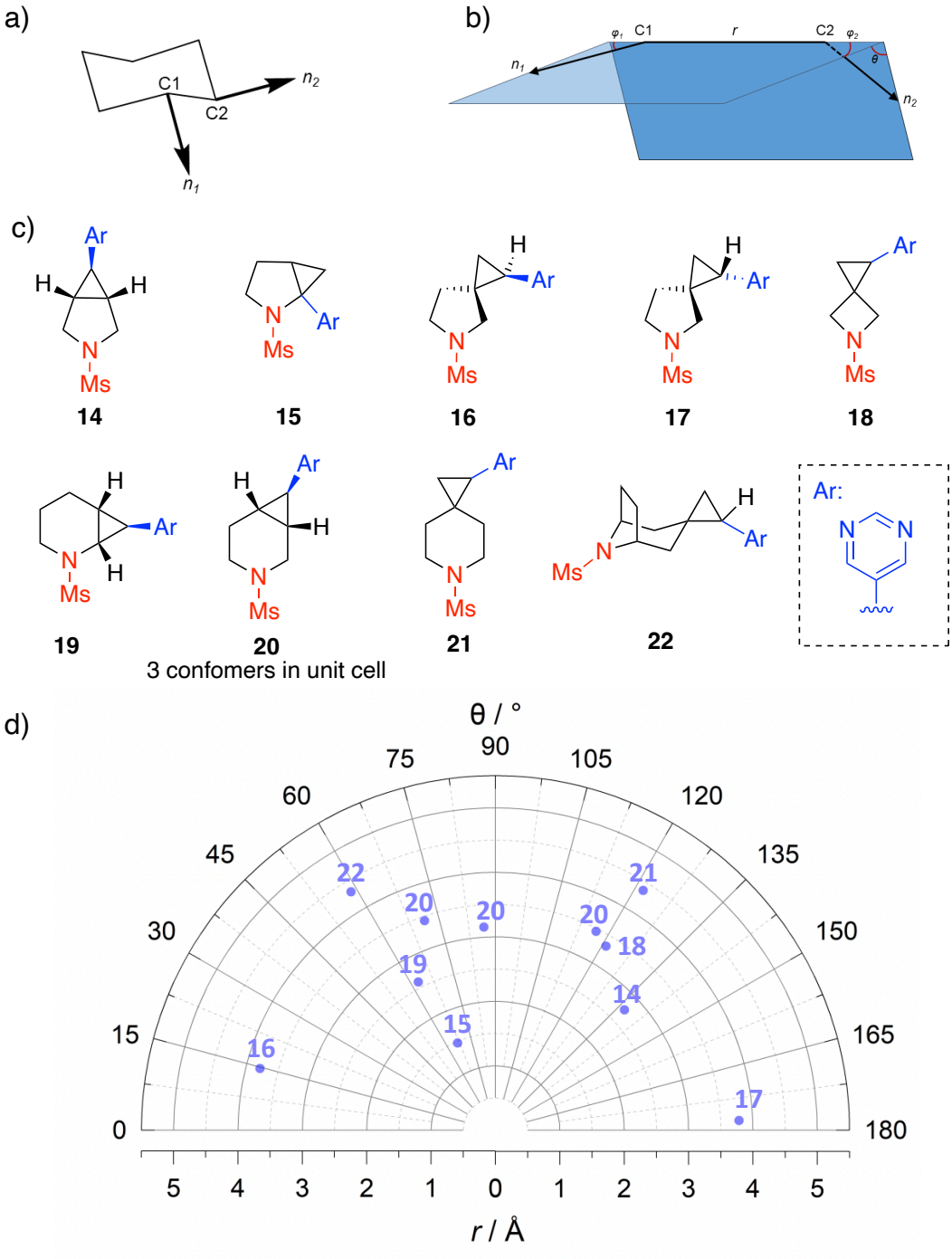

a) Definition of c_1, c_2, n_1 and n_2; b) definition of parameters r, Φ_1, Φ_2 and θ; c) structures of the nine O'Brien cyclopropyl lead-like compounds in the exit vector plot; d) exit vector plot of nine O'Brien cyclopropyl lead-like compounds based on their X-ray crystal structures.

Figure 1.8 – Distribution of O'Brien lead-like compounds in an exit vector plot

In order to demonstrate the 3-D space coverage of the nine 3-D building blocks, exit vector analysis of the X-ray crystal structures of the nine synthesised *N*-

methanesulfonamide pyrimidines (Figure 1.8c) was carried out. To do this, the X-ray crystal structures were used to determine the dihedral angle θ and r parameters and they were plotted as shown in Figure 1.8d. In these examples, n_1 represents the carbon-aryl vector (highlighted in blue), n_2 represents the nitrogen-sulfur vector (highlighted in red) and r is the through-space distance between the cyclopropyl carbon from the carbon-aryl bond and the nitrogen. Most of the compounds show a high level of conformational rigidity (compounds **14**-**19**, **21**, **22**) apart from lead-like compound *N*-methanesulfonamide pyrimidine cyclopropane **20** which had three conformations in its X-ray crystal structure and therefore appears as three coordinates on the exit vector plot. The nine *N*-methanesulfonamide pyrimidine cyclopropanes represented a diverse spread on the exit vector plot indicating that a range of chemical space was accessed by the different lead-like compounds. This highlights the potential utility of these building blocks in drug discovery projects.

With the confidence that the lead-like compounds accessed a diverse range of chemical space, it was time to demonstrate the potential for use of the synthetic platform in drug discovery. Therefore, two O'Brien group 3-D building blocks spirocyclic cyclopropyl *N*-Boc piperidinyl MIDA boronate **11** and spirocyclic cyclopropyl *N*-Boc pyrrolidine MIDA boronate *cis*-**6** were used to synthesise selective JAK3 inhibitors that mimicked the Pfizer drug Ritlecitinib. Ritlecitinib acts as a JAK3-selective inhibitor to treat patients with alopecia areata, an autoimmune disease where the immune system attacks hair follicles, causing hair loss on the scalp, face and body.[48,49] Computational modelling and docking studies, guided by the X-ray crystal structure of Ritlecitinib and JAK3, were used to determine which building blocks to use. Then, SMCC and *N*-functionalisation of two cyclopropyl building blocks gave lead-like compounds **23** and **24** (Figure 1.9).[50] Both analogues had selective binding to JAK3 over JAK1, JAK2, TYK2 kinase isoforms. Moreover, lead-like compound **24** had a high potency (IC_{50} = 69 nM) highlighting the potential for accessing drugs using this set of building blocks.

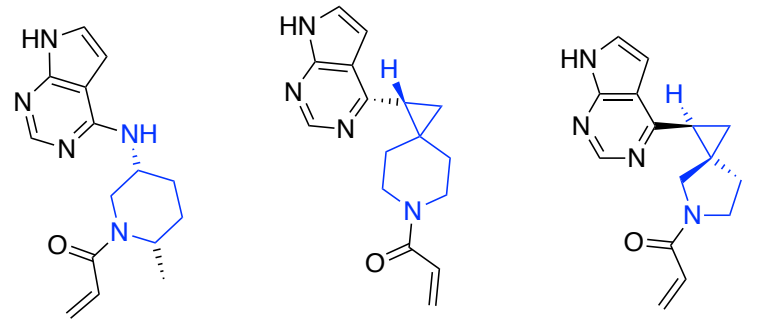

Ritlecitinib
JAK3 IC_{50} = 33 nM

23
JAK3 IC_{50} = 1420 nM

24
JAK3 IC_{50} = 69 nM

Figure 1.9 – O'Brien group selective JAK3 inhibitors and Ritlecitinib

1.4. Project Outline

The next stage in the O'Brien group's project was to expand the number of 3-D building blocks beyond the initial nine cyclopropanes. To do this, it was decided to explore cyclobutyl 3-D building blocks such as cyclobutyl trifluoroborate salt **25** (Figure 1.10) which has been the focus of the research described in this MSc thesis. Cyclobutyl trifluoroborate salt **25** possesses the same desirable features as the cyclopropyl building blocks. There are several key design features of cyclobutyl trifluoroborate salt **25**. Firstly, a cyclobutane ring is incorporated due to its conformational rigidity, providing well-defined exit vectors in regions of chemical space that are yet to be explored.[51,52] Conformational rigidity is advantageous as the conformational entropy penalty would be reduced on binding to a protein target.[53] Moreover, cyclobutanes are prevalent in at least 48 (pre)clinical drugs as of December 2022.[54] To complement the cyclobutane, a piperidine moiety was included as this is the most frequent nitrogen heterocyclic fragment present in FDA approved drugs.[55] Due to their inherent 3-dimensionality, spirocyclic compounds are an attractive scaffold for drug discovery.[33,53,56–60] Spirocyclic compounds have a high fraction of sp^3-hybridised carbons (Fsp^3), leading to a more likely and desirable "escape from flatland".[33]

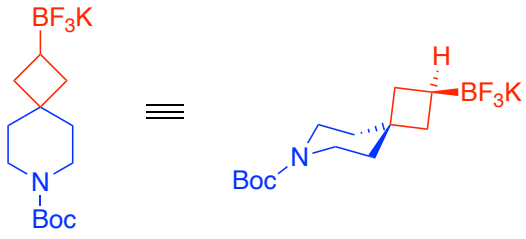

25

*Figure 1.10 – Cyclobutyl trifluoroborate salt **25***

Finally, the trifluoroborate salt moiety would be used as a synthetic handle for cross-coupling reactions. Trifluoroborate salts can be converted into boronic acids under the aqueous basic conditions typical of SMCC reactions and therefore they are widely used in SMCC reactions. In addition, as reported by Molander and Ellis,[61] alkyl trifluoroborate salts have also been successfully used as alkyl radical precursors in Ni-catalysed photoredox cross-coupling reactions. Thus, two different types of cross-coupling methodology would be available for use with cyclobutyl trifluoroborate salt **25**, whereas photoredox cross-coupling is not precedented for the MIDA alternative (see Figure 1.7).[43–45] Furthermore, trifluoroborate salts are typically air and moisture stable, easy to handle, crystalline free-flowing solids which enable ease of use for synthesis.[62]

The spirocyclic scaffold present in cyclobutyl trifluoroborate salt **25** has previously been highlighted as a contender for drug development. The same spirocyclic scaffold is part of lead-like compound **26** (Figure 1.11) which is an inhibitor of fatty acid amide hydrolase (FAAH).[63] FAAH is responsible for the breakdown of endocannabinoid anandamide (AEA).[64] Inhibition of FAAH leads to higher levels of AEA. This elevation of AEA has been found to reduce pain levels in rodent models, providing an analgesic effect. Thorarensen *et al*.[63,65] developed lead-like compound **26** which had high potency and selectivity as a FAAH inhibitor. It was therefore selected as a drug candidate in human trials. Lead-like compound **26**, which had properties in common with other CNS drugs, was potent, selective and exhibited *in vivo* efficacy.

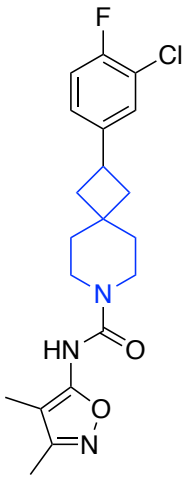

26

Figure 1.11 – FAAH inhibitor drug candidate

With the drug-like features of the building block established, we were ready to move on to its synthesis. In this MSc project, the first objective was to develop synthetic methodology to access cyclobutyl trifluoroborate salt **25** on a gram-scale. The results of our work on two different synthetic routes are described in Chapter 2. Once cyclobutyl trifluoroborate salt **25** had been synthesised, the next objective was to develop the cross-coupling of aryl bromides with cyclobutyl trifluoroborate salt **25** using Ni-catalysed photoredox cross-coupling and Pd-catalysed SMCC to produce aryl cyclobutanes **27** (Scheme 1.3). In each case, optimisation would be required to identify suitable reaction conditions. Then, it was planned to use these reaction conditions on a range of medicinally relevant aryl halides including FragLites[20] to demonstrate the scope of these cross-coupling reactions. In this way, as with the established nine cyclopropane 3-D building blocks, cyclobutyl trifluoroborate salt **25** could be used as a new structural motif in the

O'Brien group's modular synthetic platform for fragment elaboration in 3-dimensions. Progress in these areas is described in Chapter 3.

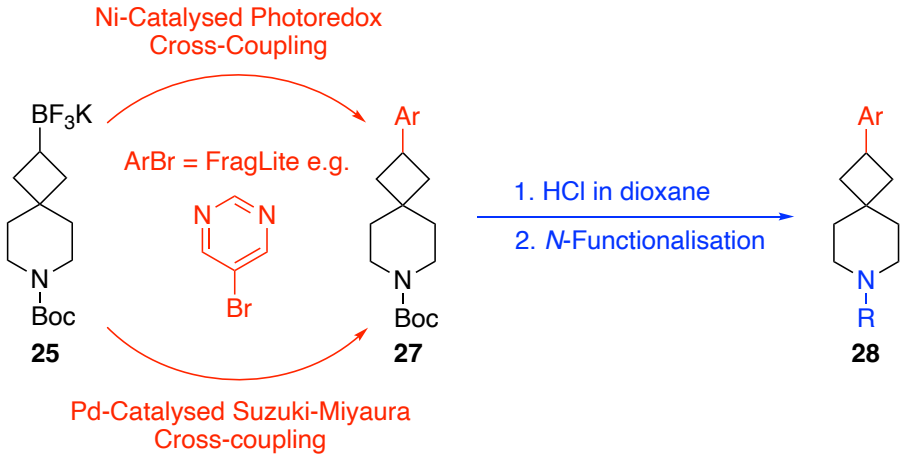

Scheme 1.3

Finally, once aryl cyclobutanes **27** were successfully synthesised, the final objective was to deprotect the amine functionality and carry out standard amine functionalisation reactions to create *N*-functionalised aryl cyclobutanes **28**. In particular, we would target a *N*-methanesulfonamide pyrimidine and attempt to obtain its X-ray crystal structure. If successful, an exit vector analysis could be carried out and the result used to show that cyclobutyl trifluoroborate salt **25** would generate lead-like compounds in areas of chemical space different to that of the nine cyclopropane 3-D building blocks. The results for the synthesis of lead-like compounds and exit vector analysis are found in Chapter 4.

2. Synthesis of Spirocyclobutane Building Block

In this Chapter, the literature background related to the synthesis of cyclobutyl trifluoroborate salt **25** and the development of synthetic methodology to access cyclobutyl trifluoroborate salt **25** is discussed. Section 2.1 introduces the previous syntheses of mono- and di-boronated spirocyclic analogues of cyclobutyl trifluoroborate salt **25**. Section 2.2 discusses the synthesis of cyclobutyl trifluoroborate salt **25** *via* a route developed by Tortosa *et al*.[66] In this approach, cyclobutyl trifluoroborate salt **25** is synthesised *via* cyclobutene **29** starting from cyclobutanone **30** and the challenges and optimisation at each stage of the synthesis are discussed (Scheme 2.1). Section 2.3 covers an alternative synthesis to the cyclobutyl trifluoroborate salt **25**, also starting from cyclobutanone **30**, which proceeds *via* Miyaura borylation of cyclobutyl enol triflate **31** (Scheme 2.1). The development of this synthetic route is discussed.

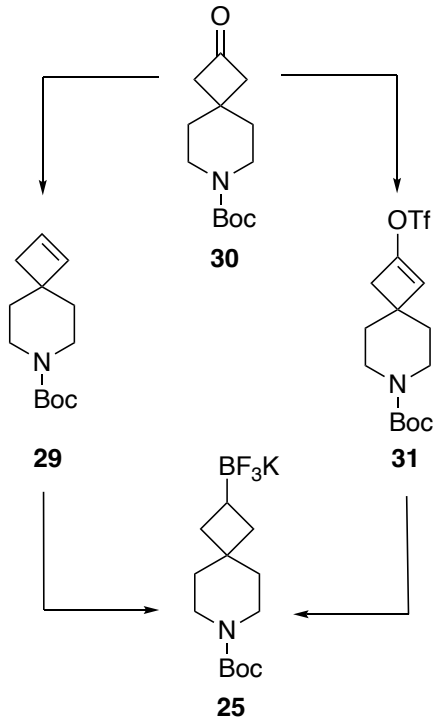

Scheme 2.1

2.1 Previous Syntheses of Mono- and Di-Boronated Spirocyclobutane Compounds

The synthesis of the spirocyclic scaffold present in cyclobutyl trifluoroborate salt **25** has previously been carried out *via* two main routes.[66–68] In one route, cyclobutanone **30** was converted into cyclobutene **29** which was then transformed into a cyclobutyl mono- or diboronate, **32** or *cis*-**33** respectively (Scheme 2.2). Alternatively, starting from cyclobutanone **30**, enol triflate formation gave cyclobutyl enol triflate **31** which was converted into cyclobutyl vinyl Bpin **34** using Miyaura borylation (Scheme 2.2). Full details on both synthetic routes are presented in this section.

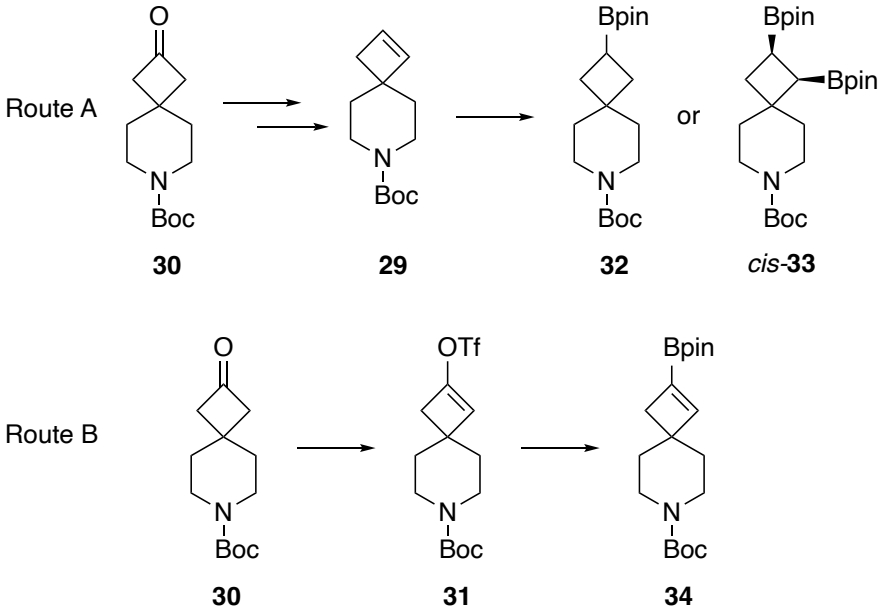

Scheme 2.2

In 2021, Tortosa *et al*.[66] reported the synthesis of a variety of spirocyclobutenes using the general synthetic route shown in Scheme 2.3. Wittig olefination of cyclic ketones **35** using methyltriphenylphosphonium bromide and KO*t*-Bu produced exocyclic alkenes **36**. Then, a [2 + 2] cycloaddition between exocyclic alkenes **36** and dichloroketene generated from trichloroacetyl chloride and a Zn-Cu couple was carried out. The dichlorocyclobutanones were then dechlorinated either using AcOH and Zn or NH_4Cl and Zn to produce cyclobutanones **37**. Next, ketone reduction using $NaBH_4$ in MeOH was carried out and subsequent tosylation using *p*-TsCl and Et_3N gave cyclobutyl tosylates **38**. Finally, elimination of the tosylate group using KO*t*-Bu in DMSO gave cyclobutenes **39**.

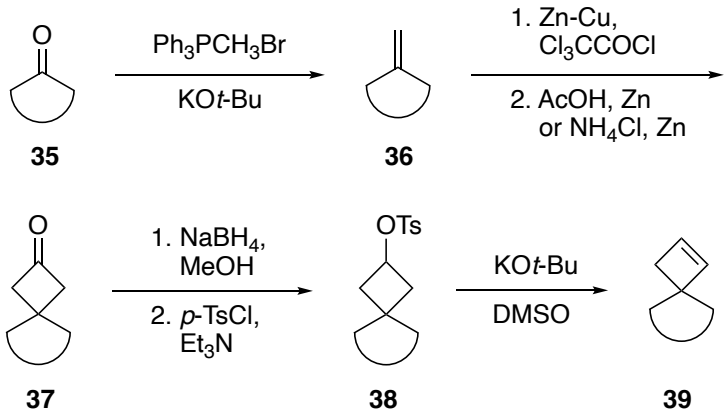

Scheme 2.3

This sequence of reactions was carried out on a variety of cyclic ketones to ultimately yield ten different cyclobutenes **39** with a variety of functional groups. The final step in the synthesis, tosylate elimination, is shown in Scheme 2.4. The cyclobutyl tosylate **38** was eliminated using KO*t*-Bu in DMSO at room temperature for 4 h. This gave cyclobutenes that included *N*-Boc, dimethyl, ether, thioether, sulfone, and acetal functionalities in spiro[3.5]nonane ring systems. Cyclobutenes with other ring systems were also prepared. The yields for the elimination step were in the range 37-91%.

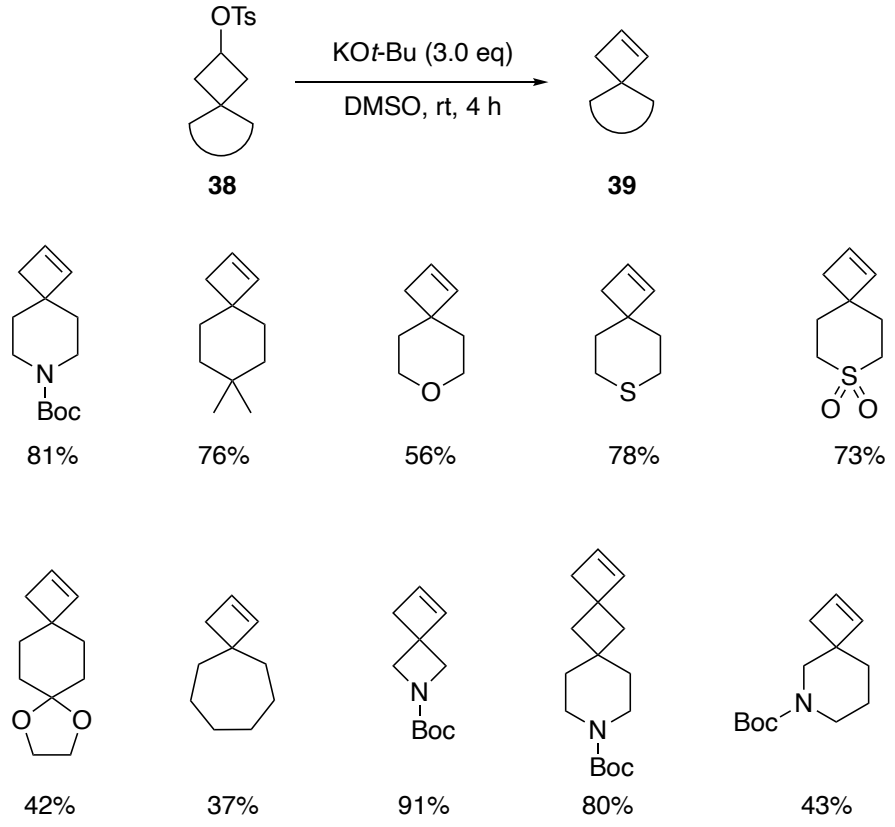

Scheme 2.4

The synthesis of cyclobutene **29** started from commercially available cyclobutanone **30**. From here, reduction and tosylation were carried out to give cyclobutyl tosylate **40** in 97% yield. Cyclobutanone **30** was reduced using $NaBH_4$ in MeOH at room temperature for 12 h. The crude cyclobutanol was then tosylated using *p*-TsCl and Et_3N in CH_2Cl_2 at room temperature for 16 h. Elimination of cyclobutyl tosylate **40** using KO*t*-Bu proceeded smoothly to form cyclobutene **29** in 81% yield (Scheme 2.5). All three steps were carried out on gram scales.

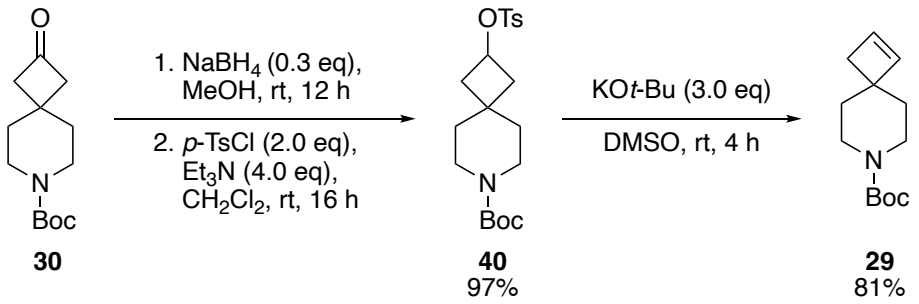

Scheme 2.5

Tortosa *et al*.[67] studied the regioselectivity of the monoborylation of cyclobutene **29** to give cyclobutyl Bpin compounds **32** and **41** (Table 2.1). Using CuCl, B_2pin_2 and a suitable ligand, it was envisaged that monoborylation products would be obtained using an *in situ* generated copper-boryl complex which would undergo migratory insertion and protonation. Cyclobutene **29** was reacted with a ligand, CuCl, B_2pin_2, KO*t*-Bu and MeOH in THF at room temperature for 16 h. It was found that the ligand had a significant effect on the regioselectivity of the monoborylation. The results are summarised in Table 2.1. For example, use of **42**-CuCl gave a 65:35 mixture of cyclobutyl Bpin compounds **32** and **41** (entry 1). With dppbz, only a 50:50 mixture of cyclobutyl Bpin compounds **32** and **41** was obtained (entry 2). Other diphosphine ligands gave improved regioselectivity in favour of cyclobutyl Bpin **32** (entries 3-6). The highest regioselectivity was obtained using Xantphos where a ≥98:2 mixture of cyclobutyl Bpin compounds **32** and **41** was generated in 86% yield (entry 3). With no ligand, a low yield and poor regioselectivity was observed (entry 7).

*Table 2.1 – Ligand effect on the copper-catalysed monoborylation of cyclobutene **29***[67]

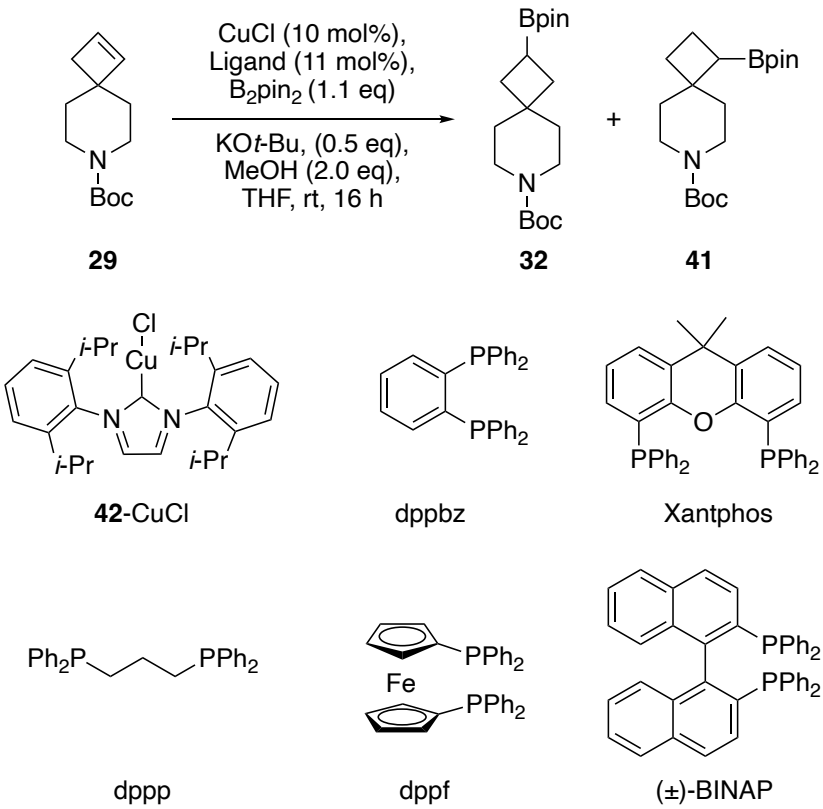

Entry	Ligand	32:41	Yield (%)[a]
1	**42**-CuCl	65:35	71
2	dppbz	50:50	84
3	Xantphos	≥98:2	86
4	dppp	83:17	58
5	dppf	64:36	79
6	(±)-BINAP	73:27	69
7	-	60:40	13

a) Yield after purification by chromatography.

With these results in hand, Tortosa *et al.*[67] proceeded to mono-borylate the previously synthesised cyclobutenes. CuCl, B_2pin_2 and Xantphos were used as these conditions had given the highest regioselectivity (≥98:2) and yield (86%) out of all the various ligands studied (see Table 2.1, entry 3). The synthesis of a variety of cyclobutyl Bpin compounds **43** were reported (Scheme 2.6), all of which were produced regioselectively and in high yields (66-90%). For example, cyclobutyl Bpin **32** was successfully obtained in 86% yield. The cyclobutenes **39** were mono-borylated on a 0.2 mmol scale, except azetidine cyclobutyl Bpin **44** which was made on both a 0.2 mmol scale and 5.1 mmol scale, in

high yields in both cases (87% and 90% respectively). An interesting result was that non-symmetric cyclobutyl Bpin **45** was synthesised as a single diastereomer. This is likely due to the copper-boryl complex adding to the opposite face to the sterically bulky *N*-Boc group.

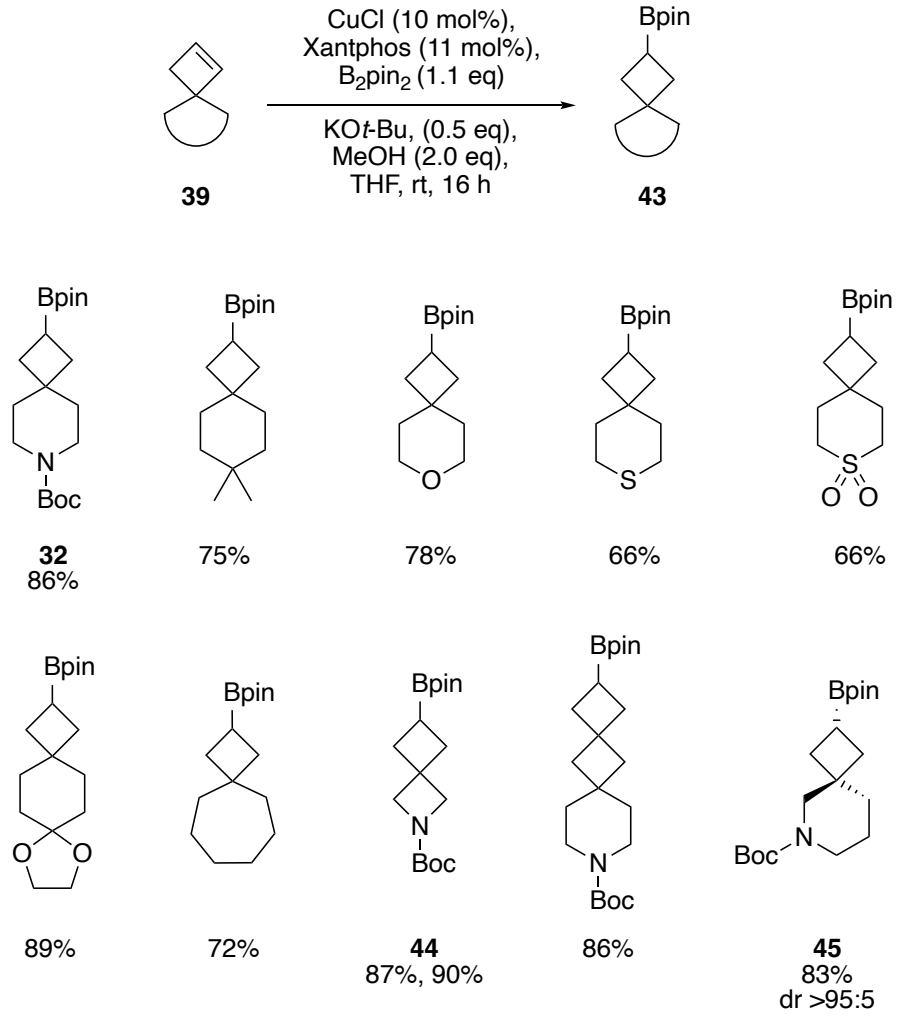

Scheme 2.6

In related work, Tortosa *et al*.[66] had reported the synthesis of a variety of *cis*-diboronated spirocycles starting from cyclobutenes. For example, reaction of cyclobutene **29** with B_2pin_2 (2.0 eq) and NaOMe (0.6 eq) in MeOH at 70 °C for 16 h resulted in *cis*-boronation stereoselectively and gave cyclobutyl diboronate *cis*-**33** in 78% yield (Scheme 2.7). *cis*-Diboronation is believed to be due to the concerted addition of a methoxide adduct of B_2pin_2 in which there are nucleophilic and electrophilic boron atoms. This was supported by DFT calculations.[69] Using this approach, a variety of diboronated spirocycles were prepared.

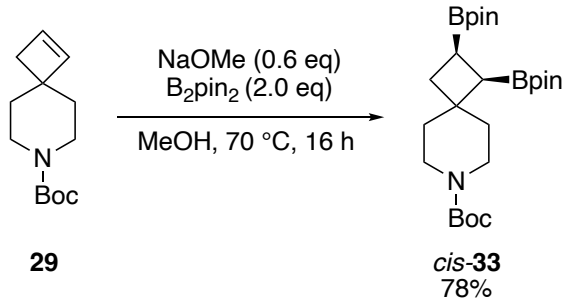

Scheme 2.7

Other synthetic work on the spirocyclobutane piperidine scaffold, namely the conversion of cyclobutanone **30** into cyclobutyl vinyl Bpin **34**, has been carried out and reported in the patent literature.[68] An enol triflate formation from cyclobutanone **30** gave cyclobutyl enol triflate **31**. Readily available cyclobutanone **30** was deprotonated α to the ketone using LiHMDS in THF at –78 °C for 1 h. The enolate was triflated using $PhNTf_2$ in THF at –78 °C to room temperature for 16 h to give cyclobutyl enol triflate **31**. The reaction proceeded in 65% yield on a 1.0 mmol scale. Subsequent Miyaura borylation of cyclobutyl enol triflate **31** produced cyclobutyl vinyl Bpin **34**. The conditions for the Miyaura borylation were: $PdCl_2$(dppf) (0.1 eq), B_2pin_2 (1.5 eq) and KOAc (3.0 eq) in dioxane at 80 °C for 4 h (Scheme 2.8). Cyclobutyl vinyl Bpin **34** was not purified and isolated; instead, the crude vinyl Bpin was used in subsequent Pd-catalysed SMCC and alkene hydrogenation.

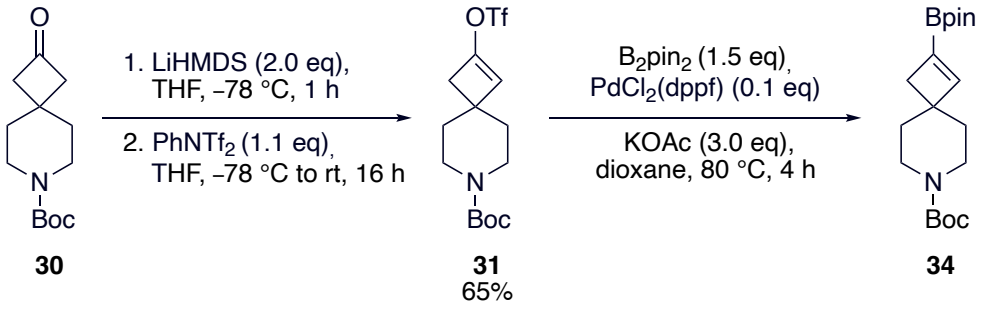

Scheme 2.8

The same synthetic route was repeated on a variety of scaffolds to give different building blocks including azetidine cyclobutyl vinyl Bpin **46** and azetidine cyclohexyl vinyl Bpin **47** (Figure 2.1).[68] In all cases, the same reagents were used for the enol triflate formation and Miyaura borylation of the spirocyclic ketone starting materials as those described in Scheme 2.8. All the building block examples were further functionalised through Pd-catalysed SMCC, alkene hydrogenation and *N*-functionalisation.

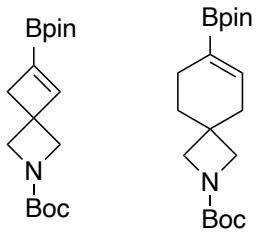

46 **47**

Figure 2.1 – Different vinyl Bpin building blocks synthesised via cyclobutyl enol triflate[68]

2.2 Synthesis of Spirocyclobutane Building Block *via* Spirocyclobutene

Our proposed synthesis of cyclobutyl trifluoroborate salt **25**, based on the work by Tortosa *et al*.[67] that was presented in the previous section, is summarised in Scheme 2.9. Cyclobutanone **30** would be synthesised in two steps. The first step would be *via* a [2 + 2] cycloaddition reaction of *N*-Boc 4-methylenepiperidine **48** with a dichloroketene generated *in situ* from Cl_3COCl and a Zn-Cu couple. This would generate dichlorocyclobutanone **49**. The second step would be dechlorination using activated Zn powder and NH_4Cl to generate cyclobutanone **30**. Cyclobutyl tosylate **40** would be generated in two steps *via* $NaBH_4$ reduction of cyclobutanone **30** to form cyclobutanol **50** followed by tosylation. This would be followed by elimination using KO*t*-Bu to produce cyclobutene **29**. Hydroboration would then be performed on cyclobutene **29** using CuCl, Xantphos, B_2pin_2 and KO*t*-Bu to produce cyclobutyl Bpin **32**. Finally, trifluoroborate salt formation from cyclobutyl Bpin **32** would be carried out using KHF_2 and MeOH to give cyclobutyl trifluoroborate salt **25**.

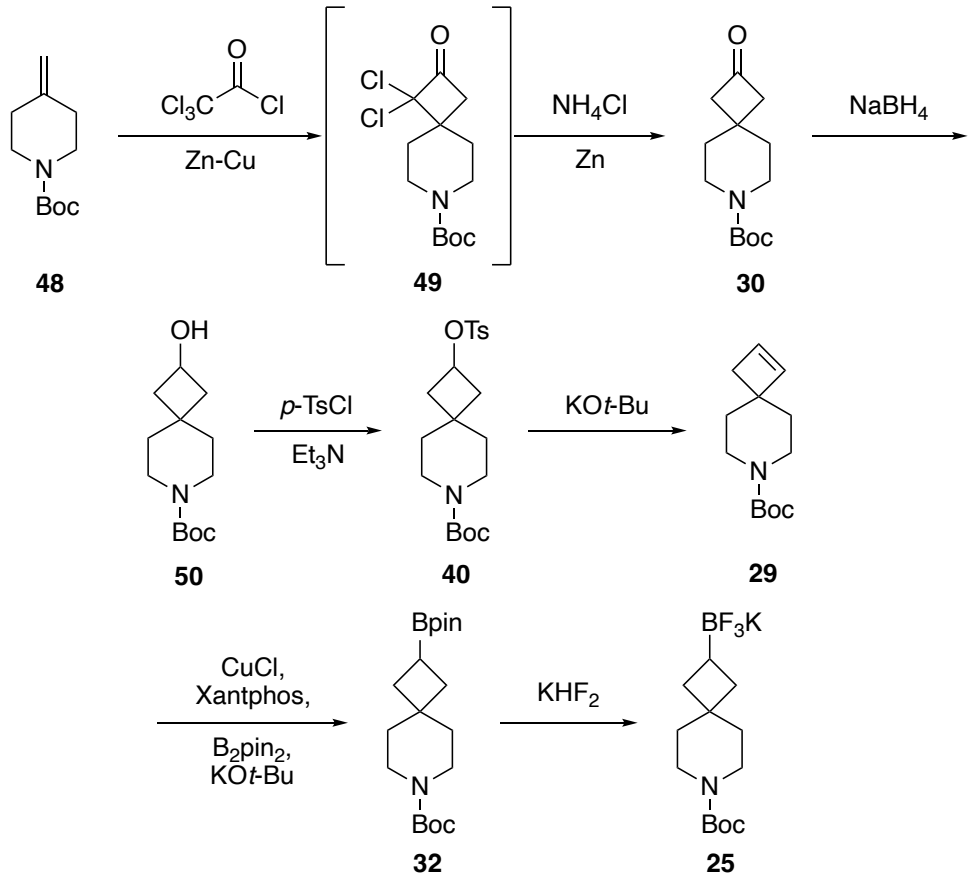

Scheme 2.9

Initially, the formation of cyclobutanone **30** was attempted using the conditions reported by Tortosa *et al*.[66] Thus, on a 1.0 mmol scale, *N*-Boc 4-methylenepiperidine **48** was reacted with Cl_3C_2OCl (4.0 eq) and Zn-Cu couple (11.0 eq) in DME and MTBE at room temperature for 16 h. The work-up of the crude dichlorocyclobutanone **49** was challenging due to the formation of emulsions. Next, dechlorination of the crude dichlorocyclobutanone **49** was carried out using activated Zn powder (10.0 eq) and NH_4Cl (7.0 eq) in MeOH at room temperature for 16 h. After another challenging work-up due to emulsion formation and purification by chromatography, cyclobutanone **30** was isolated in 39% yield (Scheme 2.10).

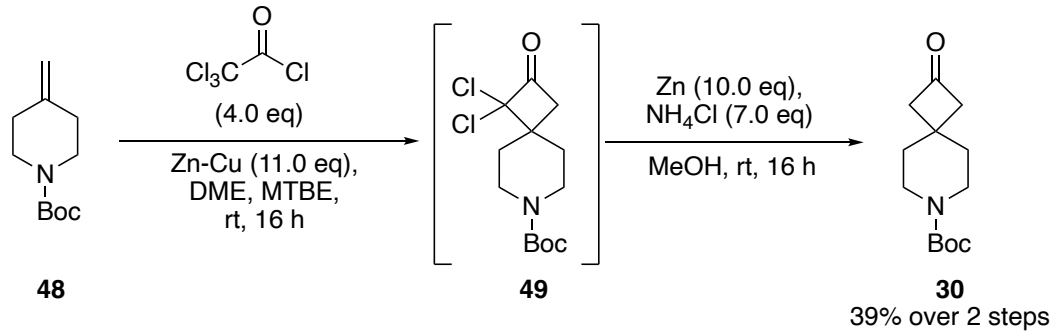

48 **49** **30**
39% over 2 steps

Scheme 2.10

The ^{1}H NMR spectrum of cyclobutanone **30** is shown in Figure 2.2. All four H_A protons are chemically equivalent and were assigned to the singlet at δ_H 2.79. The same chemical equivalence is observed for each of the sets of H_B and H_C protons which both appear as triplets. The H_C protons are the most downfield at δ_H 3.39 (t, J = 5.5 Hz) due to the electron withdrawing effects of the adjacent *N*-Boc group. The 4H singlet for H_A appears at δ_H 2.79 since it is next to the carbonyl ketone group. Finally, the most upfield protons are the H_B protons at δ_H 1.68 (t, J = 5.5 Hz) and the 9H singlet at δ_H 1.46 which is assigned to the protons on the Boc group.

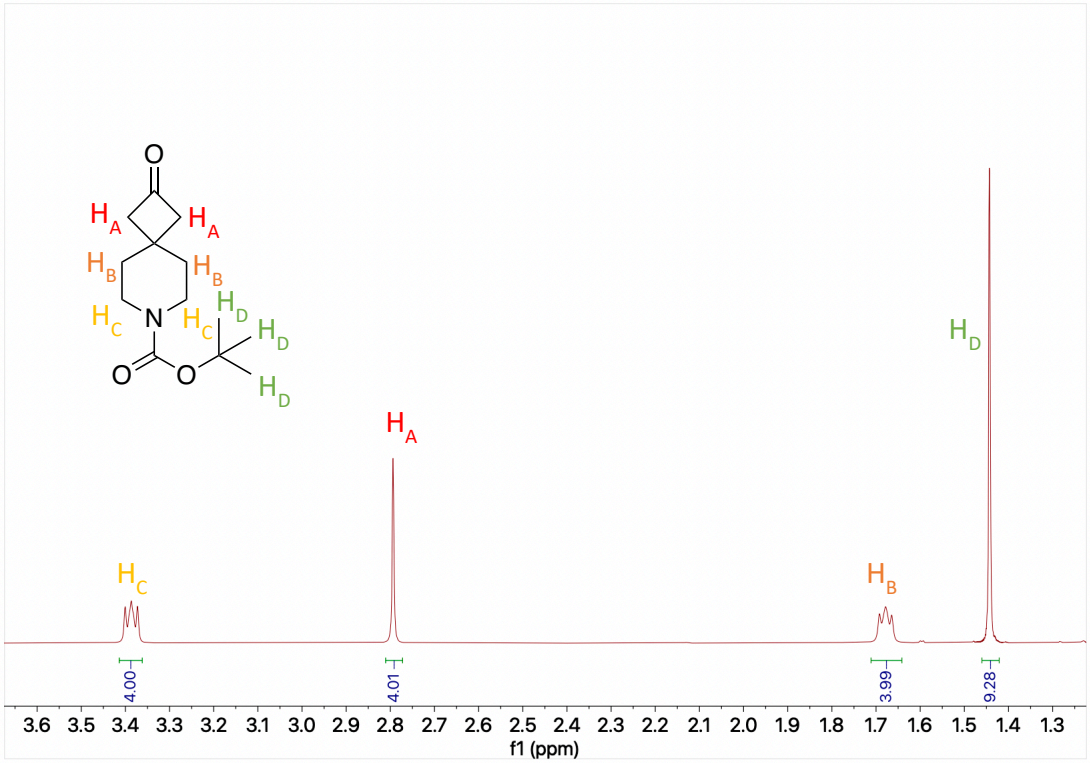

*Figure 2.2 – ^{1}H NMR spectrum of cyclobutanone **30***

Due to difficulties with emulsions forming in the work-up of both steps in the synthesis of cyclobutanone **30**, it was decided to explore other reaction conditions and work-up modifications when scaling up the reaction. In particular, conditions reported by Groblewski[70] and Kobayashi[71] were explored. The results of these variations are shown in Table 2.2, with the initially obtained 39% yield of cyclobutanone **30** shown in entry 1. Entry 1 shows the initial conditions which used 1.0 mmol of *N*-Boc 4-methylenepiperidine **48** with Cl_3C_2OCl (4.0 eq) and Zn-Cu couple (11.0 eq) in DME and MTBE at room temperature for 16 h. Next, dechlorination of the crude dichlorocyclobutanone **49** was carried out using activated Zn powder (10.0 eq) and NH_4Cl (7.0 eq) in MeOH at room temperature for 16 h. The first alteration of these conditions was as follows: on a 5.1 mmol scale, at the end of the first step, the reaction mixture was added to saturated $NaHCO_{3(aq)}$ before filtering to remove the solids rather than washing with saturated $NaHCO_{3(aq)}$ in the aqueous work-up. With this change, an emulsion did not form in the work-up but it was quite a vigorous quench when adding the reaction mixture to the saturated $NaHCO_{3(aq)}$. The dechlorination step was carried out with no changes and a 19% yield of cyclobutanone **30** was obtained over the 2 steps (entry 2). To minimise the vigorous $NaHCO_{3(aq)}$ quench at the end of the first step, saturated $NaHCO_{3(aq)}$ was added dropwise at 0 °C to the reaction mixture. This proved to be the

most practical method for basifying the reaction mixture and a 39% yield of cyclobutanone **30** (10.1 mmol scale) was obtained over the two steps (entry 3).

*Table 2.2 – Optimising the formation of cyclobutanone **30***

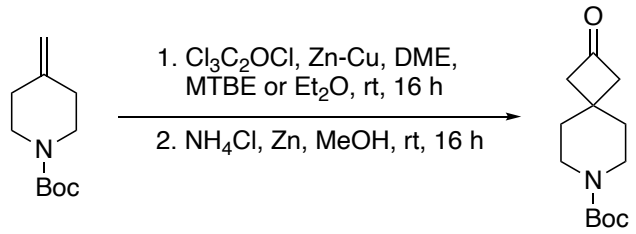

48 **30**

Entry	Scale (mmol)	Solvent	Work-up for step 1	Yield (%)[a]
1	1.0	MTBE	$NaHCO_{3(aq)}$ wash in the work-up	39
2	5.1	MTBE	Add reaction mixture to $NaHCO_{3(aq)}$	19
3	10.1	MTBE	Add $NaHCO_{3(aq)}$ to reaction mixture at 0 °C	39
4	10.1	Et_2O	Add $NaHCO_{3(aq)}$ to reaction mixture at 0 °C	79
5	20.3	Et_2O	Add $NaHCO_{3(aq)}$ to reaction mixture at 0 °C	0
6	3.0	Et_2O	Add $NaHCO_{3(aq)}$ to reaction mixture at 0 °C	37[b]

a) Yield after purification by chromatography; b) Freshly purchased Zn used.

In the next variation, Et_2O was used as the reaction solvent on a 10.1 mmol scale (instead of MTBE) for the first step and, in the second step of the reaction, the aqueous work-up was removed. Thus, the reaction mixture was filtered, and the filtrate was evaporated to give the crude product. Encouragingly, these changes led to a 79% yield of cyclobutanone **30** being achieved (entry 4). However, the high yield was not reproducible with these reaction conditions. An attempt on a 20.3 mmol scale gave no conversion to cyclobutanone **30** and a significant unidentified by-product was produced (entry 5). It was suspected that the activated Zn powder in the second step was the problem. Support for this came from the fact that a reaction with newly activated Zn gave a 37% yield of cyclobutanone **30** on a 3.0 mmol scale (entry 6). Thus, whilst it was possible to produce quantities of cyclobutanone **30** using this cycloaddition and dechlorination approach, in

our hands, we were unable to reproduce good yields of cyclobutanone **30**. Fortunately, cyclobutanone **30** is commercially available at a reasonable price (~£240 for 25 g) and so it was purchased for future work on this route to cyclobutyl trifluoroborate salt **25**.

The next two steps involved reduction of the ketone in cyclobutanone **30** to cyclobutanol **50** and subsequent tosylation. For each of these reactions, conditions reported by Pasau[72] were followed. Cyclobutanone **30** was reduced with $NaBH_4$ (1.0 eq) in MeOH at room temperature for 16 h. After purification by chromatography, cyclobutanol **50** was obtained in 89% yield (Scheme 2.11). Then, cyclobutanol **50** was tosylated using *p*-TsCl (2.0 eq) and Et_3N (2.5 eq) in CH_2Cl_2 at room temperature for 16 h. This proceeded smoothly and cyclobutyl tosylate **40** was isolated in 70% yield after chromatography (Scheme 2.11).

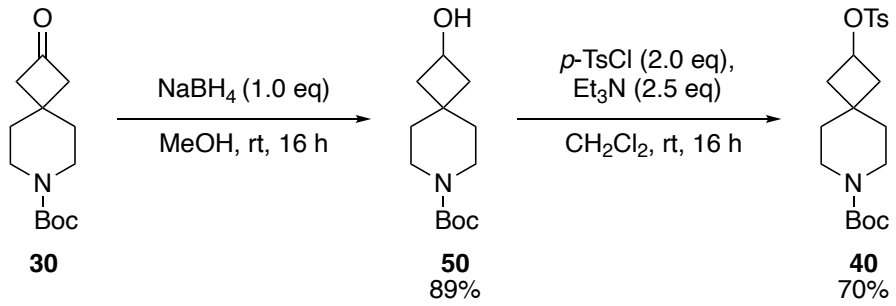

Scheme 2.11

The ^1H NMR spectrum of cyclobutyl tosylate **40** is shown in Figure 2.3. H_D appears as a triplet of triplets at δ_H 4.80 (tt, J = 7.5, 7.5 Hz) due to its coupling to the adjacent two pairs of diastereotopic H_E protons. The two sets of diastereotopic H_E protons appear as a multiplet at δ_H 1.51–1.46. The two axial protons of H_F appear as independent signals from their equatorial counterparts at δ_H 2.23–2.17 and δ_H 1.97–1.87. The H_C protons at δ_H 7.75 (d, J = 8.0 Hz) and H_B protons at δ_H 7.36 (d, J = 8.0 Hz) couple to each other so both appear as doublets. The H_C protons *ortho* to the sulfonate (δ_H 7.75) are more downfield than the *meta*-H_B protons (δ_H 7.36) due to deshielding caused by the –M mesomeric effect from the sulfonate group.

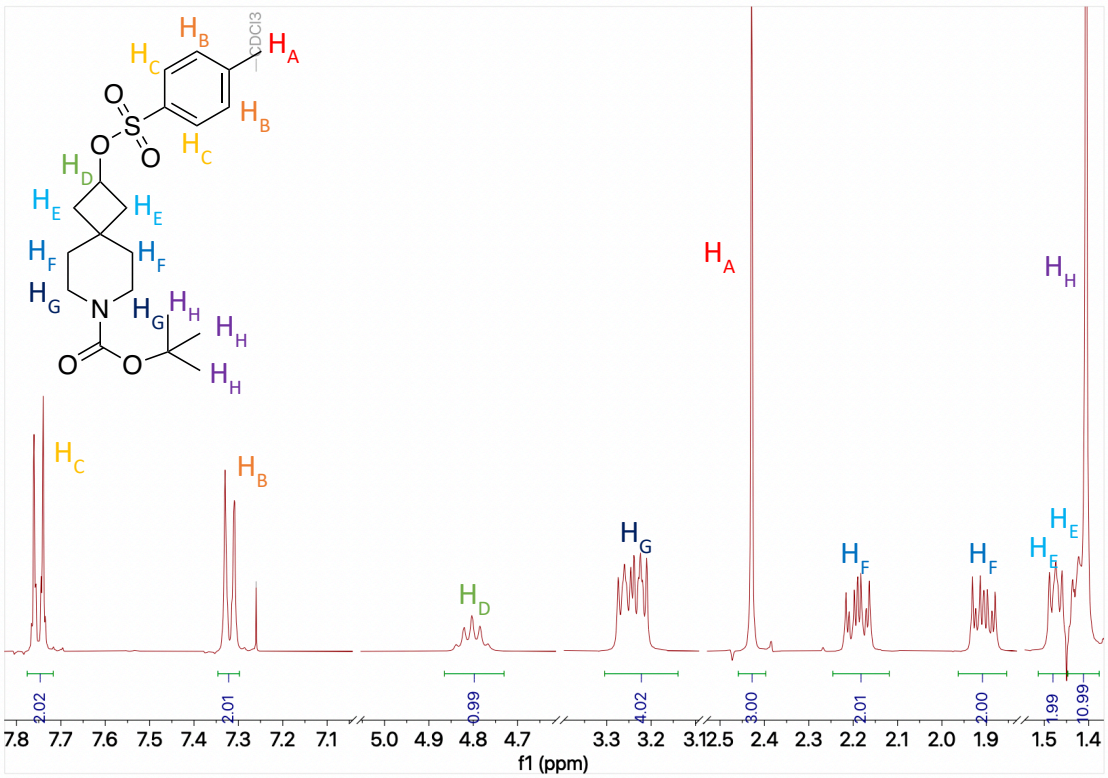

*Figure 2.3 – ^{1}H NMR spectrum of cyclobutyl tosylate **40***

It was clear that crude cyclobutanol **50** obtained from the $NaBH_4$ reduction step was of high purity and therefore it was decided to explore the synthesis of cyclobutyl tosylate **40** without purifying the intermediate alcohol. Thus, on a 0.4 mmol scale, cyclobutanone **30** was reduced in the usual way ($NaBH_4$, MeOH) and the crude cyclobutanol **50** was toslyated (*p*-TsCl, Et_3N). This gave cyclobutyl tosylate **40** in a moderate 37% yield over the two steps (Scheme 2.12). On scale-up (10.0 mmol scale), a 61% yield of cyclobutyl tosylate **40** was obtained after chromatography. These two steps were reproducible on smaller and larger scales and proceeded with few issues.

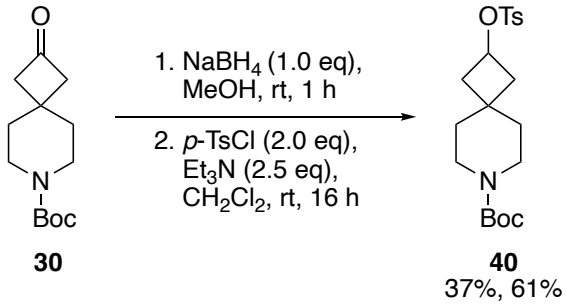

Scheme 2.12

Once cyclobutyl tosylate **40** had been successfully prepared, an elimination of the tosylate group to form cyclobutene **29** was carried out. For this reaction, conditions reported by

Tortosa *et al*.[66] were followed. Elimination of cyclobutyl tosylate **40** using KO*t*-Bu (3.0 eq) to form cyclobutene **29** was carried out in DMSO at room temperature for 4 h. After purification by chromatography, cyclobutene **29** was isolated in 81% yield (Scheme 2.13). Due to the volatility of cyclobutene **29**, care was taken when evaporating the solvent to minimise any losses of cyclobutene **29**. This step was carried out several times and yields were between 47-66% with the 81% yield being the best yield achieved on one occasion.

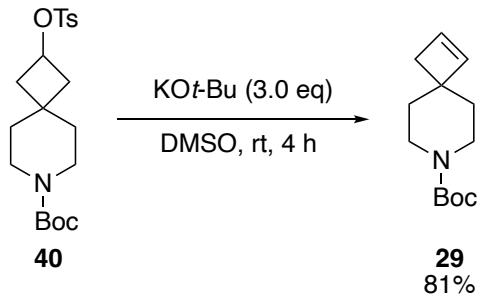

Scheme 2.13

The ^{1}H NMR spectrum of cyclobutene **29** is shown in Figure 2.4. It is likely that the axial protons of H_E are at δ_H 3.20 (ddd, J = 13.0, 8.0, 4.0 Hz) due to having two large couplings (^{2}J, $^{3}J_{\text{axial-axial}}$) and one small coupling ($^{3}J_{\text{axial-equatorial}}$). The equatorial protons of H_E are at δ_H 3.54–3.48 and appear as a multiplet. Cyclobutenes show substantially reduced ^{3}J values than larger ringed cycloalkenes and straight chain alkenes.[73] This is evident in the ^{1}H NMR spectrum of cyclobutene **29** as the H_A proton at δ_H 6.19 (d, J = 3.0 Hz) has a low ^{3}J value of 3.0 Hz compared to the high ^{3}J value usually observed for acyclic *cis*-alkenes at 8–11 Hz.[74] The CH_2 protons of the cyclobutene at H_C (δ_H 2.23) appear as an apparent singlet, with the coupling to H_A being so small that it is not resolved.

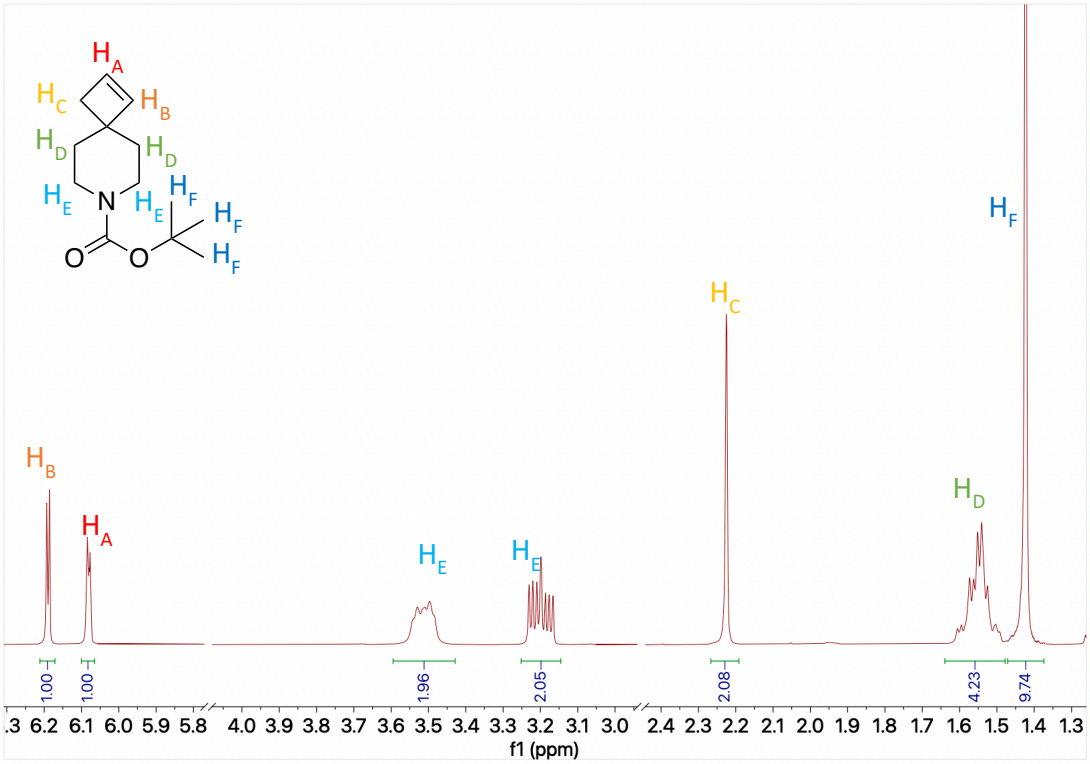

*Figure 2.4 – ^{1}H NMR spectrum of cyclobutene **29***

The next stage in the synthesis was the preparation of cyclobutyl Bpin **32** from cyclobutene **29**. Conditions optimised by Tortosa *et al.*[67] were used in the hydroboration of cyclobutene **29** to generate cyclobutyl Bpin **32** (Scheme 2.14). In this reaction, cyclobutene **29** was reacted with CuCl (10 mol%), Xantphos (11 mol%), B_2pin_2 (1.1 eq), KO*t*-Bu (0.5 eq) and MeOH (2.0 eq) in THF to produce cyclobutyl Bpin **32**. When attempting this reaction on a 0.2 mmol scale, some conversion to product was observed in the ^{1}H NMR spectrum of the crude product. However, after chromatography, no product was isolated, therefore suggesting that cyclobutyl Bpin **32** is somewhat unstable to chromatography. Therefore, eluent systems were made more polar to reduce the time cyclobutyl Bpin **32** interacted with the silica with a view to reducing boronic pinacol ester decomposition. When repeating this reaction and using a more polar eluent system in the chromatography on a 3.0 mmol scale, cyclobutyl Bpin **32** was obtained in a high yield (71%). Curiously, when the reaction was accidentally carried out with no MeOH present on a 3.4 mmol scale, an 80% yield of cyclobutyl Bpin **32** was afforded. The role of MeOH in this reaction is to provide methoxide and protons.[75] Due to no MeOH available to generate methoxide, *tert*-butoxide from KO*t*-Bu probably fulfilled the role of methoxide in this reaction. As there was no obvious proton source in the absence of MeOH, the most likely explanation of the success of this reaction would be the presence of some water in

the solvent or in the reagents providing protons for the reaction. With *tert*-butoxide from KO*t*-Bu and protons from water, MeOH was unnecessary for the reaction to be successful.

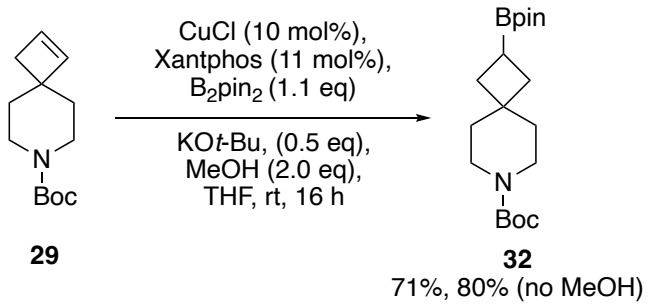

Scheme 2.14

The ^{1}H NMR spectrum of cyclobutyl Bpin **32** is shown in Figure 2.5. The spectrum shows only the symmetrical regioisomer was obtained, none of the non-symmetric isomer was seen. If the Bpin was non-symmetric, there would be four separate environments for the protons α to the nitrogen (H_E) as the two axial and the two equatorial protons would not be chemically equivalent. The same would be observed for the other piperidine protons (H_D). As this is not the case, it can be concluded that the symmetric regioisomer is the one that has been obtained. Another key feature of the ^{1}H NMR spectrum of cyclobutyl Bpin **32** is the 12H singlet assigned to the four pinacol Me groups (H_A) at δ_H 1.23.

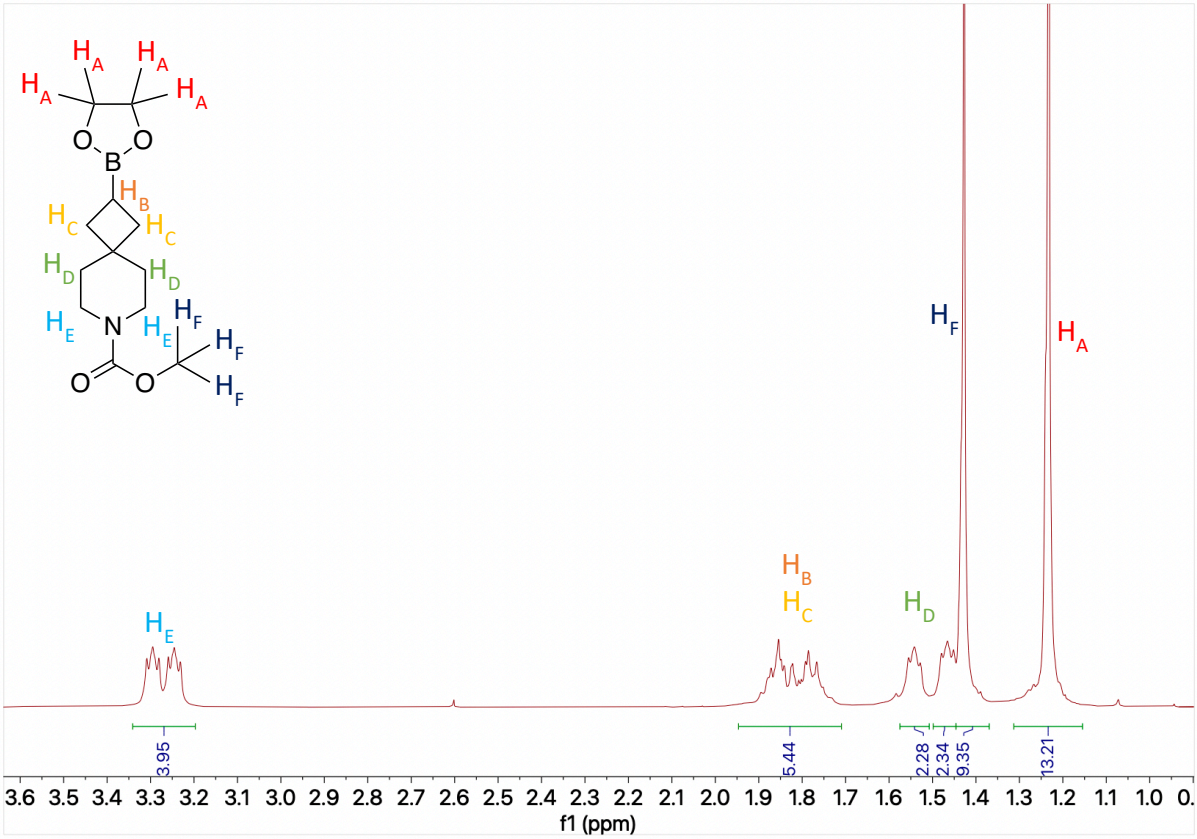

*Figure 2.5 – ^{1}H NMR spectrum of cyclobutyl Bpin **32***

Trifluoroborate salts are easily stored, stable to air and moisture and are easy to handle solids. Moreover, they are good candidates for Pd-catalysed Suzuki-Miyaura and Ni-catalysed photoredox cross-coupling reactions. Therefore, we planned to synthesise cyclobutyl trifluoroborate salt **25**. Initially, trifluoroborate salt formation from *N*-Boc piperidinyl Bpin **51** was carried out to test the reaction conditions before proceeding to cyclobutyl Bpin **32**. Conditions used by Tortosa *et al.*[67] for trifluoroborate salt formation on a similar building block were applied to *N*-Boc piperidinyl Bpin **51**. *N*-Boc piperidinyl Bpin **51** was reacted with saturated $KHF_{2(aq)}$ in MeOH at room temperature for 16 h to give *N*-Boc piperidinyl trifluoroborate salt **52**. This was carried out on a 3.0 mmol scale and *N*-Boc piperidinyl trifluoroborate salt **52** was isolated in 96% yield (Scheme 2.15).

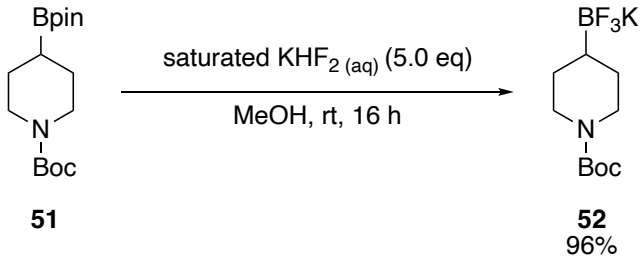

Scheme 2.15

With this knowledge, we proceeded to make cyclobutyl trifluoroborate salt **25** following the same conditions. Cyclobutyl Bpin **32** was dissolved in MeOH and saturated $KHF_{2(aq)}$ was added. After 16 h at room temperature, the solvent was evaporated, and the crude product was dissolved in hot acetone and filtered to remove any unreacted KHF_2. The filtrate was evaporated and the crude solid obtained was stirred in Et_2O and filtered to remove any organic impurities. This led to isolation of cyclobutyl trifluoroborate salt **25** as a solid. Using this method, the synthesis of cyclobutyl trifluoroborate salt **25** from cyclobutyl Bpin **32** on a 2.5 mmol scale was achieved in 97% yield (Scheme 2.16).

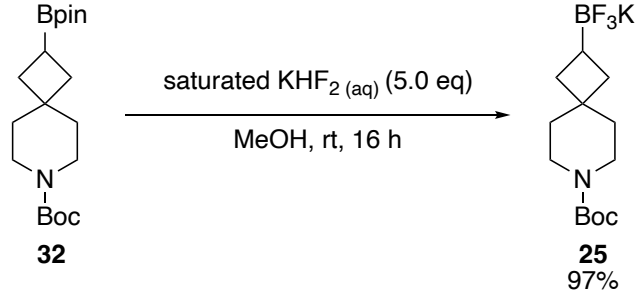

Scheme 2.16

The ^1H NMR spectrum of cyclobutyl trifluoroborate salt **25** in d_6-DMSO is presented in Figure 2.6. Proton H_A bonded to the trifluoroborate group is the most upfield at δ_H 1.13–

0.97. This is due to shielding caused by the +I inductive effect from the adjacent boron. Two of the H_C protons (on the piperidine) overlap with the four H_B protons (on the cyclobutane) leading to a multiplet signal which integrates for 6H at δ_H 1.47–1.39. The other two H_C protons occur slightly more upfield at δ_H 1.34–1.27. Finally, the most downfield protons, due to being next to the *N*-Boc group, are the H_D protons at δ_H 3.22–3.17.

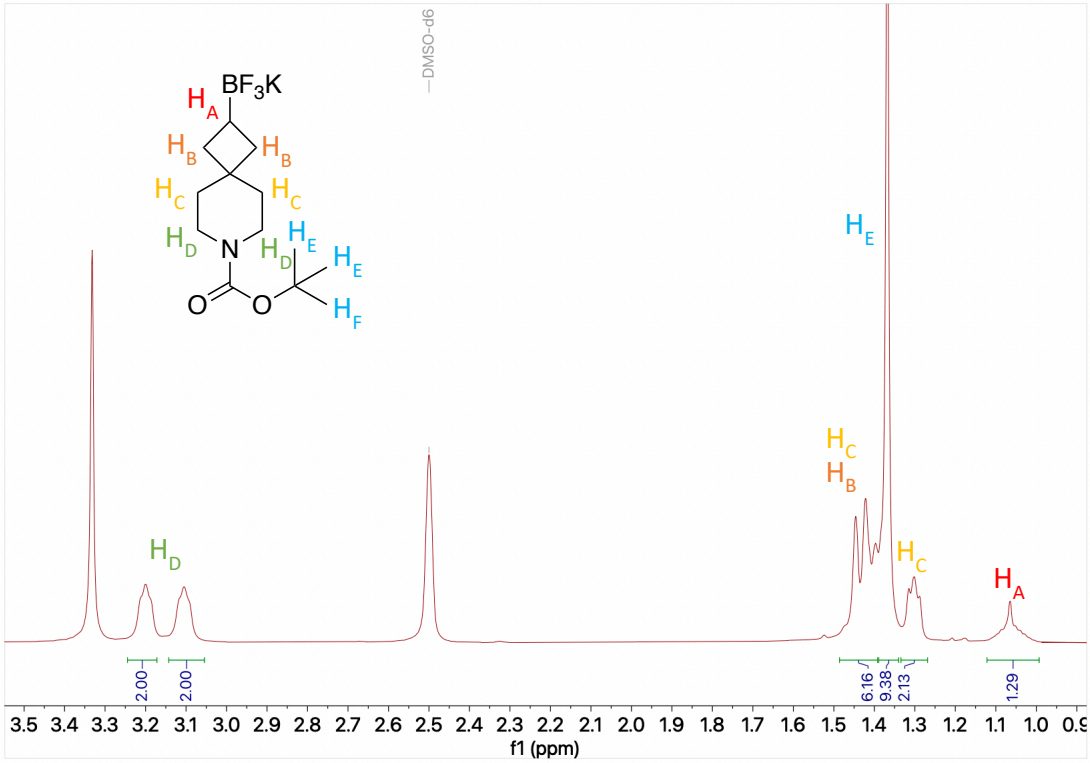

*Figure 2.6 – ^{1}H NMR spectrum of cyclobutyl trifluoroborate salt **25***

Overall, the synthesis of cyclobutyl trifluoroborate salt **25** starting from cyclobutanone **30** was achieved in good overall yield, with yields of 70% and above for each stage of the synthesis (Scheme 2.17). The overall yield from cyclobutanone **30** to cyclobutyl trifluoroborate salt **25** was 39% over five steps, showing that this is a feasible route. However, there were some issues with this synthetic route. First, the synthesis was five steps from cyclobutanone **30** and chromatography was carried out in three of the steps. Second, cyclobutene **29** was relatively volatile and challenging to work with. As a result, an alternative approach, as outlined in Section 2.3, was also explored.

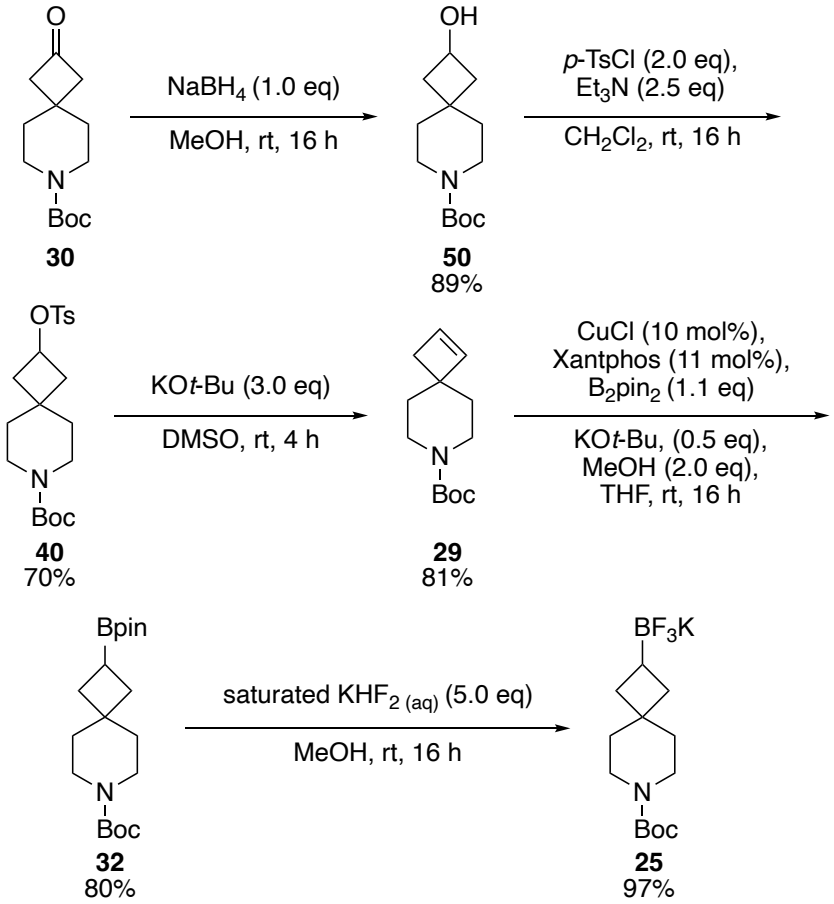
O
N
Boc
30
NaBH4 (1.0 eq)
MeOH, rt, 16 h
OH
N
Boc
50
89%
p-TsCl (2.0 eq),
Et3N (2.5 eq)
CH2Cl2, rt, 16 h
OTs
N
Boc
40
70%
KOt-Bu (3.0 eq)
DMSO, rt, 4 h
N
Boc
29
81%
CuCl (10 mol%),
Xantphos (11 mol%),
B2pin2 (1.1 eq)
KOt-Bu, (0.5 eq),
MeOH (2.0 eq),
THF, rt, 16 h
Bpin
N
Boc
32
80%
saturated KHF2 (aq) (5.0 eq)
MeOH, rt, 16 h
BF3K
N
Boc
25
97%

Scheme 2.17

2.3 Synthesis of Spirocyclobutane Building Block *via* Spirocyclic Enol Triflate

As highlighted at the end of Section 2.2, there were some issues with the previously developed synthesis of cyclobutyl trifluoroborate salt **25**. Hence, we decided to explore an alternative route to cyclobutyl trifluoroborate salt **25**. This route would also start with cyclobutanone **30** and would involve enol triflate formation and Miyaura borylation to give key intermediate, cyclobutyl vinyl Bpin **34**. Both of these steps were precedented in the patent literature (see Scheme 2.8).[68] However, we had actually devised (and investigated) the planned route shown in Scheme 2.18 before this patent literature had been found. In this route, cyclobutyl enol triflate **31** would be synthesised from cyclobutanone **30**. α-Deprotonation of cyclobutanone **30** would form the enolate and subsequent trapping using a triflating reagent would generate cyclobutyl enol triflate **31**. Miyaura borylation of cyclobutyl enol triflate **31** using $PdCl_2$(dppf), dppf, KOAc and B_2pin_2 would produce cyclobutyl vinyl Bpin **34**. In the unprecedented step of this route, cyclobutyl vinyl Bpin **34** would be hydrogenated using H_2 and Pd/C which should give cyclobutyl Bpin **32**. Finally, cyclobutyl Bpin **32** would be converted into cyclobutyl trifluoroborate salt **25** using KHF_2, as previously described.

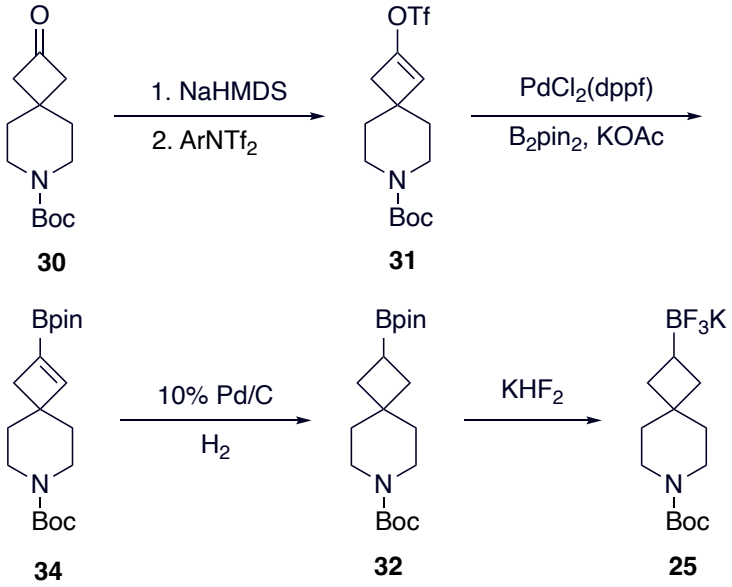

Scheme 2.18

The first step of the synthesis was to prepare cyclobutyl enol triflate **31** from cyclobutanone **30**. Initially, conditions from O'Brien *et al*.[76] were explored. To synthesise cyclobutyl enol triflate **31**, cyclobutanone **30** was deprotonated using NaHMDS (1.6 eq) in THF at –78 °C over 1 h. The enolate was then trapped with $PhNTf_2$ (1.3 eq) at –78 °C

for 10 minutes, then at room temperature for 18 h. After purification by chromatography, the product was isolated as a 50:50 inseparable mixture of cyclobutyl enol triflate **31** and sulfonamide **53**, the by-product of the triflation step. From the mass of this mixture isolated after chromatography, a 55% yield of cyclobutyl enol triflate **31** was calculated (Scheme 2.19).

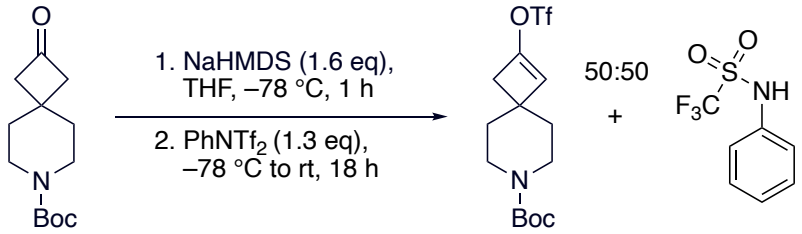

30 **31** 55% **53**

Scheme 2.19

The ^{1}H NMR spectrum of the mixture of sulfonamide **53** and cyclobutyl enol triflate **31** is shown in Figure 2.7. The diagnostic signals for sulfonamide **53** are the most downfield. A broad NH signal at δ_H 8.25 is assigned to H_G. The aromatic sulfonamide signals for H_H are assigned to δ_H 7.36–7.18. Overlap between the chloroform signal at δ_H 7.26 and the aromatic signals at δ_H 7.36–7.18 was present. Therefore, the proportion of sulfonamide **53** compared with cyclobutyl enol triflate **31** was worked out from the H_G integration. The diagnostic signals for cyclobutyl enol triflate **31** include the 1H singlet at δ_H 5.55 for H_A and the 2H singlet at δ_H 2.57 for H_B.

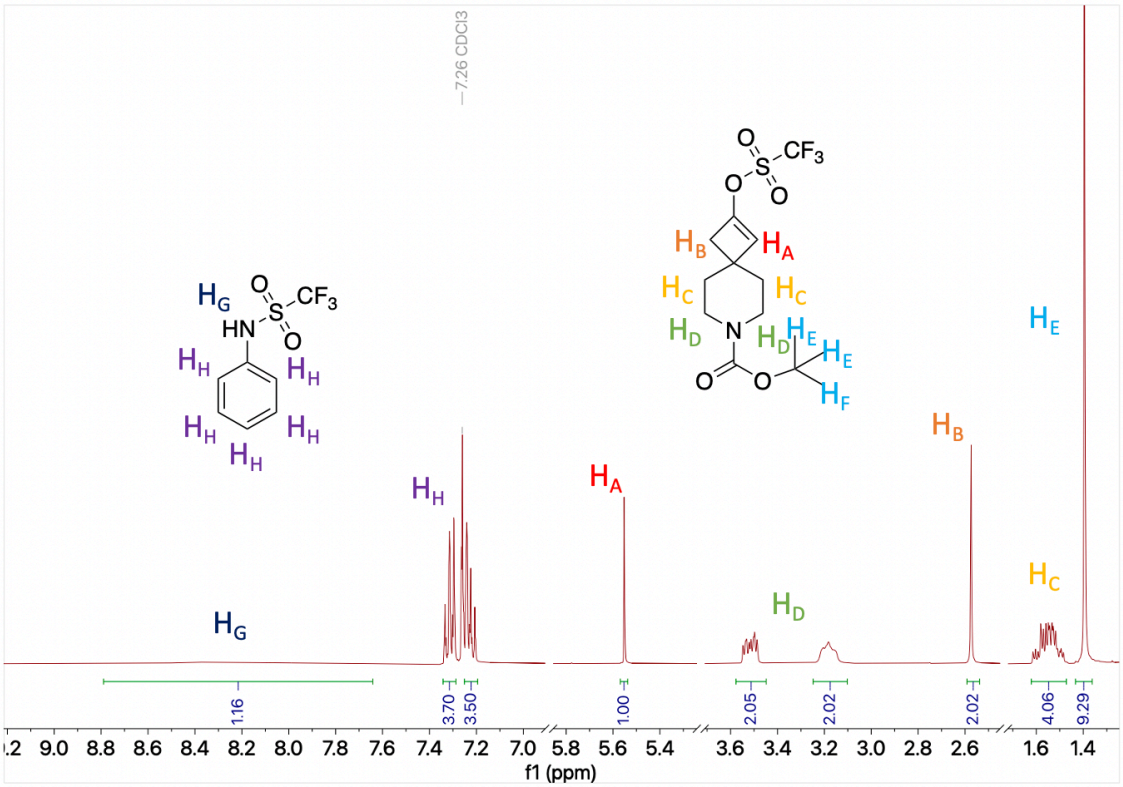

*Figure 2.7 – ^{1}H NMR spectrum of a 50:50 mixture of cyclobutyl enol triflate **31** and sulfonamide **53***

The use of triflating reagent with a different polarity could enable isolation of pure product rather than the mixture of cyclobutyl enol triflate **31** and sulfonamide **53** that was produced. Therefore, Comins' reagent **54**[77] was used as an alternative triflating reagent. Comins' reagent **54** has a similar structure to $PhNTf_2$ except that it has a 5-chloropyridin-2-yl group bonded to the nitrogen rather than a phenyl group. Cyclobutanone **30** was deprotonated using NaHMDS (1.6 eq) and then triflated with Comins' reagent **54** (1.3 eq). After purification by chromatography, pure cyclobutyl enol triflate **31** was isolated in 69% yield (Scheme 2.20).

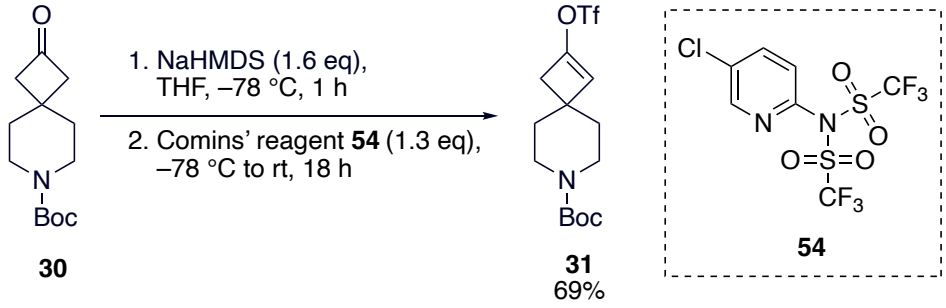

Scheme 2.20

Pleasingly, the use of Comins' reagent **54** solved the issue of isolating impure cyclobutyl enol triflate **31** and also improved the yield from 55% to 60%. Clearly, the presence of the chloropyridine functionality in Comins' reagent **54** meant that cyclobutyl enol triflate **31** had sufficient polarity difference to sulfonamide **55** (Figure 2.8), the by-product of the triflation step. With this success, Comins' reagent **54** was used in all future enol triflate forming reactions.

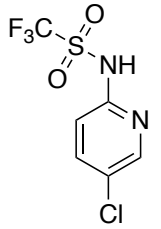

55

*Figure 2.8 – Sulfonamide **55** from Comins' reagent*

To try and improve the yield of cyclobutyl enol triflate **31** further, experimentation with the base was carried out for the enol triflate formation reaction. The results of these variations are shown in Table 2.3, with the initially obtained 69% yield of cyclobutyl enol triflate **31** using Comins' reagent **54** shown in entry 1. Rather than using NaHMDS, KHMDS was explored as an alternative base. Cyclobutanone **30** was deprotonated using KHMDS (1.6 eq) and then triflated with Comins' reagent **54** (1.3 eq). This gave cyclobutyl enol triflate **31** in 64% yield (entry 2). As changing the base to KHMDS did not improve the yield, a freshly purchased bottle of NaHMDS was explored next in a larger-scale reaction. Thus, cyclobutanone **30** (20.9 mmol) was deprotonated using NaHMDS (1.6 eq) and reacted with Comins' reagent **54** (1.3 eq) to give cyclobutyl enol triflate **31** in 83% yield (entry 3). However, in different reactions on various scales using the new bottle of NaHMDS, 71%, 69% and 52% yields of cyclobutyl enol triflate **31** were obtained. Consequently, the enol triflate reaction was reproducible in the 52-83% range.

After this work was completed, we became aware that, as discussed in Section 2.1, a patent had described the fact that cyclobutyl enol triflate **31** could be produced from cyclobutanone **30** (1.0 mmol scale) using LiHMDS (2.0 eq) and $PhNTf_2$ (1.1 eq) in THF. A 65% yield of cyclobutyl enol triflate **31** was reported after purification by chromatography.[68] As we were unaware of this literature, we did not attempt using LiHMDS as a base for this reaction. Interestingly, it was reported that cyclobutyl enol

triflate **31** could be separated from sulfonamide **53**; in our hands, this was not possible as described above.

*Table 2.3 – Base optimisation for cyclobutyl enol triflate **31** formation*

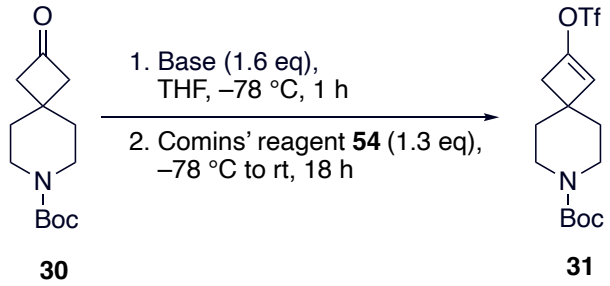

30 **31**

Entry	Scale (mmol)	Base	Yield (%)[a]
1	2.1	NaHMDS	69
2	1.0	KHMDS	64
3	20.9	NaHMDS[b]	83

a) Yield after purification by chromatography; b) Freshly purchased bottle of NaHMDS.

With cyclobutyl enol triflate **31** in hand, the next step was to carry out a Miyaura borylation to access cyclobutyl vinyl Bpin **34**. Conditions developed by Miyaura *et al.*[78] were used to carry out the Miyaura borylation. Initially, on a 0.4 mmol scale, cyclobutyl enol triflate **31** was reacted with $PdCl_2$(dppf) (6 mol%), dppf (6 mol%), KOAc (3.0 eq) and B_2pin_2 (1.2 eq) in dioxane at 80 °C for 16 h to synthesise cyclobutyl vinyl Bpin **34**. Suspecting that vinyl Bpin **34** could be unstable to silica, a polar eluent system was used in the chromatography. After purification by chromatography, a 44% yield of pure cyclobutyl vinyl Bpin **34** was obtained (Scheme 2.21), with the low yield suggesting that there had potentially been some decomposition on the column.

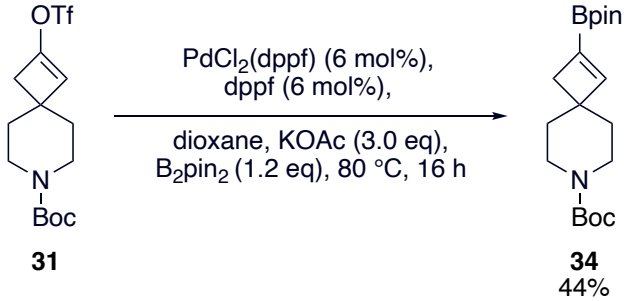

31 **34** 44%

Scheme 2.21

The next step was to convert cyclobutyl vinyl Bpin **34** into cyclobutyl Bpin **32** using a hydrogenation reaction. Some examples of hydrogenations of cyclic vinyl Bpins were reported by Knochel *et al*.[79] For example, cyclopentyl, cyclohexyl and cycloheptyl vinyl Bpins **56** were all hydrogenated using Pd/C and H_2 in MeOH at 25 °C for 1 h. Near-quantitative yields of alkyl Bpin products *cis*-**57** were achieved for all of the vinyl Bpin ring systems (Scheme 2.22).

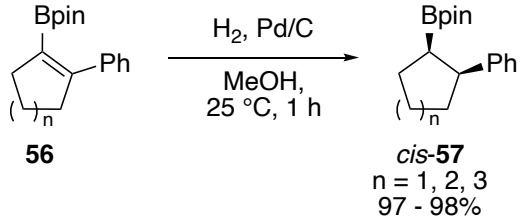

Scheme 2.22

With Knochel's precedent for successful hydrogenations of cyclic vinyl Bpins **56**, hydrogenation of cyclobutyl vinyl Bpin **34** to produce cyclobutyl Bpin **32** was attempted. To start, cyclobutyl vinyl Bpin **34** (0.12 mmol scale) was reacted with 10% Pd/C (2 mol% [Pd]) in EtOAc under H_2 at room temperature for 16 h (Scheme 2.23). The hydrogenation did not go to completion and therefore an attempt at purification by chromatography was carried out. Unfortunately, cyclobutyl vinyl Bpin **34** and cyclobutyl Bpin **32** were found to be inseparable by column chromatography and a 90:10 mixture (by ^{1}H NMR spectroscopy) of cyclobutyl Bpin **32** and cyclobutyl vinyl Bpin **34** was isolated. From this mixture, a 54% yield of cyclobutyl Bpin **32** was calculated.

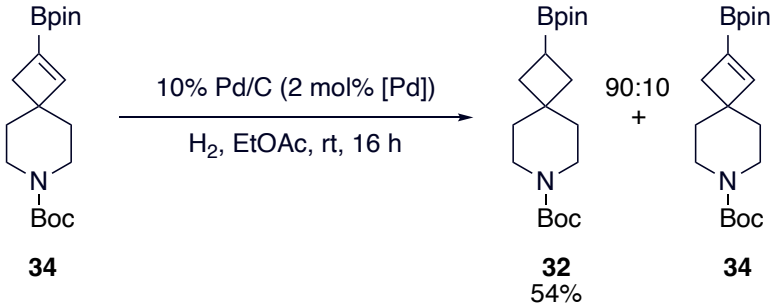

Scheme 2.23

As highlighted previously, isolating cyclobutyl vinyl Bpin **34** was challenging due to its instability to chromatography. Moreover, we were unable to separate cyclobutyl vinyl Bpin **34** from cyclobutyl Bpin **32** due to their similar polarities. Therefore, it was decided to explore a three-step route from cyclobutyl enol triflate **31** all the way through to the cyclobutyl trifluoroborate salt **25** without purifying the cyclobutyl Bpin intermediates (Scheme 2.24).

As a first attempt, starting from cyclobutyl enol triflate **31** (1.6 mmol scale), Miyaura borylation was carried out using $PdCl_2$(dppf) (6 mol%), dppf (6 mol%), KOAc (3.0 eq) and B_2pin_2 (1.2 eq) in dioxane at 80 ℃ for 16 h to give cyclobutyl vinyl Bpin **34**. After work-up, ^{1}H NMR spectroscopy indicated that a significant amount of the expected cyclobutyl vinyl Bpin **34** was generated. Since essentially no cyclobutyl enol triflate **31** was observed in the ^{1}H NMR spectrum of the crude product, the crude cyclobutyl vinyl Bpin **34** was carried through to the next stage in the synthesis. Thus, cyclobutyl vinyl Bpin **34** was hydrogenated using 10% Pd/C (2 mol% [Pd]) in EtOAc under H_2 at room temperature for 16 h. It was essential that the hydrogenation step would go to completion before transitioning to the next step. This is because if the hydrogenation had not gone to completion, in the final stage of the synthesis an inseparable mixture of cyclobutyl trifluoroborate salt **25** and cyclobutyl vinyl trifluoroborate salt would be made. On the 1.6 mmol scale, a couple of subjections of hydrogenations were needed for cyclobutyl vinyl Bpin **34** to be fully hydrogenated. Once there was no cyclobutyl vinyl Bpin **34** remaining in the ^{1}H NMR spectrum of the crude hydrogenation material, cyclobutyl Bpin **32** was taken onto the next stage of the synthesis. The final stage was a trifluoroborate salt formation using saturated $KHF_{2\,(aq)}$ (5.0 eq) and MeOH at room temperature for 16 h as previously described. The cyclobutyl trifluoroborate salt **25** was purified by dissolving it in hot acetone to remove any remaining KHF_2. The filtrate was then evaporated and stirred in Et_2O to remove any organic impurities. This approach proved to be very effective and cyclobutyl trifluoroborate salt **25** was isolated in 82% yield over the three steps, with no chromatography necessary (Scheme 2.24).

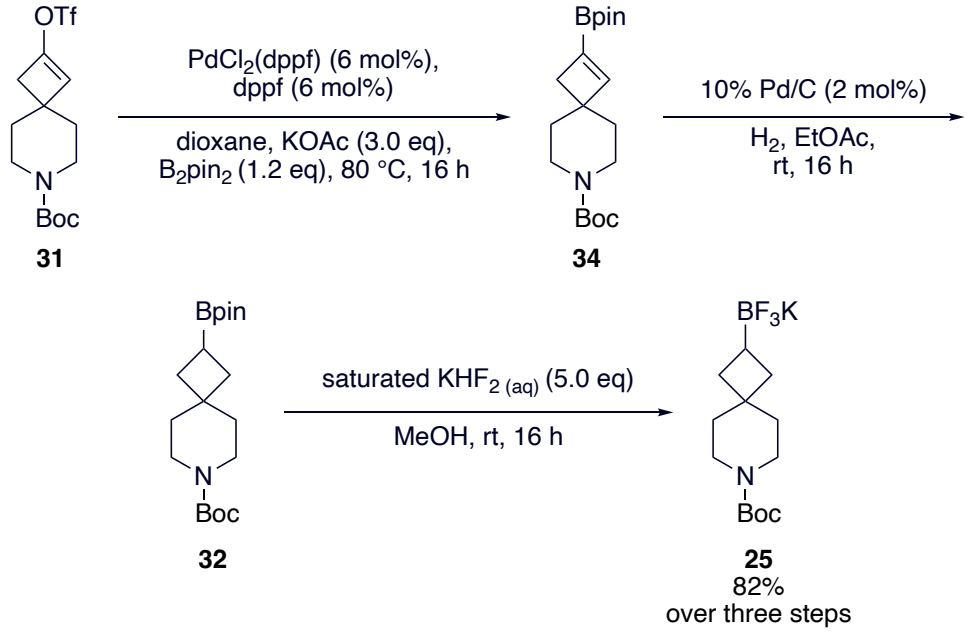

Scheme 2.24

We suspected that impurities from the Miyaura borylation step were potentially inhibiting the hydrogenation stage. Thus, when repeating the three-step synthesis of cyclobutyl trifluoroborate salt **25** on a 2.2 mmol scale of cyclobutyl enol triflate **31**, we carried out a careful filtration through a plug of Celite® before the hydrogenation step. In support of our hypothesis, this improved the hydrogenation step as only one subjection was needed. In this case, over the three steps, a 73% yield of cyclobutyl trifluoroborate salt **25** was obtained. However, this was not always the case when the three-step was repeated to bring through more material. Despite careful filtration through a plug of Celite® before the hydrogenation, sometimes multiple hydrogenations were still needed to fully hydrogenate cyclobutyl vinyl Bpin **34**.

Our optimised four-step synthesis of cyclobutyl trifluoroborate salt **25** from cyclobutanone **30** *via* cyclobutyl enol triflate **31** proceeded in a high overall yield of 68% (Scheme 2.25). This was a significant improvement compared to the route *via* cyclobutene **29** where the overall yield was 39% (see Scheme 2.17). In addition, the route *via* cyclobutyl enol triflate **31** was much less time consuming to perform than the route *via* cyclobutene **29**. This was due to the reduced number of steps and chromatographic purifications for the route *via* cyclobutyl enol triflate **31**. There were four steps to obtain cyclobutyl trifluoroborate salt **25** *via* enol triflate **31** and five steps *via* cyclobutene **29**. Only one purification by chromatography was needed for the route *via* cyclobutyl enol

triflate **31** compared to three with the route *via* cyclobutene **29**, although it should be highlighted that carrying through crude products was not explored in that route. Another benefit of the route *via* cyclobutyl enol triflate **31** is that none of the cyclobutyl piperidine intermediates are volatile, minimising any potential losses due to evaporation. In contrast, a key intermediate in the five-step route, cyclobutene **29**, is relatively volatile and challenging to work with. However, there were issues with multiple hydrogenation steps sometimes being needed for the conversion of cyclobutyl vinyl Bpin **34** to cyclobutyl Bpin **32** to go to completion in the route *via* cyclobutyl enol triflate **31**. Overall, although both routes are clearly viable, the route *via* cyclobutyl enol triflate **31** proved to be the more efficient and higher yielding route and therefore the most effective route for synthesising cyclobutyl trifluoroborate salt **25**.

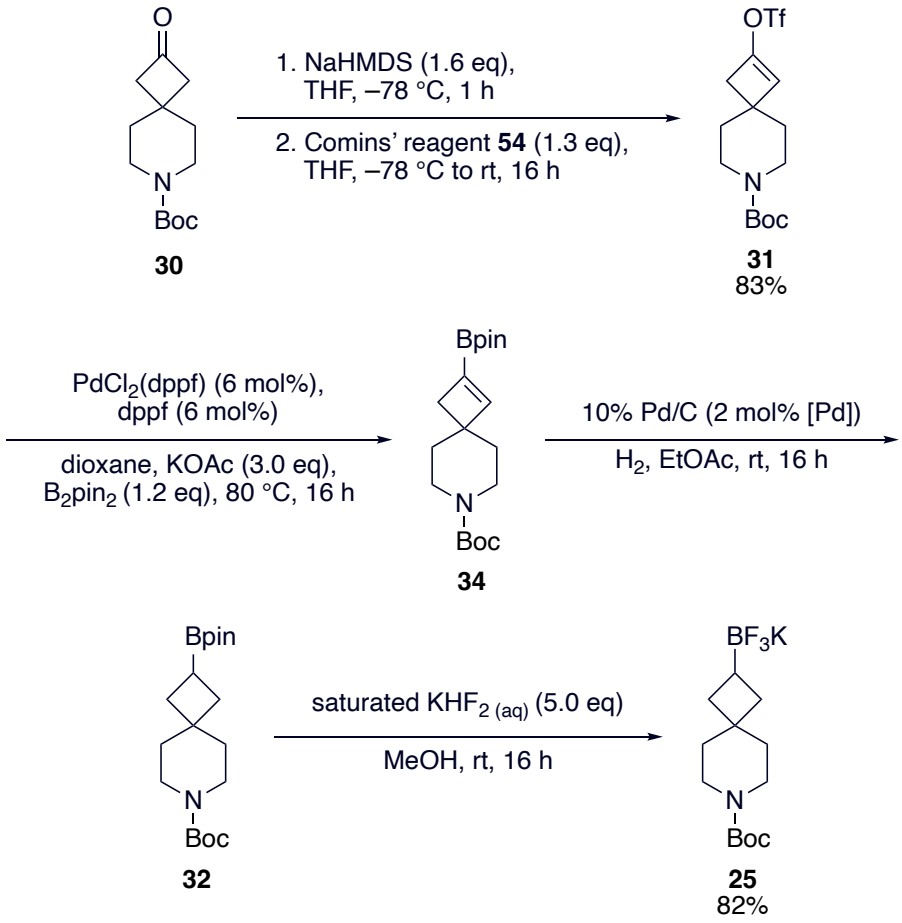

Scheme 2.25

3. Arylation of Spirocyclobutane Building Block Using Ni-catalysed and Pd-catalysed Cross-Coupling

In this Chapter, methodology for the arylation of cyclobutyl trifluoroborate salt **25** is explored. First, the literature background for Ni-catalysed photoredox cross-coupling and Suzuki-Miyaura cross-coupling (SMCC) of cyclobutyl compounds with aryl halides is presented (Section 3.1). Section 3.1.1 focuses on the relevant Ni-catalysed photoredox cross-coupling of cyclobutane systems whereas Section 3.1.2 summarises the key background on Pd-catalysed SMCC with cyclobutyl boronates. Our own efforts on utilising the Ni-catalysed photoredox cross-coupling of cyclobutyl trifluoroborate salt **25** to produce aryl cyclobutanes **27**, including model studies with cyclohexyl trifluoroborate salt and *N*-Boc piperidinyl trifluoroborate salt, are described in Section 3.2 (Scheme 3.1). The Pd-catalysed SMCC of cyclobutyl trifluoroborate salt **25** to produce aryl cyclobutanes **27** is presented in Section 3.3 (Scheme 3.1).

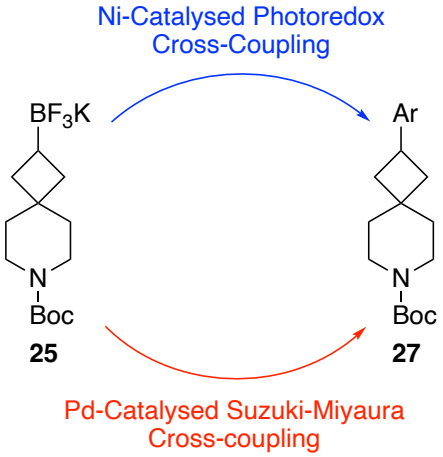

Scheme 3.1

3.1 Arylation of Cyclobutanes Using Cross-Coupling

3.1.1 Ni-Catalysed Photoredox Cross-Coupling of Cyclobutane Derivatives

A suitable method for Csp^2-Csp^3 cross-coupling is photoredox Ni-catalysed cross-coupling. Molander *et al.*[80] pioneered the Ni-catalysed photoredox cross-coupling reaction of alkyl trifluoroborate salts and aryl bromides. Light is used to excite a photocatalyst which provides all the energy needed for the reaction to take place; no heating is necessary. In this reaction, alkyl trifluoroborate salts **58** (1.5 eq) were cross-coupled with aryl bromides (1.0 eq) using $NiCl_2$-dme (5 mol%), dtbbpy (5 mol%), Ir[dFCF_3ppy]$_2$(bpy)PF_6 **59** (2.5 mol%) and Cs_2CO_3 (1.5 eq) in dioxane irradiated by a 26 W CFL lamp at room temperature for 24 h. A variety of cyclic trifluoroborate salts **58** were cross-coupled with different aryl bromides (including heteroaromatics) to give aryl products **60** in high yields (Scheme 3.2).

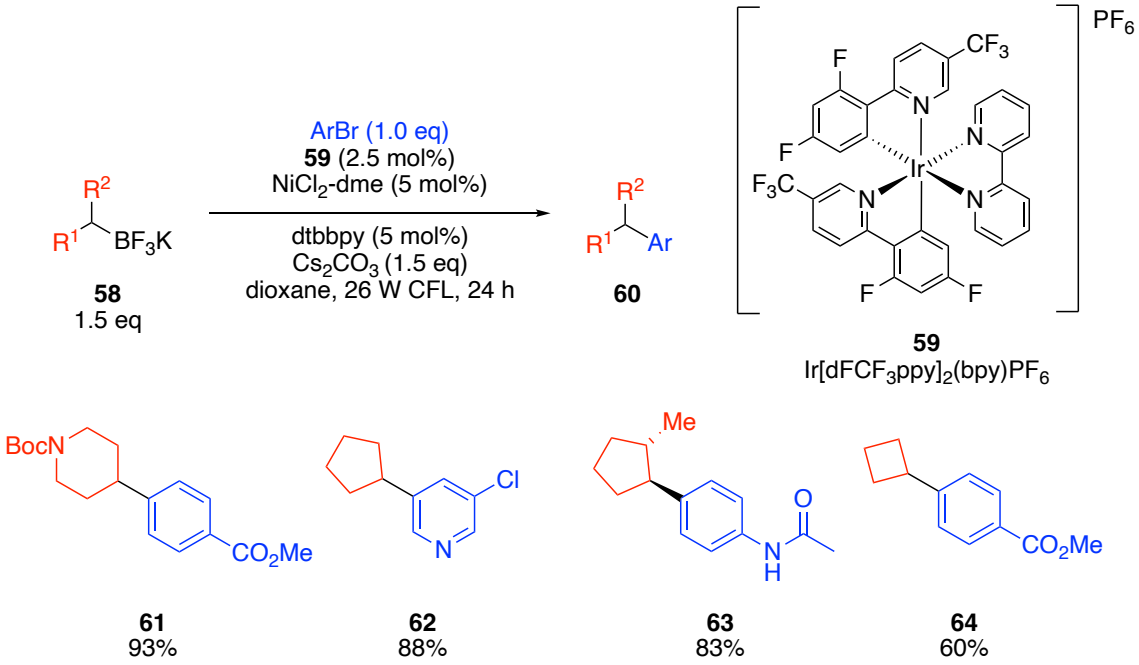

Scheme 3.2

High yields (83-93%) were achieved using *N*-Boc piperidine- and cyclopentane-containing trifluoroborate salts to give aryl products **61**, **62** and **63**.[80] However, when moving on to smaller ring systems such as a cyclobutyl trifluoroborate salt, aryl cyclobutane **64** was obtained in only 60% yield. The reaction was unsuccessful with cyclopropyl trifluoroborate salt. It was hypothesised that this trend was due to the greater s-character present in 3- and 4-membered rings, leading to destabilisation of the radical

that would form. The cross-coupling was successful with a variety of aryl bromides including electron poor and electron rich aryl bromides. Moreover, the cross-coupling with an acetanilide FragLite[20] and heteroaromatic 3-bromo-5-chloropyridine with cyclopentyl trifluoroborate salt gave aryl products **63** and **62** in good yields. Finally, one example on a gram scale was demonstrated using a ~125 mL long thin-walled vacuum flask to enable sufficient light for irradiation and reduced catalyst loading.

The catalytic cycle for Molander's photoredox cross-coupling reaction is shown in Scheme 3.3. Visible light is used to excite Ir^{III} photocatalyst **A** which generates photoexcited $*Ir^{III}$ catalyst **B**. This photoexcited catalyst oxidises trifluoroborate salt **58** to an alkyl radical **C** using single-electron transfer, reducing $*Ir^{III}$ catalyst **B** to Ir^{II} **D**. Alkyl radical **C** binds to ligated Ni^0 complex **E** to form alkyl-Ni complex **F** which undergoes oxidative addition with the aryl bromide to form aryl-Ni complex **G**. Subsequent reductive elimination releases aryl product **60** and Ni^I complex **H**. A single-electron transfer between Ni^I complex **H** and Ir^{II} complex **D** thus regenerates the two catalysts and the dual catalytic cycles repeat.

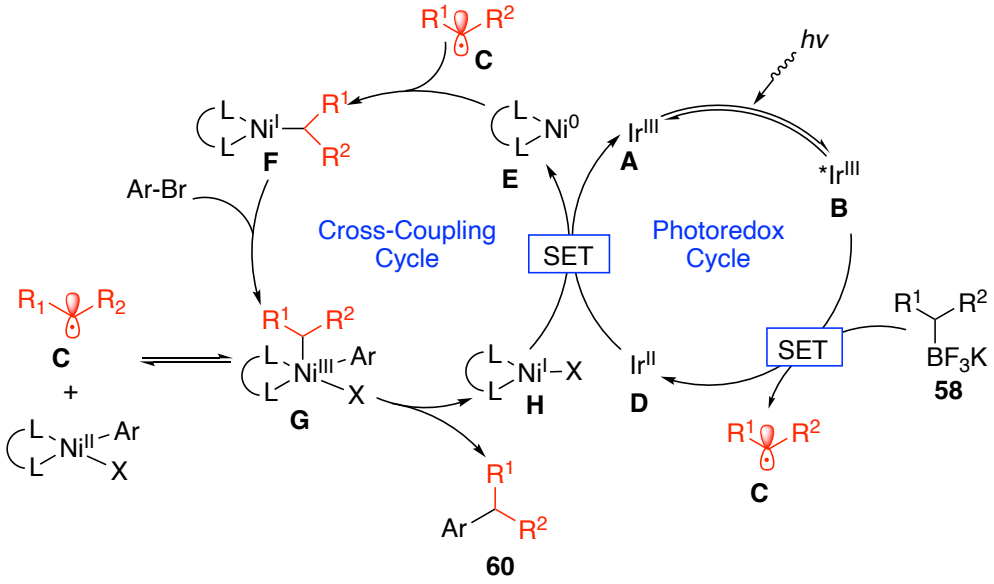

Scheme 3.3

In subsequent work, Molander *et al.*[81] cross-coupled cyclobutyl trifluoroborate salt **65** with 2-(4-bromophenyl)-1,1,1-trifluoro-3-(trimethylsilyl)propan-2-ol to give aryl cyclobutene **66** in 70% yield (Scheme 3.4). The Ni-catalysed photoredox cross-coupling conditions used were: cyclobutyl trifluoroborate salt **65** (1.5 eq), aryl bromide (1.0 eq), KF (1.5 eq), $[Ni(dtbbpy)(H_2O)_4]Cl_2$ (5 mol%) and $[Ir[dF(CF_3)ppy]_2(bpy)]PF_6$ (2.5 mol%)

in THF (0.05 M) using blue LEDs to excite the photocatalyst at room temperature for 18 h. KF was reported as an effective additive to increase yields, despite doubts that this would not be compatible due to its high affinity for silicon.

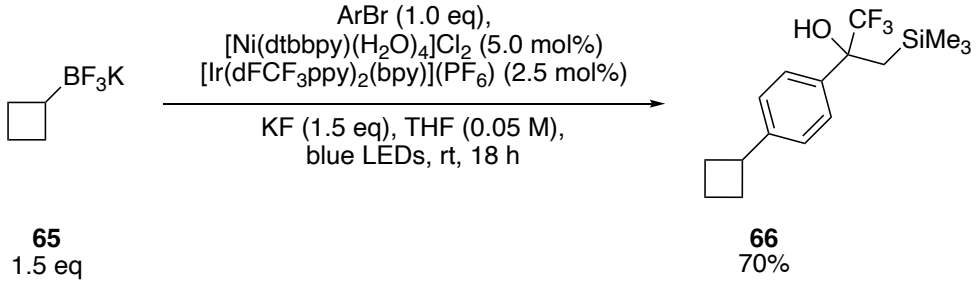

65
1.5 eq

66
70%

Scheme 3.4

Hall *et al.*[82] cross-coupled enantioenriched β-trifluoroborate cyclobutylcarboxyester *cis*-**67** (99% ee) with a variety of aryl bromides using photoredox cross-coupling conditions. Due to the intermediate planar radical that is formed, arylation occurred *trans* to the sterically bulky ester group to give aryl cyclobutanes *trans*-**68** in >20:1 dr (Scheme 3.5). In this way, the carboxy ester substituent acted as a chirality relay group. Hall *et al.*[82] used the conditions developed by Molander,[80] namely $[Ni(dtbbpy)(H_2O)_4]Cl_2$ (5.0 mol%), $[Ir(dFCF_3ppy)_2(bpy)]PF_6$ (7.5 mol%), β-trifluoroborate cyclobutylcarboxyester *cis*-**67** (1.5 eq), aryl bromide (1.0 eq) and Cs_2CO_3 (1.7 eq) in dioxane at room temperature for 24 h irradiated by a 40 W kessil lamp. A variety of aryl bromides were cross-coupled under these conditions, a few of which are depicted in Scheme 3.5. For example, nitrogen-containing pyridines and FragLite[20] pyrimidine were cross-coupled to give pyrimidine and pyridine cyclobutanes in moderate to excellent yields and high % ee. Nitrogen-containing heterocycles can be challenging to cross-couple in metal-catalysed reactions due to their affinity for metal centres,[83] so it is noteworthy that pyridine and pyrimidine aryl bromides were cross-coupled in good yields in this reaction. Cross-coupling with aryl bromides that had a *para*-substituted electron-donating methoxy group and an electron-withdrawing nitro group to β-trifluoroborate cyclobutylcarboxyester *cis*-**67** were less successful.

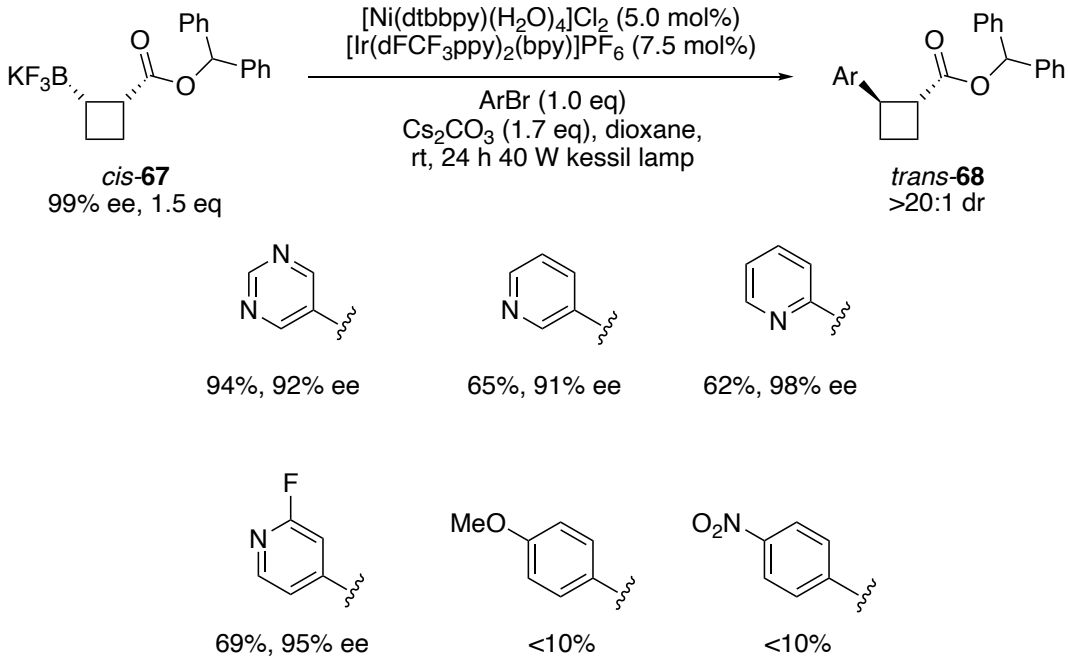

Scheme 3.5

Fused cyclobutyl trifluoroborate salt *cis*-**69** was successfully cross-coupled using Molander's method to give tetra-substituted aryl cyclobutane *cis*-**70**, as reported by Yoon *et al.*[84] Thus, cyclobutyl trifluoroborate salt *cis*-**69** (1.5 eq) was reacted with 1-bromo-4-(trifluoromethyl)benzene (1.0 eq) in the presence of $NiCl_2$-dme (10 mol%), $[Ir[dF(CF_3)ppy]_2(bpy)]PF_6$ (2.5 mol%) and Cs_2CO_3 (1.5 eq) in dioxane (3.5 mL) irradiated by blue light (LED) for 42 h to give aryl cyclobutane *cis*-**70** in 77% yield (Scheme 3.6). The diastereoselectivity presumably arose from the planar radical intermediate reacting on the less sterically hindered *exo*-face of the fused bicyclic system. It was stated that the reaction performed poorly at temperatures above ambient, highlighting the importance of maintaining a consistent ambient temperature using a fan during photoredox cross-coupling reactions.

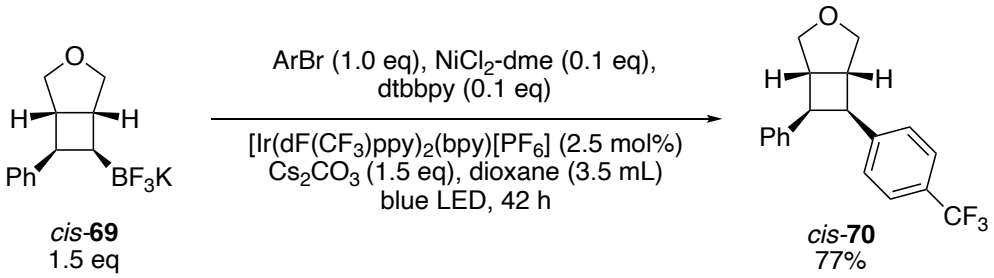

Scheme 3.6

One limitation of Ni-catalysed photoredox cross-coupling reactions is that, for small scale reactions, weighing out of the small amounts of catalyst and other reagents can be time

consuming. Jolit *et al*.[85] from Abbvie developed a solution to this problem by making tablets with the required mass of catalysts and reagents for photoredox cross-coupling which can be added to the reaction, without the need for weighing anything out. Using conditions developed by Molander *et al*.,[80] $[Ir[dF(CF_3)ppy]_2(dtbbpy)]PF_6$ (2.5 mol%), $NiCl_2$(dtbbpy) (5 mol%) and Cs_2CO_3 (1.5 eq) were premixed and compressed to form tablets. Ac-Di-Sol® (15 wt%), an internally cross-linked sodium carboxymethyl cellulose that assists dissolution, was also added in this tablet. Ac-Di-Sol® reduced the time taken for the tablet to disintegrate in the solvent, with no effect on the yield. This avoided the use of stock solutions or spending excess time weighing out reagents. The trifluoroborate salt (1.5 eq), aryl bromide (1.0 eq) and the tablet were dissolved in dioxane and irradiated with blue light (LED) for 18 h. The reaction was carried out on several different trifluoroborate salt substrates. For example, cyclobutyl trifluoroborate salt **71** was cross-coupled with methyl 4-bromobenzoate to produce aryl cyclobutane **72** in 56% yield (Scheme 3.7).

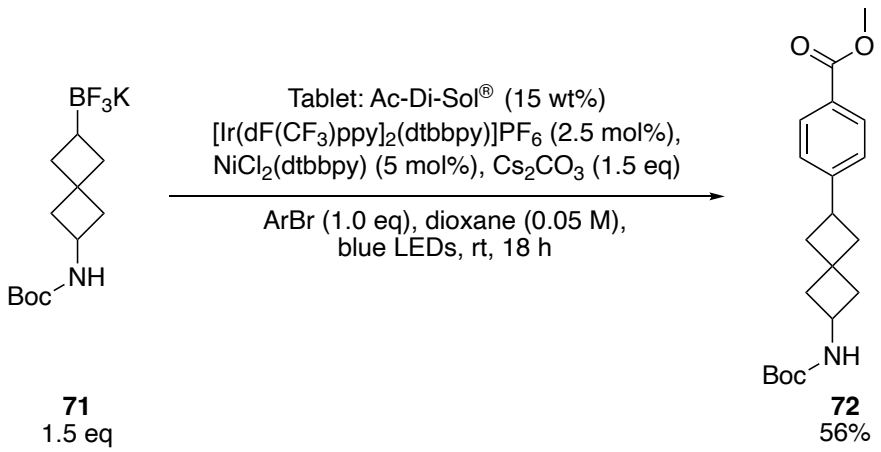

71
1.5 eq

72
56%

Scheme 3.7

Another limitation of Molander's Ni-catalysed photoredox cross-coupling reaction is that scale-up is difficult due to the large surface area-to-volume ratio needed for the efficient penetration of light essential for the reaction to take place. Boyd *et al*.[86] addressed this difficulty by using continuous flow equipment to enable scale-up. The reaction mixture was continuously pumped through tubing, which was irradiated with light, allowing for more efficient irradiation due to the larger surface area-to-volume ratio of the flow reactor compared to the traditional reaction vessel. As Cs_2CO_3 is not fully soluble in dioxane, this base was replaced with 2,6-lutidine in a 1:4 solvent mixture of DMA-dioxane to create a homogenous solution, essential for carrying out this reaction in flow. For these reactions, cyclobutyl trifluoroborate salt **65** (1.5 eq), $NiCl_2$-dme/dtbbpy (12 mol%),

[Ir(dFCF$_3$ppy)$_2$(bpy)]PF$_6$ (3 mol%), aryl bromide (1.0 eq) and 2,6-lutidine (1.6 eq) in a solvent mixture of 1:4 DMA-dioxane at room temperature for 40 min irradiated by a 450 nm LED were used. It was concluded that the reaction could be scaled up to gram scale as a 1.0 mmol scale reaction was carried out with 81 mg/h of aryl cyclobutane **73** collected. It may be possible to obtain gram-scale quantities with this reaction set-up but Boyd *et al.*[86] only carried out the reaction for an hour so did not actually make a gram of aryl cyclobutane **73** (Scheme 3.8).

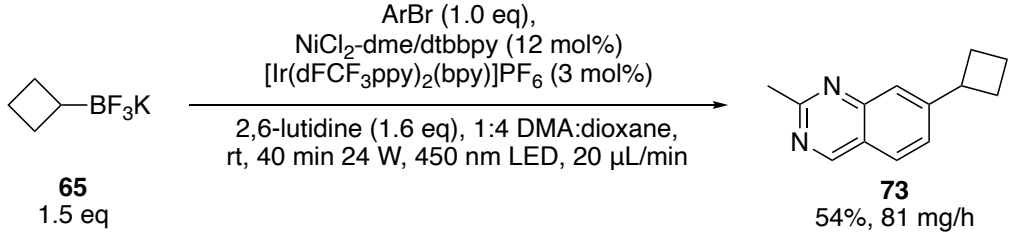

65
1.5 eq

73
54%, 81 mg/h

Scheme 3.8

In a recent 2022 paper by Speckmeier and Maier,[87] an ART (Amino Radical Transfer) reaction process was developed using Ni/photoredox dual catalysis to cross-couple alkyl Bpin compounds with aryl bromides in a scalable reaction using visible light. The reactions were carried out under air with no protective argon or nitrogen atmosphere necessary. Furthermore, dry solvents were not needed for this reaction. As the photoredox cross-coupling reaction pioneered by Molander requires exclusion of oxygen, this is an exciting alternative with a simpler set up. In the air-insensitive reaction, amino radicals add into the vacant p-orbital of boronic esters, leading to C–B bond homolytic cleavage. This then releases an alkyl radical to enter the catalytic cross-coupling cycle. Electron donating solvents were used to help enable this radical transfer. Only 2 h of irradiation was necessary for these reactions to take place and a variety of alkyl Bpin compounds and aryl bromides were successfully cross-coupled.

The conditions of the reaction are similar to Molander's but differ in a few key aspects. Specifically, alkyl Bpin (2.0 eq) was reacted with aryl bromide (1.0 eq) in the presence of [Ir(dF(CF$_3$)ppy)$_2$(dtbbpy)]PF$_6$ (1.0 mol%), NiCl$_2$-dme (5 mol%), dtbbpy (5 mol%) and morpholine (1.5 eq) in DMF irradiated by blue light at 445 nm for 2 h. The most promising results were achieved with 2.0 equivalents of alkyl Bpin, although this is quite an excess for reactions of more complex alkyl Bpin compounds. Using this new approach, Speckmeier and Maier[87] successfully cross-coupled cyclobutyl Bpin **74** with two

medicinally relevant FragLites[20] to give aryl cyclobutanes **75** and **76** in good yields (Scheme 3.9).

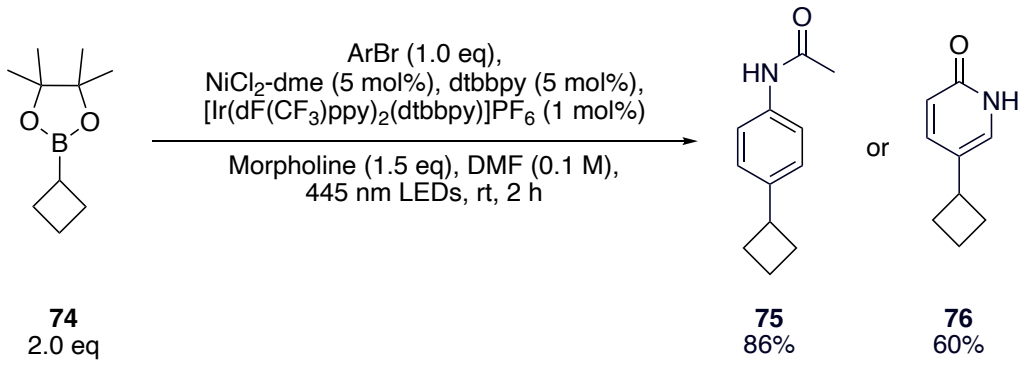

74
2.0 eq

75
86%

76
60%

Scheme 3.9

As discussed previously, it is usually quite challenging to scale up photoredox cross-coupling reactions due to the large surface area-to-volume ratio needed for optimum light penetration. Due to the low molar extinction coefficient of $[Ir(dF(CF_3)ppy)_2(dtbbpy)]PF_6$ in DMF, Speckmeier and Maier[87] were able to scale up the Ni-catalysed photoredox cross-coupling reaction with a different Bpin substrate on a 5.0 mmol scale with only a slight reduction in yield. This was possible in a round-bottomed flask with no flow equipment necessary for scaling up, a significant advantage of using these conditions.

The proposed mechanism for the ART reaction is shown in Scheme 3.10. Ir^{III} catalyst **A** is excited to its triplet state $*Ir^{III}$ catalyst **B** which oxidises the amine from morpholine to nitrogen centred radical **C**. By oxidising this amine, $*Ir^{III}$ catalyst **B** reduces to Ir^{II} **D**. After this, the amino radical transfer can begin. The amine radical interacts with the empty p-orbital of alkyl Bpin **77** to give adduct **E**. From here, homolytic cleavage of the C–B bond takes place, releasing alkyl radical **F** to enter the nickel catalytic cycle. In the cross-coupling cycle, an oxidative addition takes place between Ni^0 catalyst **G** and the aryl bromide. Intermediate **H** traps alkyl radical **F** in a second oxidative addition reaction to produce Ni^{III} complex **I**. Finally, reductive elimination takes place to release aryl product **60** and Ni^I catalyst **J**. A single-electron transfer between Ni^I catalyst **J** and Ir^{II} catalyst **D** regenerates Ir^{III} photocatalyst **A** and Ni^0 catalyst **G** so that the cycles can repeat.

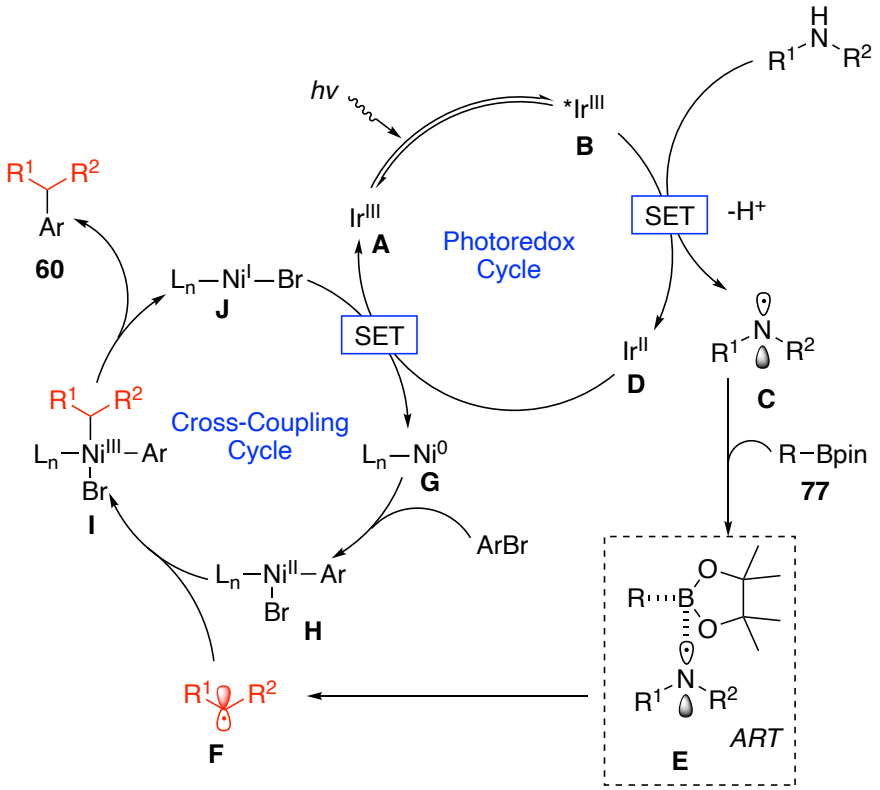

Scheme 3.10

In a different cross-coupling approach, visible-light mediated Minisci reactions were used by Wang *et al.*[88] to react alkyl boronic acids and heteroarenes using molecular oxygen as the oxidant. The Minisci reaction involves radical alkylation of heteroarenes.[89] Nitrogen-containing heterocycles were cross-coupled with primary or secondary alkyl boronic acids. Thus, heteroarene (1.0 eq) was reacted with alkyl boronic acid (3.0 eq) in the presence of $[Ir(dF(CF_3)ppy)_2(dtbbpy)]PF_6$ (1 mol%), TFA (2.0 eq) in DCE (0.1 M) under an O_2 atmosphere. The reaction was irradiated by 36 W blue light at room temperature for 24 h. For example, 4-methylquinoline **78** was reacted with cyclobutyl boronic acid **79** to give aryl cyclobutane **80** in 54% yield using these conditions (Scheme 3.11).

Scheme 3.11

The proposed reaction mechanism is shown in Scheme 3.12. Ir^{III} photocatalyst **A** is excited by visible light to produce excited state $*Ir^{III}$ catalyst **B**. A single-electron transfer from $*Ir^{III}$ catalyst **B** to oxygen forms a superoxide radical anion **C** as well as highly oxidised Ir^{IV} catalyst **D**. Superoxide radical anion **C** reacts with boronic acid **81** to form alkyl radical **E** which reacts with protonated heteroarene **F** *via* a Minisci-type reaction to produce radical cation **G**. A single-electron transfer to radical cation **G** from Ir^{IV} catalyst **D** and then deprotonation affords aryl product **82**.

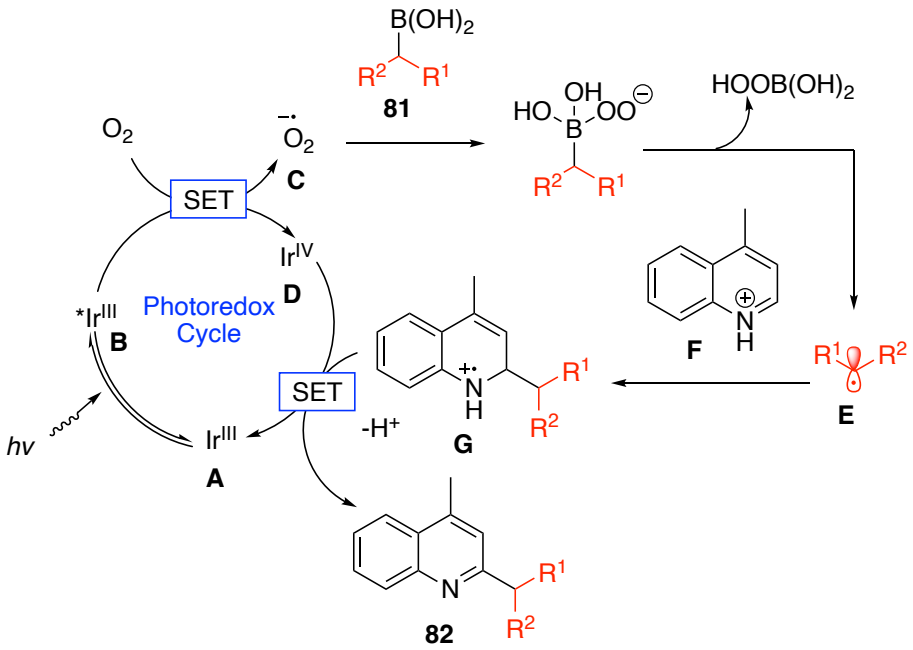

Scheme 3.12

Herrmann *et al.*[90] cross-coupled aryl halides with aliphatic *N*-(acyloxy)phthalimides as redox-active esters using Ni/photoredox catalysis. The benefit of using redox-active esters is that there is an abundance of carboxylic building block scaffold analogues which can be easily reacted to form redox-active esters, leading to a diverse set of substrates for cross-coupling. After attempts using various substituents on the 4-chloropyrimidine, an electron-withdrawing group at the 5-position and an electron-donating group at the 2-position was found to achieve the best yields in this reaction. Thus, 4-chloropyrimidine **83** (3.0 eq) was reacted with the redox active ester (1.0 eq) in the presence of Hünig's base (5.0 eq), $[Ir(dtbbpy)(ppy)_2]PF_6$ (2.5 mol%), $NiCl_2$-dme (40 mol%) and dtbbpy (50 mol%) in either DMSO or dioxane irradiated by blue light (LED, 465 nm) at room temperature for 16 h. A variety of cyclic and acyclic secondary alkanes were successfully cross-coupled using this method. For example, cyclobutane redox-active ester **84** was cross-coupled with 4-chloropyrimidine **83** to produce aryl cyclobutane **85** (Scheme 3.13). When

dioxane was used as a solvent, a higher yield (58%) was achieved in this reaction compared to DMSO (47%).

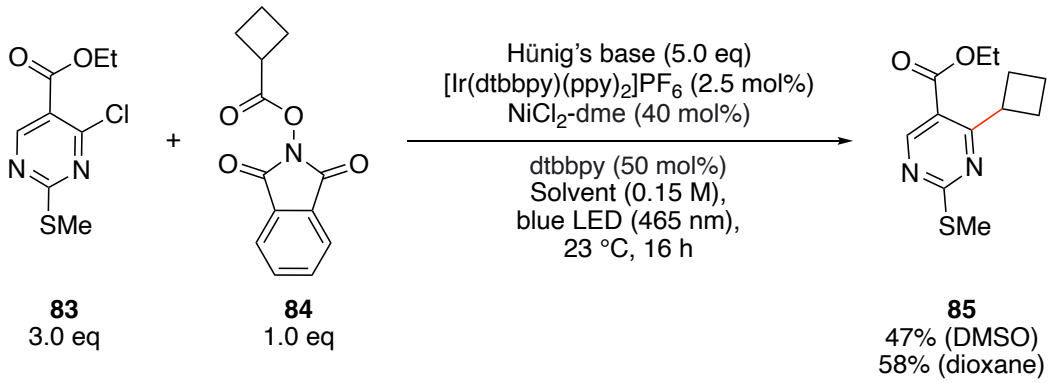

Scheme 3.13

The proposed mechanism for cross-coupling aryl halides with aliphatic *N*-(acyloxy)phthalimides is depicted in Scheme 3.14. Three interlinked catalytic cycles are shown, including the radical generation cycle, the nickel reduction cycle and the cross-coupling cycle. Firstly, in the radical generation cycle, Ir^{III} photocatalyst **A** is excited with 465 nm blue light to generate photoexcited $*Ir^{III}$ species **B**. Hünig's base **C** reduces $*Ir^{III}$ catalyst **B** to generate the radical cation **D** and Ir^{II} catalyst **E**. A single-electron transfer from Ir^{II} catalyst **E** to redox-active ester **86** takes place. This generates a carboxyl radical which decomposes into stable phthalimide through loss of carbon dioxide and generates carbon-centered radical **F**. Through this single-electron transfer, Ir^{III} catalyst **A** is regenerated to repeat the radical reduction catalytic cycle. Ni^0 catalyst **G** and heteroaryl halide **83** undergo oxidative addition in the cross-coupling cycle to create Ni^{II} complex **H**. Alkyl radical **F** and Ni^{II} complex **H** react to form Ni^{III} complex **I**. Aryl product **87** is released through reductive elimination, forming Ni^{I} complex **J** in the process. Finally, the nickel reduction cycle allows the regeneration of Ni^0 complex **G** through the single-electron transfer from Ir^{II} catalyst **E**.

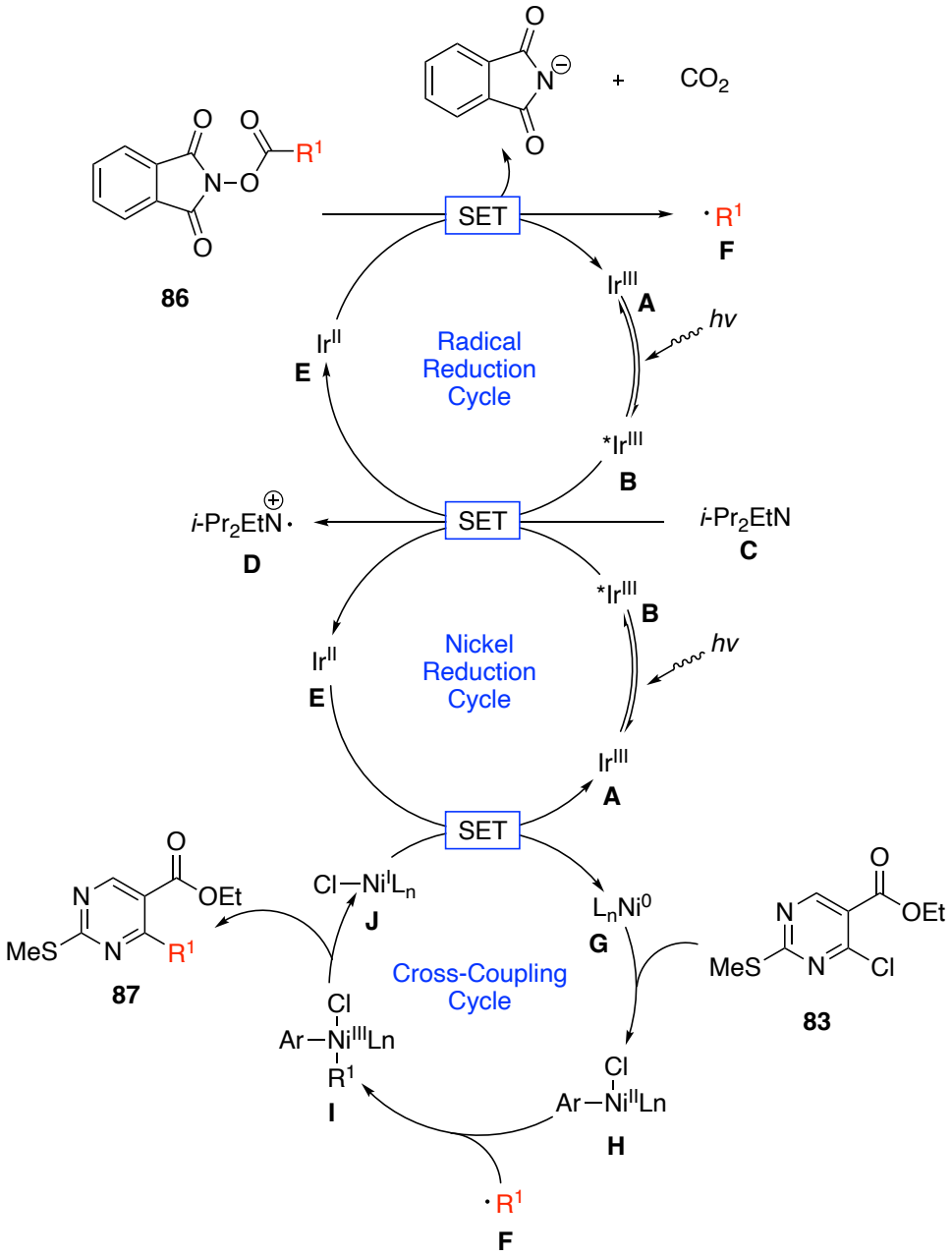

Scheme 3.14

A method for cross-coupling primary, secondary and tertiary alcohols with aryl bromides and chlorides was very recently developed by Dong and MacMillan.[91] The advantage of using alcohols in cross-coupling is they are the most versatile alkyl source with simple syntheses, allowing for more diverse scaffolds for cross-coupling. These cross-coupling reactions act *via* a deoxygenative mechanism using an *N*-heterocyclic carbene (NHC) precursor where the NHC precursor condenses with the hydroxyl group to form an NHC-alcohol adduct. Oxidation of this adduct leads to the formation of an aromatic by-product through heterolytic bond cleavage, a driving force for this reaction.

To make the NHC-alcohol adduct, a primary, secondary or tertiary alcohol **88** (1.75 eq) and NHC precursor **89** (1.6 eq) were combined in MTBE (0.13 M) and then pyridine (1.6 eq) was added. The NHC-alcohol adduct thus formed was reacted with the aryl halide (1.0 eq) in the presence of $Ir[ppy]_2(dtbbpy)PF_6$ (1.5 mol%), $NiBr_2(dtbbpy)$ (5 mol%) and quinuclidine (1.75 eq) in DMA (5.0 mL) under nitrogen. The reaction was irradiated under 450 nm LED lights for 2 h for the cross-coupling to take place. A wide variety of primary, secondary and tertiary alcohols were explored for this photoredox cross-coupling reaction. Some examples of alcohols that were cross-coupled with methyl 5-bromopyridine-2-carboxylate to produce aryl products **90** include cyclopropanol **91**, cyclobutanol **92**, azetidine alcohol **93** and two examples of spirocyclobutyl alcohols (**94** and **95**) (Scheme 3.15). When using spirocyclic azetidine alcohol **94**, a better result was obtained with a higher loading of $NiBr_2(dtbbpy)$ and the use of phthalimide as an additive.

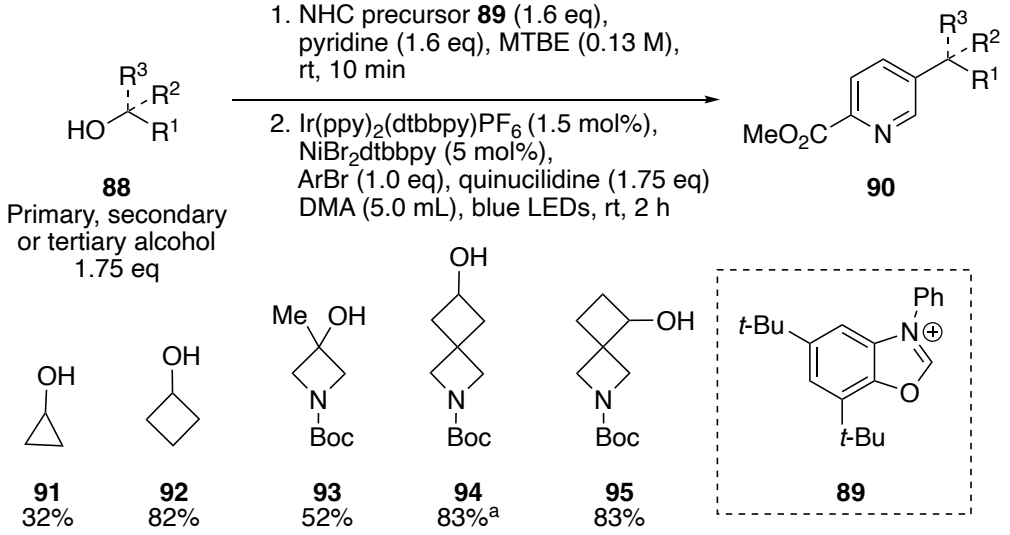

a) 7.5 mol% Ni catalyst with 22.5 mol% phthalimide.

Scheme 3.15

The mechanism proposed by Dong and MacMillan[91] for the photoredox cross-coupling of alcohols and aryl bromides using NHC precursors is shown in Scheme 3.16. Alcohol **88** condenses with NHC precursor **89** forming NHC-alcohol adduct **96**. Ir^{III} photocatalyst **A** is excited by blue light to generate excited $*Ir^{III}$ photocatalyst **B**. The excited photocatalyst oxidises the nitrogen lone pair on NHC-alcohol adduct **96** *via* a single-electron transfer mechanism, releasing Ir^{II} catalyst **C**. The oxidation of the nitrogen on the NHC-alcohol adduct **D** weakens the adjacent C–H bond allowing deprotonation of this proton using a base, in this case quinuclidine. The deprotonation produces a radical α to nitrogen to produce deprotonated NHC-alcohol adduct **E**. β-Scission then occurs to

produce a carbamate and deoxygenated radical **F**. The formation of the strong C=O bond in the carbamate is the thermodynamic driving force for this reaction. As for the cross-coupling cycle, Ni^{I} catalyst **G** is reduced to Ni^{0} catalyst **H** using a single-electron transfer with Ir^{II} photocatalyst **C**. Oxidative addition occurs with Ni^{0} catalyst **H** and the aryl bromide to form Ni^{II} species **I**. Alkyl radical **F** binds to Ni^{II} catalyst **I**, forming Ni^{III} complex **J**. Reductive elimination takes place on Ni^{III} complex **J** to release aryl product **60** and reform Ni^{I} catalyst **G** to repeat the cycle.

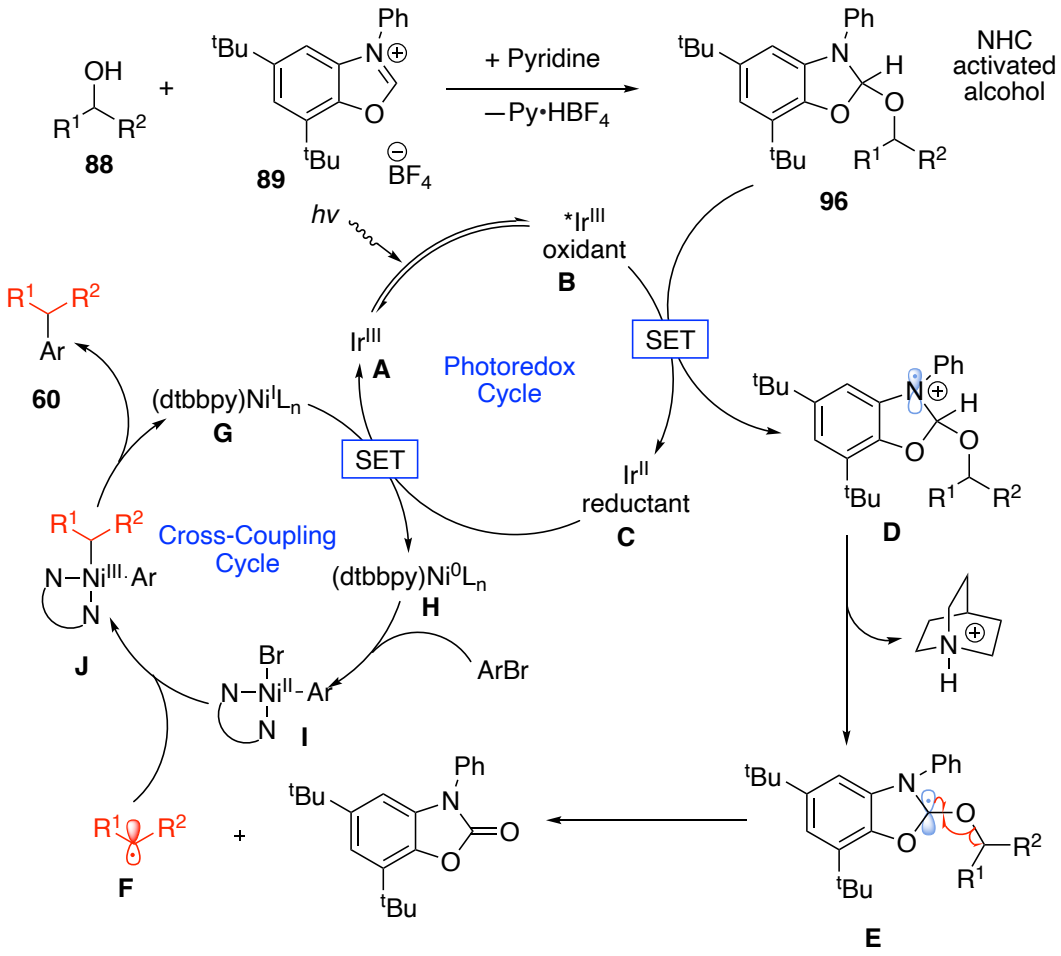

Scheme 3.16

Overall, the literature on photoredox cross-coupling of cyclobutanes is extensive and includes a variety of cyclobutyl substrates including examples where enantioenriched, spirocyclic and fused cyclobutyl rings readily partake in cross-coupling. Moreover, photoredox cross-coupling reactions from a variety of starting materials are possible including trifluoroborate salts, Bpin compounds, alcohols and redox-active esters under different conditions. Although there are some issues with scale-up, this problem has been addressed by using either a long thin-walled vacuum flask, flow photochemistry or the

ART platform. Furthermore, issues with not being able to make enantioenriched cross-coupled products have also been addressed by using chirality relay groups.

3.1.2 Pd-Catalysed Suzuki-Miyaura Cross-Coupling of Cyclobutane Boronates and Trifluoroborate Salts

Pd-catalysed Suzuki-Miyaura cross-coupling (SMCC) is a versatile and widely used method for the formation of Csp^2-Csp^2 bonds.[92,93] The SMCC reaction usually involves the cross-coupling of an organoboron reagent (*e.g.* boronic acid or pinacol boronate) and an organic halide in the presence of palladium(0) as a catalyst under basic conditions. The ligands are often electron-rich, sterically bulky phosphine ligands to allow facile oxidative addition and reductive elimination.

The general mechanism for Csp^2-Csp^2 SMCC is shown in Scheme 3.17. If a palladium(II) precatalyst is used then the activation of the precatalyst to generate palladium(0) complex **A** must occur first. Alternatively, palladium(0) complex **A** can be accessed through ligand dissociation. An oxidative addition of organic halide **97** and palladium(0) catalyst **A** occurs to produce organopalladium(II) complex **B**. Electrophiles other than organic halides can also be used such as organic triflates and tosylates. Transmetallation of the organoboron nucleophile **98** to the organopalladium(II) electrophile **B** takes place in the presence of aqueous base to produce diorganopalladium(II) complex **C** and release boronate **99**. *cis/trans* Isomerisation of the organic groups on diorganopalladium(II) complex **C** occurs. This isomerisation allows for reductive elimination to take place from the diorganopalladium(II) species **C** to release cross-coupled product **100** and regenerate palladium(0) catalyst **A**.[94,95]

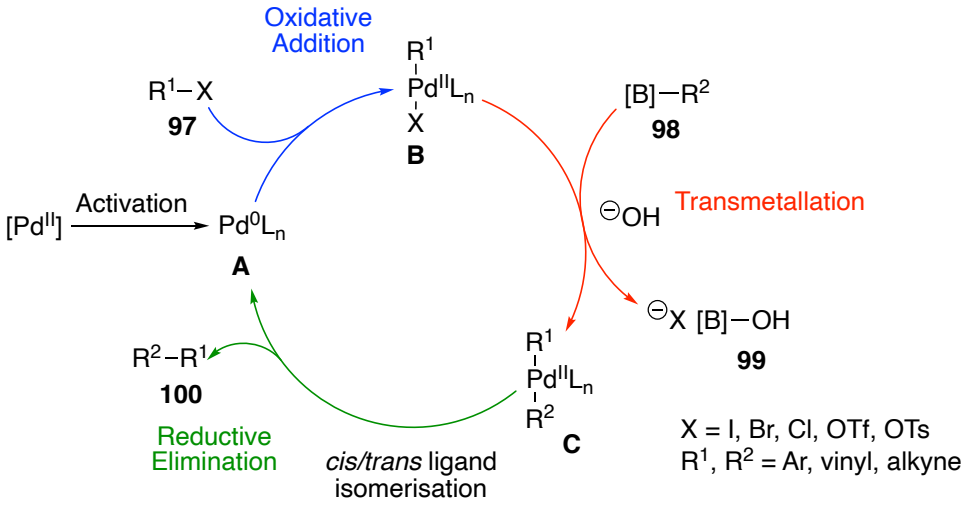

Scheme 3.17

Although the mechanisms for oxidative addition and reductive elimination are well-known, the mechanism of transmetallation is debated.[96] Two potential pathways for

transmetallation of boronic acids are presented in Scheme 3.18.[97–100] Firstly, hydroxide is generated *in situ* from an inorganic base and water. The transmetallation pathways differ in the role of hydroxide, highlighted in red.[98] The difference lies in whether the hydroxide attacks the boronic acid or the palladium. Pathway A displays what is known as the boronate pathway. In this pathway, hydroxide attacks the boronic acid to make nucleophilic four-coordinate anionic boronate **A**. The halide from palladium(II) complex **B** substitutes with boronate **A**, generating intermediate palladium(II) boronate **C** and releasing KX. Intermediate palladium(II) boronate **C** decomposes, releasing $B(OH)_3$ and transferring the organic group R^2 from the boronic acid to the palladium(II) complex, producing transmetallation palladium(II) complex **D**, thus completing the transmetallation step for pathway A. Alternatively, pathway B is known as the oxo-palladium pathway. In this pathway, the halide from palladium(II) complex **B** undergoes a substitution with the hydroxide ion to generate nucleophilic oxo-palladium(II) complex **E**. Neutral boronic acid **F** is attacked by nucleophilic oxo-palladium(II) complex **E** to generate intermediate palladium(II) boronate **C**, the same intermediate made in pathway A. Although there is debate as to which pathway is most likely to occur, kinetic studies in one system showed that pathway B is favoured.[99]

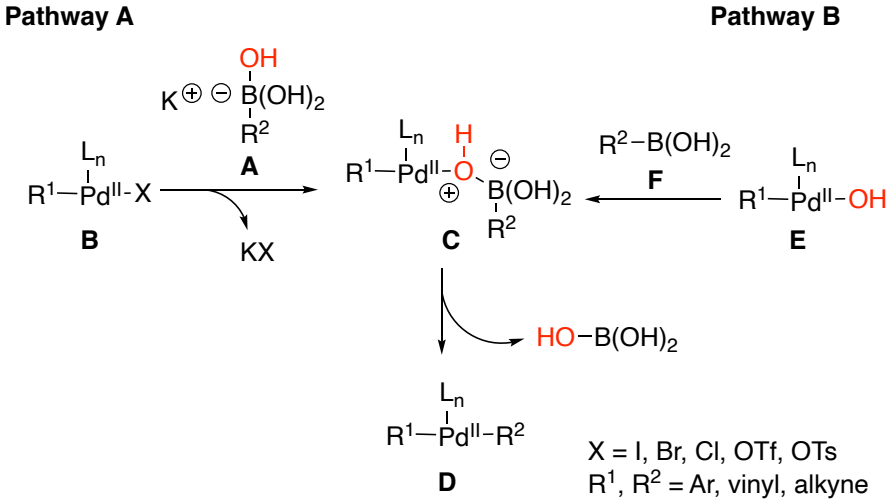

Scheme 3.18

There are fewer reports on Csp^2-Csp^3 variants for cross-coupling compared to Csp^2-Csp^2 variants. This may be due to alkyl-palladium complexes forming with the Csp^3 centres which can undergo β-hydrogen elimination rather than reductive elimination.[101] Therefore, for Csp^2-Csp^3 variants, the rate of reductive elimination must be fast in order to avoid β-hydrogen elimination side-reactions. Another issue with Csp^2-Csp^3 variants for cross-coupling is protodeboronation. Rather than unprotected boronic acids,

tetrahedral boronates such as trifluoroborate salts and MIDA boronates can be used to minimise protodeboronation. The electron-withdrawing groups that trifluoroborate salts and MIDA boronates have make the boron less nucleophilic in SMCC. Therefore, under basic conditions, the boronic acid is released slowly in solution. The slow release of boronic acid reduces the availability of boronic acid in the reaction and therefore reduces the probability of protodeboronation.[95,102–104]

There are a few previous examples of Csp^2-Csp^3 SMCC reactions of cyclobutyl trifluoroborate salts. For example, Gormisky and Molander[105] developed SMCC conditions for cyclobutyl trifluoroborate salt **65**. Cyclobutyl trifluoroborate salt **65** was cross-coupled with a variety of different aryl chlorides (Scheme 3.19). Despite being less reactive than their bromo- and iodo- analogues, aryl chlorides are less expensive and more readily available electrophiles.[105] Thus, cyclobutyl trifluoroborate salt **65** (1.01 eq) was reacted with aryl chloride (1.0 eq) in the presence of $Pd(OAc)_2$ (2 mol%), CataCXium A **101** (3 mol%) and Cs_2CO_3 (3.0 eq) in a 10:1 mixture of toluene-H_2O at 100 ℃ for 24 h. Four different aryl chlorides were successfully cross-coupled with cyclobutyl trifluoroborate salt **65** to give aryl cyclobutanes **102** in moderate to high yields (45-82%). For example, heteroaryl-containing cyclobutanes **103** and **104** were generated using these conditions. However, the SMCC conditions were not universal and three aryl chlorides gave none of the aryl products.

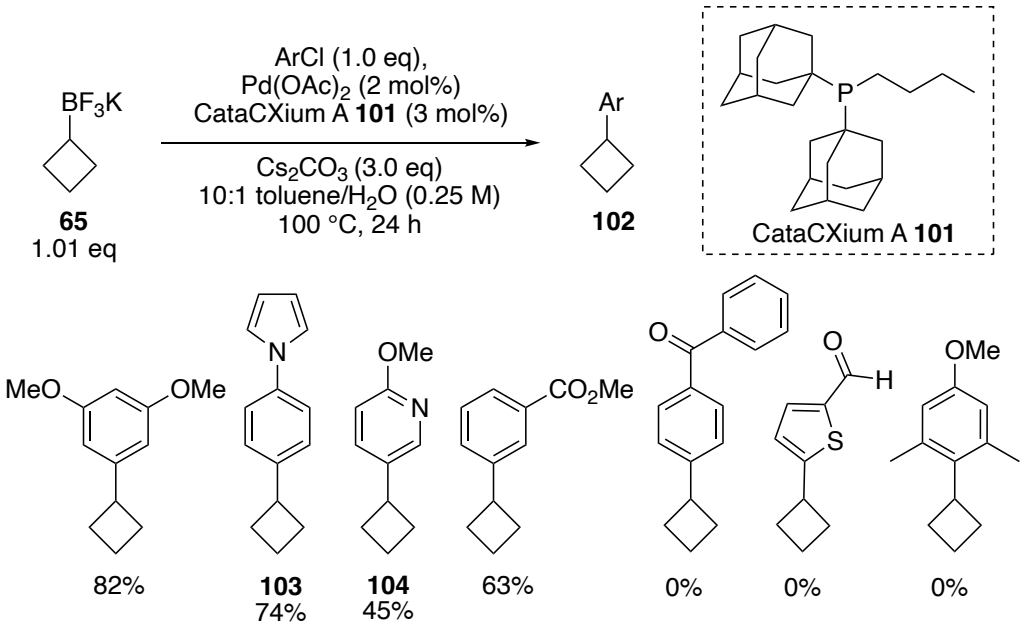

Scheme 3.19

An alternative to using $Pd(OAc)_2$ is to use a palladium precatalyst that generates the palladium(0) *in situ*. Biscoe *et al.*[106] carried out SMCC reactions with a palladium precatalyst on cyclobutyl trifluoroborate salt **65**. As an example, cyclobutyl trifluoroborate salt **65** (1.5 eq) was reacted with 1-(4-chlorophenyl)-1H-pyrrole (1.0 eq) in the presence of K_2CO_3 (3.0 eq) and P*t*-Bu_3 Pd G3 precatalyst **105** (5 mol%) in 2:1 toluene-H_2O at 100 ℃ for 24 h to produce aryl cyclobutane **103** in 86% yield (Scheme 3.20). These conditions were a slight improvement on the result from Gormisky and Molander's[105] where a 74% yield of aryl cyclobutane **103** was achieved (see Scheme 3.19).

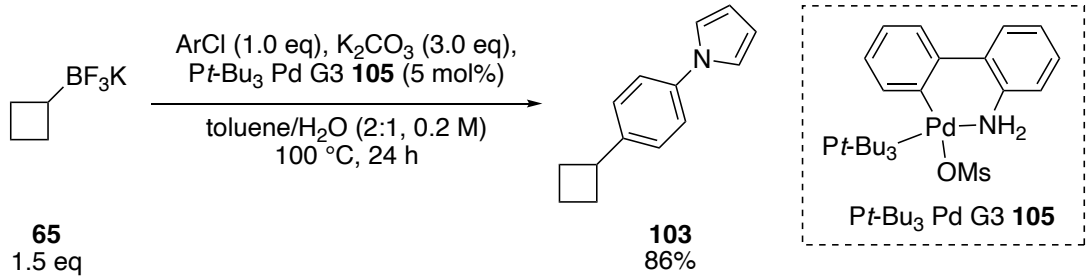

Scheme 3.20

Yu *et al.*[107] were able to successfully stereospecifically cross-couple an aryl amide cyclobutyl trifluoroborate salt *cis*-**106** with 1-chloro-4-nitrobenzene to produce aryl product *cis*-**107** (Scheme 3.21). Using conditions developed by Molander *et al.*,[108] cyclobutyl trifluoroborate salt *cis*-**106** (1.2 eq) and 1-chloro-4-nitrobenzene (1.0 eq) were reacted in the presence of $Pd(OAc)_2$ (10 mol%), SPhos **108** (20 mol%) and Cs_2CO_3 (3.0 eq) in a 67:10 mixture of CPME-H_2O under a nitrogen atmosphere at 95 ℃ for 20 h. Aryl cyclobutane *cis*-**107** was successfully obtained in 58% yield. The SMCC reaction proceeded with retention of stereochemistry and this may be due to the amide directing the transmetallation step.

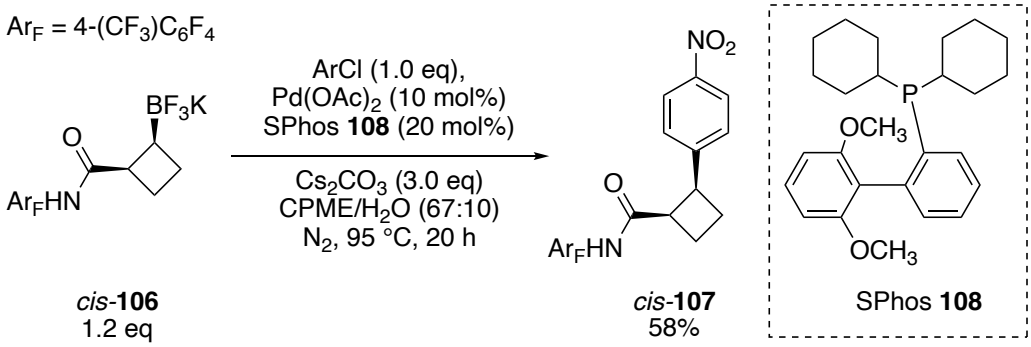

Scheme 3.21

Hall *et al.*[82] were unable to cross-couple cyclobutyl trifluoroborate salt *cis*-**67** or Bpin analogue *cis*-**109** to produce aryl cyclobutanes *cis*-**110** or *trans*-**111** using a variety of different Pd-catalysed SMCC conditions (Scheme 3.22). Six different conditions were attempted varying equivalents, use of cyclobutyl trifluoroborate salt *cis*-**67** or Bpin analogue *cis*-**109**, type and amount of palladium catalyst, type and amount of ligand, type of base, solvent system, temperature and time.[108–113] These were all conditions which had previously worked on different Csp^2-Csp^3 cross-couplings of secondary alkyl Bpin compounds or trifluoroborate salts and one example from a cyclobutyl trifluoroborate salt,[109] but none of the conditions were successful on their substrates. These results highlight the difficulty and nuances with SMCC cross-coupling of sp^3 cyclobutyl boronates.

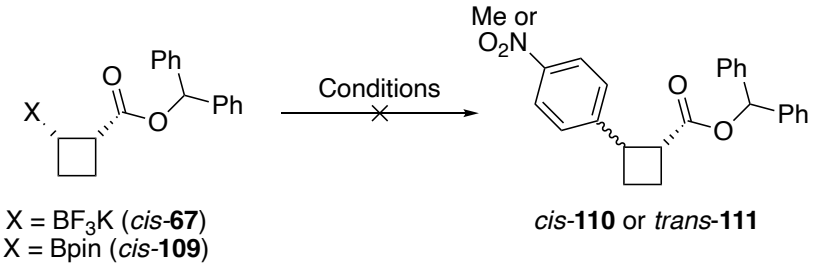

Scheme 3.22

Hall *et al.*[82] also attempted two different SMCC conditions on a morpholine amide cyclobutyl trifluroborate salt *cis*-**112**. Unfortunately, cross-coupling to produce aryl cyclobutane *cis*-**113** or *trans*-**114** was unsuccessful when using Molander's or Yu's conditions (Scheme 3.23). A major side-product **115** was observed which was believed to arise from a Buchwald-Hartwig amination of the released morpholine (due to the basic SMCC conditions) and the aryl bromide.

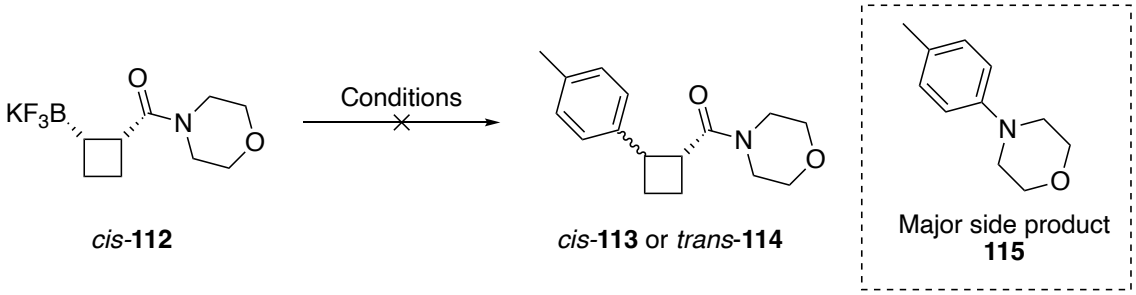

Scheme 3.23

Finally, Tortosa *et al.*[66] were able to regioselectively and stereospecifically cross-couple a variety of different aryl bromides (including electron-rich, electron-poor and heterocycles) to different diborylated spirocyclobutyl systems (Scheme 3.24). A high

catalyst loading was needed for these reactions. Thus, cyclobutyl di-Bpin *cis*-**116** (1.0 eq) and aryl bromide (1.2 eq) were reacted in the presence of $Pd(OAc)_2$ (5 mol%), RuPhos **117** (12.5 mol%) and KOH (2.0 eq) in a 10:1 mixture of THF-H_2O at 80 ℃ for 16 h. Examples of symmetric and non-symmetric *N*-Boc piperidine spirocyclobutyl di-Bpin compounds were cross-coupled as well as an *N*-Boc azetidine spirocyclobutyl di-Bpin compound. The yields ranged from 49-80%. In the cross-coupling reaction, the least sterically hindered cyclobutyl Bpin group cross-coupled with the aryl bromide to regioselectively give mono-Bpin aryl cyclobutane *cis*-**118**. Attempts to remove the more sterically hindered pinacol boronic ester which had not cross-coupled by proto-deborylation were unsuccessful. Morken *et al*.[114] found improvements in yield when cross-coupling adjacent 1,2-bis(boronates) rather than mono-borylated species. Tortosa *et al*.[66] were able to replicate results from Morken *et al*.[114] hypothesising that the boron from one boronic pinacol ester acted as a Lewis acid and accepted electron density from the adjacent pinacoloto oxygen as shown by cyclobutyl di-Bpin **119** (Scheme 3.24). Therefore, the electrophilicity of the cross-coupling boron would be increased as the electron density is pulled away from it through the Lewis basic oxygen. Consequently, the rate of transmetallation of cyclobutyl di-Bpin *cis*-**116** would increase and ultimately efficient cross-coupling would be achieved.

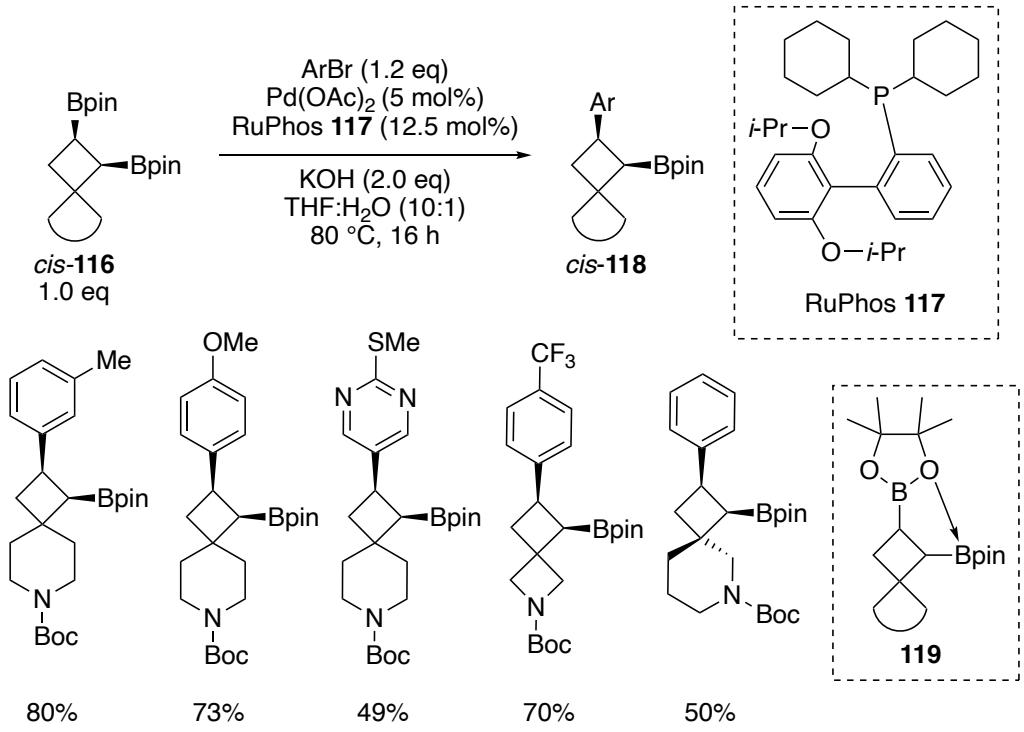

Scheme 3.24

Overall, Csp^2-Csp^3 SMCC of cyclobutyl boronates is not well precedented but there are a few examples where cross-coupling of cyclobutyl boronates has been successful. From the examples of cyclobutyl boronate SMCC reactions, only simple substrates have been cross-coupled with the more complicated examples such as those reported by Tortosa *et al*.[66] needing extra aid through Lewis acidity of the second Bpin. For cross-coupling of cyclobutyl boronates with predefined *cis*-stereochemistry, a retention of stereochemistry was seen on Tortosa's and Yu's substrates.

3.2 Ni-Catalysed Photoredox Cross-Coupling Results

3.2.1 Cross-Coupling with Cyclohexyl and Piperidinyl Trifluoroborates

The next stage of the project was to demonstrate that elaboration of cyclobutyl trifluoroborate salt **25** at the trifluoroborate functional handle could be achieved. For this, the plan was to explore the cross-coupling of cyclobutyl trifluoroborate salt **25** with different aryl bromides using Ni-catalysed photoredox cross-coupling. However, as there was limited experience of using such photoredox methodology in the O'Brien group, it was decided to carry out some preliminary work on more readily available cyclic trifluoroborate salts. Thus, following the procedure developed by Molander *et al.*,[80] photoredox cross-coupling of six-membered trifluoroborate salts **120** (cyclohexyl) and **52** (*N*-Boc piperidinyl) with aryl bromides was carried out.

To start, the cross-coupling between cyclohexyl trifluoroborate salt **120** and ethyl 4-bromobenzoate **121** was investigated using an in-house photoredox set-up. The reagents/conditions were: $[Ir(dFCF_3ppy)_2(dtbpy)]PF_6$ **122** (2.5 mol%), $NiCl_2$-dme (5 mol%), dtbbpy (5 mol%) and Cs_2CO_3 (1.5 eq) in dioxane at room temperature for 24 h with irradiation of light using a 30 W CFL. These conditions were the same as those reported by Molander *et al.*[80] (see Scheme 3.2) except that the equivalents of trifluoroborate salt and aryl bromides were varied, a 30 W bulb rather than 26 W was used and $[Ir(dFCF_3ppy)_2(dtbpy)]PF_6$ **122** (which was available in the group) was used rather than $Ir[dFCF_3ppy]_2(bpy)PF_6$ **59**.

The set-up for Ni-catalysed photoredox cross-coupling is shown in Figure 3.1. A test tube rack held three pressure vials, each containing the reaction mixture for an individual photoredox cross-coupling reaction. The lid to each vial was sealed with parafilm. The vials were secured in a test tube rack on top of a stirrer plate. A 30 W CFL lamp irradiated the vials with light from roughly 2 cm distance from the vials. Once the vials were secured in place and the stirrer plate and light turned on, a black box was placed over the top of the whole set-up. A fan was placed in a hole at the top of the box to ensure that the heat from the light did not increase the temperature too much.

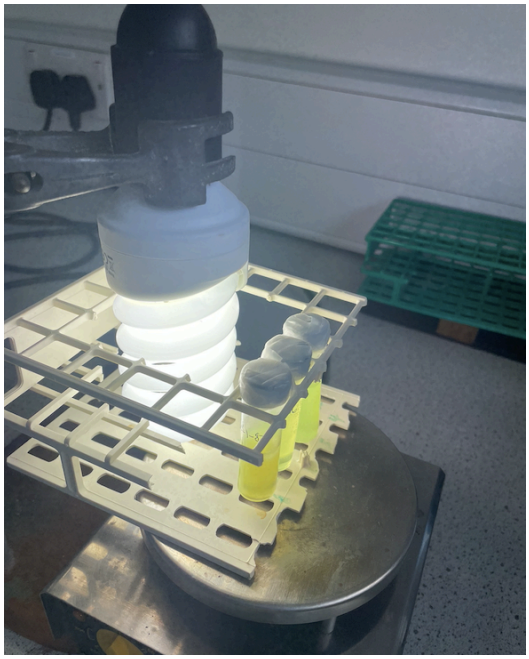


Figure 3.1 – Ni-catalysed photoredox cross-coupling set-up

The standard scale of the reactions was a 0.25 mmol scale. As a first attempt, 1.5 equivalents of cyclohexyl trifluoroborate salt **120** was reacted with 1.0 equivalent of ethyl 4-bromobenzoate **121** under the standard photoredox set-up and conditions. After chromatography, ethyl ester phenyl cyclohexane **123** was obtained in approximately 88% yield (Table 3.1, entry 1). The yield is approximate since the product co-eluted with small amounts of an unknown side-product. Nevertheless, it was particularly pleasing that we could carry out this Molander-style photoredox cross-coupling reaction in high yield.

The initially explored conditions were based on Molander's use of 1.0 equivalent of aryl bromide and 1.5 equivalents of trifluoroborate salt. This would be undesirable for eventually carrying out photoredox reactions on cyclobutyl trifluoroborate salt **25** as the precious building block would be used in excess. Thus, reactions with cyclohexyl trifluoroborate salt **120** as the limiting reagent were explored. Use of 1.0 equivalent of ethyl 4-bromobenzoate **121** and 1.0 equivalent of cyclohexyl trifluoroborate salt **120** gave a 68% yield of ethyl ester phenyl cyclohexane **123** (entry 2). Similarly, when using 1.5 equivalents of ethyl 4-bromobenzoate **121** and 1.0 equivalent of cyclohexyl trifluoroborate salt **120**, a 66% yield of ethyl ester phenyl cyclohexane **123** was obtained (entry 3). Unfortunately, ethyl ester phenyl cyclohexane **123** could not be separated from unreacted ethyl 4-bromobenzoate **121** in these cases. However, it was possible to

calculate the yield of ethyl ester phenyl cyclohexane **123** using the ^{1}H NMR spectrum of the mixture after chromatography.

*Table 3.1 – Ni-catalysed photoredox cross-coupling using different equivalents of cyclohexyl trifluoroborate salt **120** and 4-ethyl bromobenzoate **121***

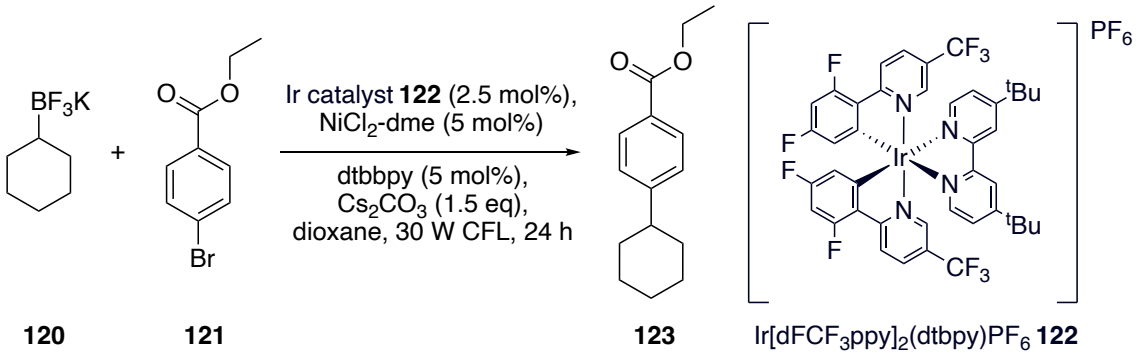

120 **121** **123** Ir[dFCF$_3$ppy]$_2$(dtbpy)PF$_6$ **122**

Entry	Eq BF_3K	Eq ArBr	Yield (%)[a]
1	1.5	1.0	88[b]
2	1.0	1.0	68[c]
3	1.0	1.5	66[c]

a) Yield after purification by chromatography; b) Approximate yield as the product co-eluted with an unidentified compound; c) Co-eluted with aryl bromide – yield determined by ^{1}H NMR spectroscopy of a mixture of **121** and **123**.

Next, cross-coupling cyclohexyl trifluoroborate salt **120** with various heteroaryl bromides to produce aryl cyclohexanes **124** was explored. The results are shown in Scheme 3.25. A cross-coupling reaction following Molander's conditions, using cyclohexyl trifluoroborate salt **120** (1.5 eq) and 3-bromopyridine (1.0 eq), yielded none of pyridine cyclohexane **125** (conditions a). Although there are examples of Ni-catalysed photoredox cross-coupling reactions between other alkyl boronates and 3-bromopyridine,[82,83,87] there was no specific precedent for a Ni-catalysed photoredox cross-coupling reaction to produce pyridine cyclohexane **125**. In contrast, using these conditions, cross-coupling was successful using 5-bromopyrimidine (1.0 eq), a FragLite,[20] and cyclohexyl trifluoroborate salt **120** (1.5 eq), to produce pyrimidine cyclohexane **126** in 43% yield. It was decided to further explore the lower equivalents of alkyl trifluoroborate salts in other cross-coupling examples before moving on to cyclobutyl trifluoroborate salt **25**

(conditions b). Therefore, 5-bromopyrimidine (1.5 eq), was reacted with cyclohexyl trifluoroborate salt **120** (1.0 eq) to produce pyrimidine cyclohexane **126** in 63% yield. Clearly, lowering the equivalents of trifluoroborate salt did not negatively affect the reaction. Moreover, cyclohexyl trifluoroborate salt **120** (1.0 eq) was reacted with 4-bromo-2-fluoropyridine (1.5 eq) to produce fluoropyridine cyclohexane **127** in 51% yield (Scheme 3.25).

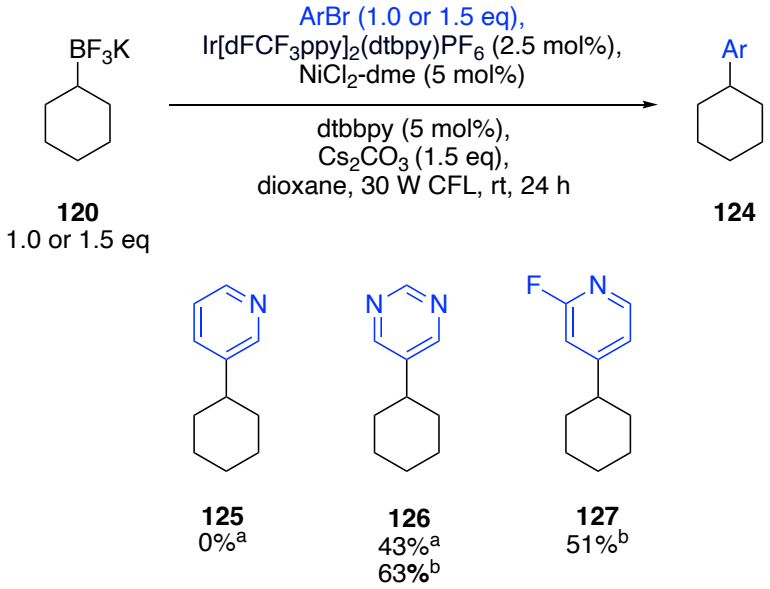

a) 1.5 eq BF_3K, 1.0 eq. ArBr; b) 1.0 eq BF_3K, 1.5 eq ArBr.

Scheme 3.25

Once cross-coupling cyclohexyl trifluoroborate salt **120** with various aryl bromides was attempted, cross-coupling of *N*-Boc piperidinyl trifluoroborate salt **52** to produce aryl *N*-Boc piperidines **128** was explored due to its more similar structure to the 3-D building block, cyclobutyl trifluoroborate salt **25**. For all these reactions, 1.0 equivalent of *N*-Boc piperidinyl trifluoroborate salt **52** was reacted with 1.5 equivalents of aryl bromide as these would be the conditions we expected to use with cyclobutyl trifluoroborate salt **25**. Firstly, cross-coupling ethyl 4-bromobenzoate with *N*-Boc piperidinyl trifluoroborate salt **52** gave ethyl ester phenyl *N*-Boc piperidine **129** in 61% yield (Scheme 3.26). No conversion to pyrimidine *N*-Boc piperidine **130** by ^{1}H NMR spectroscopy of the crude mixture was observed when cross-coupling *N*-Boc piperidinyl trifluoroborate salt **52** and 5-bromopyrimidine. It was not clear why this reaction failed since 5-bromopyrimidine cross-coupled well with cyclohexyl trifluoroborate salt **120** (see Scheme 3.25). As a result, more recent work by a member of the O'Brien group has revisited this exact reaction and, with no obvious explanation, a reproducible 66-72% yield of pyrimidine *N*-

Boc piperidine **130** was obtained.[115] 4-Bromo-2-fluoropyridine and *N*-Boc piperidinyl trifluoroborate salt **52** were cross-coupled to give impure fluoropyridine *N*-Boc piperidine **131**. After purification by chromatography, ^{1}H NMR spectroscopy revealed a 70% pure product with an unidentified side product. From these data, an approximate yield of ~39% of fluoropyridine *N*-Boc piperidine **131** was calculated.

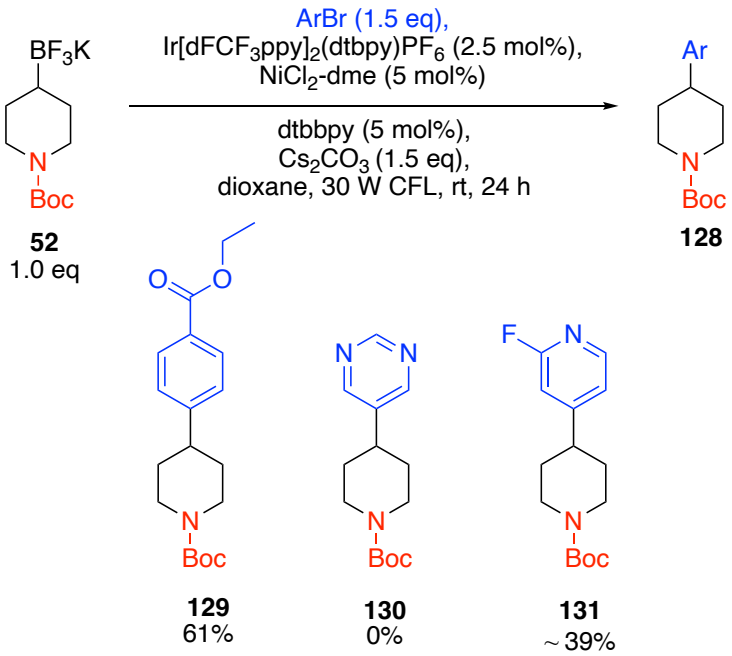

Scheme 3.26

Although cyclohexyl trifluoroborate salt **120** and *N*-Boc piperidinyl trifluoroborate salt **52** are both similar in structure, the results of cross-coupling these substrates with aryl bromides was varied. For example, cross-coupling of 5-bromopyrimidine with cyclohexyl trifluoroborate salt **120** produced pyrimidine cyclohexane **126** in 43-63% yield. However, no conversion to pyrimidine *N*-Boc piperidine **130** was observed when attempting this reaction on *N*-Boc piperidinyl trifluoroborate salt **52**, although there has now been recent success in the group with this reaction. Despite this, some aryl bromides behaved similarly when cross-coupling with cyclohexyl trifluoroborate salt **120** and *N*-Boc piperidinyl trifluoroborate salt **52**. This included reactions with 4-bromo-2-fluoropyridine where similar yields of 39% (**131**) and 51% (**127**) for the fluoropyridine *N*-Boc piperidinyl and cyclohexyl cross-coupled products were achieved respectively. Cross-coupling ethyl 4-bromobenzoate with cyclohexyl trifluoroborate salt **120** or *N*-Boc piperidinyl trifluoroborate salt **52** also yielded similar results (66% yield of ethyl ester phenyl cyclohexane **123** and 61% yield of ethyl ester phenyl *N*-Boc piperidine **129**).

In summary, cross-coupling six-membered cyclic trifluoroborate salts with aryl bromides under Molander's conditions was achieved. When using lower equivalents of trifluoroborate salt, the yield was not significantly affected, which is beneficial for future use on more complicated trifluoroborate salt substrates. The Ni-catalysed photoredox cross-coupling reaction was consistently successful with 4-bromo-2-fluoropyridine and cyclohexyl trifluoroborate salt **120** as well as *N*-Boc piperidinyl trifluoroborate salt **52**. The reaction was also successful with 5-bromopyrimidine and cyclohexyl trifluoroborate salt **120**. These are important results due to the medicinal relevance of these heterocyclic aryl bromides. However, unexpected variability was observed when cross-coupling 5-bromopyrimidine and *N*-Boc piperidinyl trifluoroborate salt **52** as this reaction failed in our hands.

3.2.2 Cross-Coupling with Cyclobutyl Trifluoroborate Salt

At this point, with the success so far with the Ni-catalysed photoredox cross-coupling methodology, we were ready to explore attaching aryl groups to cyclobutyl trifluoroborate salt **25**. Thus, Ni-catalysed photoredox cross-coupling was carried out using 1.5 equivalents of a range of aryl bromides. The aim of this part of the project was to demonstrate that cross-coupling with medicinally relevant aryl bromides could be accomplished. In particular, for this, we were keen to use Waring's FragLites[20] (see Figure 1.3) as this would show that our proposed fragment elaboration methodology would be compatible with these useful fragments.

To start, ethyl 4-bromobenzoate was cross-coupled with cyclobutyl trifluoroborate salt **25** using the standard conditions ([Ir(dFCF$_3$ppy)$_2$(dtbpy)]PF$_6$ (2.5 mol%), NiCl$_2$-dme (5 mol%), dtbbpy (5 mol%) and Cs$_2$CO$_3$ (1.5 eq) in dioxane at room temperature for 24 h with irradiation using a 30 W CFL). Pleasingly, this reaction proceeded smoothly and gave a 53% yield of ethyl ester phenyl cyclobutane **132** after purification by chromatography (Scheme 3.27). This was a similar, but slightly lower yield, to those achieved under the same conditions for ethyl ester phenyl cyclohexane **123** (66%) and ethyl ester phenyl *N*-Boc piperidine **129** (61%).

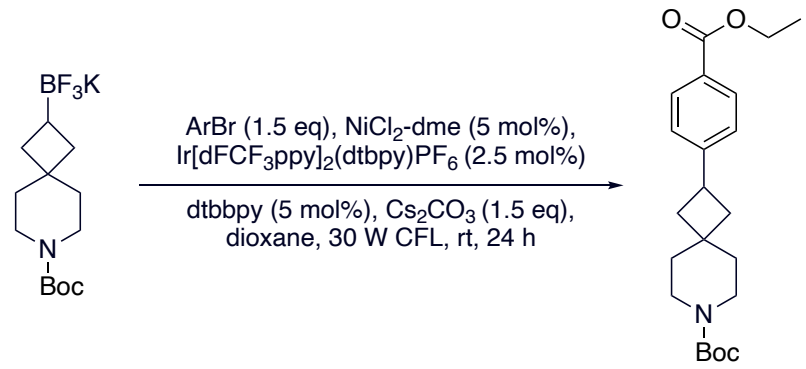

25
1.0 eq

132
53%

Scheme 3.27

The ^{1}H NMR spectrum of ethyl ester phenyl cyclobutane **132** is shown in Figure 3.2. In the upfield part of the spectrum, the H$_A$ protons appear as a triplet at δ_H 1.39 (t, J = 7.0 Hz, 3H). The H$_A$ protons couple to the H$_B$ protons which appear as a quartet at δ_H 4.36 (q, J = 7.0 Hz, 2H). The aryl H$_C$ protons appear at δ_H 7.97 (d, J = 8.5 Hz, 2H) and aryl H$_D$ protons at δ_H 7.25 (d, J = 8.5 Hz, 2H) which couple to each other and both appear as doublets. The H$_C$ protons *ortho* to the ester (δ_H 7.97) are more downfield than the *meta*-

H_D protons (δ_H 7.25) due to deshielding caused by the –M mesomeric effect from the ester group. H_E appears as a triplet of triplets at δ_H 3.57 (tt, J = 9.0, 9.0 Hz, 1H) due to its coupling to the adjacent two pairs of diastereotopic H_F protons. Electron withdrawing effects of the adjacent aromatic group lead to a downfield H_E proton at δ_H 3.57. The two sets of diastereotopic H_F protons appear as two sets of multiplets at δ_H 2.37–2.27 and δ_H 2.00–1.83. Similarly, the two axial protons of H_G appear as independent signals from their equatorial counterparts at δ_H 1.77–1.67 and δ_H 1.54–1.48. Finally, the H_H protons are more downfield than the H_G protons at δ_H 3.45–3.34 and δ_H 3.33–3.22 due to the electron withdrawing effects of the adjacent *N*-Boc group.

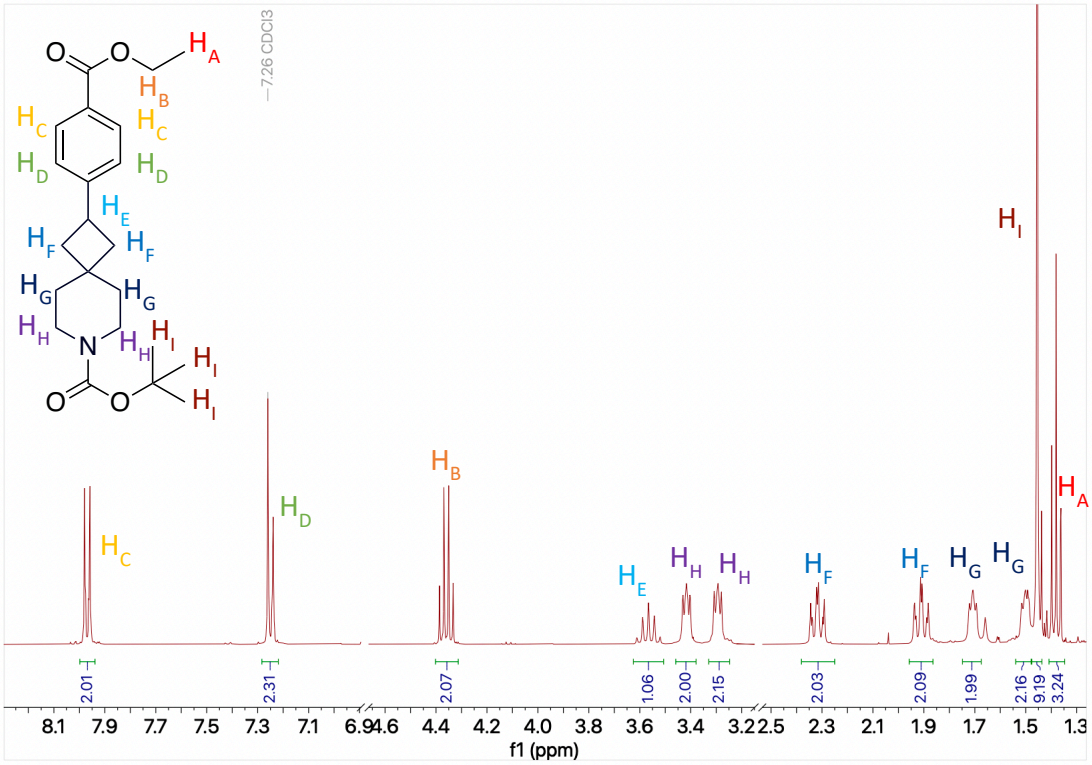

*Figure 3.2 – ^{1}H NMR spectrum of ethyl ester phenyl cyclobutane **132***

With the success of cross-coupling ethyl 4-bromobenzoate with cyclobutyl trifluoroborate salt **25**, cross-coupling of some FragLites[20] with cyclobutyl trifluoroborate salt **25** to produce aryl cyclobutanes **27** was attempted (Scheme 3.28). 5-Bromopyrimidine was cross-coupled with cyclobutyl trifluoroborate salt **25** to produce pyrimidine cyclobutane **133** in excellent 84% yield. 4-Bromo-2-methoxypyridine, a different heteroaromatic FragLite, was also successfully cross-coupled to cyclobutyl trifluoroborate salt **25** to produce methoxypyridine cyclobutane **134** in 63% yield. 4-Bromoacetanilide was cross-coupled to cyclobutyl trifluoroborate salt **25** to produce

acetanilide cyclobutane **135** in 46% yield. This last example is notable as the free NH from the amide did not cause any issues in this reaction.

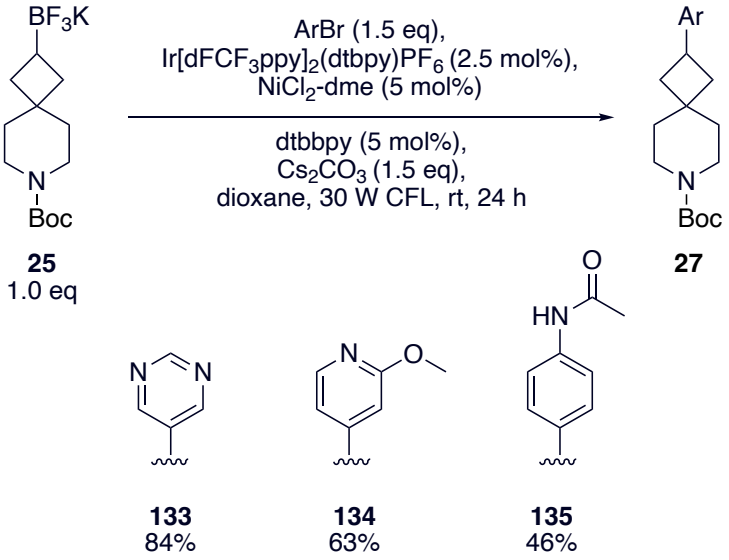

Scheme 3.28

The ^{1}H NMR spectrum of pyrimidine cyclobutane **133** is shown in Figure 3.3. At the downfield end of the spectrum, H_A is found at δ_H 9.03. The H_A proton is the most downfield due to –I inductive effects from the two nitrogen atoms. The H_B protons are the next most downfield, appearing as a 2H singlet at δ_H 8.56. The H_B protons are adjacent to only one nitrogen and so the –I inductive effects are less pronounced. The rest of the protons in pyrimidine cyclobutane **133** follow the same appearance in the ^{1}H NMR spectrum as that of ethyl ester phenyl cyclobutane **132** (see Figure 3.2).

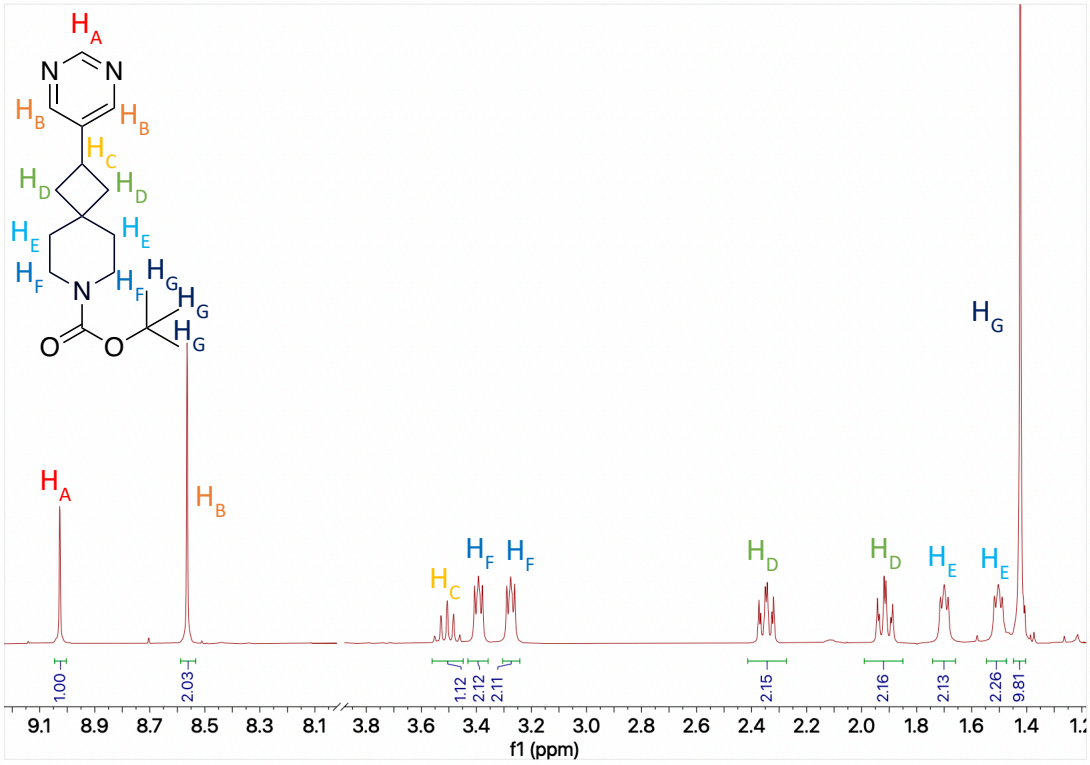

*Figure 3.3 – ^{1}H NMR spectrum of pyrimidine cyclobutane **133***

Although some FragLites[20] were cross-coupled effectively, others were not as successful (Scheme 3.29). For example, 4-bromophenyl methyl sulfone cross-coupled to cyclobutyl trifluoroborate salt **25** to give methanesulfonylphenyl cyclobutane **136** in a low 12% yield. 4-Bromobenzene sulfonamide failed to cross-couple with cyclobutyl trifluoroborate salt **25** to produce sulfamoylphenyl cyclobutane **137**. 4-Bromopyrazole also failed to cross-couple with cyclobutyl trifluoroborate salt **25** to give pyrazole cyclobutane **138**. Finally, 2-amino-4-bromopyridine was cross-coupled with cyclobutyl trifluoroborate salt **25** to give trace amounts of aminopyridine cyclobutane **139** by mass spectrometry. These results were reproducible by another member of the group, supporting the idea that some aryl bromides are unable to cross-couple to the trifluoroborate salt using this method.[115] There may have been issues due to the iridium catalyst oxidising the lone pairs on the amino groups in 4-bromobenzene sulfonamide, pyrazole and 2-amino-4-bromopyridine rather than the iridium catalyst cleaving the C-B bond, resulting in the reaction failing for these aryl bromides.

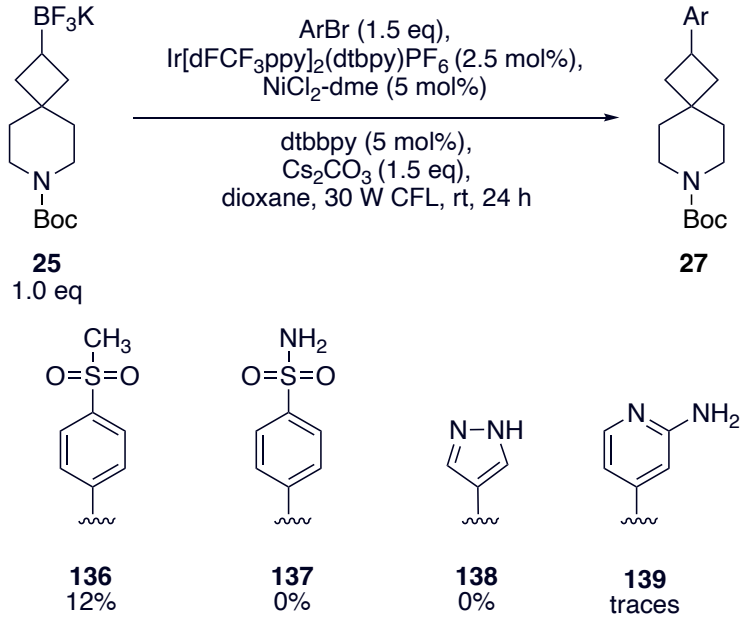

Scheme 3.29

In order to try and improve the yield of methanesulfonylphenyl cyclobutane **136**, the reaction with 4-bromophenyl methyl sulfone was repeated. Disappointingly, this reaction failed to give methanesulfonylphenyl cyclobutane **136**, despite yielding 12% of product in the first attempt. It appeared that the Ni-catalysed photoredox cross-coupling reactions were not working as efficiently as they were previously. Thus, we returned to the cross-coupling of cyclobutyl trifluoroborate salt **25** with 5-bromopyrimidine which had previously given an 84% yield of pyrimidine cyclobutane **133**. Upon repetition under identical conditions, only a 46% yield was obtained.

To determine what might be leading to the problems carrying out previously successful photoredox reactions, several studies were executed to explore the reaction of cyclobutyl trifluoroborate salt **25** with 5-bromopyrimidine as this aryl bromide had previously given a high yield (84%). To rule out issues with the building block itself, investigations were carried out to determine whether cyclobutyl trifluoroborate salt **25** could be affecting the reaction. Our hypothesis was that if there was an issue with cyclobutyl trifluoroborate salt **25**, then the reaction should be successful with cyclohexyl trifluoroborate salt **120**. Therefore, cyclohexyl trifluoroborate salt **120** and 5-bromopyrimidine were cross-coupled. Despite achieving a previous yield of 63%, none of pyrimidine cyclohexane **126** was obtained when repeating the reaction (Scheme 3.30). To further confirm it was not a problem with cyclobutyl trifluoroborate salt **25**, *N*-Boc piperidinyl trifluoroborate salt **52** and ethyl 4-bromobenzoate were cross-coupled to produce ethyl ester phenyl *N*-Boc

piperidine **129**. Likewise, this reaction failed when previously a 61% yield of ethyl ester phenyl *N*-Boc piperidine **129** had been obtained. From these results, it was concluded that there was an issue with something other than the cyclobutyl trifluoroborate salt **25**.

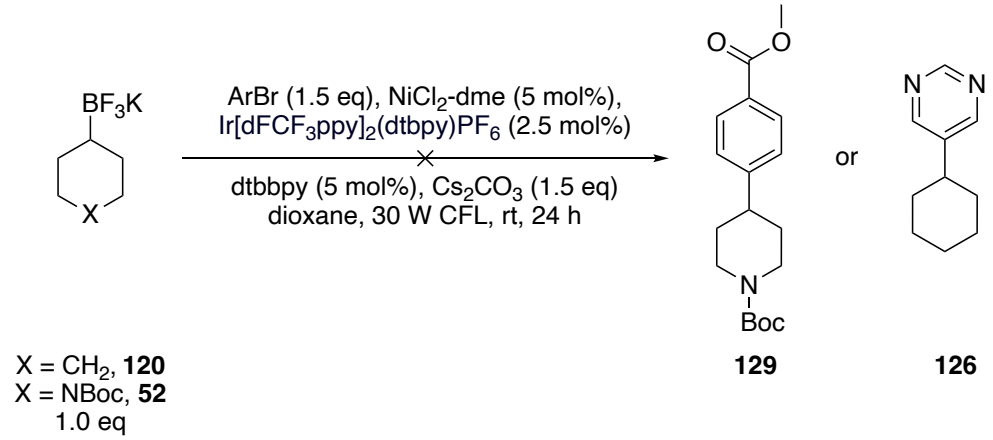

Scheme 3.30

It was decided to explore a range of different conditions when cross-coupling cyclobutyl trifluoroborate salt **25** and 5-bromopyrimidine to try to determine what the issue was in the Ni-catalysed photoredox cross-coupling reaction. The different conditions investigated are presented in Table 3.2, with the first two entries in the table being the previously obtained results. When carrying out Ni-catalysed photoredox cross-coupling under standard conditions, the capped vial would be purged with argon for 20 minutes before being exposed to the 30 W CFL lamp. This degassing is to remove oxygen from the reaction mixture. To determine whether variable degassing could be the cause of variations in yields, we attempted to cross-couple 5-bromopyrimidine and cyclobutyl trifluoroborate salt **25** with no degassing. This reaction failed to give any of pyrimidine cyclobutane **133** (entry 3) and shows that an oxygen-free system is vital for the reaction to take place.

*Table 3.2 – Exploring issues with the Ni-catalysed photoredox cross-coupling reaction using 5-bromopyrimidine and cyclobutyl trifluoroborate salt **25***

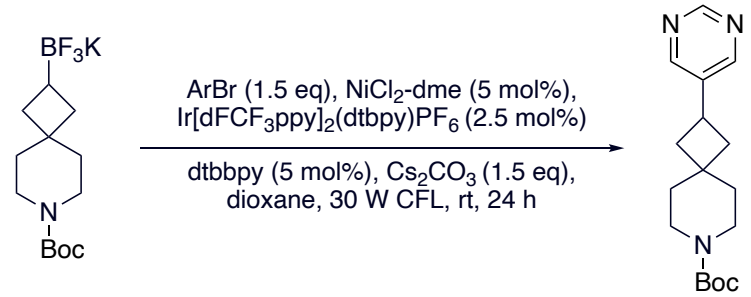

25
1.0 eq

133

Entry	Conditions differing from original[a]	Yield (%)[b]
1	None	84
2	None	46
3	No degassing	0
4	7 mL solvent	<17[c]
5	Sonicated solvent	<13[c]
6	0.125 mmol scale	29
7	Recrystallised Ir, different Ni batch	<27[c]
8	Recrystallised Ir, different dtbbpy batch	<17[c]
9	Recrystallised Ir, new dioxane	41

a) original conditions: 20 min degassing, 5 mL solvent, no sonication, 0.25 mmol; b) Yield after purification by chromatography; c) Approximate yield, unable to quantify yield due to significant impurities present.

Another potential area of concern was that the solid reagents, $[Ir(dFCF_3ppy)_2(dtbpy)]PF_6$, $NiCl_2$-dme, dtbbpy, Cs_2CO_3, cyclobutyl trifluoroborate salt **25** and aryl bromide were not all dissolving in the dioxane reaction solvent. Three side-by-side experiments were carried out: the first a normal reaction on a 0.25 mmol scale with 5 mL of solvent and no sonication (A), the second with 7 mL of solvent (B) (instead of the usual 5 mL of dioxane) and the third with the solution sonicated (C) (Figure 3.4). As Cs_2CO_3 is not fully soluble in dioxane, it was difficult to tell whether it was only Cs_2CO_3 not dissolving or if the other reagents were also not dissolving. The more dilute reaction conditions led to a yield of <17% of pyrimidine cyclobutane **133** (Table 3.2, entry 4). A number of these experiments led to significant impurities being present after chromatography, hence it was not possible to quantify an accurate yield (entries 4, 5, 7 and 8). The final experiment that was carried

out to improve solubility of solid reagents into the reaction mixture was to sonicate the reaction mixture for 10 minutes before degassing the mixture. The sonicating was to encourage more of the solids to dissolve in the dioxane. Although the reaction mixture appeared more concentrated (vial C, Figure 3.4), the yield was <13% of pyrimidine cyclobutane **133** (entry 5). Interestingly, there was a colour change from lime green to maroon for the two vials without sonication but the colour change was from lime green to amber coloured with sonication (Figure 3.4).

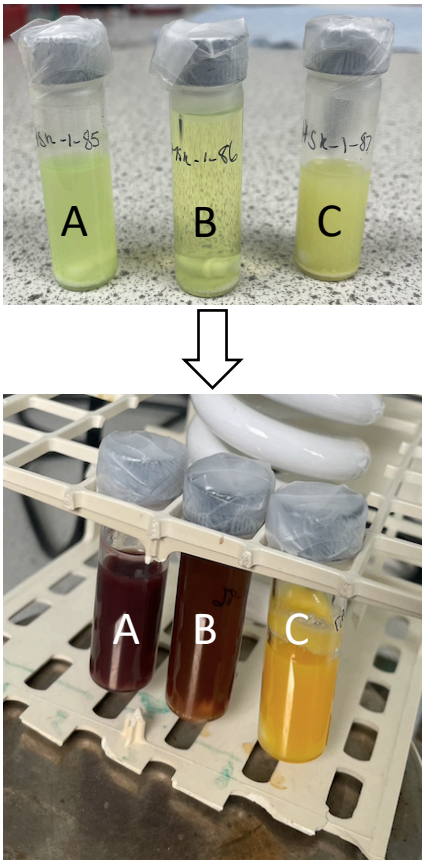

Top image depicts reaction mixture before stirring irradiated by 30 W CFL lamp for 24 hours. Bottom image shows the vials after 24 hours. A = 5 mL solvent, no sonication; B = 7 mL solvent, no sonication; C = 5 mL solvent, 10 min sonication.

Figure 3.4 – Solubility tests for Ni-catalysed photoredox cross-coupling

As these tests were using a high quantity of cyclobutyl trifluoroborate salt **25**, a half scale reaction was carried out to see if the reaction would be feasible on a 0.125 mmol scale without affecting the yield. As the yield was 29% of pyrimidine cyclobutane **133** when attempting the reaction on a half scale, the tests continued at full scale (Table 3.2, entry 6). Another hypothesis as to what could be causing issues in the reaction was that light could have caused some of the photocatalyst, $[Ir(dFCF_3ppy)_2(dtbpy)]PF_6$, to decompose

as it was stored without the exclusion of light. Therefore, the catalyst may have had lower reactivity in the Ni-catalysed photoredox cross-coupling reaction. To ensure only working catalyst was used, the catalyst was freshly recrystallised. When using the new recrystallised catalyst and a different batch of $NiCl_2$-dme, a yield of <27% of pyrimidine cyclobutane **133** was obtained (entry 7). Similarly, a different batch of dtbbpy ligand led to a yield of <17% of pyrimidine cyclobutane **133** (entry 8). Lastly, the dioxane was investigated. The bottle which was being used for the previous reactions was found to have multiple peaks in its ^{1}H NMR spectrum. Some of these impurities may have been due to oxygen forming peroxides upon storage. Such peroxides could have been interfering with the photoredox cross-coupling process. Therefore, a freshly purchased bottle of dioxane was used as the solvent when cross-coupling cyclobutyl trifluoroborate salt **25** and 5-bromopyrimidine. This gave pyrimidine cyclobutane **133** in 41% yield which was of much higher purity than the experiments carried out with the older bottle of dioxane (entry 9).

The freshly purchased bottle of dioxane was used in a further Ni-catalysed photoredox cross-coupling reaction. In this case, cyclobutyl trifluoroborate salt **25** was reacted with 4-bromophenyl methyl sulfone under standard conditions to give methanesulfonylphenyl cyclobutane **136** in 39% yield (Scheme 3.31). The 39% yield was a major achievement as the reaction failed previously and gave a 12% yield before this. Another member of the O'Brien group managed to increase the yield even further to 69%.[115] From this, it was concluded that the older bottle of dioxane, possibly contaminated with peroxides, was contributing to producing the low yields.

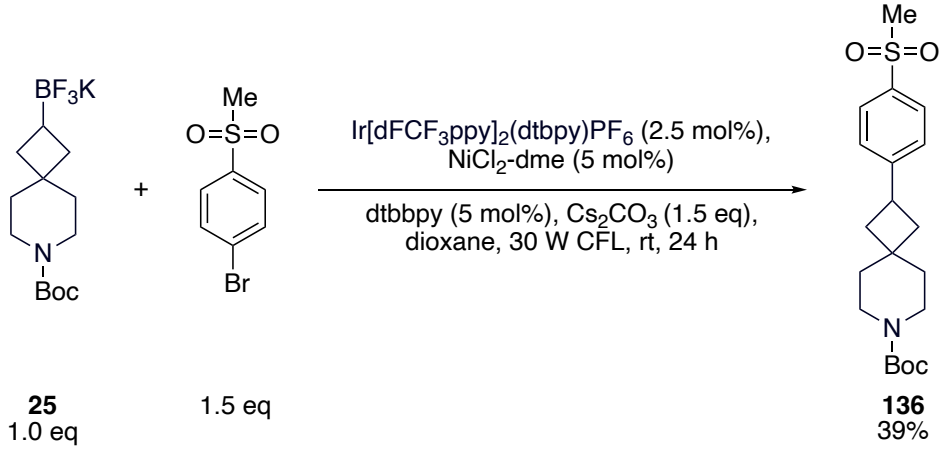

25
1.0 eq

1.5 eq

136
39%

Scheme 3.31

Overall, Ni-catalysed photoredox cross-coupling from cyclobutyl trifluoroborate salt **25** was a viable method for cross-coupling the building block with a variety of aryl bromides including FragLites[20] such as 5-bromopyrimidine, 3-methoxypyridine, 4-bromoacetanilide and 4-bromophenyl methyl sulfone in yields from 39-84%. Some FragLites were not successfully cross-coupled such as 4-bromobenzene sulfonamide, 4-bromopyrazole and 2-amino-4-bromopyridine, perhaps due to these aryl bromides being oxidised and interfering with the photoredox cross-coupling rection. This technique proved to be substrate-dependent, sensitive, and not fully reproducible. Although using a new bottle of dioxane helped to bring the yield up slightly, there is more work needed to be done to figure out what is the root cause of the low yields and variability observed in this reaction. Nevertheless, there was some success on a range of medicinally relevant aryl bromides with complex cyclobutyl trifluoroborate salt **25**. Moreover, a new member of the O'Brien group has broadly found these results to be reproducible.[115]

3.2.3 Cross-Coupling with the Cyclobutanol

During the course of the project, we discovered a 2021 paper by Dong and MacMillan[91] on an alternative method to cross-couple aryl halides with alcohols rather than trifluoroborate salts. A brief overview of this work was described in Section 3.1.1 (see Scheme 3.15). In our case, cyclobutanol **50** would be used as the building block rather than cyclobutyl trifluoroborate salt **25** to explore cross-coupling from the alcohol. Using MacMillan's method reduces the number of steps to the building block since cyclobutanol **50** can be synthesised in one step from commercially available cyclobutanone **30** (see Scheme 2.11). The two-step Ni-catalysed photoredox cross-coupling reaction from the cyclobutanol is highlighted in Scheme 3.32 (see Scheme 3.16 for full mechanistic details). The first step is to make the NHC-alcohol adduct **140**. This step proceeds *via* condensation of cyclobutanol **50** with NHC precursor **141**. In this step, NHC precursor **141** (1.6 eq), cyclobutanol **50** (1.75 eq) and pyridine (1.6 eq) are combined in MTBE (4.0 mL) at room temperature for 30 min to produce NHC-alcohol adduct **140** to be used *in situ*. In the second step, the NHC-alcohol adduct **140** is reacted with aryl bromide (1.0 eq), $NiBr_2$-dme (7.5 mol%), dtbbpy (7.5 mol%), $[Ir(dFCF_3ppy]_2(dtbpy)]PF_6$ (1.5 mol%), quinuclidine (1.75 eq), (and phthalimide (0.22 eq) if using) in DMA (5.0 mL) at room temperature for 24 h to produce aryl cyclobutanes **27** (Scheme 3.32).

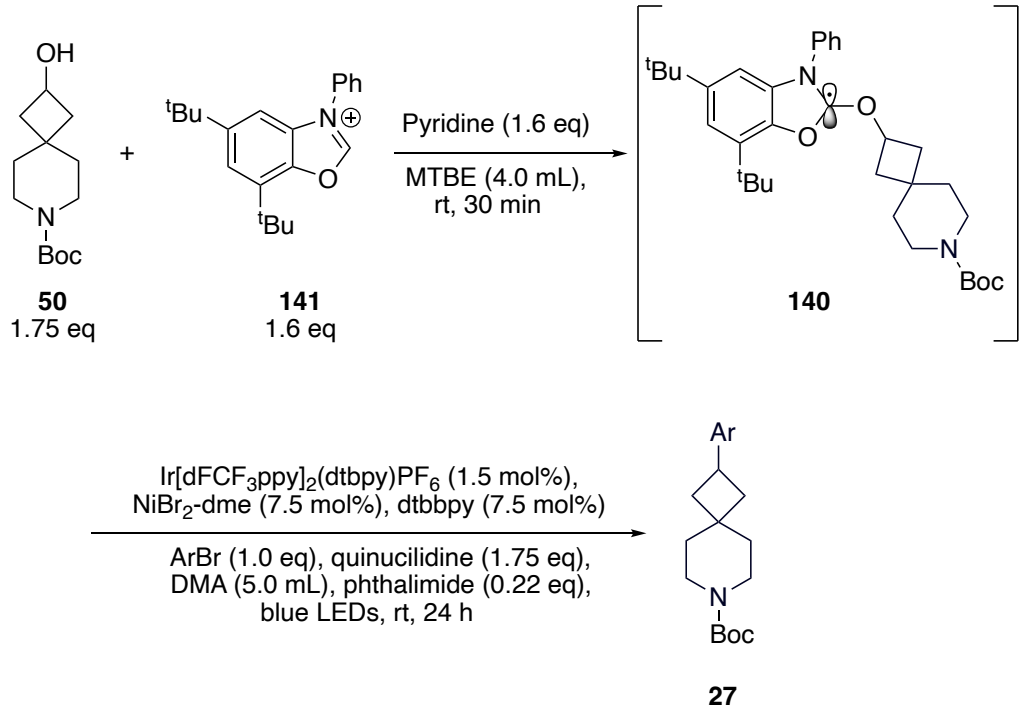

Scheme 3.32

Initially, cyclobutanol **50**, which had previously been prepared as part of one of the routes to cyclobutyl trifluoroborate salt **25** (see Scheme 2.11), was cross-coupled with ethyl 4-bromobenozate to give ethyl ester phenyl cyclobutane **132** on a 0.25 mmol scale using MacMillan's conditions without phthalimide. There were many spots on the TLC which meant it was challenging to isolate pure product. Despite our best efforts, ethyl ester phenyl cyclobutane **132** could not be separated from phthalimide **142**. After purification by chromatography, an 80:20 mixture of ethyl ester phenyl cyclobutane **132** and phthalimide **142** was isolated, from which a 43% yield of ethyl ester phenyl cyclobutane **132** was calculated (Scheme 3.33).

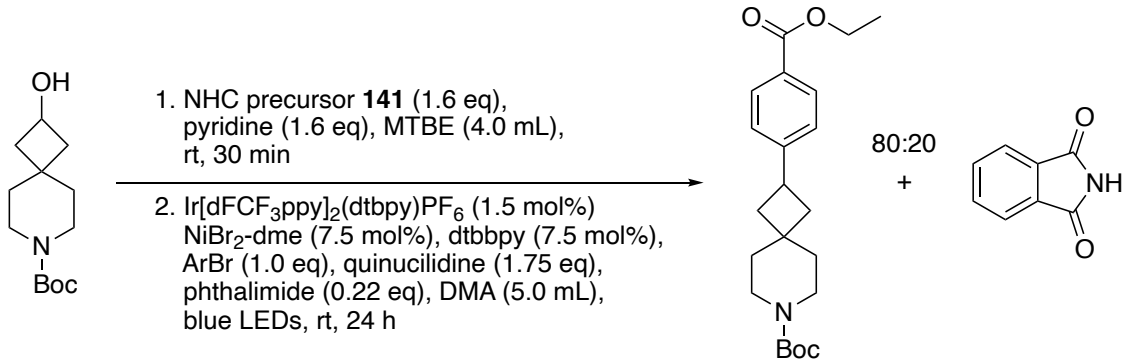

50 **132** 43%[a] **142**

a) 80:20 mixture of ethyl ester phenyl cyclobutane **132** and phthalimide **142**.

Scheme 3.33

With the successful cross-coupling of ethyl 4-bromobenzoate with cyclobutanol **50**, the cross-coupling of a FragLite[20] was attempted. 4-Bromobenzene sulfonamide was cross-coupled to cyclobutanol **50** to produce sulfamoylphenyl cyclobutane **137**. Due to the challenging purification in the previous reaction, the additive phthalimide was removed as it may not have been necessary for the reaction to take place and its presence complicated purification. Pleasingly, sulfamoylphenyl cyclobutane **137** was isolated in 19% yield (Scheme 3.34). However, despite the removal of phthalimide, purification continued to prove challenging with five significant spots eluting, and so some product was sacrificed in order to ensure high purity. It was interesting to note that 4-bromobenzene sulfonamide cross-coupled successfully using Macmillan's method *via* cyclobutanol **50** but not using Molander's conditions *via* cyclobutyl trifluoroborate salt **25**.

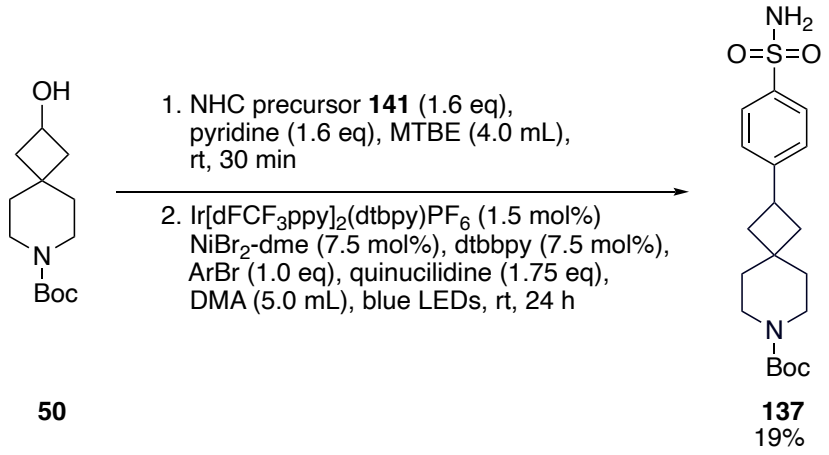

50 **137** 19%

Scheme 3.34

One advantage of cross-coupling under MacMillan's conditions was the potential for cross-coupling aryl bromides to cyclobutanol **50** that are more difficult to cross-couple using Molander's conditions such as 4-bromobenzene sulfonamide. Futhermore, cyclobutanol **50** is easily accessed, requiring one step to synthesise it from cyclobutanone **30**. A minimum of four steps to make cyclobutyl trifluoroborate salt **25** were required so the reduced number of steps to cyclobutanol **50** as a building block for cross-coupling is appealing. Therefore, although the yields of photoredox cross-coupling cyclobutanol **50** were low, cross-coupling from cyclobutanol **50** may be more efficient overall than cross-coupling from cyclobutyl trifluoroborate salt **25**. However, although Ni-catalysed photoredox cross-coupling using Macmillan's conditions from cyclobutanol **50** worked, purification proved to be more challenging than cross-coupling using Molander's conditions from cyclobutyl trifluoroborate salt **25**. As purification was challenging, this method was deemed to be unfavourable compared to cross-coupling *via* cyclobutyl trifluoroborate salt **25** under Molander's conditions.

3.3 Pd-Catalysed Suzuki-Miyaura Cross-Coupling Results

After carrying out several successful photoredox cross-coupling reactions with cyclobutyl trifluoroborate salt **25**, our attention turned to briefly exploring whether Suzuki-Miyaura cross-coupling (SMCC) would also be feasible. As this is a cyclobutyl building block, Pd-catalysed SMCC reactions are less precedented for Csp^2-Csp^3 couplings (as discussed in Section 3.1.2) than Ni-catalysed photoredox cross-coupling which is why the photoredox cross-coupling approach was investigated first. Moreover, more complex cyclobutanes were able to be cross-coupled using Ni-catalysed photoredox cross-coupling than SMCC which led us to think that Ni-catalysed photoredox cross-coupling would be more likely to be successful on the complex building block substrate in comparison to SMCC.

Initially, SMCC conditions reported by Gormisky and Molander[105] with the unsubstituted cyclobutyl trifluoroborate salt **65** were selected. Another member of the O'Brien group had used these conditions to cross-couple 5-chloro-3-dimethoxybenzene with *N*-Boc azetidinyl trifluoroborate salt **143** to give aryl azetidine **144** in 8% yield[116] (Scheme 3.35). The conditions used were 5-chloro-3-dimethoxybenzene (1.0 eq), *N*-Boc azetidinyl trifluoroborate salt **143** (1.01 eq), $Pd(OAc)_2$ (2 mol%), CataCXium A **145** (3 mol%) and Cs_2CO_3 (3.0 eq) in a 10:1 mixture of toluene-H_2O at 0.25 M concentration of aryl chloride at 100 °C for 24 h.

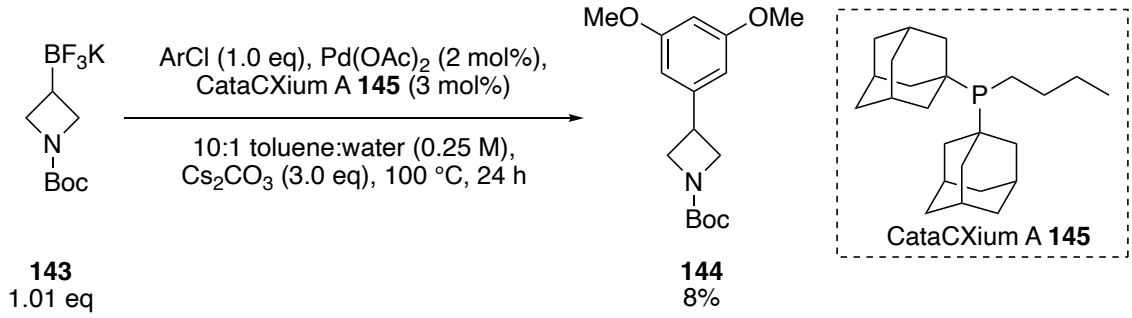

Scheme 3.36

As these conditions worked on the azetidine (albeit in very low yield), we decided to test these conditions in a SMCC of cyclobutyl trifluoroborate salt **25**. Higher equivalents of cyclobutyl trifluoroborate salt **25** were used initially to try to increase the yield. Thus, cyclobutyl trifluoroborate salt **25** (1.5 eq) was reacted with 5-chloro-3-dimethoxybenzene (1.0 eq) in the presence of $Pd(OAc)_2$ (2 mol%), CataCXium A (3 mol%) and Cs_2CO_3 (3.0 eq) in a 10:1 mixture of toluene-H_2O at 0.25 M concentration of aryl chloride in attempt

to produce dimethoxyphenyl cyclobutane **146**. The reaction was attempted at 100 ℃ and 120 ℃ for 24 h. Unfortunately, there was no product observed in the ^{1}H NMR spectrum of the crude products at either of these temperatures (Scheme 3.37).

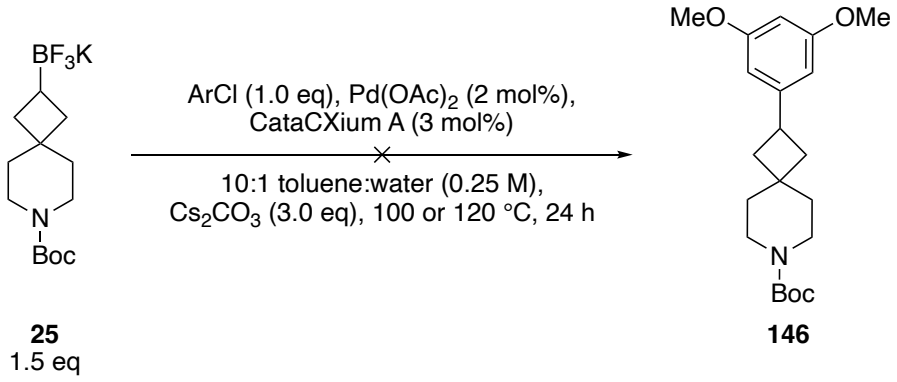

Scheme 3.37

Recently, a member of the O'Brien group was investigating the SMCC reaction of *N*-Boc piperidinyl trifluoroborate salt **52** with chlorobenzene to produce phenyl *N*-Boc piperidine **147**.[116] It was shown that increasing the loading of $Pd(OAc)_2$ from 5 mol% to 10 mol% alongside increasing the loading of CataCXium A from 10 mol% to 20 mol% resulted in a change in yield from 25% to 37%, a significant increase (Scheme 3.38).

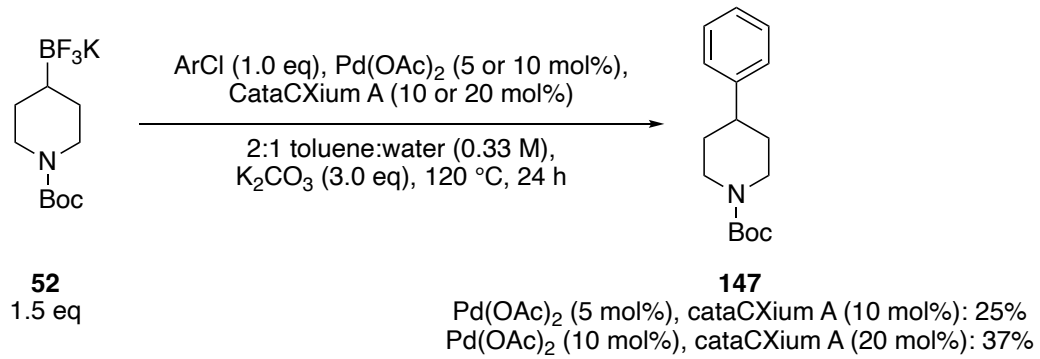

Scheme 3.38

Despite the lack of success using SMCC conditions by Gormisky and Molander[105] on cyclobutyl trifluoroborate salt **25**, it was decided to try a higher catalyst loading due to the success doing so in the O'Brien group[116] (see Scheme 3.38). The reaction conditions were the same apart from 10 mol% of $Pd(OAc)_2$ and 20 mol% CataCXium A were used. Moreover, chlorobenzene **148** was used rather than the more complicated 5-chloro-3-dimethoxybenzene. Also, the reaction was only tried at 120 ℃. To our delight, cross-coupling of cyclobutyl trifluoroborate salt **25** with chlorobenzene **148** was successful, giving a 55% yield of phenyl cyclobutane **149** (Table 3.3, entry 1). As cyclobutyl trifluoroborate salt **25** is more precious than chlorobenzene, the reaction was attempted

using chlorobenzene in excess and the yield was not affected (53%, entry 2). Moving forward, it would be ideal to use aryl bromides rather than aryl chlorides as the FragLites[20] which were readily available to us were aryl bromides. Therefore, the cross-coupling was attempted with bromobenzene **150** rather than chlorobenzene **148**. Unfortunately, this gave a yield of <24% of phenyl cyclobutane **149** (entry 3). In this case, it was not possible to quantify the yield due to unidentified impurities that were present.

*Table 3.3 – Optimising equivalents and halide used for SMCC cross-coupling PhCl **148** or PhBr **150** with cyclobutyl trifluoroborate salt **25***

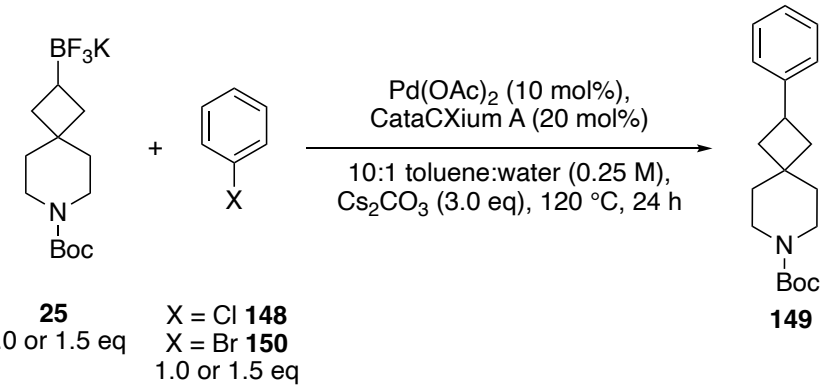

Entry	Eq BF_3K	Eq PhX	X	Yield (%)[a]
1	1.5	1.0	Cl	55
2	1.0	1.5	Cl	53
3	1.0	1.5	Br	<24

a) Yield after purification by chromatography.

With these results in hand, more complicated FragLites[20] were cross-coupled using SMCC conditions with 1.0 equivalent of cyclobutyl trifluoroborate salt **25** to produce aryl cyclobutanes **27** (Scheme 3.39). 5-Bromopyrimidine was cross-coupled with cyclobutyl trifluoroborate salt **25** to produce pyrimidine cyclobutane **133** in 45% yield. With 4-bromophenyl methyl sulfone, a 15:30:55 mixture of methanesulfonylphenyl cyclobutane **136**, cyclobutanol **50** and 4-bromophenyl methyl sulfone was obtained after the first purification. A 28% yield of methanesulfonylphenyl cyclobutane **136** was determined from this mixture. After a second column, a 28% yield of cyclobutanol **50** was isolated. Based on previous work in the O'Brien group, we believe that cyclobutanol **50** forms as follows. During the reaction, cyclobutyl trifluoroborate salt **25** is presumably hydrolysed to the corresponding boronic acid. In other systems in the group, it has been shown that alkyl boronic acids can be converted into alcohols upon chromatography on silica. We

presume that a similar process is occurring in this case. When separately cross-coupling 4-bromobenzene sulfonamide and 4-bromoacetanilide with cyclobutyl trifluoroborate salt **25** to produce aryl products **137** and **135** respectively, no product was isolated.

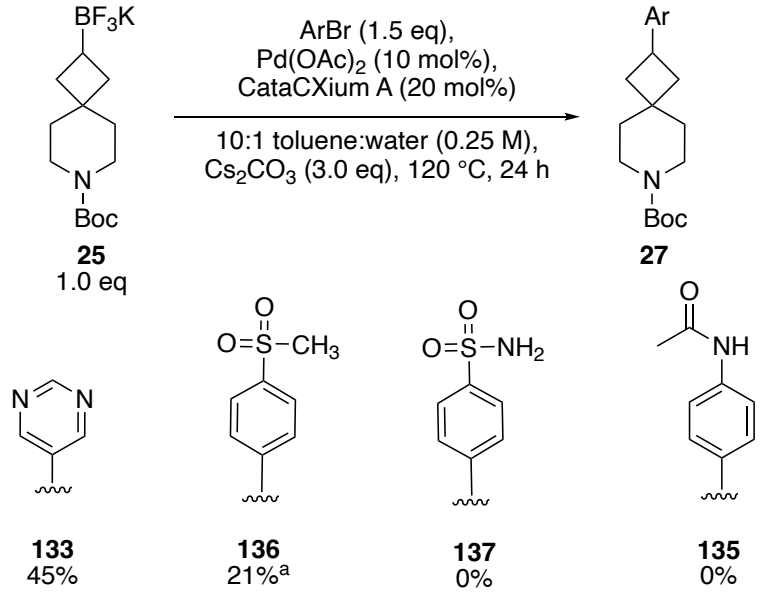

a) 15:30:55 mixture of methanesulfonylphenyl cyclobutane **136**, cyclobutanol **50** and 4-bromophenyl methyl sulfone.

Scheme 3.39

Overall, SMCC of cyclobutyl trifluoroborate salt **25** with aryl halides has potential to be a viable method for cross-coupling. This is an exciting finding as Csp^2-Csp^3 SMCC cross-coupling is challenging on more complex cyclobutyl systems. For example, a second Lewis acid Bpin group was necessary for cross-coupling to be able to take place on a similar substrate[66] (see Scheme 3.24, Section 3.1.2). The key to enabling SMCC from cyclobutyl trifluoroborate salt **25** was to use a high catalyst loading. However, optimisation is still important for this reaction as there were some examples where the yields were low (**136**), or the reaction did not work at all (**135** and **137**).

4. *N*-Functionalisation of Aryl Cyclobutanes

In this Chapter, *N*-functionalisation reactions on aryl cyclobutanes **27** to create *N*-functionalised aryl cyclobutanes **28** will be discussed (Scheme 4.1). Section 4.1 discusses the literature background of *N*-functionalisation reactions on aryl cyclobutanes **27**. Section 4.2 presents the synthesis to make lead-like compounds for potential use in medicinal chemistry through Boc removal and *N*-functionalisation of aryl cyclobutanes **27** to produce *N*-functionalised aryl cyclobutanes **28**. Section 4.2 also discusses the exit vector analysis of one *N*-functionalised aryl cyclobutane **28** (Ar = pyrimidine, R = methanesulfonamide) using its X-ray crystal structure.

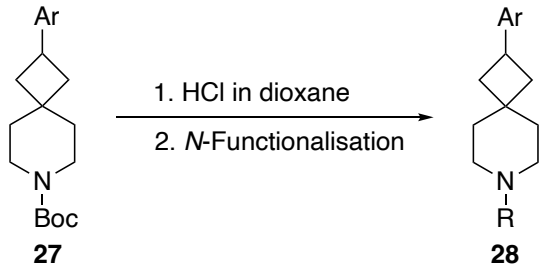

Scheme 4.1

4.1 Cyclobutane Piperidine Scaffold in Drug Discovery

The final step to creating lead-like compounds from aryl cyclobutanes **27** would be the removal of the Boc group and *N*-functionalisation of the free amine to obtain *N*-functionalised aryl cyclobutanes **28**. There are several examples of aryl cyclobutanes in the patent literature that are structurally similar to the types of lead-like compounds that we planned to synthesise. A few of these known lead-like compounds are shown in Figure 4.1, with the aryl motifs simplified to 'Ar'.

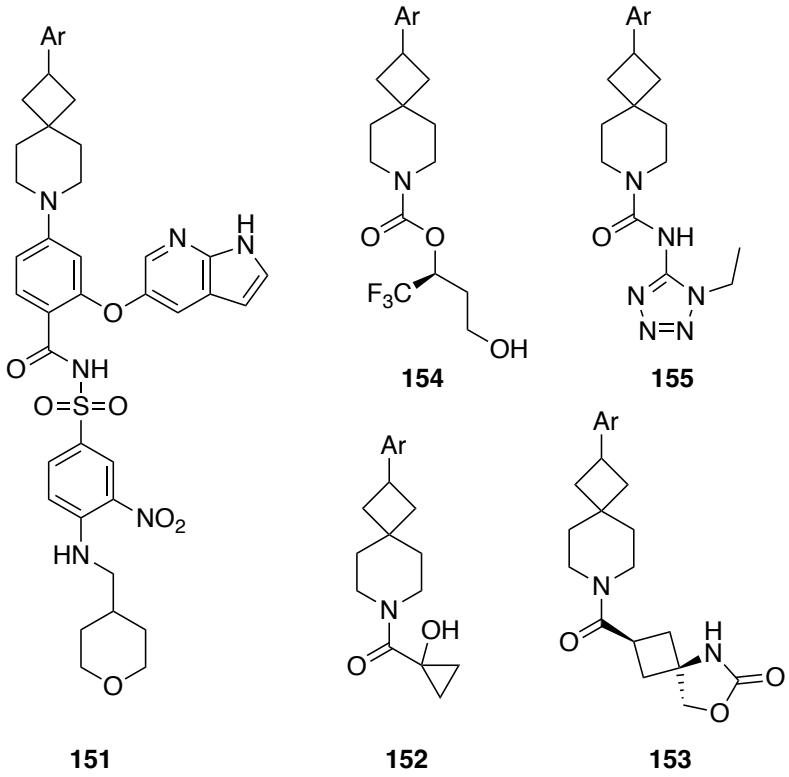

Figure 4.1 – Patent examples of N-functionalised aryl cyclobutanes

For example, researchers at BeiGene synthesised a variety of Bcl-2 inhibitors to treat Bcl-2 related diseases such as cancer and autoimmune disease.[117] An example of one of their synthesised compounds is the complex *N*-functionalised aryl cyclobutane **151** where a nitrogen-aryl bond formation was achieved. Two examples of amide *N*-functionalised aryl cyclobutanes are depicted as **152** and **153**. Forma Therapeutics produced *N*-functionalised aryl cyclobutane **152** in an attempt to inhibit fatty acid synthase, implicated in non-alcoholic steatohepatitis.[118] Researchers at Janssen Pharmaceuticals synthesised *N*-functionalised aryl cyclobutane **153** as a modulator of monoacylglycerol lipase (MAGL), an enzyme implicated in neurological disorders and cancers.[119] Alternatively, carbamate *N*-functionalised aryl cyclobutane **154** and analogues of this compound were

synthesised by medicinal chemists at Pfizer.[120] These lead-like compounds were also synthesised with the intention of acting as MAGL inhibitors. In a separate publication, researchers at Pfizer prepared a selection of carbamide lead-like compounds to act as fatty acid amide hydrolase (FAAH) inhibitors to treat pain, inflammation, anxiety and depression.[121] This work was previously discussed in Section 1.4[63,65] (see Figure 1.11). The structure of one of these carbamides is *N*-functionalised aryl cyclobutane **155**. The variety of *N*-functionalised aryl cyclobutanes previously synthesised to target a diverse set of diseases highlights the utility of the building block scaffold for the pharmaceutical industry.

One example of *N*-functionalisation as a route to *N*-functionalised aryl cyclobutane **156**, reported by Assembly Biosciences in 2021, is shown in Scheme 4.2.[68] The goal was to synthesise compounds for the treatment of hepatitis caused by the Hepatitis B virus. To obtain *N*-functionalised aryl cyclobutane **156**, initially the Boc group was removed from *N*-Boc aryl cyclobutane **27** using TFA in CH_2Cl_2 to produce amine aryl cyclobutane **157** in 90% yield. Then, a nucleophilic aromatic substitution reaction was carried out with amine aryl cyclobutane **157** (1.0 eq), 3,4,5-trifluoropyridine (1.0 eq) and Et_3N (3.0 eq) in MeCN to give *N*-functionalised aryl cyclobutane **156** in 29% yield (Scheme 4.2).

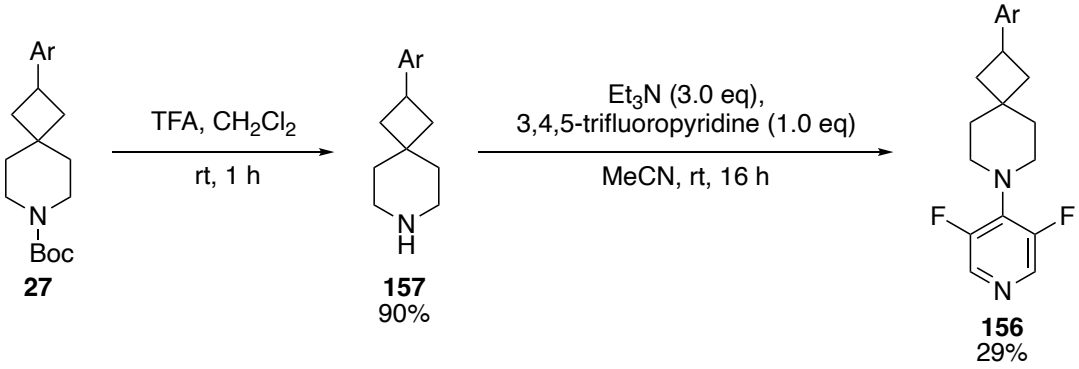

Scheme 4.2

4.2 *N*-Functionalisation of Aryl Cyclobutanes

After the successful cross-coupling of several aryl halides with cyclobutyl trifluoroborate salt **25** to produce aryl cyclobutanes **27**, the final stage was to explore the *N*-functionalisation of some of these compounds. In all of the *N*-functionalisation reactions, the first step was to remove the Boc group under acidic conditions. After this, robust *N*-functionalisation reactions such as sulfonamide formation and amide coupling were to be used to obtain a selection of lead-like compounds.

As a first example, Boc removal on pyrimidine cyclobutane **133** using 4 N HCl in dioxane at room temperature for 1 h produced pyrimidine cyclobutyl HCl salt **158**. Then, using conditions from Whitlock *et al*.,[122] pyrimidine cyclobutyl HCl salt **158** was mesylated using mesyl chloride (2.2 eq) and Et_3N (4.8 eq) in CH_2Cl_2 at room temperature for 16 h. After purification by chromatography, *N*-methanesulfonamide pyrimidine cyclobutane **159** was obtained in 67% yield (Scheme 4.3). Thus, it was demonstrated that lead-like compounds could be produced from the developed 3-D building block, cyclobutyl trifluoroborate salt **25**.

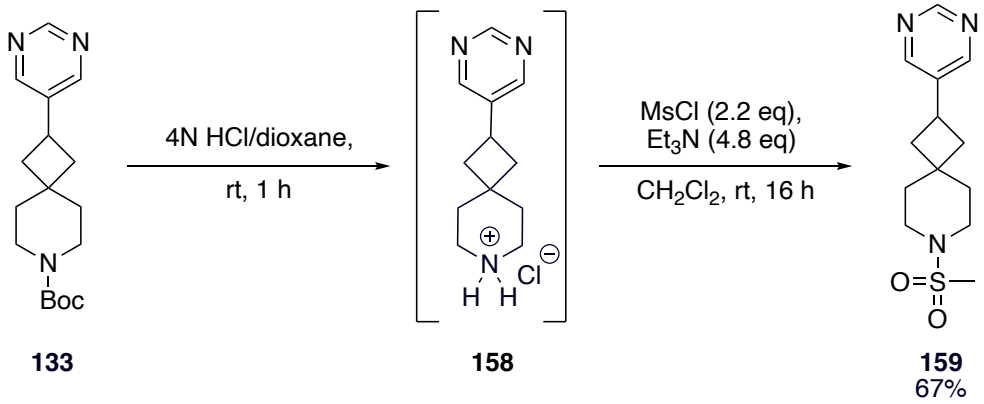

Scheme 4.3

The ^{1}H NMR spectrum of *N*-methanesulfonamide pyrimidine cyclobutane **159** is shown in Figure 4.2. One key feature of this spectrum is the absence of the Boc signal at ~δ_H 1.4. Of note, a 3H singlet at δ_H 2.77 from the protons of the methyl group of the sulfonamide is present. Other than this difference, the ^{1}H NMR spectrum of *N*-methanesulfonamide pyrimidine cyclobutane **159** does not significantly differ from that of its Boc protected precursor pyrimidine cyclobutane **133** (see Figure 3.3).

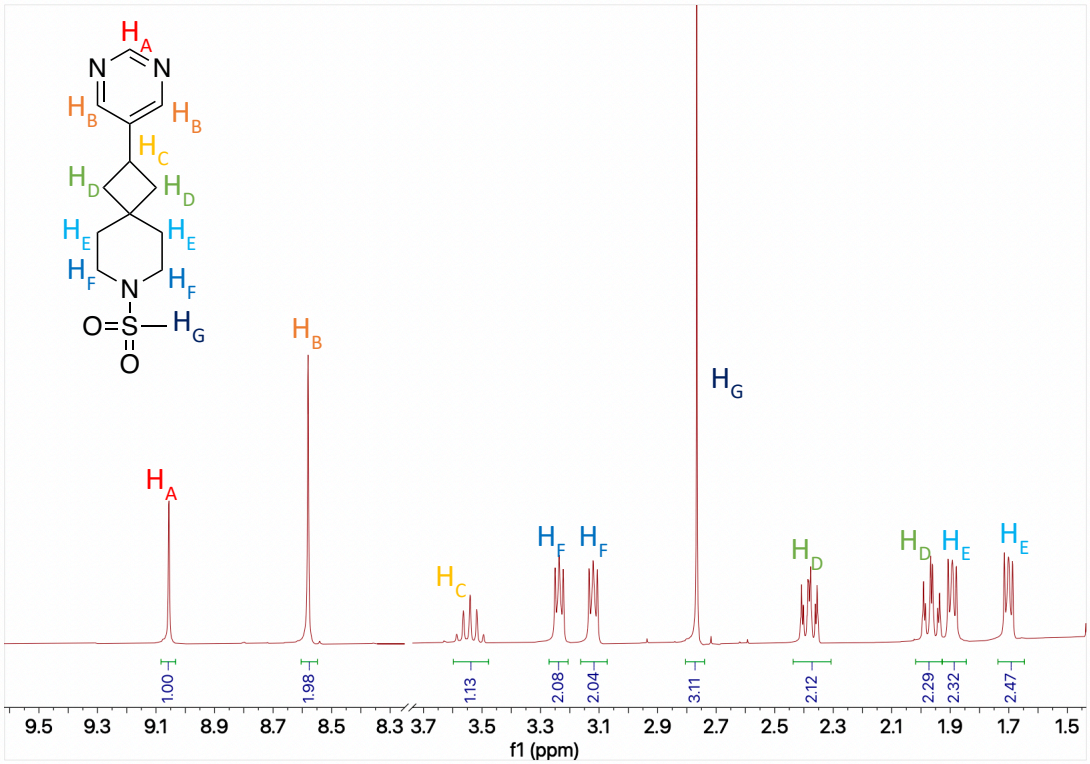

*Figure 4.2 – ^{1}H NMR spectrum of N-methanesulfonamide pyrimidine cyclobutane **159***

Once *N*-methanesulfonamide pyrimidine cyclobutane **159** was obtained, crystals of it were grown and its X-ray crystal structure determined (Figure 4.3a). This lead-like compound was specifically targeted in order to obtain an X-ray crystal structure to allow comparison with the nine previously prepared cyclopropane pyrimidine methanesulfonamides described in Section 1.3. With the information from its X-ray crystal structure, the parameters for exit vector analysis could be determined for *N*-methanesulfonamide pyrimidine cyclobutane **159** and the coordinates plotted on an exit vector plot alongside the nine O'Brien *N*-methanesulfonamide pyrimidine cyclopropanes.[123] The results of the vector analysis are visualised in Figure 4.3b. To our delight, *N*-methanesulfonamide pyrimidine cyclobutane **159** appeared in a new area of chemical space (red coordinate) compared to the other nine O'Brien *N*-methanesulfonamide pyrimidine cyclopropanes (blue coordinates). See Figure 1.8 for more information on the exit vector analysis for the nine O'Brien *N*-methanesulfonamide pyrimidine cyclopropanes.

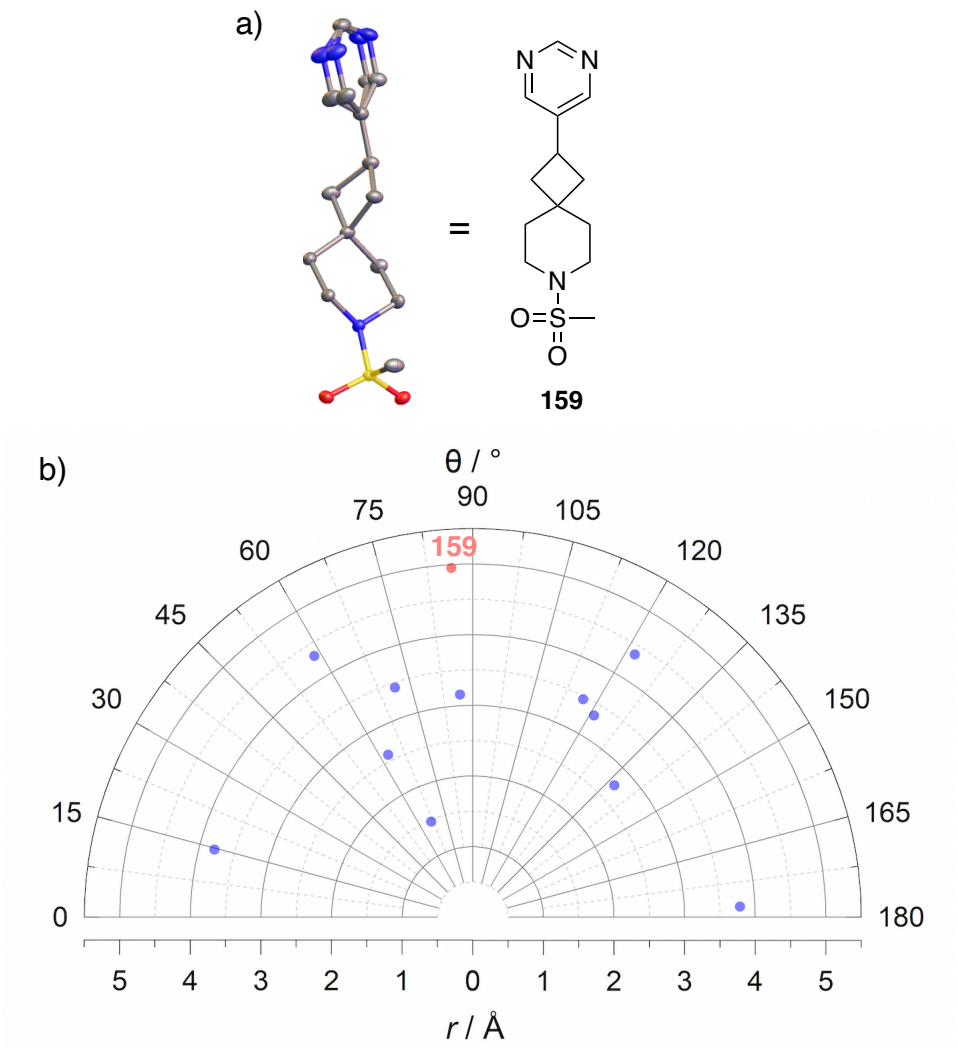

a) X-ray crystal structure of *N*-methanesulfonamide pyrimidine cyclobutane **159**; b) exit vector plot of *N*-methanesulfonamide pyrimidine cyclobutane **159** (red) and nine O'Brien cyclopropyl building blocks (blue).

*Figure 4.3 – X-ray crystal structure and exit vector plot of N-methanesulfonamide pyrimidine cyclobutane **159***

With the success of obtaining *N*-methanesulfonamide pyrimidine cyclobutane **159**, a different sulfonamide formation reaction was carried out. This time, Boc removal on ethyl ester phenyl cyclobutane **132** was carried out using the same conditions as previously described. Conditions for the sulfonamide formation reaction were taken from Weber *et al.*,[124] with the addition of DMAP as a catalyst. The HCl salt and medicinally relevant heteroaromatic 3,5-dimethylisoxazole-4-sulfonyl chloride (1.25 eq) were reacted in the presence of Et_3N (5.0 eq) and DMAP (0.1 eq) in CH_2Cl_2 at 0 °C to room temperature for 18 h. After purification by chromatography, *N*-dimethyloxazolylsulfonyl ethyl ester phenyl cyclobutane **160** was obtained in 79% yield (Scheme 4.4).

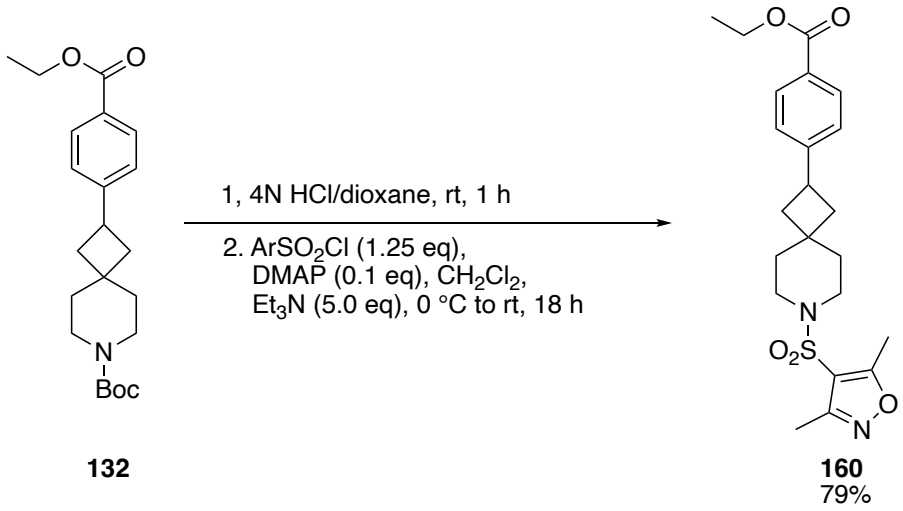

Scheme 4.4

To demonstrate diversity in *N*-functionalisation reactions with aryl cyclobutanes **27**, amide coupling reactions were also carried out. The first substrate used in an amide coupling reaction was acetanilide cyclobutane **135**. This substrate underwent Boc removal, as previously described, before carrying out an amide coupling on the HCl salt. Conditions for this amide coupling were taken from Maryanoff *et al*.[125] The HCl salt was reacted with benzoyl chloride (1.25 eq) and Et_3N (2.0 eq) in CH_2Cl_2 at 0 ℃ to room temperature for 18 h. Chemoselectivity could have been a potential issue with this reaction as the amide nitrogen could also have been acylated. This would be unlikely as amines are more reactive than amides in acylation. We saw no evidence of amide acylation and the desired product *N*-benzamide acetanilide cyclobutane **161** was isolated in 61% yield after chromatography (Scheme 4.5).

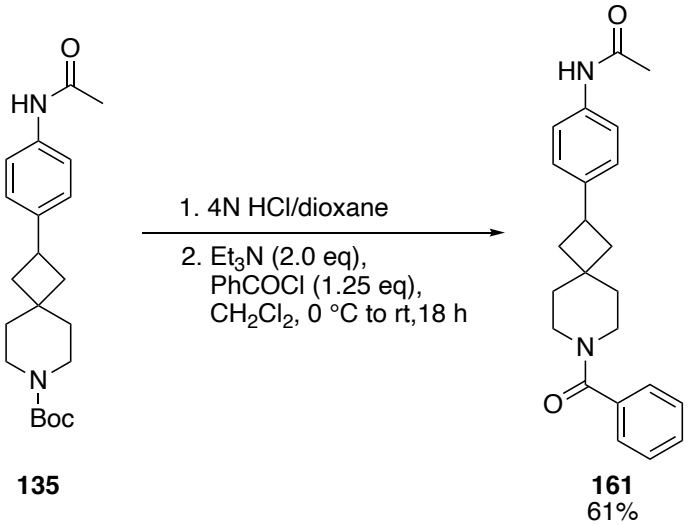

Scheme 4.5

A different amide coupling reaction was carried out on methoxypyridine cyclobutane **134**. The HCl salt was prepared in the usual way. Conditions for the amide coupling were taken from Lee *et al.*[126] Thus, acetic anhydride (6.0 eq) was reacted with the HCl salt in pyridine at room temperature for 18 h. After purification by chromatography, *N*-acetamide methoxypyridine cyclobutane **162** was isolated in an excellent 90% yield (Scheme 4.6).

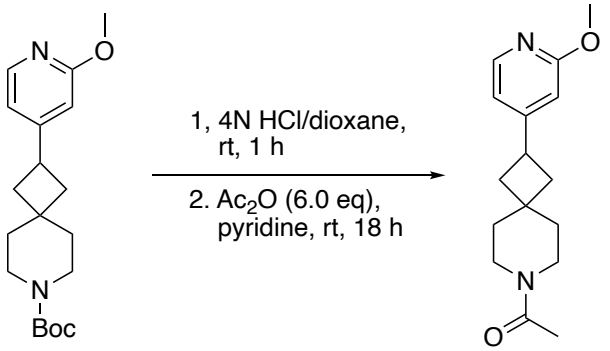

Scheme 4.6

A final amide coupling reaction was executed on phenyl cyclobutane **149**. After Boc removal using the standard conditions, the HCl salt was reacted with heteroaromatic indole-3-carboxylic acid (1.2 eq) in the presence of 50% T3P in toluene (2.0 eq) and Et_3N (4.0 eq) in ethyl acetate at 0 ℃ to 80 ℃ for 18 h, following conditions from Bamberg *et al.*[127] After purification by chromatography, *N*-indoleamide phenyl cyclobutane **163** was isolated in 55% yield (Scheme 4.7).

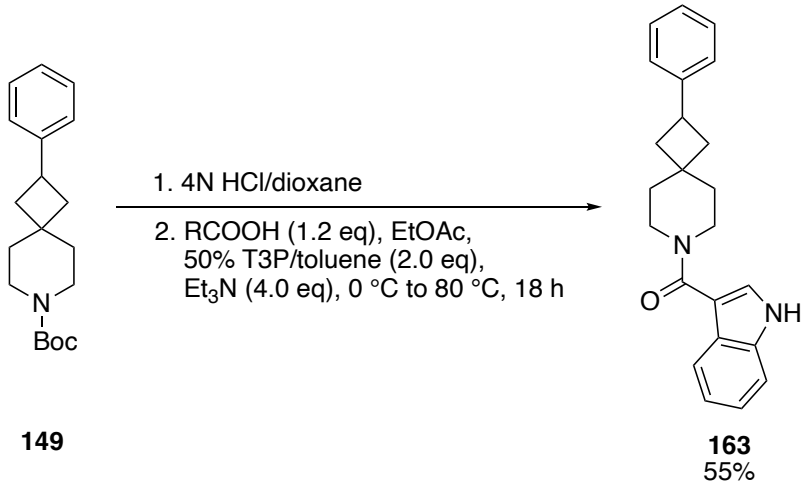

Scheme 4.7

Overall, both sulfonamide formation and amide coupling reactions from different aryl cyclobutanes **27** were accomplished. A variety of aryl cyclobutanes were *N*-

functionalised with success (55-90%, Scheme 4.8). Moreover, the *N*-functionalisation reactions introduced a variety of moieties including medicinally relevant heteroaromatic substrates. This demonstrates the potential to create lead-like compounds for drug development from aryl cyclobutanes **27**. With the X-ray crystal structure from *N*-methanesulfonamide pyrimidine cyclobutane **159**, vector analysis was carried out and it was possible to show that a new area of chemical space was accessed by this lead-like compound compared to the other nine O'Brien pyrimidine mesylate cyclopropanes. This exciting result presents the potential for *N*-functionalised aryl cyclobutanes **28** to access a different area of a target protein in drug design, therefore potentially increasing interactions between the drug and the protein and increasing potency, leading to more possibilities in the future for drug design.

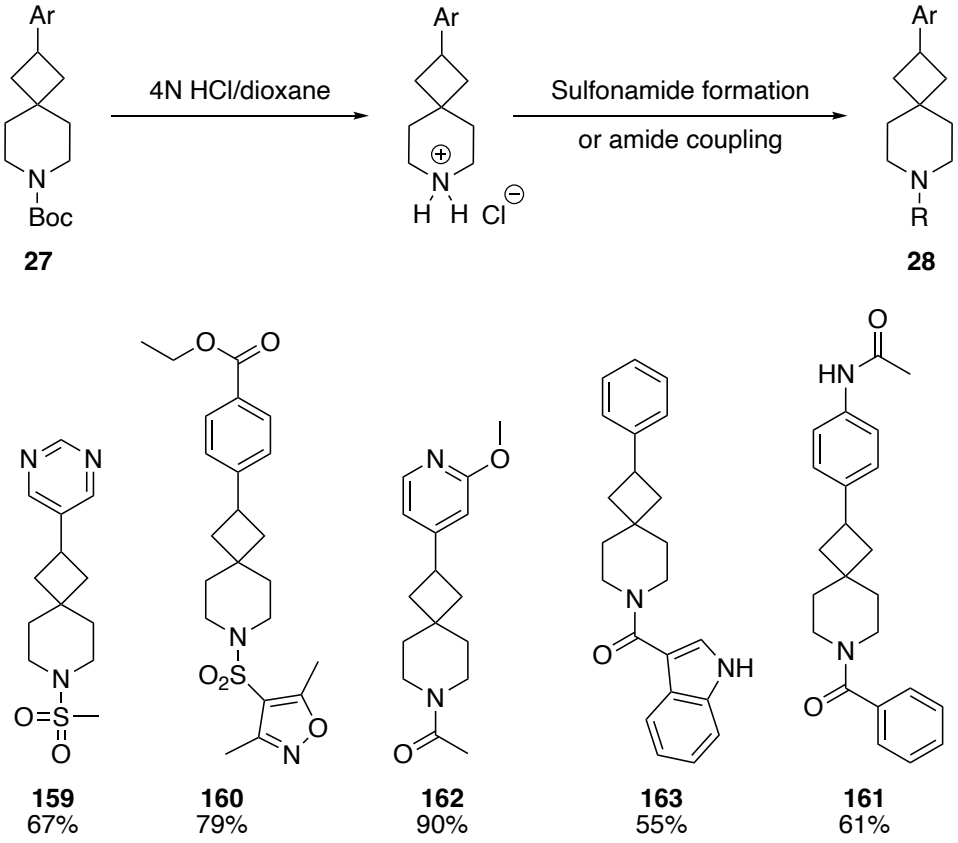

Scheme 4.8

5. Conclusions and Future Work

In summary, the work described in this MSc thesis has demonstrated that it will be possible to utilise cyclobutyl trifluoroborate salt **25** (Figure 5.1) as a new 3-D building block in the O'Brien group modular synthetic platform for fragment elaboration in 3-dimensions. This would be the first cyclobutyl-based 3-D building block added into the library.

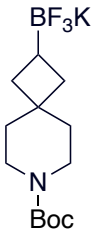

25

*Figure 5.1 – Cyclobutyl trifluoroborate salt **25***

Cyclobutyl trifluoroborate salt **25** (Figure 5.1) was successfully synthesised in gram quantities using two separate synthetic routes. The first route was a five-step synthetic route including reduction, tosylation, elimination, hydroboration and trifluoroborate salt formation reactions with four purifications, and gave cyclobutyl trifluoroborate salt **25** in 39% overall yield. This route was time-consuming and one of the key synthetic intermediates was volatile. Therefore, a higher yielding and more time-efficient route was developed. This was a four-step synthetic route to produce cyclobutyl trifluoroborate salt **25** using enol triflate formation, Miyaura borylation, hydrogenation and trifluoroborate salt formation reactions. Cyclobutyl trifluoroborate salt **25** was prepared in 68% overall yield using the four-step route. The four-step synthesis was preferred due to the higher yields, reduced number of steps and time efficiency, as only one chromatographic purification was necessary.

Ni-catalysed photoredox cross-coupling with cyclobutyl trifluoroborate salt **25** using conditions developed by Molander *et al.*[80] and a variety of aryl bromides including medicinally relevant FragLites[20] was successfully carried out. Pyrimidine cyclobutane **133**, methoxypyridine cyclobutane **134**, ethyl ester phenyl cyclobutane **132**, acetanilide cyclobutane **135**, and methanesulfonylphenyl cyclobutane **136** were obtained in 39%-84% yields (Scheme 5.1). However, the results of the cross-couplings were variable as some of the FragLites failed to cross-couple to cyclobutyl trifluoroborate salt **25**. For

example, sulfamoylphenyl cyclobutane **137**, pyrazole cyclobutane **138** and aminopyridine cyclobutane **139** were not obtained (Scheme 5.1). This could have been due to oxidation of the lone pairs of the amino groups inhibiting the reaction.

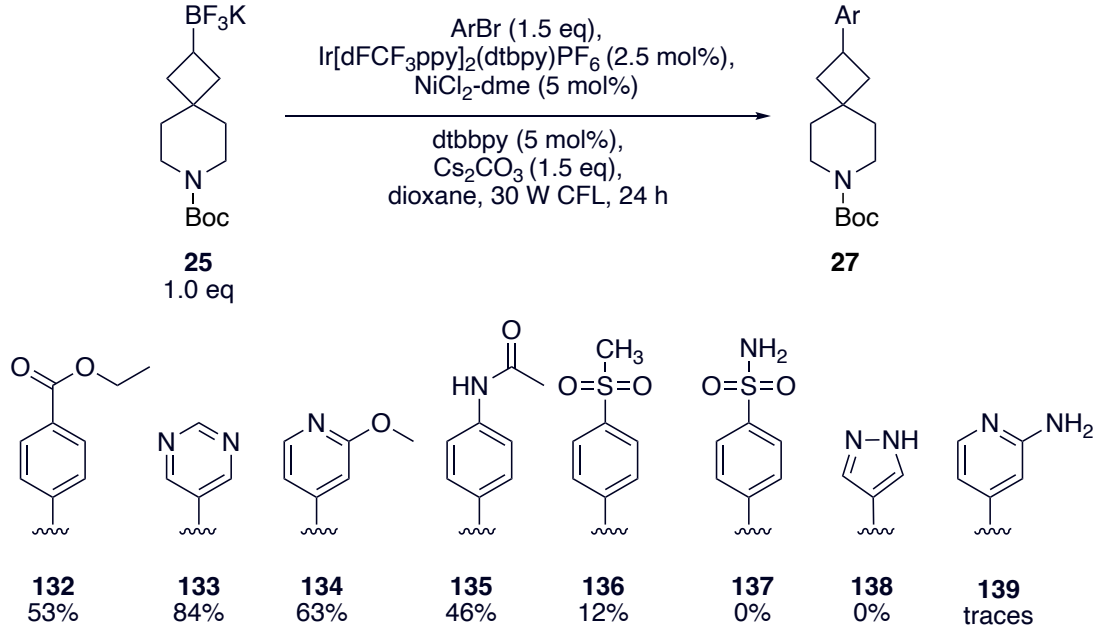

Scheme 5.1

Ni-catalysed photoredox cross-coupling from cyclobutanol **50** using conditions developed by Dong and MacMillan[91] were also successful as ethyl ester phenyl cyclobutane **132** and sulfonamide aryl cyclobutane **135** were both produced (Scheme 5.2). Interestingly, sulfonamide aryl cyclobutane **135** was successfully produced using conditions from Dong and MacMillan[91] but not using conditions from Molander *et al.*[80] highlighting the potential to use both methods to cross-couple a wider range of aryl bromides to the building block. Despite this, purifications were challenging for cross-coupled products from conditions by Dong and MacMillan.[91] Therefore, cross-coupling from cyclobutyl trifluoroborate salt **25** was preferred and is recommended for future studies.

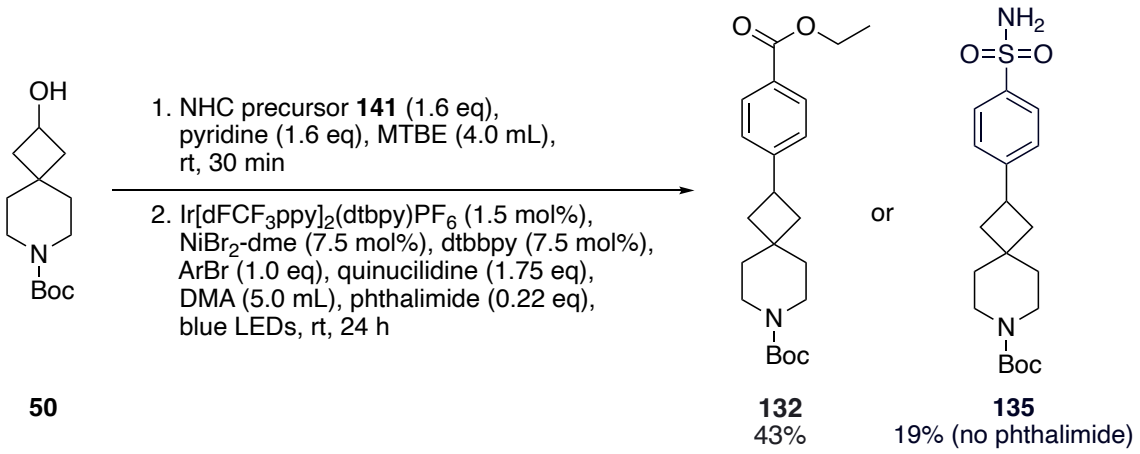

Scheme 5.2

During this project, Pd-catalysed Suzuki-Miyaura cross-coupling (SMCC) reactions of cyclobutyl trifluoroborate salt **25** have been developed, albeit with a high catalyst loading (10 mol% $Pd(OAc)_2$) (Scheme 5.3). Chlorobenzene produced higher yields of phenyl cyclobutane **149** than bromobenzene. Varying equivalents of aryl halide and cyclobutyl trifluoroborate salt **25** had a negligible effect on the yield. Finally, a substrate scope using SMCC with FragLites[20] was explored. Pyrimidine cyclobutane **133** and methanesulfonylphenyl cyclobutane **136** were both successfully cross-coupled. Due to the lack of SMCC reactions on cyclobutyl substrates in the literature, it was particularly exciting that it was possible to cross-couple two FragLites to cyclobutyl trifluoroborate salt **25**. Sulfamoylphenyl cyclobutane **137** and acetanilide cyclobutane **135** were not formed in the attempted SMCC reactions.

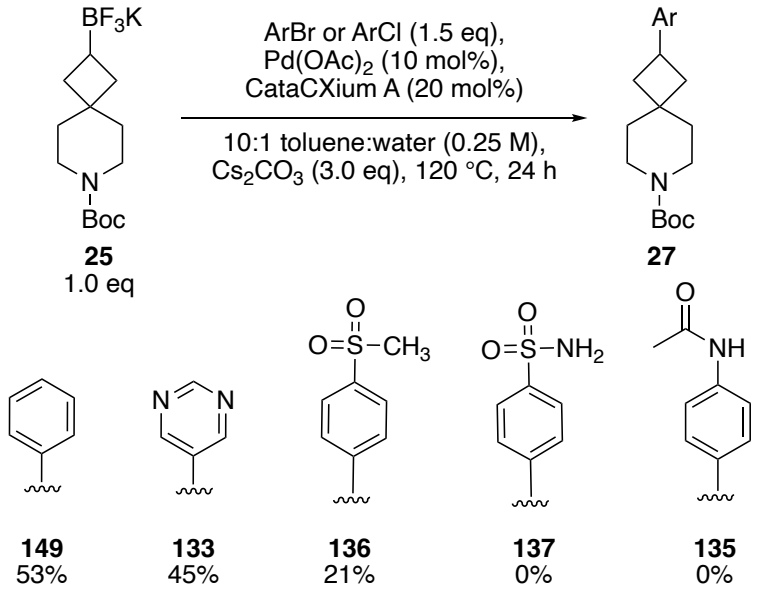

Scheme 5.3

Finally, *N*-functionalisation reactions of aryl cyclobutanes **27** afforded five diverse lead-like compounds for potential use in medicinal chemistry (Figure 5.2). An X-ray crystal structure of *N*-methanesulfonamide pyrimidine cyclobutane **159** was obtained and used in exit vector analysis. This exit vector analysis revealed that *N*-methanesulfonamide pyrimidine cyclobutane **159** accessed a new area of chemical space compared to the other nine O'Brien pyrimidine *N*-methanesulfonamide cyclopropanes.

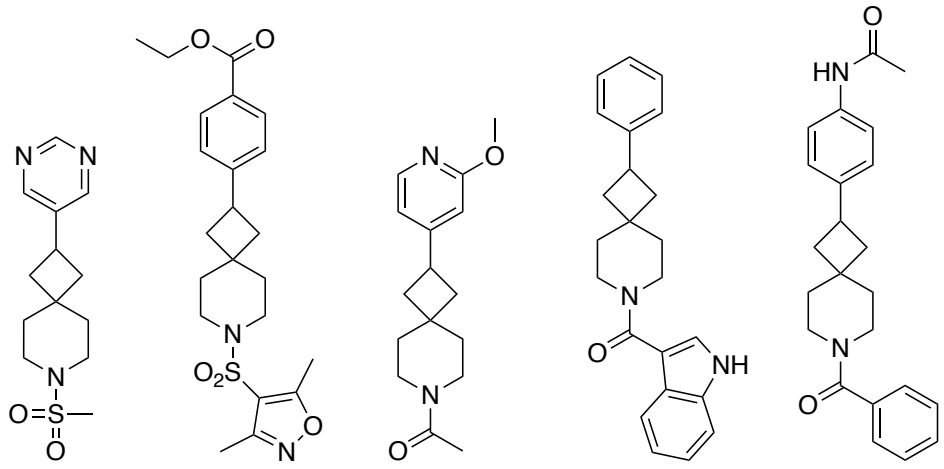

Figure 5.2 – N-functionalised lead-like compounds synthesised using sulfonamidation and amidation reactions

Future work could include cross-coupling the full set of FragLites[20] to the building block, and it may be necessary to use both Ni-catalysed photoredox cross-coupling and Pd-catalysed SMCC methods to achieve this. Protecting groups could be used on some of the FragLites due to potentially reactive functionalities interfering with the cross-coupling methods. Another possibility for future work is to expand the set of cyclobutyl building blocks and ultimately functionalise these to demonstrate that lead-like compounds can be generated. Some building blocks of interest include azetidine spirocyclobutyl trifluoroborate salt **164**, fused pyrrolidine cyclobutyl trifluoroborate salt *exo*-**165** and fused pyrrolidine cyclobutyl trifluoroborate salts *endo*-**166** and *exo*-**167** (Figure 5.3). With the success of synthesising, cross-coupling and *N*-functionalising cyclobutyl trifluoroborate salt **25**, the knowledge gained from this process could be applied to the synthesis and cross-coupling of other, more hindered building blocks. Indeed, fused pyrrolidine cyclobutyl trifluoroborate salt *exo*-**165** has already been successfully synthesised and cross-coupled using Ni-catalysed photoredox and Pd-catalysed SMCC reactions.[128]

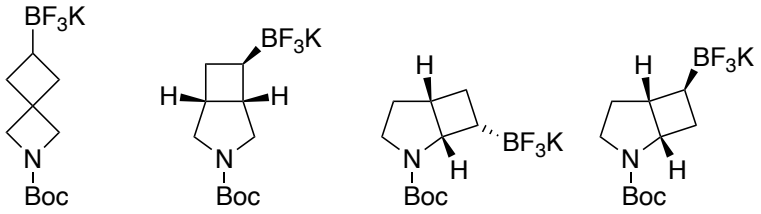

164 *exo*-**165** *endo*-**166** *exo*-**167**

Figure 5.3 – Possible future cyclobutane building blocks

6. Experimental Section

6.1. General Methods

All non-aqueous reactions were carried out under oxygen-free Ar or N_2 atmosphere using flame-dried glassware. Brine refers to a saturated $NaCl_{(aq)}$ solution. Water is distilled water. Flash column chromatography was carried out using Fluka Chemie GmbH silica (220-440 mesh). Thin layer chromatography was carried out using commercially available Merck F254 aluminium backed silica plates. Spots were visualised by UV and appropriate stains ($KMnO_4$ and Ninhydrin). Proton (400 MHz) and carbon (100.6 MHz) NMR spectra were recorded on a Jeol ECX-400 instrument using an internal deuterium lock. For samples recorded in $CDCl_3$, chemical shifts are quoted in parts per million relative to $CHCl_3$ (δ_H 7.26) and $CDCl_3$ (δ_C 77.0, central line of triplet). For samples recorded in *d*$_6$-DMSO, chemical shifts are quoted in parts per million relative to DMSO (δ_H 2.50, central line of quintet) and *d*$_6$-DMSO (δ_C 39.5, central line of septet). Carbon NMR spectra were recorded with broad band proton decoupling and assigned using DEPT and HSQC experiments. Coupling constants (*J*) are quoted in Hertz. Melting points were carried out on a Gallenkamp melting point apparatus. Infrared spectra were recorded on an ATI Mattson Genesis FT-IR spectrometer. Electrospray high and low resonance mass spectra were recorded at room temperature on a Bruker Daltronics microOTOF spectrometer.

6.2. General Procedures

General procedure A: Ni-catalysed photoredox cross-coupling of alkyl trifluoroborate salts

4,4'-Di-*tert*-butyl-2,2'-bipyridine (4 mg, 0.0125 mmol, 5 mol%), $NiCl_2$-dme (3 mg, 0.0125 mmol, 5 mol%) and THF (0.5 mL) were added to a glass vial equipped with a Teflon-coated magnetic stirrer bar. The vial was capped and the resulting suspension was heated with a heat gun until the nickel and ligand were fully solubilised. This gave a pale green solution. The solvent was evaporated under reduced pressure to give a fine coating of the ligated nickel complex on the side of the vial. Then, alkyl trifluoroborate salt (0.25-0.375 mmol, 1.0-1.5 eq), aryl bromide (0.25-0.375 mmol, 1.0-1.5 eq), $[Ir(dFCF_3ppy]_2(dtbpy)]PF_6$ (7 mg, 0.00625 mmol, 2.5 mol%), Cs_2CO_3 (123 mg, 0.375 mmol, 1.5 eq) and dioxane (5 mL) were added. The vial was capped and purged with Ar for 20 min. The vial was sealed with parafilm and stirred approximately 4 cm away from a 30 W fluorescent light bulb at ~24 ℃ for 16 h. A fan was blown across the reaction set-up to maintain a temperature of ~24 ℃. Then, the solids were removed by filtration through a plug of Celite® washing with EtOAc (10 mL). The filtrate was evaporated under reduced pressure to give the crude product.

General procedure B: Suzuki-Miyaura cross-coupling of cyclobutyl trifluoroborate salt 25

Cyclobutyl trifluoroborate salt **25** (0.3-0.45 mmol, 1.0-1.5 eq), aryl halide (0.3-0.45 mmol, 1.0-1.5 eq), $Pd(OAc)_2$ (2 mol% or 10 mol%), CataCXium A (3 mol% or 20 mol%) and Cs_2CO_3 (293 mg, 0.9 mmol, 3.0 eq) were added to a 7 mL vial. The vial was sealed with a screw top cap with a PTFE/silicone septum. The vial was purged under N_2 for 20 min. Then, degassed toluene and degassed water (10:1, 1.2 mL) were added under N_2. The resulting mixture was stirred at 1000 rpm and heated at either 100 ℃ or 120 ℃ (heater block temperature) for 24 h. After being allowed to cool to rt, saturated $NH_4Cl_{(aq)}$ (3 mL) was added and the two layers were separated. The aqueous layer was extracted with EtOAc (3 × 3 mL) and the combined organics were washed with brine (10 mL), dried ($MgSO_4$) and evaporated under reduced pressure to give the crude product.

General procedure C: Suzuki-Miyaura cross-coupling of cyclobutyl trifluoroborate salt 25

Cyclobutyl trifluoroborate salt **25** (0.3-0.45 mmol, 1.0-1.5 eq), $Pd(OAc)_2$ (7 mg, 30 μmol, 10 mol%), CataCXium A (21.5 mg, 60 μmol, 20 mol%), and Cs_2CO_3 (293 mg, 0.9 mmol, 3.0 eq) were added to a 7 mL vial. The vial was sealed with a screw top cap with a PTFE/silicone septum. The vial was purged under N_2 for 20 min. Then, aryl halide (0.3-0.45 mmol, 1.0-1.5 eq), degassed toluene and degassed water (10:1, 1.2 mL) were added under N_2. The resulting mixture was stirred at 1000 rpm and heated at 120 °C (heater block temperature) for 24 h. After being allowed to cool to rt, saturated $NH_4Cl_{(aq)}$ (3 mL) was added and the two layers were separated. The aqueous layer was extracted with EtOAc (3 × 3 mL), and the combined organics were washed with brine (10 mL), dried ($MgSO_4$) and evaporated under reduced pressure to give the crude product.

6.3. Experimental Procedures and Characterisation Data

***tert*-Butyl 2-oxo-7-azaspiro[3.5]nonane-7-carboxylate 30**

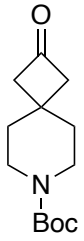

30

Zn-Cu couple (721 mg, 11.0 mmol, 11.0 eq) was added to a stirred solution of *N*-Boc-4-methylene piperidine **48** (197 mg, 1.0 mmol, 1.0 eq) in MTBE (4 mL) under Ar. Then, a solution of trichloroacetyl chloride (0.5 mL, 4.0 mmol, 4.0 eq) in DME (1.6 mL) was added dropwise at 0 ℃. The resulting mixture was stirred at rt for 16 h. The solids were removed by filtration through a plug of Celite®. The filtrate was evaporated under reduced pressure and dissolved in EtOAc (20 mL). This solution was washed with H_2O (20 mL) and saturated $NaHCO_{3(aq)}$ (20 mL). Then, the basic aqueous layer was extracted with EtOAc (3 × 20 mL). The combined organic extracts and the original EtOAc extract were washed with brine (25 mL), dried ($MgSO_4$) and evaporated under reduced pressure to give the crude dichlorocyclobutanone **49**. The crude dichlorocyclobutanone **49** was dissolved in MeOH (5 mL). NH_4Cl (375 mg, 7.0 mmol, 7.0 eq) and activated Zn powder (654 mg, 10.0 mmol, 10.0 eq) were added and the resulting mixture was stirred at rt for 16 h. The solids were removed by filtration through a plug of Celite®. The filtrate was evaporated under reduced pressure and dissolved in EtOAc (20 mL). This solution was washed with H_2O (20 mL). Then, the aqueous layer was extracted with EtOAc (3 × 20 mL). The combined organic extracts and the original EtOAc extract were washed with brine (25 mL), dried ($MgSO_4$) and evaporated under reduced pressure to give the crude product. Purification by flash column chromatography on silica with 9:1 to 17:3 hexane-EtOAc as eluent gave cyclobutanone **30** (92 mg, 39%) as a white solid, mp 49-51 ℃ (lit.,[129] 55-56 ℃); R_F (17:3 hexane-EtOAc) 0.22; IR (ATR) 2919, 1782 (C=O, ketone), 1686 (C=O, Boc), 1417, 1166, 770 cm^{-1}; ^1H NMR (400 MHz, $CDCl_3$) δ 3.39 (t, J = 5.5 Hz, 4H, NCH), 2.79 (s, 4H, CHCO), 1.68 (t, J = 5.5 Hz, 4H, CH), 1.44 (s, 9H, CMe_3); ^{13}C NMR (100.6 MHz, $CDCl_3$) (rotamers) δ 206.7 (C=O, ketone), 154.9 (C=O, Boc), 79.8 (O*C*Me_3), 56.5 (*C*H_2C=O), 42.3 (br, NCH_2), 36.6 (C), 29.2 (C*Me*$_3$), 28.6 (CH_2), 28.5

(CH_2); HRMS (ESI) *m/z* calcd for $C_{13}H_{21}NO_3$ $(M + Na)^+$ 262.1414, found 262.1418 (–1.7 ppm error). Spectroscopic data consistent with those reported in the literature.[70]
Lab book reference: HSK-1-1

Zn-Cu couple (3.65 g, 55.8 mmol, 11.0 eq) was added to a stirred solution of *N*-Boc-4-methylene piperidine **48** (1 g, 5.07 mmol, 1.0 eq) in MTBE (21 mL) under Ar. Then, a solution of trichloroacetyl chloride (2.3 mL, 20.3 mmol, 4.0 eq) in DME (9 mL) was added dropwise at 0 ℃. The resulting mixture was stirred at rt for 16 h. The solids were removed by filtration through a plug of Celite®. The filtrate was evaporated under reduced pressure and added to saturated $NaHCO_{3(aq)}$ (20 mL), dried ($MgSO_4$) and the solids removed by filtration through a plug of Celite®. The reaction mixture was dissolved in EtOAc (20 mL) and washed with H_2O (2 × 20 mL). The organic extracts and the original EtOAc extract were washed with brine (25 mL), dried ($MgSO_4$) and evaporated under reduced pressure to give the crude dichlorocyclobutanone **49**. The crude dichlorocyclobutanone **49** was dissolved in MeOH (25 mL). NH_4Cl (1.87 g, 35.0 mmol, 7.0 eq) and activated Zn powder (3.32 g, 50.7 mmol, 10.0 eq) were added and the resulting mixture stirred at rt for 16 h. The solids were removed by filtration through a plug of Celite®. The filtrate was evaporated under reduced pressure, dissolved in EtOAc (20 mL) and washed with H_2O (20 mL). Then, the aqueous layer was extracted with EtOAc (3 × 20 mL). The combined organic extracts and the original EtOAc extract were washed with brine (25 mL), dried ($MgSO_4$) and evaporated under reduced pressure to give the crude product. Purification by flash column chromatography on silica with 9:1 to 17:3 hexane-EtOAc as eluent gave cyclobutanone **30** (236 mg, 19%) as a white solid, identical (by ^1H NMR spectroscopy) to that described above.
Lab book reference: HSK-1-11

Zn-Cu couple (7.3 g, 112 mmol, 11.0 eq) was added to a stirred solution of *N*-Boc-4-methylene piperidine **48** (2 g, 10.1 mmol, 1.0 eq) in MTBE (42 mL) under Ar. Then, a solution of trichloroacetyl chloride (4.6 mL, 40.6 mmol, 4.0 eq) in DME (18 mL) was added dropwise at 0 ℃. The resulting mixture was stirred at rt for 16 h. The solids were removed by filtration through a plug of Celite®. The filtrate was evaporated under reduced pressure. The filtrate was cooled to 0 ℃. Saturated $NaHCO_{3(aq)}$ was added (20 mL) and stirred at 0 ℃ for 10 min. The solids were removed by filtration through a plug

of Celite®. The reaction mixture was dissolved in EtOAc (20 mL) and washed with H_2O (20 mL). The organic extracts and the original EtOAc extract were washed with brine (25 mL), dried ($MgSO_4$) and evaporated under reduced pressure to give the crude dichlorocyclobutanone **49**. The crude dichlorocyclobutanone **49** was dissolved in MeOH (50 mL). NH_4Cl (3.74 g, 70.0 mmol, 7.0 eq) and activated Zn powder (6.64 g, 101 mmol, 10.0 eq) were added and the resulting mixture stirred at rt for 16 h. The solids were removed by filtration through a plug of Celite®. The filtrate was evaporated under reduced pressure, dissolved in EtOAc (20 mL) and washed with H_2O (20 mL). Then, the aqueous layer was extracted with EtOAc (3 × 20 mL). The combined organic extracts and the original EtOAc extract were washed with brine (25 mL), dried ($MgSO_4$) and evaporated under reduced pressure to give the crude product. Purification by flash column chromatography on silica with 9:1 to 17:3 hexane-EtOAc as eluent gave cyclobutanone **30** (946 mg, 39%) as a white solid, identical (by ^{1}H NMR spectroscopy) to that described above.

Lab book reference: HSK-1-16

Zn-Cu couple (7.3 g, 112 mmol, 11.0 eq) was added to a stirred solution of *N*-Boc-4-methylene piperidine **48** (2 g, 10.0 mmol, 1.0 eq) in Et_2O (42 mL) at 0 ℃ under Ar. Then, a solution of trichloroacetyl chloride (4.6 mL, 41.0 mmol, 4.0 eq) in DME (18 mL) was added dropwise at 0 ℃. The resulting mixture was stirred at rt for 16 h. The filtrate was cooled to 0 ℃. Saturated $NaHCO_{3(aq)}$ was added (20 mL) and stirred at 0 ℃ for 10 min. The solids were removed by filtration through a plug of Celite®, eluting with Et_2O. The filtrate was evaporated under reduced pressure, dissolved in Et_2O (20 mL), and washed with H_2O (20 mL). Then, the aqueous layer was extracted with Et_2O (3 × 20 mL). The combined organic extracts and the original Et_2O extract were washed with brine (25 mL), dried ($MgSO_4$) and evaporated under reduced pressure to give the crude dichlorocyclobutanone **49**. The crude dichlorocyclobutanone **49** was dissolved in MeOH (50 mL). NH_4Cl (3.74 g, 70.0 mmol, 7.0 eq) and activated Zn powder (6.64 g, 101 mmol, 10.0 eq) were added and the resulting mixture stirred at rt for 16 h. The solids were removed by filtration through a plug of Celite®. The filtrate was evaporated under reduced pressure to give the crude product. Purification by flash column chromatography on silica with 19:1 to 3:1 hexane-EtOAc as eluent gave cyclobutanone **30** (1.919 g, 79%) as a white solid, identical (by ^{1}H NMR spectroscopy) to that described above.

Lab book reference: HSK-1-22

Zn-Cu couple (14.633 g, 223 mmol, 11.0 eq) was added to a stirred solution of *N*-Boc-4-methylene piperidine **48** (4 g, 20.3 mmol, 1.0 eq) in Et_2O (81.5 mL) at 0 ℃ under Ar. Then, a solution of trichloroacetyl chloride (9.1 mL, 81.0 mmol, 4.0 eq) in DME (32.5 mL) was added dropwise at 0 ℃. The resulting mixture was stirred at rt for 16 h. The filtrate was cooled to 0 ℃. Saturated $NaHCO_{3(aq)}$ was added (20 mL) and stirred at 0 ℃ for 10 min. The solids were removed by filtration through a plug of silica, eluting with Et_2O. The filtrate was evaporated under reduced pressure, dissolved in Et_2O (20 mL) and washed with H_2O (20 mL). Then, the aqueous layer was extracted with Et_2O (3 × 20 mL). The combined organic extracts and the original Et_2O extract were washed with brine (25 mL), dried ($MgSO_4$) and evaporated under reduced pressure to give the crude dichlorocyclobutanone **49**. The crude dichlorocyclobutanone **49** was dissolved in MeOH (101.5 mL). NH_4Cl (7.603 g, 142 mmol, 7.0 eq) and activated Zn powder (13.272 g, 203 mmol, 10.0 eq) were added and the resulting mixture stirred at rt for 16 h. The solids were removed by filtration through a plug of silica. The filtrate was evaporated under reduced pressure to give the crude product. Purification by flash column chromatography on silica with 99:1 to 49:1 CH_2Cl_2-acetone as eluent gave none of cyclobutanone **30** by ^{1}H NMR spectroscopy.

Lab book reference: HSK-1-29

Zn-Cu couple (2.162 g, 33.0 mmol, 11.0 eq) was added to a stirred solution of *N*-Boc-4-methylene piperidine **48** (592 mg, 3.0 mmol, 1.0 eq) in Et_2O (12 mL) at 0 ℃ under Ar. Then, a solution of trichloroacetyl chloride (1.4 mL, 12.0 mmol, 4.0 eq) in DME (4.8 mL) was added dropwise at 0 ℃. The resulting mixture was stirred at rt for 16 h. The filtrate was cooled to 0 ℃. Saturated $NaHCO_{3(aq)}$ was added (20 mL) and stirred at 0 ℃ for 10 min. The solids were removed by filtration through a plug of Celite®, eluting with Et_2O. The filtrate was evaporated under reduced pressure, dissolved in Et_2O (20 mL) and washed with H_2O (20 mL). Then, the aqueous layer was extracted with Et_2O (3 × 20 mL). The combined organic extracts and the original Et_2O extract were washed with brine (25 mL), dried ($MgSO_4$) and evaporated under reduced pressure to give the crude dichlorocyclobutanone **49**. The crude dichlorocyclobutanone **49** was dissolved in MeOH (15 mL). NH_4Cl (1.124 g, 21.0 mmol, 7.0 eq) and activated Zn powder (1.961 g, 30.0

mmol, 10.0 eq) were added and the resulting mixture stirred at rt for 16 h. The solids were removed by filtration through a plug of Celite®. The filtrate was evaporated under reduced pressure to give the crude product. Purification by flash column chromatography on silica with 9:1 to 4:1 hexane-EtOAc as eluent gave cyclobutanone **30** (267 mg, 37%) as a white solid, identical (by ^{1}H NMR spectroscopy) to that described above.
Lab book reference: HSK-1-41

***tert*-Butyl 2-hydroxy-7-azaspiro[3.5]nonane-7-carboxylate 50**

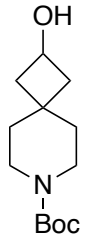

50

$NaBH_4$ (190 mg, 5.0 mmol, 1.0 eq) was added to a stirred solution of cyclobutanone **30** (1.197 g, 5.0 mmol, 1.0 eq) in MeOH (25 mL) at rt under Ar. The resulting solution was stirred at rt for 16 h. Then, the solvent was evaporated under reduced pressure and the residue was dissolved in EtOAc (20 mL) and washed with H_2O (20 mL). The aqueous layer was extracted with EtOAc (3 × 20 mL). The combined organic extracts and the original EtOAc extract were washed with brine (25 mL), dried ($MgSO_4$) and evaporated under reduced pressure to give crude cyclobutanol **50**. Purification by flash column chromatography on silica with 9:1 to 1:1 hexane-Et_2O as eluent gave cyclobutanol **50** (1.079 g, 89%) as a white solid, mp 88-90 ℃, R_F (7:3 hexane-EtOAc) 0.1; IR (ATR) 3439 (br, OH), 2927, 1664 (C=O), 1436, 1268, 1150, 1061, 879, 549 cm^{-1}; ^{1}H NMR (400 MHz, $CDCl_3$) δ 4.30–4.26 (m, 1H, C*H*OH), 3.33–3.22 (m, 4H, NCH), 2.73–2.42 (m, 1H, CHO*H*), 2.28–2.18 (m, 2H, C*H*CHO), 1.70–1.61 (m, 2H, C*H*CHO), 1.52–1.43 (m, 4H, CH), 1.41 (s, 9H, CMe_3); ^{13}C NMR (100.6 MHz, $CDCl_3$) (rotamers) δ 155.1 (C=O), 79.5 (O*C*Me_3), 63.1 (HOCH), 42.6 (CH_2) , 41.0 (br, NCH_2), 39.5 (CH_2), 36.5 (CH_2), 30.2 I, 28.5 (OC*Me*$_3$); HRMS (ESI) *m/z* calcd for $C_{13}H_{23}NO_3$ $(M + Na)^+$ 264.1570 found 264.1579 (–3.2 ppm error). Spectroscopic data consistent with those reported in the literature.[67]
Lab book reference: HSK-1-55

***tert*-Butyl 2-[(4-methylbenzenesulfonyl)oxy]-7-azaspiro[3.5]nonane-7-carboxylate 40**

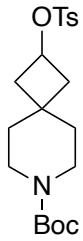

40

$NaBH_4$ (15 mg, 0.38 mmol, 1.0 eq) was added to a stirred solution of cyclobutanone **30** (92 mg, 0.38 mmol, 1.0 eq) in MeOH (1.9 mL) at rt under Ar. The resulting solution was stirred at rt for 1 h. Then, the solvent was evaporated under reduced pressure and the residue was dissolved in EtOAc (20 mL) and washed with H_2O (20 mL). The aqueous layer was extracted with EtOAc (3 × 20 mL). The combined organic extracts and the original EtOAc extract were washed with brine (25 mL), dried ($MgSO_4$) and evaporated under reduced pressure to give crude cyclobutanol **50**. *p*-TsCl (123 mg, 0.65 mmol, 1.7 eq) and Et_3N (0.11 mL, 0.81 mmol, 2.1 eq) were added to a stirred solution of the crude cyclobutanol **50** in CH_2Cl_2 (2 mL) at rt under Ar. The resulting solution was stirred at rt for 16 h. CH_2Cl_2 (20 mL) was added and the organic solution was washed with H_2O (20 mL), 1 M $HCl_{(aq)}$ (20 mL) and brine (25 mL), dried ($MgSO_4$) and evaporated under reduced pressure to give the crude product. Purification by flash column chromatography on silica with 9:1 to 4:1 hexane-EtOAc as eluent gave cyclobutyl tosylate **40** (56 mg, 37%) as a white solid, mp 50-52 ℃; R_F (4:1 hexane-EtOAc) 0.40; IR (ATR) 2930, 1689 (C=O), 1364, 1174, 1013, 5560 cm^{-1}; ^1H NMR (400 MHz, $CDCl_3$); δ 7.75 (d, *J* = 8.0 Hz, 2H, Ar), 7.36 (d, *J* = 8.0 Hz, 2H, Ar), 4.80 (tt, *J* = 7.5, 7.5 Hz, 1H, CHOTs), 3.31–3.20 (m, 2H, NCH), 2.44 (s, 3H, Me), 2.23–2.17 (m, 2H, C*H*CHO), 1.97–1.87 (m, 2H, C*H*CHO), 1.51–1.46 (m, 4H, CH), 1.42 (s, 9H, CMe_3); ^{13}C NMR (100.6 MHz, $CDCl_3$) (rotamers) δ 154.9 (C=O), 144.9 (*ipso*-Ar), 134.1 (*ipso*-Ar), 130.0 (Ar), 128.9 (Ar), 79.6 (O*C*Me_3), 71.7 (OCH), 40.9 (br, NCH_2), 40.0 (*C*H_2CHO), 39.0 (CH_2), 36.0 (CH_2), 32.1 (C), 28.5 (C*Me*$_3$), 21.8 (Me); HRMS (ESI) *m/z* calcd for $C_{20}H_{29}NO_5S$ $(M + Na)^+$ 418.1659, found 418.1658 (+0.3 ppm error). Spectroscopic data consistent with those reported in the literature.[66]

Lab book reference: HSK-1-4

p-TsCl (159 mg, 0.84 mmol, 2.0 eq) and Et_3N (0.15 mL, 1.05 mmol, 2.5 eq) were added to cyclobutanol **50** (100 mg, 0.42 mmol, 1.0 eq) in CH_2Cl_2 (2.1 mL) under Ar and stirred at rt for 16 h. CH_2Cl_2 (20 mL) was added and the resulting solution washed with H_2O (20 mL), 1 M $HCl_{(aq)}$ (20 mL) and brine (25 mL), dried ($MgSO_4$) and evaporated under reduced pressure to give the crude product. Purification by flash column chromatography on silica with 99:1 to 17:3 hexane-EtOAc as eluent gave cyclobutyl tosylate **40** (116 mg, 70%) as a white solid, identical (by ^{1}H NMR spectroscopy) to that described above.
Lab book reference: HSK-1-58

$NaBH_4$ (378 mg, 10.0 mmol, 1.0 eq) was added to cyclobutanone **30** (2.393 g, 10.0 mmol, 1.0 eq) in MeOH (50 mL) under Ar and stirred at rt for 16 h. Then, the solvent was evaporated under reduced pressure and the residue dissolved in EtOAc (20 mL) and washed with H_2O (20 mL). The aqueous layer was extracted with EtOAc (3 × 20 mL). The combined organic extracts and the original EtOAc extract were washed with brine (25 mL), dried ($MgSO_4$) and evaporated under reduced pressure to give the crude cyclobutanol **50**. *p*-TsCl (3.813 g, 20.0 mmol, 2.0 eq) and Et_3N (3.5 mL, 25.0 mmol, 2.5 eq) were added to the crude cyclobutanol **50** in CH_2Cl_2 (50 mL) and stirred at rt for 16 h. CH_2Cl_2 (20 mL) was added and the resulting solution was washed with H_2O (20 mL), 1 M $HCl_{(aq)}$ (20 mL) and brine (25 mL), dried ($MgSO_4$) and evaporated under reduced pressure to give the crude product. Purification by flash column chromatography on silica with 99:1 to 4:1 hexane-EtOAc as eluent gave cyclobutyl tosylate **40** (2.402 g, 61%) as a white solid identical (by ^{1}H NMR spectroscopy) to that described above.
Lab book reference: HSK-2-106

tert-Butyl 7-azaspiro[3.5]non-1-ene-7-carboxylate 29

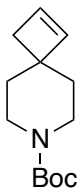

29

A solution of cyclobutyl tosylate **40** (1.232 g, 3.39 mmol, 1.0 eq) in DMSO (6.8 mL) was added dropwise to a stirred suspension of KO*t*-Bu (1.131 g, 10.2 mmol, 3.0 eq) in DMSO (20.4 mL) under Ar. The resulting suspension was stirred at rt for 4 h. Et_2O (20 mL) was added and the organic solution was washed with H_2O (20 mL) and brine (20 mL). The

aqueous layer was extracted with Et_2O (2 × 10 mL). The combined organic extracts and the original Et_2O extract were washed with brine (2 × 25 mL), dried ($MgSO_4$) and evaporated under reduced pressure to give crude cyclobutene **29**. Purification by flash column chromatography on silica with 99:1 to 49:1 hexane-EtOAc as eluent gave cyclobutene **29** (611 mg, 81%) as a colourless oil, R_F (49:1 hexane-EtOAc) 0.38; IR (ATR) 2919, 1692 (C=O), 1415, 1130, 899, 710 cm^{-1}; ^1H NMR (400 MHz, $CDCl_3$) δ 6.19 (d, *J* = 3.0 Hz, 1H, =CH), 6.11–6.05 (m, 1H, CH_2CH=), 3.55–3.47 (m, 2H, NCH), 3.20 (ddd, *J* = 13.0, 8.0, 4.0 Hz, 2H, NCH), 2.25–2.20 (m, 2H, CH_2CH=), 1.61–1.48 (m, 4H, CH), 1.42 (s, 9H, CMe_3); ^{13}C NMR (100.6 MHz, $CDCl_3$) δ 155.1 (C=O), 143.5 (CC=CH), 134.4 (CH_2C=CH), 79.3 ($OCMe_3$), 47.6 (C), 42.4 (NCH_2), 41.6 (CH_2C=C), 35.4 (CH_2), 28.6 (CMe_3); HRMS (ESI) *m/z* calcd for $C_{13}H_{21}NO_2$ $(M + Na)^+$ 246.1464, found 246.1468 (–1.4 ppm error). Spectroscopic data consistent with those reported in the literature.[66]
Lab book reference: HSK-1-28

***tert*-Butyl 2-(4,4,5,5-tetramethyl-1,3,2-dioxaborolan-2-yl)-7-azaspiro[3.5]nonane-7-carboxylate 32**

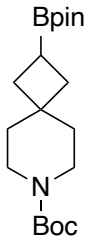

32

A suspension of CuCl (29 mg, 0.30 mmol, 0.1 eq), B_2pin_2 (830 mg, 3.27 mmol, 1.1 eq), KO*t*-Bu (167 mg, 1.49 mmol, 0.5 eq) and Xantphos (189 mg, 0.33 mmol, 0.11 eq) in THF (7.4 mL) under Ar was stirred at rt for 15 min. Then, a solution of cyclobutene **29** (663 mg, 2.97 mmol, 1.0 eq) in THF (14.9 mL) was added dropwise to the reaction mixture followed by the dropwise addition of MeOH (0.2 mL, 5.94 mmol, 2.0 eq). The resulting suspension was stirred at rt for 16 h. The solids were removed by filtration through a plug of Celite® eluting with EtOAc (10 mL). The filtrate was evaporated under reduced pressure to give the crude product. Purification by flash column chromatography on silica with 19:1 to 7:3 hexane-EtOAc as eluents gave cyclobutyl Bpin **32** (736 mg, 71%) as a white semi-solid, R_F (19:1 hexane-EtOAc) 0.22; IR (ATR) 2976, 2922, 1691 (C=O), 1417, 1242, 1142, 1112, 983 cm^{-1}; ^1H NMR (400 MHz, $CDCl_3$) δ 3.33–3.21 (m, 4H, NCH), 1.92–1.71 (m, 5H, C*H*CHB, BCH), 1.58–1.51 (m, 2H, CH), 1.50–1.44 (m, 2H,

CH), 1.44 (s, 9H, CMe_3), 1.23 (s, 12H, CMe_2); ^{13}C NMR (100.6 MHz, $CDCl_3$) δ 155.1 (C=O), 83.2 (O*C*Me_2), 79.2 (O*C*Me_3), 40.5 (br, NCH_2), 38.1 (C), 37.3 (CH_2), 36.7 (CH_2), 33.1 (BCH), 29.0 (C*Me*$_2$), 24.9 (C*Me*$_3$); ^{11}B NMR (128 MHz, $CDCl_3$) δ 33.4; HRMS (ESI) *m/z* calcd for $C_{19}H_{34}BNO_4$ $(M + Na)^+$ 374.2473, found 374.2481 (–1.7 ppm error). Spectroscopic data consistent with those reported in the literature.[67]
Lab book reference: HSK-1-32

A suspension of CuCl (2 mg, 0.022 mmol, 0.1 eq), B_2pin_2 (63 mg, 0.246 mmol, 1.1 eq), KO*t*-Bu (13 mg, 0.11 mmol, 0.5 eq) and Xantphos (14 mg, 0.025 mmol, 0.11 eq) in THF (0.6 mL) was stirred at rt for 15 min under Ar. Then, a solution of cyclobutene **29** (50 mg, 0.224 mmol, 1.0 eq) in THF (1.1 mL) was added dropwise to the reaction mixture followed by the dropwise addition of MeOH (18 μL, 0.448 mmol, 2.0 eq). The resulting suspension was stirred at rt for 16 h. The solids were removed by filtration through a plug of Celite® eluting with EtOAc (10 mL). The filtrate was evaporated under reduced pressure to give the crude product. Purification by flash column chromatography on silica with 49:1 to 9:1 hexane-EtOAc as eluent gave none of cyclobutyl Bpin **32**.
Lab book reference: HSK-1-7

A suspension of CuCl (31 mg, 0.31 mmol, 0.1 eq), B_2pin_2 (861 mg, 3.39 mmol, 1.1 eq), KO*t*-Bu (173 mg, 1.54 mmol, 0.5 eq) and Xantphos (197 mg, 0.34 mmol, 0.11 eq) in THF (7.7 mL) under Ar was stirred at rt for 15 min. Then, a solution of cyclobutene **29** (687 mg, 3.08 mmol, 1.0 eq) in THF (15.4 mL) was added dropwise to the reaction mixture. The resulting suspension was stirred at rt for 16 h. The solids were removed by filtration through a plug of Celite® eluting with EtOAc (10 mL). The filtrate was evaporated under reduced pressure to give the crude product. Purification by flash column chromatography on silica with 19:1 to 9:1 hexane-EtOAc as eluents gave cyclobutyl Bpin **32** (898 mg, 80%) as a white semi-solid, identical (by ^1H NMR spectroscopy) to that described above.
Lab book reference: HSK-2-108

***tert*-Butyl 4-(trifluoro- λ-4-boranyl)piperidine-1-carboxylate potassium 52**

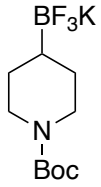

52

Saturated $KHF_{2(aq)}$ (4.5 M, 3.3 mL, 15.0 mmol, 5.0 eq) was added dropwise to a stirred solution of *N*-Boc piperdinyl Bpin **51** (934 mg, 3.0 mmol, 1.0 eq) in MeOH (15 mL). The resulting mixture was stirred at rt for 16 h. The solvent was evaporated under reduced pressure to give the crude product. The residue was dissolved in the minimum amount of hot acetone and the solids were removed by filtration. The filtrate was evaporated under reduced pressure. Et_2O (100 mL) was added and the resulting mixture was stirred at rt for 1 h. The solid was collected by filtration to give *N*-Boc piperidinyl trifluoroborate salt **52** (836 mg, 96%) as a white solid, mp 210-220 ℃ (lit.,[130] 213-215 ℃); IR (ATR) 2850, 1671 (C=O), 1420, 1286, 1115, 979 cm^{-1}; ^1H NMR (400 MHz, d_6-DMSO) δ 3.88–3.81 (m, 2H, NCH), 2.57–2.32 (m, 2H, NCH), 1.41–1.38 (m, 2H, CH), 1.36 (s, 9H, CMe_3), 1.08–0.93 (m, 2H, CH), 0.18–0.04 (m, 1H, BCH); ^{13}C NMR (100.6 MHz, d_6-DMSO) (rotamers) δ 154.0 (C=O), 77.7 (O*C*Me_3), 46.1 (br, NCH_2), 45.3 (br, NCH_2), 28.4 (C*Me*$_3$), 28.0 (CH_2) (BCH resonance not resolved); ^{11}B NMR (128 MHz, d_6-DMSO) δ 3.77; ^{19}F NMR (375 MHz, d_6-DMSO) δ –144.52; HRMS (ESI) *m/z* calcd for $C_{10}H_{18}BF_3NO_2$ M^- 252.1388 found 252.1393 (–2.1 ppm error). Spectroscopic data consistent with those reported in the literature.[131]

Lab book reference: HSK-1-43

***tert*-Butyl 2-(trifluoro-λ-4-boranyl)-7-azaspiro[3.5]nonane-7-carboxylate potassium 25**

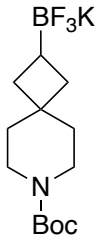

25

Saturated $KHF_{2(aq)}$ (4.5 M, 2.7 mL, 12.28 mmol, 5.0 eq) was added dropwise to a stirred solution of cyclobutyl Bpin **32** (863 mg, 2.46 mmol, 1.0 eq) in MeOH (12.3 mL) at rt.

The resulting mixture was stirred at rt for 16 h. The solvent was evaporated under reduced pressure to give the crude product. The residue was dissolved in the minimum amount of hot acetone and the solids were removed by filtration. The filtrate was evaporated under reduced pressure. Et_2O (100 mL) was added and the resulting mixture was stirred at rt for 1 h. The solid was collected by filtration to give cyclobutyl trifluoroborate salt **25** (794 mg, 97%) as a white solid, mp 240-241 °C; IR (ATR) 2916, 1668 (C=O), 1425, 1245, 1146, 970 cm^{-1}; ^1H NMR (400 MHz, d_6-DMSO) δ 3.22–3.17 (m, 2H, NCH), 3.13–3.08 (m, 2H, NCH), 1.47–1.39 (m, 6H, CH, C*H*CHB), 1.37 (s, 9H, CMe_3), 1.34–1.27 (m, 2H, CH), 1.13–0.97 (m, 1H, BCH); ^{13}C NMR (100.6 MHz, d_6-DMSO) δ 154.1 (C=O), 78.2 (O*C*Me_3, Boc), 40.0 (br, NCH, detected by HSQC), 35.1 (CH), 33.0 (CH), 28.2 (C*Me*$_3$) (BCH and C resonances not resolved); ^{11}B NMR (128 MHz, d_6-DMSO) δ 3.92; ^{19}F NMR (376 MHz, d_6-DMSO) δ –143.48; HRMS (ESI) *m/z* calcd for $C_{13}H_{22}BF_3NO_2$ M^- 292.1709, found 292.1701 (–2.3 ppm error).
Lab book reference: HSK-2-111

***tert*-Butyl 2-[(4-methylbenzenesulfonyl)oxy]-7-azaspiro[3.5]non-1-ene-7-carboxylate 31**

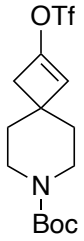

31

NaHMDS (3.3 mL of a 1 M solution in THF, 3.34 mmol, 1.6 eq) was added dropwise to a stirred solution of cyclobutanone **30** (500 mg, 2.09 mmol, 1.0 eq) in THF (14 mL) under Ar at –78 °C. The resulting solution was stirred at –78 °C for 1 h. Then, a solution of Comins' reagent **54** (1.067 g, 2.72 mmol, 1.3 eq) in THF (3.4 mL) was added and the resulting solution was stirred at –78 °C for 10 min. The solution was then allowed to warm slowly to rt and stirred at rt for 18 h. Saturated $NH_4Cl_{(aq)}$ (30 mL) was added and the mixture was extracted with Et_2O (4 × 30 mL). The combined organic extracts were washed with brine (20 mL), dried ($MgSO_4$) and evaporated under reduced pressure to give the crude product. Purification by flash column chromatography on silica with 19:1 to 17:3 hexane-Et_2O as eluent gave cyclobutyl enol triflate **31** (536 mg, 69%) as a white solid, mp 54-55 °C, R_F (2:3 hexane-Et_2O) 0.44; IR (ATR) 2933, 1673 (C=O), 1422, 1206,

1132, 851, 609 cm^{-1}; ^{1}H NMR (400 MHz, $CDCl_3$) δ 5.62 (s, 1H, =CH), 3.62–3.54 (m, 2H, NCH), 3.30–3.19 (m, 2H, NCH), 2.64 (s, 2H, CHCO), 1.70–1.53 (m, 4H, CH), 1.46 (s, 9H, CMe_3); ^{13}C NMR (100.6 MHz, $CDCl_3$); δ 154.9 (C=O), 140.7 (O*C*=CH), 122.6 (=CH), 117.0 (q, J = 321.0 Hz, CF_3), 79.8 (O*C*Me_3), 44.4 (CH_2), 42.5 (br, NCH_2), 39.9 (C), 34.6 (CH_2), 28.5 (C*Me*$_3$); ^{19}F NMR (375 MHz, $CDCl_3$) –73.65; HRMS (ESI) *m/z* calcd for $C_{14}H_{20}F_3NO_5$ $(M + Na)^+$ 394.0905 found 394.0906 (+4.7 ppm error).
Lab book reference: HSK-1-53

NaHMDS (0.7 mL of a 1 M solution in THF, 0.70 mmol, 1.6 eq) was added dropwise to a stirred solution of cyclobutanone **30** (100 mg, 0.42 mmol, 1.0 eq) in THF (2.1 mL) at –78 °C under Ar. The resulting solution was stirred at –78 °C for 1 h. Then, a solution of $PhNTf_2$ (194 mg, 0.54 mmol, 1.3 eq) in THF (0.7 mL) was added and the resulting solution was stirred at –78 °C for 10 min. The solution was then allowed to warm slowly to rt and stirred at rt for 16 h. Saturated $NH_4Cl_{(aq)}$ (10 mL) was added and the mixture was extracted with Et_2O (4 × 20 mL). The combined organic extracts were washed with brine (20 mL), dried ($MgSO_4$) and evaporated under reduced pressure to give the crude product. Purification by flash column chromatography on silica with 19:1 to 13:7 hexane-Et_2O as eluent gave a 50:50 mixture (by ^{1}H NMR spectroscopy) of sulfonamide **53** and cyclobutyl enol triflate **31** (185 mg, i.e. 86 mg (55%) of cyclobutyl enol triflate **31**) as a clear oil. Diagnostic signals for sulfonamide **53**: ^{1}H NMR (400 MHz, $CDCl_3$) δ 8.49–7.93 (br, s, 1H, NH), 7.36–7.28 (m, 2H, Ph), 7.28–7.17 (m, 3H, Ph).
Lab book reference: HSK-1-45

KHMDS (3.2 mL of a 0.5 M solution in toluene, 1.6 mmol, 1.6 eq) was added dropwise to a stirred solution of cyclobutanone **30** (239 mg, 1.0 mmol, 1.0 eq) in THF (5 mL) at –78 °C under Ar. The resulting solution was stirred at –78 °C for 1 h. Then, a solution of Comins' reagent **54** (511 mg, 1.3 mmol, 1.3 eq) in THF (1.6 mL) was added and the resulting solution was stirred at –78 °C for 10 min. The solution was then allowed to warm slowly to rt and stirred at rt for 18 h. Saturated $NH_4Cl_{(aq)}$ (30 mL) was added and the mixture was extracted with Et_2O (4 × 30 mL). The combined organic extracts were washed with brine (20 mL), dried ($MgSO_4$) and evaporated under reduced pressure to give the crude product. Purification by flash column chromatography on silica with 49:1

to 17:3 hexane-Et_2O as eluent gave cyclobutyl enol triflate **31** (236 mg, 64%) as a white solid, identical (by ^1H NMR spectroscopy) to that described above.
Lab book reference: HSK-1-74

NaHMDS (33.4 mL of a 1 M solution in THF, 33.4 mmol, 1.6 eq) was added dropwise to a stirred solution of cyclobutanone **30** (5.0 g, 20.9 mmol, 1.0 eq) in THF (52 mL) at –78 °C under Ar. The resulting solution was stirred at –78 °C for 1 h. Then, a solution of Comins' reagent **54** (10.081 g, 27.2 mmol, 1.3 eq) in THF (34 mL) was added and the resulting solution was stirred at –78 °C for 10 min. The solution was then allowed to warm slowly to rt and stirred at rt for 18 h. Saturated $NH_4Cl_{(aq)}$ (50 mL) was added and the mixture was extracted with Et_2O (4 × 50 mL). The combined organic extracts were washed with brine (50 mL), dried ($MgSO_4$) and evaporated under reduced pressure to give the crude product. Purification by flash column chromatography on silica with 19:1 to 17:3 hexane-Et_2O as eluent gave cyclobutyl enol triflate **31** (6.471 g, 83%) as a white solid, identical (by ^1H NMR spectroscopy) to that described above.
Lab book reference: HSK-1-90

***tert*-Butyl 2-(4,4,5,5-tetramethyl-1,3,2-dioxaborolan-2-yl)-7-azaspiro[3.5]non-1-ene-7-carboxylate 34**

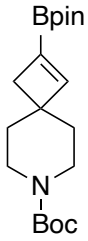

34

$PdCl_2$(dppf) (12 mg, 0.02 mmol, 0.06 eq), dppf (9 mg, 0.02 mmol, 0.06 eq), KOAc (79 mg, 0.8 mmol, 3.0 eq) and B_2pin_2 (82 mg, 0.3 mmol, 1.2 eq) were added to a stirred solution of cyclobutyl enol triflate **31** (100 mg, 0.3 mmol, 1.0 eq) in dioxane (3 mL) under Ar. The resulting mixture was stirred at 80 °C for 16 h. H_2O (10 mL) was added and the mixture was extracted with EtOAc (3 × 10 mL). The combined organic extracts were washed with brine (20 mL), dried ($MgSO_4$) and evaporated under reduced pressure to give the crude product. Purification by flash column chromatography on silica with 19:1 to 7:3 hexane-Et_2O gave cyclobutyl vinyl Bpin **34** (41 mg, 44%) as a white solid, mp 98-99 °C; R_F (4:1 hexane-Et_2O) 0.14; IR (ATR) 2974, 2926, 1676 (C=O), 1601 (C=C), 1419,

1136, 1032, 854, 659 cm^{-1}; ^{1}H NMR (400 MHz, $CDCl_3$) δ 7.02 (s, 1H, =CH), 3.52–3.45 (m, 2H, NCH), 3.29–3.18 (m, 2H, NCH), 2.32 (s, 2H, CHCB), 1.64–1.47 (m, 4H, CH), 1.43 (s, 9H, CMe_3), 1.25 (s, 12H, CMe_2); ^{13}C NMR (100.6 MHz, $CDCl_3$) δ 159.4 (=CH), 155.1 (C=O), 83.6 (O*C*Me_2) , 79.3 (O*C*Me_3), 48.0 (C), 42.2 (br, NCH_2), 41.5 (CH), 34.8 (CH), 28.6 (C*Me*$_3$), 24.9 (C*Me*$_2$) (BC= resonance not resolved); ^{11}B NMR (128 MHz, $CDCl_3$) δ 26.26; HRMS (ESI) *m/z* calcd for $C_{19}H_{32}BNO_4$ $(M + Na)^+$ 372.2317 found 372.2325 (+2.0 ppm error).

Lab book reference: HSK-1-52

tert-Butyl 2-(4,4,5,5-tetramethyl-1,3,2-dioxaborolan-2-yl)-7-azaspiro[3.5]nonane-7-carboxylate 32

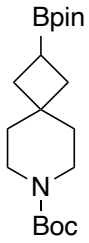

32

Cyclobutyl vinyl Bpin **34** (41 mg, 0.12 mmol, 1.0 eq) and 10% Pd/C (0.3 mg, 0.0028 mmol, 2 mol%) were dissolved in EtOAc (0.6 mL). The reaction flask was evacuated under reduced pressure and back-filled with Ar three times, and then with H_2 three times. The resulting mixture was stirred at rt under a balloon of H_2 for 16 h. The solids were removed by filtration through a plug of Celite® eluting with EtOAc (10 mL). The filtrate was evaporated under reduced pressure to give the crude product. Purification by flash column chromatography on silica with 19:1 to 9:1 hexane-EtOAc as eluent gave a 90:10 mixture (by ^{1}H NMR spectroscopy) of cyclobutyl Bpin **32** and cyclobutyl vinyl Bpin **34** (24 mg, i.e. 22 mg (54%) of cyclobutyl Bpin **32**) as a white semi-solid.

Lab book reference: HSK-1-54

tert-Butyl 2-(trifluoro-_λ_-4-boranyl)-7-azaspiro[3.5]nonane-7-carboxylate potassium 25

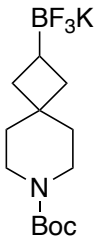

25

$PdCl_2$(dppf) (72 mg, 0.1 mmol, 0.06 eq), dppf (54 mg, 0.1 mmol, 0.06 eq), KOAc (482 mg, 4.9 mmol, 3.0 eq) and B_2pin_2 (498 mg, 2.0 mmol, 1.2 eq) were added to a stirred solution of cyclobutyl enol triflate **31** (608 mg, 1.6 mmol, 1.0 eq) in dioxane (16 mL) under Ar. The resulting mixture was stirred at 80 ℃ for 16 h. H_2O (30 mL) was added and the mixture was extracted with EtOAc (3 × 20 mL). The combined organic extracts were washed with brine (30 mL), dried ($MgSO_4$) and evaporated under reduced pressure to give the crude cyclobutyl vinyl Bpin **34**. The crude cyclobutyl vinyl Bpin **34** and 10% Pd/C (3.5 mg, 0.03 mmol, 2 mol%) were dissolved in EtOAc (8 mL). The reaction flask was evacuated under reduced pressure and back-filled with Ar three times, and then with H_2 three times. The resulting mixture was stirred at rt under a balloon of H_2 for 16 h. The solids were removed by filtration through a plug of Celite® eluting with EtOAc (20 mL). The filtrate was evaporated under reduced pressure to give a crude mixture of cyclobutyl Bpin **32** and cyclobutyl vinyl Bpin **34**. The crude mixture and 10% Pd/C (3.5 mg, 0.03 mmol, 2 mol%) were dissolved in EtOAc (8 mL) under Ar. The reaction flask was evacuated under reduced pressure and back-filled with Ar three times, and then with H_2 three times. The resulting mixture was stirred at rt under a balloon of H_2 for 16 h. The solids were removed by filtration through a plug of Celite® eluting with EtOAc (20 mL). The filtrate was evaporated under reduced pressure to give crude cyclobutyl Bpin **32**. The crude cyclobutyl Bpin **32** was dissolved in MeOH (8 mL) and saturated $KHF_{2(aq)}$ (4.5 M, 1.8 mL, 8.19 mmol, 5.0 eq) was added dropwise. The resulting mixture was stirred at rt for 16 h. The solvent was evaporated under reduced pressure to give the crude product. The residue was dissolved in the minimum amount of hot acetone and the solids were removed by filtration. The filtrate was evaporated under reduced pressure. Et_2O (100 mL) was added and the resulting mixture was stirred for 1 h. The solid was collected by filtration to give cyclobutyl trifluoroborate salt **25** (447 mg, 82%) as a white solid, identical (by ^1H, ^{11}B and ^{19}F NMR spectroscopy) to that described above.

Lab book reference: HSK-1-76

$PdCl_2$(dppf) (95 mg, 0.13 mmol, 0.06 eq), dppf (72 mg, 0.13 mmol, 0.06 eq), KOAc (640 mg, 6.52 mmol, 3.0 eq) and B_2pin_2 (663 mg, 2.61 mmol, 1.2 eq) were added to a stirred solution of cyclobutyl enol triflate **31** (807 mg, 2.17 mmol, 1.0 eq) in dioxane (21.7 mL) under Ar. The resulting mixture was stirred at 80 ℃ for 16 h. H_2O (30 mL) was added and the mixture was extracted with EtOAc (3 × 20 mL). The combined organic extracts were washed with brine (10 × 30 mL), dried ($MgSO_4$) and evaporated under reduced pressure to give the crude cyclobutyl vinyl Bpin **34**. The crude mixture was filtered through Celite®, washing with EtOAc (10 mL) and evaportated under reduced pressure. The crude mixture and 10% Pd/C (9.2 mg, 0.043 mmol, 2 mol%) were dissolved in EtOAc (10.9 mL). The reaction flask was evacuated under reduced pressure and back-filled with Ar three times, and then with H_2 three times. The resulting mixture was stirred at rt under a balloon of H_2 for 16 h. The solids were removed by filtration through a plug of Celite® eluting with EtOAc (20 mL). The filtrate was evaporated under reduced pressure to give crude cyclobutyl Bpin **32**. The crude mixture was dissolved MeOH (10.9 mL). Then, saturated $KHF_{2(aq)}$ (4.5 M, 2.4 mL, 10.87 mmol, 5.0 eq) was added dropwise, and the resulting mixture was stirred at rt for 16 h. The reaction mixture was evaporated under reduced pressure to give the crude product. The residue was dissolved in the minimum amount of hot acetone and the filtrate was collected and evaporated under reduced pressure. Et_2O (100 mL) was added and the resulting mixture was stirred for 1 h. The mixture was filtered to give cyclobutyl trifluoroborate salt **25** (522 mg, 73%) as a white solid, identical (by ^1H, ^{11}B, and ^{19}F NMR spectroscopy) to that described above.
Lab book reference: HSK-1-80

Ethyl 4-cyclohexylbenzoate 123

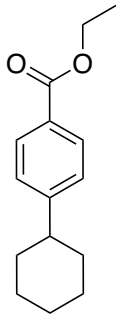

123

Using general procedure A, cyclohexyl trifluoroborate salt **120** (72 mg, 0.375 mmol, 1.5 eq) and ethyl 4-bromobenzoate (41 μL, 0.25 mmol, 1.0 eq) gave the crude product.

Purification by flash column chromatography on silica with 1000:1 hexane-Et_2O as eluent gave ethyl ester phenyl cyclohexane **123** (53 mg, 96% pure by ^1H NMR spectroscopy with an unidentified side product, ~88%) as a yellow solid, mp 50-51 ℃ (lit.,[132] 59 ℃); R_F (49:1 hexane-EtOAc) 0.27; IR (ATR): 2925, 1715 (C=O), 1610, 1271, 1099, 1021, 706 cm^{-1}; ^1H NMR (400 MHz, $CDCl_3$) δ 7.95 (d, J = 8.5 Hz, 2H, Ar), 7.25 (d, J = 8.5 Hz, 2H, Ar), 4.37 (q, J = 7.0 Hz, 2H, OCH), 2.59–2.48 (m, 1H, ArCH), 1.90–1.84 (m, 4H, CH), 1.80–1.73 (m, 1H, CH), 1.51–1.33 (m, 7H, CH, Me), 1.33–1.18 (m, 1H, CH); ^{13}C NMR (100.6 MHz, $CDCl_3$) δ 166.8 (C=O), 153.5 (*ipso*-Ar), 129.8 (Ar), 128.2 (*ipso*-Ar), 126.9 (Ar), 60.8 (OCH_2), 44.8 (Ar*C*H), 34.3 (CH_2), 26.9 (CH_2), 26.2 (CH_2), 14.5 (Me); HRMS (ESI) *m/z* calcd for $C_{15}H_{20}O_2$ $(M + Na)^+$ 255.1356 found 255.1361 (–2.8 ppm error). Spectroscopic data consistent with those reported in the literature.[133]
Lab book reference: HSK-1-39

Using general procedure A, cyclohexyl trifluoroborate salt **120** (48 mg, 0.25 mmol, 1.0 eq) and ethyl 4-bromobenzoate (41 μL, 0.25 mmol, 1.0 eq) gave the crude product. Purification by flash column chromatography on silica with 1000:1 hexane-Et_2O as eluent gave a 70:30 mixture of ethyl ester phenyl cyclohexane **123** and ethyl-4-bromobenzoate (51 mg, i.e. 39 mg (68%) of ethyl ester phenyl cyclohexane **123**) as a yellow oil.
Lab book reference: HSK-1-34

Using general procedure A, cyclohexyl trifluoroborate salt **120** (48 mg, 0.25 mmol, 1.0 eq) and ethyl 4-bromobenzoate (62 μL, 0.375 mmol, 1.5 eq) gave the crude product. Purification by flash column chromatography on silica with 1000:1 hexane-Et_2O as eluent gave a 55:45 mixture of ethyl ester phenyl cyclohexane **123** and ethyl-4-bromobenzoate (70 mg, i.e. 38.5 mg (66%) of ethyl ester phenyl cyclohexane **123**) as a yellow oil.
Lab book reference: HSK-1-40

Attempted synthesis of 3-cyclohexylpyridine 125

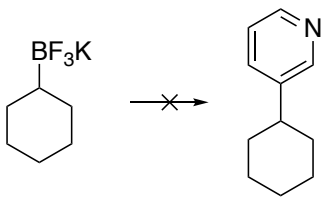

125

Using general procedure A, cyclohexyl trifluoroborate salt **120** (72 mg, 0.375 mmol, 1.5 eq) and 3-bromopyridine (24 μL, 0.25 mmol, 1.0 eq) gave the crude product which contained none of pyridine cyclohexane **125** by ^{1}H NMR spectroscopy.
Lab book reference: HSK-1-33

5-Cyclohexylpyrimidine 126

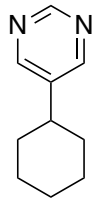

126

Using general procedure A, cyclohexyl trifluoroborate salt **120** (72 mg, 0.375 mmol, 1.5 eq) and 5-bromopyrimidine (40 mg, 0.25 mmol, 1.0 eq) gave the crude product. Purification by flash column chromatography on silica with 9:1 to 4:1 hexane-EtOAc as eluent gave pyrimidine cyclohexane **126** (17 mg, 43%) as a yellow solid, mp 49-50 °C (lit.,[134] 55-56 °C); R_F (4:1 hexane-EtOAc) 0.19; IR (ATR) 2924, 1559, 1411, 733, 630 cm^{-1}; ^{1}H NMR (400 MHz, $CDCl_3$) δ 9.04 (s, 1H, Ar), 8.57 (s, 2H, Ar), 2.57–2.45 (m, 1H, CHAr), 1.92–1.83 (m, 4H, CH), 1.82–1.72 (m, 1H, CH), 1.51–1.33 (m, 4H, CH), 1.32–1.19 (m, 1H, CH); ^{13}C NMR (100.6 MHz, $CDCl_3$) δ 156.9 (Ar), 155.7 (Ar), 140.2 (*ipso*-Ar), 40.0 (*C*HAr), 33.8 (CH_2), 26.6 (CH_2), 25.8 (CH_2); HRMS (ESI) *m/z* calcd for $C_{10}H_{14}N_2$ $(M + H)^+$ 163.2298 found 163.2295 (–0.2 ppm error). Spectroscopic data consistent with those reported in the literature.[135]
Lab book reference: HSK-1-38

Using general procedure A, cyclohexyl trifluoroborate salt **120** (48 mg, 0.25 mmol, 1.0 eq) and 5-bromopyrimidine (60 mg, 0.375 mmol, 1.5 eq) gave the crude product. Purification by flash column chromatography on silica with 9:1 to 4:1 hexane-EtOAc as eluent gave pyrimidine cyclohexane **126** (26 mg, 63%) as a yellow solid, identical (by ^{1}H NMR spectroscopy) to that described above.
Lab book reference: HSK-1-49

4-Cyclohexyl-2-fluoropyridine 127

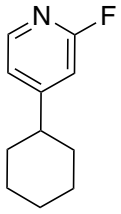

127

Using general procedure A, cyclohexyl trifluoroborate **120** (48 mg, 0.25 mmol, 1.0 eq) and 4-bromo-2-fluoropyridine (39 μL, 0.375 mmol, 1.5 eq) gave the crude product. Purification by flash column chromatography on silica with 40:1 to 20:1 hexane-EtOAc as eluent gave fluoropyridine cyclohexane **127** (23 mg, 51%) as a colourless oil, R_F (10:1 hexane-EtOAc) 0.26; IR (ATR) 2926, 2853 1609, 1410, 948, 843 cm^{-1}; ^1H NMR (400 MHz, $CDCl_3$) δ 8.09 (d, J = 5.5 Hz, 1H, Ar), 7.01 (d, J = 5.5 Hz, 1H, Ar), 6.75 (s, 1H, Ar), 2.54 (tt, J = 11.5, 3.0 Hz, 1H, ArCH), 1.91–1.83 (m, 4H, CH), 1.81–1.73 (m, 1H, CH), 1.47–1.28 (m, 5H, CH); ^{13}C NMR (100.6 MHz, $CDCl_3$) δ 164.4 (d, J = 238.0 Hz, *ipso*-Ar), 162.9 (d, J = 7.0 Hz, *ipso*-Ar), 147.4 (d, J = 15.0 Hz, Ar), 120.4 (d, J = 4.0 Hz, Ar), 107.6 (d, J = 37.0 Hz, Ar), 44.0 (Ar*C*H), 33.5 (CH), 26.5 (CH_2), 26.0 (CH_2); ^{19}F NMR (375 MHz, $CDCl_3$) δ –69.07; HRMS (ESI) *m/z* calcd for $C_{11}H_{14}FN$ $(M + H)^+$ 180.1180 found 180.1183 (–0.9 ppm error). Spectroscopic data consistent with those reported in the literature.[136]

Lab book reference: HSK-1-42

***tert*-Butyl 4-[4-(ethoxycarbonyl)phenyl]piperidine-1-carboxylate 129**

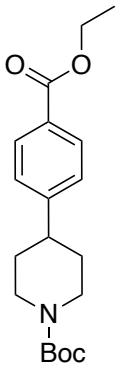

129

Using general procedure A, *N*-Boc piperidinyl trifluoroborate salt **52** (73 mg, 0.25 mmol, 1.0 eq) and ethyl 4-bromobenzoate (62 μL, 0.375 mmol, 1.5 eq) gave the crude product. Purification by flash column chromatography on silica with 999:1 to 9:1 hexane-Et_2O as eluent gave ethyl ester phenyl *N*-Boc piperidine **129** (51 mg, 61%) as a white semi-solid,

R_F (9:1 hexane-Et_2O) 0.05; IR (ATR) 2977, 1715 (C=O, ester), 1688 (C=O, Boc), 1271, 1164, 1016, 76 cm^{-1}; ^1H NMR (400 MHz, $CDCl_3$) δ 7.98 (d, J = 8.0 Hz, 2H, Ar), 7.26 (d, J = 8.0 Hz, 2H, Ar), 4.36 (q, J = 7.0 Hz, 2H, OCH), 4.29–4.24 (m, 2H, NCH), 2.86–2.75 (m, 2H, NCH), 2.70 (tt, J = 12.0, 3.5 Hz, 1H, ArCH), 1.91–1.78 (m, 2H, CH), 1.70–1.55 (m, 2H, CH), 1.48 (s, 9H, CMe_3), 1.38 (t, J = 7.0 Hz, 3H, Me); ^{13}C NMR (100.6 MHz, $CDCl_3$) δ 166.7 (C=O, ester), 154.9 (C=O, Boc), 151.1 (*ipso*-Ar), 130.0 (Ar), 128.8 (*ipso*-Ar), 126.9 (Ar), 79.7 (O*C*Me_3), 61.0 (OCH_2), 44.4 (NCH_2), 42.9 (Ar*C*H), 33.0 (CH_2), 28.6 (C*Me*$_3$), 14.5 (Me); HRMS (ESI) *m/z* calcd for $C_{22}H_{31}NO_4$ $(M + Na)^+$ 356.1832 found 356.1832 (+0.1 ppm error). Spectroscopic data consistent with those reported in the literature.[137]

Lab book reference: HSK-1-46

Attempted synthesis of *tert*-butyl 4-(pyrimidin-5-yl)piperidine-1-carboxylate 130

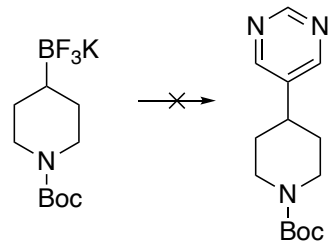

130

Using general procedure A, *N*-Boc piperidinyl trifluoroborate salt **52** (73 mg, 0.25 mmol, 1.0 eq) and 3-bromopyrimidine (60 mg, 0.375 mmol, 1.5 eq) gave the crude product which contained none of pyrimidine *N*-Boc piperidine **130** by ^1H NMR spectroscopy.

Lab book reference: HSK-1-47

***tert*-Butyl 4-(2-fluoropyridin-4-yl)piperidine-1-carboxylate 131**

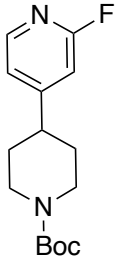

131

Using general procedure A, *N*-Boc piperidinyl trifluoroborate salt **52** (73 mg, 0.25 mmol, 1.0 eq) and 4-bromo-2-fluoropyridine (39 μL, 0.375 mmol, 1.5 eq) gave the crude product. Purification by flash column chromatography on silica with 99:1 to 7:3 hexane-

Et_2O as eluent gave fluoropyridine *N*-Boc piperidine **131** (38 mg, 70% pure by ^1H NMR spectroscopy with an unidentified side product, ~39%) as a colourless oil, R_F (7:3 hexane-Et_2O) 0.14; IR (ATR) 2932, 1686 (C=O), 1609, 1412, 1160, 951, 1769, 561 cm^{-1}; ^1H NMR (400 MHz, $CDCl_3$) δ 8.12 (d, *J* = 5.5 Hz, 1H, Ar), 7.00 (d, *J* = 5.5 Hz, 1H, Ar), 6.75 (s, 1H, Ar), 4.33–4.23 (m, 2H, NCH), 2.85–2.73 (m, 2H, NCH), 2.69 (tt, *J* = 12.0, 3.5 Hz, 1H, ArCH), 1.87–1.79 (m, 2H, CH), 1.68–1.50 (m, 2H, CH), 1.47 (s, 9H, CMe_3); ^{13}C NMR (100.6 MHz, $CDCl_3$) δ 164.3 (d, *J* = 238.0 Hz, *ipso*-Ar) 160.6 (d, *J* = 7.5 Hz, *ipso*-Ar), 154.8 (C=O), 147.7 (Ar), 120.1 (Ar), 107.7 (d, *J* = 37.0 Hz, Ar), 79.9 ($OCMe_3$), 44.4 (br, NCH_2), 42.1 (Ar*C*H), 32.3 (CH_2), 28.6 (CMe_3); ^{19}F NMR (375 MHz, $CDCl_3$) δ –68.25; HRMS (ESI) *m/z* calcd for $C_{15}H_{21}FN_2O_2$ $(M + H)^+$ 281.1660 found 281.1668 (–1.3 ppm error). Spectroscopic data consistent with those reported in the literature.[138]
Lab book reference: HSK-1-48

***tert*-Butyl 2-[4-(ethoxycarbonyl)phenyl]-7-azaspiro[3.5]nonane-7-carboxylate 132**

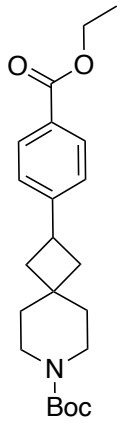

132

Using general procedure A, cyclobutyl trifluoroborate salt **25** (83 mg, 0.25 mmol, 1.0 eq) and ethyl 4-bromobenzoate (61 μL, 0.375 mmol, 1.5 eq) gave the crude product. Purification by flash column chromatography on silica with 19:1 to 4:1 hexane-Et_2O as eluent gave ethyl ester phenyl cyclobutane **132** (49 mg, 53%) as a white solid, mp 69-70 °C; R_F (4:1 hexane-Et_2O) 0.19; IR (ATR) 2924, 1704 (C=O, ester), 1682 (C=O, Boc), 1410, 1242, 1109, 766, 576 cm^{-1}; ^1H NMR (400 MHz, $CDCl_3$) δ 7.97 (d, *J* = 8.5 Hz, 2H, Ar), 7.25 (d, *J* = 8.5 Hz, 2H, Ar), 4.36 (q, *J* = 7.0 Hz, 2H, OCH_2), 3.57 (tt, *J* = 9.0, 9.0 Hz, 1H, ArCH), 3.45–3.34 (m, 2H, NCH), 3.33–3.22 (m, 2H, NCH), 2.37–2.27 (m, 2H, C*H*CHAr), 2.00–1.83 (m, 2H, C*H*CHAr), 1.77–1.67 (m, 2H, CH), 1.54–1.48 (m, 2H, CH), 1.46 (s, 9H, CMe_3), 1.39 (t, *J* = 7.0 Hz, 3H, CH_2Me); ^{13}C NMR (100.6 MHz, $CDCl_3$);

δ 166.7 (C=O, ester), 155.1 (C=O, Boc), 151.5 (*ipso*-Ar), 129.7 (Ar), 128.2 (*ipso*-Ar), 126.4 (Ar), 79.4 (O*C*Me$_3$), 60.9 (OCH$_2$), 40.9 (br, NCH$_2$), 39.3 (CH$_2$), 39.0 (CH$_2$), 35.9 (CH$_2$), 34.1 (C), 33.6 (Ar*C*H), 28.6 (OC*Me$_3$*), 14.5 (Me); HRMS (ESI) *m/z* calcd for $C_{22}H_{31}NO_4$ $(M + Na)^+$ 396.2145 found 396.2149 (–1.1 ppm error).

Lab book reference: HSK-1-79

***tert*-Butyl 2-(pyrimidin-5-yl)-7-azaspiro[3.5]nonane-7-carboxylate 133**

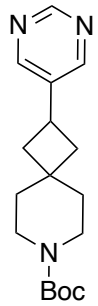

133

Using general procedure A, cyclobutyl trifluoroborate salt **25** (83 mg, 0.25 mmol, 1.0 eq) and 5-bromopyrimidine (60 mg, 0.375 mmol, 1.5 eq) gave the crude product. Purification by flash column chromatography on silica with 4:1 to 3:7 hexane-EtOAc as eluent gave pyrimidine cyclobutane **133** (64 mg, 84%) as a white solid, mp 55-60 ℃; R_F (3:2 hexane-EtOAc) 0.08; IR (ATR) 2971, 1687 (C=O), 1411, 1243, 1146, 975, 728 cm^{-1}; ^{1}H NMR (400 MHz, $CDCl_3$) δ 9.03 (s, 1H, Ar), 8.56 (s, 2H, Ar), 3.51 (tt, *J* = 9.0 Hz, 9.0 Hz, 1H, ArCH), 3.42–3.36 (m, 2H, NCH), 3.31–3.24 (m, 2H, NCH), 2.40–2.30 (m, 2H, C*H*CHAr), 1.96–1.87 (m, 2H, C*H*CHAr), 1.74–1.66 (m, 2H, CH), 1.54–1.44 (m, 2H, CH), 1.42 (s, 9H, CMe$_3$); ^{13}C NMR (100.6 MHz, $CDCl_3$) δ 156.7 (Ar), 155.4 (Ar), 155.0 (C=O), 138.5 (*ipso*-Ar), 79.5 (O*C*Me$_3$), 39.2 (br, NCH$_2$), 38.7 (CH$_2$), 35.6 (CH$_2$), 34.8 (C), 29.1 (ArCH), 28.5 (C*Me$_3$*); HRMS (ESI) *m/z* calcd for $C_{17}H_{25}N_3O_2$ $(M + Na)^+$ 326.1839 found 326.1842 (–1.2 ppm error).

Lab book reference: HSK-1-67

***tert*-Butyl 2-(2-methoxypyridin-4-yl)-7-azaspiro[3.5]nonane-7-carboxylate 134**

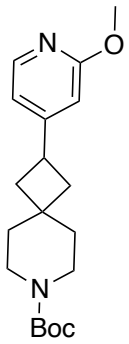

134

Using general procedure A, cyclobutyl trifluoroborate salt **25** (83 mg, 0.25 mmol, 1.0 eq) and 4-bromo-2-methoxypyridine (71 mg, 0.375 mmol, 1.5 eq) gave the crude product. Purification by flash column chromatography on silica with 19:1 to 23:2 hexane-EtOAc as eluent gave methoxypyridine cyclobutane **134** (52 mg, 63%) as a clear oil, R_F (9:1 hexane-EtOAc) 0.2; IR (ATR) 2923, 1672 (C=O), 1428, 1242, 762 cm^{-1}; ^1H NMR (400 MHz, $CDCl_3$) δ 8.05 (d, J = 5.5 Hz, 1H, Ar), 6.73–6.67 (m, 1H, Ar), 6.55 (s, 1H, Ar), 3.91 (s, 3H, OMe), 3.55–3.43 (m, 1H, ArCH), 3.43–3.33 (m, 2H, NCH), 3.31–3.24 (m, 2H, NCH), 2.32–2.22 (m, 2H, C*H*CHAr), 1.92–1.82 (m, 2H, C*H*CHAr), 1.71–1.64 (m, 2H, CH), 1.52–1.47 (m, 2H, CH), 1.45 (s, 9H, CMe_3); ^{13}C NMR (100.6 MHz, $CDCl_3$) δ 164.6 (*ipso*-Ar), 157.9 (*ipso*-Ar), 155.0 (C=O), 146.7 (Ar), 115.6 (Ar), 108.3 (Ar), 79.4 (O*C*Me_3), 53.4 (OMe), 41.2 (br, NCH_2), 39.1 (CH_2), 38.3 (CH_2), 35.9 (CH_2), 34.2 (C), 32.7 (Ar*C*H), 28.5 (C*Me*$_3$); HRMS (ESI) *m/z* calcd for $C_{19}H_{28}N_2O_3$ $(M + H)^+$ 333.2173 found 333.2180 (–1.8 ppm error).

Lab book reference: HSK-1-71

***tert*-Butyl 2-(4-acetamidophenyl)-7-azaspiro[3.5]nonane-7-carboxylate 135**

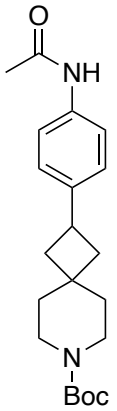

135

Using general procedure A, cyclobutyl trifluoroborate salt **25** (83 mg, 0.25 mmol, 1.0 eq) and 4-bromoacetanilide (81 mg, 0.375 mmol, 1.5 eq) gave the crude product. Purification by flash column chromatography on silica with 4:1 to 3:2 hexane-EtOAc then 99:1 to 19:1 CH_2Cl_2-acetone as eluent gave acetanilide cyclobutane **135** (41 mg, 46%) as an off-white solid, mp 155-165 ℃; R_F (9:1 CH_2Cl_2-acetone) 0.49; IR (ATR) 2919, 2853, 1681 (C=O, amide), 1662 (C=O, Boc), 1429, 1243, 1147, 823, 545 cm^{-1}; ^1H NMR (400 MHz, $CDCl_3$) δ 7.87 (d, J = 8.0 Hz, 2H, Ar), 7.38 (d, J = 8.0 Hz, 2H, Ar), 3.61 (tt, J = 9.0, 9.0 Hz ArCH), 3.46– 3.39 (m, 2H NCH), 3.34–3.26 (m, 2H, NCH), 3.04 (s, 3H, Me), 2.41–2.31 (m, 2H, C*H*CHAr), 1.97–1.87 (m, 2H, C*H*CHAr), 1.76–1.68 (m, 2H, CH), 1.59 (br s, 1H, NH), 1.55–1.48 (m, 2H, CH), 1.46 (s, 9H, CMe_3); ^{13}C NMR (100.6 MHz, $CDCl_3$) δ 155.0 (C=O, Boc), 152.7 (C=O, amide), 138.0 (*ipso*-Ar), 127.6 (Ar), 127.4 (Ar), 79.5 (O*C*Me_3), 44.7 (Me), 40.6 (br, NCH_2, identified by HSQC), 39.2 (CH_2), 39.0 (CH_2), 35.8 (CH_2), 34.2 (C), 33.5 (ArCH), 28.6 (C*Me*$_3$) (*ipso*-Ar resonance not resolved); HRMS (ESI) *m/z* calcd for $C_{21}H_{30}N_2O_3$ $(M + Na)^+$ 381.2149 found 381.2154 (–1.4 ppm error).
Lab book reference: HSK-1-70

***tert*-Butyl 2-(4-methanesulfonylphenyl)-7-azaspiro[3.5]nonane-7-carboxylate 136**

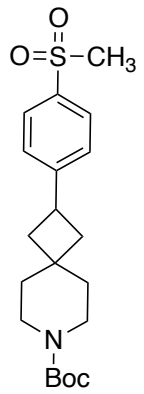

136

Using general procedure A, cyclobutyl trifluoroborate salt **25** (83 mg, 0.25 mmol, 1.0 eq) and 1-bromo-4-methane sulfonyl benzene (88 mg, 0.375 mmol, 1.5 eq) gave the crude product. Purification by flash column chromatography on silica with 9:1 to 3:1 hexane-EtOAc as eluent gave methanesulfonylphenyl cyclobutane **136** (11 mg, 12%) as a white solid, mp 110-120 ℃; R_F (6:4 hexane-EtOAc) 0.50; IR (ATR) 2925, 1683 (C=O), 1427, 1308, 1145, 772 cm^{-1}; ^1H NMR (400 MHz, $CDCl_3$) δ 7.86 (d, J = 8.0 Hz, 2H, Ar), 7.38 (d, J = 8.0 Hz, 2H, Ar), 3.61 (tt, J = 9.0 Hz, 9.0 Hz 1H, ArCH), 3.46–3.38 (m, 2H, NCH), 3.33–3.26 (m, 2H, NCH), 3.04 (s, 3H, Me), 2.35 (m, 2H, C*H*CHAr), 1.92 (m, 2H,

C*H*CHAr), 1.72 (m, 2H, CH), 1.51 (m, 2H, CH), 1.46 (s, 9H, CMe_3); ^{13}C NMR (100.6 MHz, $CDCl_3$); 155.1 (C=O), 152.7 (*ipso*-Ar), 138.1 (*ipso*-Ar), 127.6 (Ar), 127.5 (Ar), 79.5 (O*C*Me_3), 44.7 (Me), 41.0 (br, NCH_2), 39.3 (CH_2), 39.0 (CH_2), 35.9 (CH_2), 34.3 (C), 33.5 (ArCH), 28.6 (C*Me₃*); HRMS (ESI) *m/z* calcd for $C_{20}H_{29}NO_4S$ $(M + Na)^+$ 402.1710 found 402.1711 (–2.2 ppm error).
Lab book reference: HSK-1-68

Attempted synthesis of *tert*-butyl 2-(4-sulfamoylphenyl)-7-azaspiro[3.5]nonane-7-carboxylate 137

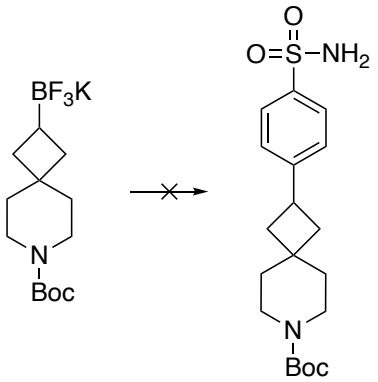

137

Using general procedure A, cyclobutyl trifluoroborate salt **25** (83 mg, 0.25 mmol, 1.0 eq) and 4-bromobenzene sulfonamide (89 mg, 0.375 mmol, 1.5 eq) gave the crude product which contained none of sulfamoylphenyl cyclobutane **137** by ^1H NMR spectroscopy.
Lab book reference: HSK-1-77

Attempted synthesis of *tert*-butyl 2-(1H-pyrazol-4-yl)-7-azaspiro[3.5]nonane-7-carboxylate 138

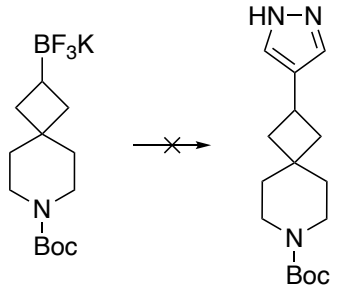

138

Using general procedure A, cyclobutyl trifluoroborate salt **25** (83 mg, 0.25 mmol, 1.0 eq) and 4-bromopyrazole (55 mg, 0.375 mmol, 1.5 eq) gave the crude product which contained none of pyrazole cyclobutane **138** by ^1H NMR spectroscopy.

Lab book reference: HSK-1-81

tert-Butyl 2-(2-aminopyridin-4-yl)-7-azaspiro[3.5]nonane-7-carboxylate 139

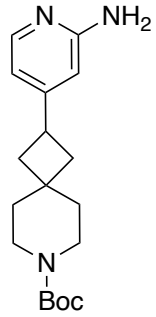

139

Using general procedure A, cyclobutyl trifluoroborate salt **25** (83 mg, 0.25 mmol, 1.0 eq) and 2-amino-4-bromopyridine (65 mg, 0.375 mmol, 1.5 eq) gave trace amounts of aminopyridine cyclobutane **139** by mass spectrometry, HRMS (ESI) *m/z* calcd for $C_{13}H_{19}N_3O_2S$ $(M + H)^+$ 318.2176 found 318.2185 (–2.3 ppm error).

Lab book reference: HSK-1-82

Attempted synthesis of _tert_-butyl 2-(4-methanesulfonylphenyl)-7-azaspiro[3.5]nonane-7-carboxylate 136

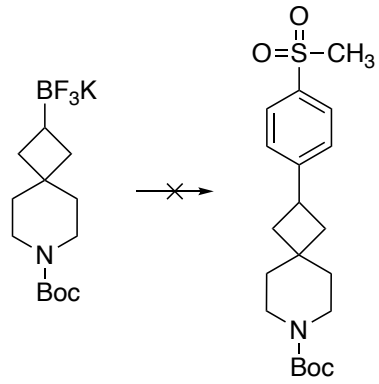

136

Using general procedure A, cyclobutyl trifluoroborate salt **25** (83 mg, 0.25 mmol, 1.0 eq) and 1-bromo-4-methane sulfonyl benzene (88 mg, 0.375 mmol, 1.5 eq) gave the crude product which contained none of methanesulfonylphenyl cyclobutane **136** by ^{1}H NMR spectroscopy.

Lab book reference: HSK-2-96

Attempted synthesis of _tert_-butyl 4-[4-(ethoxycarbonyl)phenyl]piperidine-1-carboxylate 129

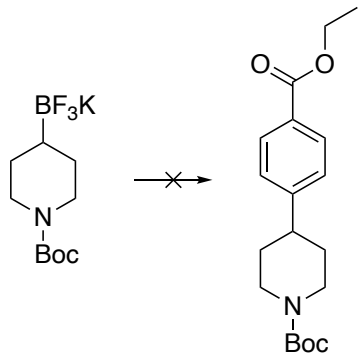

129

Using general procedure A, *N*-Boc piperidinyl trifluoroborate salt **52** (73 mg, 0.25 mmol, 1.0 eq) and ethyl 4-bromobenzoate (62 μL, 0.375 mmol, 1.5 eq) gave the crude product which contained none of ethyl ester phenyl *N*-Boc piperidine **129** by ^{1}H NMR spectroscopy.

Lab book reference: HSK-2-104

Attempted synthesis of 5-cyclohexylpyrimidine 126

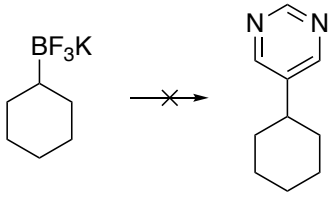

126

Using general procedure A, cyclohexyl trifluoroborate salt **120** (48 mg, 0.25 mmol, 1.0 eq) and 5-bromopyrimidine (60 mg, 0.375 mmol, 1.5 eq) gave the crude product which contained none of pyrimidine cyclohexane **126** by ^{1}H NMR spectroscopy.

Lab book reference: HSK-2-105

***tert*-Butyl 2-(pyrimidin-5-yl)-7-azaspiro[3.5]nonane-7-carboxylate 133**

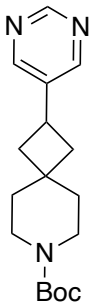

133

Using general procedure A, cyclobutyl trifluoroborate salt **25** (83 mg, 0.25 mmol, 1.0 eq) and 5-bromopyrimidine (60 mg, 0.375 mmol, 1.5 eq) gave the crude product. Purification by flash column chromatography on silica with 9:1 hexane-EtOAc to EtOAc as eluent gave pyrimidine cyclobutane **133** (35 mg, 46%) as a yellow solid, identical (by ^{1}H NMR spectroscopy) to that described above.
Lab book reference: HSK-1-84

Using general procedure A without solvent degassing, cyclobutyl trifluoroborate salt **25** (83 mg, 0.25 mmol, 1.0 eq) and 5-bromopyrimidine (60 mg, 0.375 mmol, 1.5 eq) gave the crude product which contained none of pyrimidine cyclobutane **133** by ^{1}H NMR spectroscopy.
Lab book reference: HSK-1-83

Using general procedure A in dioxane (7 mL), cyclobutyl trifluoroborate salt **25** (83 mg, 0.25 mmol, 1.0 eq) and 5-bromopyrimidine (60 mg, 0.375 mmol, 1.5 eq) gave the crude product. Purification by flash column chromatography on silica with 7:3 to 2:3 hexane-EtOAc as eluent gave impure pyrimidine cyclobutane **133** (14 mg, <17%, unable to quantify yield due to significant impurities present) as a yellow oil.
Lab book reference: HSK-1-86

Using general procedure A with the reaction mixture sonicated for 10 min before degassing, cyclobutyl trifluoroborate salt **25** (83 mg, 0.25 mmol, 1.0 eq) and 5-bromopyrimidine (60 mg, 0.375 mmol, 1.5 eq) gave the crude product. Purification by flash column chromatography on silica with 9:1 to 1:1 hexane-EtOAc as eluent gave impure pyrimidine cyclobutane **133** (13 mg, <13%, unable to quantify yield due to significant impurities present) as a yellow oil.
Lab book reference: HSK-1-87

Using general procedure A with 0.5 scale, 4,4'-di-tert-butyl-2,2'-bipyridine (2 mg, 0.00625 mmol, 5 mol%), $NiCl_2$-dme (1.5 mg, 0.00625 mmol, 5 mol%), THF (0.25 mL), cyclobutyl trifluoroborate salt **25** (42 mg, 0.125 mmol, 1.0 eq), 5-bromopyrimidine (30 mg, 0.1875 mmol, 1.5 eq), $[Ir(dFCF_3ppy]_2(dtbpy)]PF_6$ (3.5 mg, 0.003125 mmol, 2.5 mol%), Cs_2CO_3 (62 mg, 0.1875 mmol, 1.5 eq) and dioxane (2.5 mL) gave the crude product. Purification by flash column chromatography on silica with 9:1 to 1:1 hexane-

EtOAc as eluent gave pyrimidine cyclobutane **133** (11 mg, 29%) as a white solid, identical (by ^{1}H NMR spectroscopy) to that described above.
Lab book reference: HSK-1-91

Using general procedure A with freshly recrystallised [Ir(dFCF$_3$ppy]$_2$(dtbpy)]PF$_6$ and a different batch of NiCl$_2$-dme, cyclobutyl trifluoroborate salt **25** (83 mg, 0.25 mmol, 1.0 eq) and 5-bromopyrimidine (60 mg, 0.375 mmol, 1.5 eq) gave the crude product. Purification by flash column chromatography on silica with 9:1 to 1:1 hexane-EtOAc as eluent gave impure pyrimidine cyclobutane **133** (21 mg, <27% unable to quantify yield due to significant impurities present) as a yellow oil.
Lab book reference: HSK-2-101

Using general procedure A using a different batch of dtbbpy, cyclobutyl trifluoroborate salt **25** (83 mg, 0.25 mmol, 1.0 eq) and 5-bromopyrimidine (60 mg, 0.375 mmol, 1.5 eq) gave the crude product. Purification by flash column chromatography on silica with 9:1 to 1:1 hexane-EtOAc as eluent gave impure pyrimidine cyclobutane **133** (13 mg, <17% unable to quantify yield due to significant impurities present) as a yellow oil.
Lab book reference: HSK-2-102

Using general procedure A with a freshly purchased bottle of dioxane, cyclobutyl trifluoroborate salt **25** (83 mg, 0.25 mmol, 1.0 eq) and 5-bromopyrimidine (60 mg, 0.375 mmol, 1.5 eq) gave the crude product. Purification by flash column chromatography on silica with 9:1 to 1:1 hexane-EtOAc as eluent gave pyrimidine cyclobutane **133** (31 mg, 41%) as a yellow solid, identical (by ^{1}H NMR spectroscopy) to that described above.
Lab book reference: HSK-2-119

***tert*-Butyl 2-(4-methanesulfonylphenyl)-7-azaspiro[3.5]nonane-7-carboxylate 136**

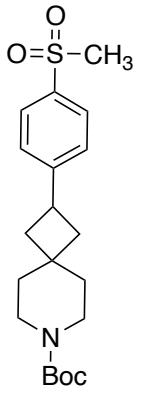

136

Using general procedure A with a freshly purchased bottle of dioxane, cyclobutyl trifluoroborate salt **25** (83 mg, 0.25 mmol, 1.0 eq) and 1-bromo-4-methane sulfonyl benzene (88 mg, 0.375 mmol, 1.5 eq) gave the crude product. Purification by flash column chromatography on silica with 19:1 hexane-EtOAc to EtOAc as eluent gave methanesulfonylphenyl cyclobutane **136** (37 mg, 39%) as a white solid, identical (by ^{1}H NMR spectroscopy) to that described above.

Lab book reference: HSK-2-127

***tert*-Butyl 2-[4-(ethoxycarbonyl)phenyl]-7-azaspiro[3.5]nonane-7-carboxylate 132**

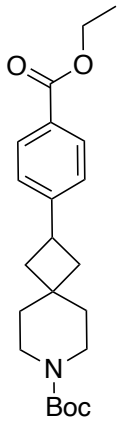

132

4,4'-Di-*tert*-butyl-2,2'-bipyridine (5 mg, 0.019 mmol, 7.5 mol%), $NiBr_2$-dme (4 mg, 0.019 mmol, 7.5 mol%), and THF (0.5 mL) were added to a glass vial equipped with a Teflon-coated magnetic stirrer bar. The vial was capped and the resulting suspension was heated with a heat gun until the nickel and ligand were fully solubilised. This gave a pale green solution. The solvent was evaporated under reduced pressure to give a fine coating of the ligated nickel complex on the side of the vial. Then, $[Ir(dFCF_3ppy]_2(dtbpy)]PF_6$ (4

mg, 0.00375 mmol, 1.5 mol%), quinuclidine (49 mg, 0.44 mmol, 1.75 eq), ethyl 4-bromobenzoate (41 μL, 0.25 mmol, 1.0 eq) and phthalimide (8 mg, 0.056 mmol, 0.22 eq) in DMA (2.5 mL) were added. The vial was capped and purged with Ar for 30 min. Cyclobutanol **50** (106 mg, 0.44 mmol, 1.75 eq) and the NHC precursor **141** (158 mg, 0.40 mmol, 1.6 eq) were added to a second pressure vial and MTBE (2.5 mL) was added. Pyridine (32 μL, 0.40 mmol, 1.6 eq) was added to the mixture. The resulting mixture was stirred at rt for 30 min whereupon a colour change of white to pink was observed. This mixture was taken up in a syringe and transferred to the first vial using a syringe filter. The mixed suspension was purged with Ar for 15 min. The vial was sealed with parafilm and stirred approximately 4 cm away from a blue LED light at ~24 ℃ for 16 h. A fan was blown across the reaction set-up to maintain a temperature of ~24 ℃. EtOAc (10 mL) was added and the organic layer was washed with H_2O (15 mL). The organic layer was washed with 1 M $HCl_{(aq)}$ (10 mL), 15% $CuSO_{4(aq)}$ (10 mL) and brine (2 × 15 mL), dried ($MgSO_4$) and evaporated under reduced pressure to give the crude product. Purification by flash column chromatography on silica with hexane to 17:3 hexane-Et_2O as eluent gave a 80:20 mixture of ethyl ester phenyl cyclobutane **132** and phthalimide (44 mg, i.e. 40 mg (43%) of ethyl ester phenyl cyclobutane **132**) as a white solid.
Lab book reference: HSK-1-62

***tert*-Butyl 2-(4-sulfamoylphenyl)-7-azaspiro[3.5]nonane-7-carboxylate 137**

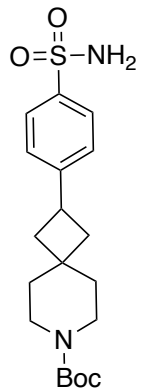

137

4,4'-Di-*tert*-butyl-2,2'-bipyridine (5 mg, 0.019 mmol, 7.5 mol%), $NiBr_2$-dme (4 mg, 0.019 mmol, 7.5 mol%), and THF (0.5 mL) were added to a glass vial equipped with a Teflon-coated magnetic stirrer bar. The vial was capped and the resulting suspension was heated with a heat gun until the nickel and ligand were fully solubilised. This gave a pale green solution. The solvent was evaporated under reduced pressure to give a fine coating

of the ligated nickel complex on the side of the vial. Then, $[Ir(dFCF_3ppy]_2(dtbpy)]PF_6$ (4 mg, 0.00375 mmol, 1.5 mol%), quinuclidine (49 mg, 0.44 mmol, 1.75 eq) and 4-bromobenzene sulfonamide (59 mg, 0.25 mmol, 1.0 eq) in DMA (2.5 mL) were added. The vial was capped and purged with Ar for 30 min. Cyclobutanol **50** (106 mg, 0.44 mmol, 1.75 eq) and the NHC precursor **141** (158 mg, 0.40 mmol, 1.6 eq) were added to a second pressure vial and MTBE (2.5 mL) was added. Pyridine (32 μL, 0.40 mmol, 1.6 eq) was added to the mixture. The resulting mixture was stirred at rt for 30 min whereupon a colour change of white to pink was observed. This mixture was taken up in a syringe and transferred to the first vial using a syringe filter. The mixed suspension was purged with Ar for 15 min. The vial was sealed with parafilm and stirred approximately 4 cm away from a blue LED light at ~24 ℃ for 16 h. A fan was blown across the reaction set-up to maintain a temperature of ~24 ℃. EtOAc (10 mL) was added and the organic layer was washed with H_2O (15 mL). The organic layer was washed with 1 M $HCl_{(aq)}$ (10 mL), 15% $CuSO_{4(aq)}$ (10 mL) and brine (2 × 15 mL), dried ($MgSO_4$) and evaporated under reduced pressure to give the crude product. Purification by flash column chromatography on silica with 99:1 to 9:1 CH_2Cl_2-acetone as eluent gave sulfamoylphenyl cyclobutane **137** (18 mg, 19%) as a white solid, mp 195-200 ℃, R_F (9:1 CH_2Cl_2-acetone) 0.58; IR (ATR) 3285 (N–H), 2923, 1668 (C=O), 1438, 1333, 1154, 908, 721, 568 cm^{-1}; ^1H NMR (400 MHz, $CDCl_3$) δ 7.86 (d, J = 8.0 Hz, 2H, Ar), 7.33 (d, J = 8.0 Hz, 2H, Ar), 4.91 (s, 2H, NH_2), 3.59 (tt, J = 9.0, 9.0 Hz, 1H, ArCH), 3.45–3.34 (m, 2H, NCH), 3.33–3.25 (m, 2H, NCH), 2.45–2.29 (m, 2H, C*H*CHAr), 2.01–1.85 (m, 2H, C*H*CHAr), 1.75–1.68 (m, 2H, CH), 1.54–1.47 (m, 2H, CH), 1.45 (s, 9H, CMe_3); ^{13}C NMR (100.6 MHz, $CDCl_3$) δ 155.1 (C=O), 151.7 (*ipso*-Ar), 139.4 (*ipso*-Ar), 127.2 (Ar), 126.7 (Ar), 79.5 (O*C*Me_3), 40.9 (br, NCH_2), 39.2 (CH_2), 39.0 (CH_2), 35.9 (CH_2), 34.3 (C), 33.5 (ArCH), 28.6 (C*Me*$_3$); HRMS (ESI) *m/z* calcd for $C_{19}H_{28}N_2O_4S$ $(M + Na)^+$ 403.1662 found 403.1664 (–1.6 ppm error).

Lab book reference: HSK-1-66

Attempted synthesis of *tert*-butyl 2-(3,5-dimethoxyphenyl)-7-azaspiro[3.5]nonane-7-carboxylate 146

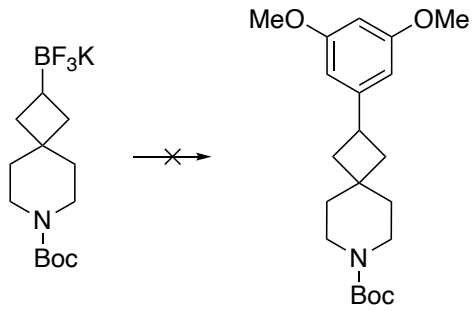

146

Using general procedure B, cyclobutyl trifluoroborate salt **25** (149 mg, 0.45 mmol, 1.5 eq), 5-chloro-3-dimethoxybenzene (52 mg, 0.30 mmol, 1.0 eq), $Pd(OAc)_2$ (1.4 mg, 6 μmol, 2 mol%), and CataCXium A (3.2 mg, 9 μmol, 3 mol%), heated at 120 ℃ (heater block temperature), gave the crude product which contained none of dimethoxyphenyl cyclobutane **146** by ^{1}H NMR spectroscopy.
Lab book reference: HSK-2-109

Using general procedure B, cyclobutyl trifluoroborate salt **25** (149 mg, 0.45 mmol, 1.5 eq), 5-chloro-3-dimethoxybenzene (52 mg, 0.30 mmol, 1.0 eq), $Pd(OAc)_2$ (1.4 mg, 6 μmol, 2 mol%), and CataCXium A (3.2 mg, 9 μmol, 3 mol%), heated at 100 ℃ (heater block temperature), gave the crude product which contained none of dimethoxyphenyl cyclobutane **146** by ^{1}H NMR spectroscopy.
Lab book reference: HSK-2-110

***tert*-Butyl 2-phenyl-7-azaspiro[3.5]nonane-7-carboxylate 149**

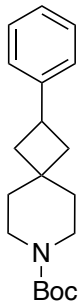

149

Using general procedure C, cyclobutyl trifluoroborate salt **25** (149 mg, 0.45 mmol, 1.5 eq) and chlorobenzene (30 μL, 0.30 mmol, 1.0 eq) gave the crude product. Purification by flash column chromatography on silica with 99:1 to 1:1 hexane-EtOAc as eluent gave

phenyl cyclobutane **149** (43 mg, 55%) as a yellow solid, mp 70-80 °C; R_F (6:4 hexane-EtOAc) 0.71; IR (ATR) 2921, 1691 (C=O), 1603, 1420, 1242, 1145, 975, 697 cm^{-1}; ^1H NMR (400 MHz, $CDCl_3$); δ 7.44–7.28 (m, 2H, Ph), 7.23–7.14 (m, 3H, Ph), 3.52 (tt, *J* = 9.0, 9.0 Hz, 1H, PhCH), 3.46–3.38 (m, 2H, NCH), 3.33–3.27 (m, 2H, NCH), 2.37–2.25 (m, 2H, C*H*CHAr), 1.96–1.86 (m, 2H, C*H*CHAr), 1.80–1.68 (m, 2H, CH), 1.60–1.50 (m, 2H, CH), 1.47 (s, 9H, CMe_3); ^{13}C NMR (100.6 MHz, $CDCl_3$) δ 155.1 (C=O), 146.2 (*ipso*-Ph), 128.4 (Ph), 126.5 (Ph), 125.9 (Ph), 79.4 (O*C*Me_3), 40.9 (br, NCH_2), 39.3 (CH_2), 39.2 (CH_2), 36.0 (CH_2) 34.0 (C), 33.5 (PhCH), 28.6 (OC*Me*$_3$); HRMS (ESI) *m/z* calcd for $C_{19}H_{27}NO_2$ $(M + Na)^+$ 324.1934, found 324.1937 (–1.6 ppm error). Spectroscopic data consistent with those reported in the literature.[139]
Lab book reference: HSK-2-113

Using general procedure C, cyclobutyl trifluoroborate salt **25** (99 mg, 0.3 mmol, 1.0 eq) and chlorobenzene (46 μL, 0.45 mmol, 1.5 eq) gave the crude product. Purification by flash column chromatography on silica with 1000:1 to 4:1 hexane-EtOAc as eluent gave phenyl cyclobutane **149** (48 mg, 53%) as a yellow solid, identical (by ^1H NMR spectroscopy) to that described above.
Lab book reference: HSK-2-118

Using general procedure C, cyclobutyl trifluoroborate salt **25** (99 mg, 0.3 mmol, 1.0 eq), and bromobenzene (47 μL, 0.45 mmol, 1.5 eq) gave the crude product. Purification by flash column chromatography on silica with 1000:1 to 4:1 hexane-EtOAc as eluent gave impure phenyl cyclobutane **149** (22 mg, <24% unable to quantify yield due to significant impurities present) as a yellow solid.
Lab book reference: HSK-2-120

***tert*-Butyl 2-(pyrimidin-5-yl)-7-azaspiro[3.5]nonane-7-carboxylate 133**

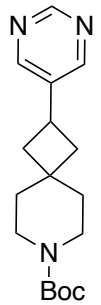

133

Using general procedure B cyclobutyl trifluoroborate salt **25** (99 mg, 0.3 mmol, 1.0 eq), and 5-bromopyrimidine (72 mg, 0.45 mmol, 1.5 eq) gave the crude product. Purification by flash column chromatography on silica with 9:1 to 1:1 hexane-EtOAc as eluent gave pyrimidine cyclobutane **133** (41 mg, 45%) as a yellow solid, identical (by ^{1}H NMR spectroscopy) to that described above.

Lab book reference: HSK-2-122

***tert*-Butyl 2-(4-methanesulfonylphenyl)-7-azaspiro[3.5]nonane-7-carboxylate 136 and *tert*-butyl 2-hydroxy-7-azaspiro[3.5]nonane-7-carboxylate 50**

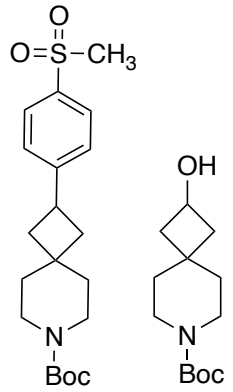

136 **50**

Using general procedure C, cyclobutyl trifluoroborate salt **25** (99 mg, 0.3 mmol, 1.0 eq) and 1-bromo-4-methane sulfonyl benzene (106 mg, 0.45 mmol, 1.5 eq) gave the crude product. Purification by flash column chromatography on silica with 1:1 hexane-EtOAc as eluent gave a 15:30:55 mixture of methanesulfonylphenyl cyclobutane **136**, cyclobutanol **50** and 4-bromophenyl methyl sulfone (115 mg, i.e. 24 mg (21%) of methanesulfonylphenyl cyclobutane **136**) as a yellow oil. Purification by flash column chromatography on silica with 1:1 hexane-EtOAc as eluent a second time gave cyclobutanol **50** (20 mg, 28%) as a white solid, identical (by ^{1}H NMR spectroscopy) to that described above.

Lab book reference: HSK-2-123

Attempted synthesis of *tert*-butyl 2-(4-sulfamoylphenyl)-7-azaspiro[3.5]nonane-7-carboxylate 137

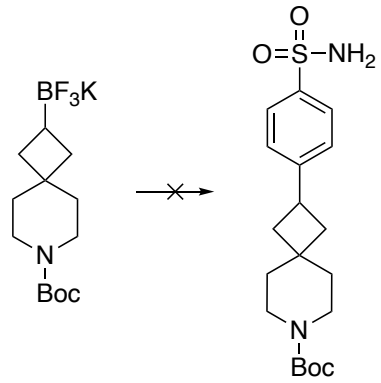

137

Using general procedure C, cyclobutyl trifluoroborate salt **25** (99 mg, 0.3 mmol, 1.0 eq), and 4-bromobenzene sulfonamide (106 mg, 0.45 mmol, 1.5 eq) gave the crude product which contained none of sulfamoylphenyl cyclobutane **137** by ^{1}H NMR spectroscopy.
Lab book reference: HSK-2-121

Attempted synthesis of *tert*-butyl 2-(4-acetamidophenyl)-7-azaspiro[3.5]nonane-7-carboxylate 135

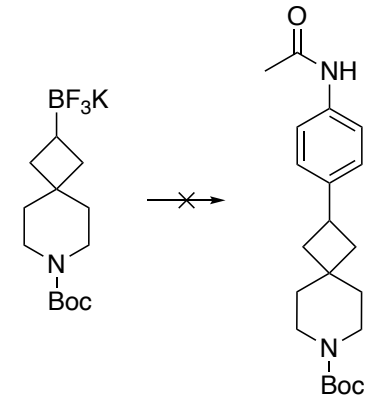

135

Using general procedure C, cyclobutyl trifluoroborate salt **25** (99 mg, 0.3 mmol, 1.0 eq), and 4-bromoacetanilide (96 mg, 0.45 mmol, 1.5 eq) gave the crude product which contained none of acetanilide cyclobutane **135** by ^{1}H NMR spectroscopy.
Lab book reference: HSK-2-124

7-Methanesulfonyl-2-(pyrimidin-5-yl)-7-azaspiro[3.5]nonane 159

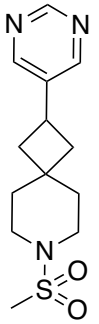

159

A solution of pyrimidine cyclobutane **133** (69 mg, 0.23 mmol, 1.0 eq) in 4 N HCl in dioxane (5 mL) under Ar was stirred at rt for 1 h. The dioxane was evaporated under reduced pressure to give the crude HCl salt as a yellow solid. The solid was suspended in CH_2Cl_2 (5 mL) and Et_3N (0.15 mL, 1.1 mmol, 4.8 eq) was added. The resulting mixture was stirred at rt until all of the solids had dissolved. Then, MsCl (39 μL, 0.50 mmol, 2.2 eq) was added and the resulting solution was stirred at rt for 16 h. CH_2Cl_2 (20 mL) was added and the solution was washed with saturated $NaHCO_{3(aq)}$ (10 mL) and brine (25 mL), dried ($MgSO_4$) and evaporated under reduced pressure to give the crude product. Purification by flash column chromatography on silica with EtOAc to 9:1 EtOAc-hexane as eluent gave *N*-methanesulfonamide pyrimidine **159** (37 mg, 67%) as a white solid, mp 148-150 ℃; R_F (9:1 EtOAc-hexane) 0.1; IR (ATR) 2924, 2331, 1558, 1411, 1312, 1144, 787, 519 cm^{-1}; ^1H NMR (400 MHz, $CDCl_3$); δ 9.06 (s, 1H, Ar), 8.58 (s, 2H, Ar), 3.54 (tt, *J* = 9.0, 9.0 Hz 1H, ArCH), 3.27–3.18 (m, 2H, NCH), 3.16–3.08 (m, 2H, NCH), 2.77 (s, 3H, Me), 2.43–2.33 (m, 2H, C*H*CHAr), 2.01–1.92 (m, 2H, C*H*CHAr), 1.92–1.86 (m, 2H, CH), 1.74–1.66 (m, 2H, CH); ^{13}C NMR (100.6 MHz, $CDCl_3$) δ 156.9 (Ar), 155.3 (Ar), 138.1 (*ipso*-Ar), 43.1 (NCH_2), 42.8 (NCH_2), 38.7 (CH_2), 38.5 (CH_2), 35.3 (CH_2), 34.9 (Me), 34.1 (C), 29.0 (ArCH); HRMS (ESI) *m/z* calcd for $C_{13}H_{19}N_3O_2S$ $(M + Na)^+$ 304.1090 found 304.1093 (–1.2 ppm error).

Lab book reference: HSK-1-75

Ethyl 4-{7-[(3,5-dimethyl-1,2-oxazol-4-yl)sulfonyl]-7-azaspiro[3.5]nonan-2-yl}benzoate 160

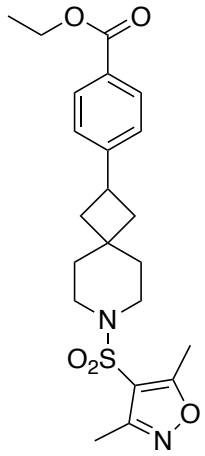

160

A solution of ethyl ester phenyl cyclobutane **132** (48 mg, 0.129 mmol, 1.0 eq) in 4 N HCl in dioxane (5 mL) under Ar was stirred at rt for 1 h. The solvent was evaporated under reduced pressure to give the crude HCl salt. CH_2Cl_2 (5 mL), DMAP (1.5 mg, 0.0129 mmol, 0.1 eq) and Et_3N (90 µL, 0.643 mmol, 5.0 eq) were added under Ar. The resulting solution was cooled to 0 ℃ and 3,5-dimethylisoxazole-4-sulfonyl chloride (31.5 mg, 0.161 mmol, 1.25 eq) was added. The resulting solution stirred was stirred at rt for 18 h. 1 M $HCl_{(aq)}$ (10 mL) was added, and the two layers were separated. The aqueous layer was extracted with CH_2Cl_2 (3 × 10 mL). The combined organic extracts and the original CH_2Cl_2 extract were washed with brine (15 mL), dried ($MgSO_4$) and evaporated under reduced pressure to give the crude product. Purification by flash column chromatography on silica with 9:1 to 7:3 hexane-EtOAc as eluent gave *N*-dimethyloxazolylsulfonyl ethyl ester phenyl cyclobutane **160** (44 mg, 79%) as a white solid, mp 130-135 ℃; R_F (1:1 hexane-EtOAc) 0.8; IR (ATR) 2926, 1713 (C=O), 1588, 1273, 1177, 1106, 726, 624, 571 cm^{-1}; ^1H NMR (400 MHz, $CDCl_3$) δ 7.96 (d, J = 8.0 Hz, 2H, Ar), 7.21 (d, J = 8.0 Hz, 2H, Ar), 4.35 (q, J = 7.0 Hz, 2H, OCH_2), 3.55 (tt, J = 9.0, 9.0 Hz, 1H, ArCH), 3.18–3.11 (m, 2H, NCH), 3.06–2.99 (m, 2H, NCH), 2.64 (s, 3H, Me), 2.41 (s, 3H, Me), 2.33–2.23 (m, 2H, C*H*CHAr), 1.93–1.89 (m, 2H, C*H*CHAr), 1.88–1.84 (m, 2H, CH), 1.82–1.60 (m, 2H, CH), 1.37 (t, J = 7.0 Hz, 3H, *Me*CH_2); ^{13}C NMR (100.6 MHz, $CDCl_3$) δ 173.7 (C=O), 166.6 (*ipso*-Ar), 158.2 (*ipso*-Ar), 150.8 (*ipso*-Ar), 129.8 (Ar), 128.4 (*ipso*-Ar), 126.4 (Ar), 113.9 (*ipso*-Ar), 61.0 (OCH_2), 42.8 (NCH_2), 42.5 (NCH_2), 38.7 (CH_2), 38.5 (CH_2), 35.3

(CH_2), 33.4 (ArCH), 14.5 (*Me*CH_2), 13.1 (Me), 11.5 (Me); HRMS (ESI) *m/z* calcd for $C_{22}H_{28}N_2O_5S$ $(M + Na)^+$ 455.1611, found 455.1618 (–2.1 ppm error).
Lab book reference: HSK-2-114

_N_-(4-{7-Benzoyl-7-azaspiro[3.5]nonan-2-yl}phenyl)acetamide 161

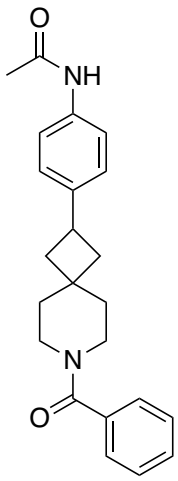

161

A solution of acetanilide cyclobutane **135** (39 mg, 0.109 mmol, 1.0 eq) in 4 N HCl in dioxane (5 mL) under Ar was stirred at rt for 1 h. The solvent was evaporated under reduced pressure to give the crude HCl salt. CH_2Cl_2 (5 mL) and Et_3N (30 µL, 0.217 mmol, 2.0 eq) were added under Ar. The resulting solution was cooled to 0 ℃ and benzoyl chloride (16 µL, 0.136 mmol, 1.25 eq) was added dropwise. The resulting solution was stirred at rt for 18 h. The solution was washed with H_2O (10 mL) and the aqueous layer was extracted with CH_2Cl_2 (3 × 10 mL). The combined organic extracts and the original CH_2Cl_2 extract were washed with brine (15 mL), dried ($MgSO_4$) and evaporated under reduced pressure to give the crude product. Purification by flash column chromatography on silica with 1:1 to 1:4 hexane-EtOAc as eluent gave *N*-benzamide acetanilide cyclobutane **161** (24 mg, 61%) as a white solid, mp 175-180 ℃; R_F (7:3 hexane-EtOAc) 0.18; IR (ATR) 3303 (N–H), 2922, 2854, 1667 (C=O), 1601 (C=O), 1514, 1275, 730, 709 cm^{-1}; ^1H NMR (400 MHz, $CDCl_3$) (rotamers) δ 7.60–7.56 (br m, 1H, NH), 7.45–7.37 (br m, 7H, Ar), 7.16–7.10 (br m, 2H, Ar), 3.79–3.74 (br m, 1H, NCH), 3.67–3.61 (br m, 1H, NCH), 3.55–3.43 (br m, 1H, ArCH), 3.41–3.36 (br m, 1H, NCH), 3.29–3.25 (br m, 1H, NCH), 2.33–2.28 (m, 2H, C*H*CHAr), 2.13 (s, 3H, Me), 1.91–1.87 (br m, 2H, C*H*CHAr), 1.70–1.65 (br m, 2H, CH), 1.53–1.48 (br, m, 2H, CH); ^{13}C NMR (100.6 MHz, $CDCl_3$) δ 170.6 (C=O), 168.6 (C=O), 141.8 (*ipso*-Ar), 136.4 (*ipso*-Ar), 136.0 (*ipso*-Ar), 129.6 (Ar),

128.6 (Ar), 126.9 (Ar), 120.2 (Ar), 45.2 (br, NCH_2), 39.3 (CH_2), 39.2 (br, NCH_2, identified by HSQC), 38.7 (CH_2, identified by HSQC), 35.4 (CH_2, identified by HSQC), 34.2 (C), 33.0 (ArCH), 24.5 (Me) (one Ar resonance not resolved); HRMS (ESI) *m/z* calcd for $C_{23}H_{26}N_2O_2$ $(M + Na)^+$ 385.1886, found 385.1876 (+2.6 ppm error).
Lab book reference: HSK-2-115

1-[2-(2-Methoxypyridin-4-yl)-7-azaspiro[3.5]nonan-7-yl]ethan-1-one 162

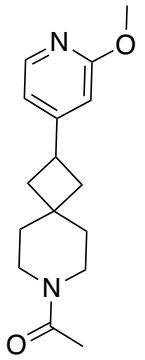

162

A solution of methoxypyridine cyclobutane **134** (42 mg, 0.126 mmol, 1.0 eq) in 4 N HCl in dioxane (5 mL) under Ar was stirred at rt for 1 h.. The solvent was evaporated under reduced pressure to give the crude HCl salt. The crude HCl salt was dissolved in pyridine (5 mL) and Ac_2O (71 μL, 0.756 mmol, 6.0 eq) was added dropwise. The resulting solution was stirred at rt for 18 h. The solvent was evaporated under reduced pressure to give the crude product. Purification by flash column chromatography on silica with 1:1 to 1:4 hexane-EtOAc as eluent gave *N*-acetamide methoxypyridine cyclobutane **162** (31 mg, 90%) as a yellow oil, R_F (7:3 hexane-EtOAc) 0.12; IR (ATR) 2922, 2853, 1640 (C=O), 1607 1556, 1393, 1265, 1044, 987, 658 cm^{-1}; ^1H NMR (400 MHz, $CDCl_3$) (50:50 mixture of rotamers) δ 8.05 (d, *J* = 5.5 Hz, 1H, Ar), 6.72–6.66 (m, 1H, Ar), 6.57–6.52 (m, 1H, Ar), 3.91 (s, 3H, OMe), 3.61–3.54 (m, 1H, NCH), 3.52–3.45 (m, 1H, ArCH), 3.45–3.38 (m, 2H, NCH), 3.33–3.25 (m, 1H, NCH), 2.34–2.22 (m, 2H, C*H*CHAr), 2.08 (s, 1.5 H, Me), 2.06 (s, 1.5 H, Me), 2.00–1.84 (m, 2H, C*H*CHAr), 1.77–1.66 (m, 2H, CH), 1.55–1.39 (m, 2H, CH); ^{13}C NMR (100.6 MHz, $CDCl_3$) (rotamers) δ 169.00 (C=O), 168.96 (C=O), 164.6 (*ipso*-Ar), 157.7 (*ipso*-Ar), 157.6 (*ipso*-Ar), 146.8 (Ar), 115.6 (Ar), 115.5 (Ar), 108.3 (Ar), 108.3 (Ar), 53.5 (OMe), 43.8 (NCH_2), 43.4 (NCH_2), 39.7 (CH_2), 38.9 (CH_2), 38.8 (CH_2), 38.5 (NCH_2), 38.2 (NCH_2), 36.6 (CH_2), 35.7 (CH_2), 34.4 (C), 34.3 (C), 32.7 (ArCH), 21.6 (Me), 21.6 (Me); HRMS (ESI) *m/z* calcd for $C_{16}H_{22}N_2O_2$ $(M + Na)^+$ 297.1573, found 297.1572 (+0.5 ppm error).

Lab book reference: HSK-2-116

7-(1H-Indole-3-carbonyl)-2-phenyl-7-azaspiro[3.5]nonane 163

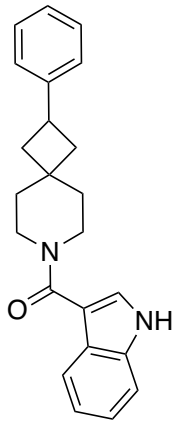

163

A solution of phenyl cyclobutane **149** (48 mg, 0.159 mmol, 1.0 eq) in 4 N HCl in dioxane (5 mL) under Ar was stirred at rt for 1 h. The solvent was evaporated under reduced pressure to give the crude HCl salt. The crude HCl salt was suspended in EtOAc (3 mL). Then, Et_3N (88 μL, 0.637 mmol, 4.0 eq) and indole-3-carboxylic acid (31 mg, 0.192 mmol, 1.2 eq) were added under Ar. The resulting solution was cooled to 0 ℃ and a 50% solution of T3P in toluene (0.l9 mL, 0.318 mmol, 2.0 eq) was added dropwise. The resulting solution was stirred and heated at 80 ℃ for 18 h. After being allowed to cool to rt, EtOAc (20 mL) was added and the solution was washed with saturated $NaHCO_{3(aq)}$ (10 mL). The organic layer was washed with 0.5 M $HCl_{(aq)}$ (10 mL). The combined organic extracts were washed with brine (15 mL), dried ($MgSO_4$) and evaporated under reduced pressure to give the crude product. Purification by flash column chromatography on silica with 7:3 to 2:3 hexane-EtOAc as eluent gave *N*-indoleamide phenyl cyclobutane **163** (30 mg, 55%) as a beige solid, mp 160-165 ℃; R_F (7:3 hexane-EtOAc) 0.32; IR (ATR) 3173 (N–H), 2922, 2853, 1592 (C=O), 1444, 747, 735, 698 cm^{-1}; ^1H NMR (400 MHz, $CDCl_3$) δ 9.77 (s, 1H, NH), 7.71–7.64 (m, 1H, Ar), 7.39–7.01 (m, 10H, Ar), 3.74–3.69 (m, 2H, NCH), 3.62–3.57 (m, 2H, NCH), 3.56–3.45 (m, 1H, ArCH), 2.40–2.30 (m, 2H, C*H*CHAr), 2.00–1.90 (m, 2H, C*H*CHAr), 1.82–1.78 (m, 2H, CH), 1.62–1.58 (m, 2H, CH); ^{13}C NMR (100.6 MHz, $CDCl_3$) δ 146.0 (C=O), 135.8 (*ipso*-Ar), 128.4 (Ar), 126.5 (Ar), 126.0 (Ar), 125.6 (*ipso*-Ar), 122.7 (Ar), 121.0 (Ar), 120.3 (Ar), 112.0 (Ar), 39.7 (CH_2, detected by HSQC), 39.3 (CH_2), 36.2 (CH_2, detected by HSQC), 34.3 (C), 33.5

(ArCH) (CH_2 and 2 × *ipso*-Ar resonances not resolved); HRMS (ESI) *m/z* calcd for $C_{23}H_{24}N_2O$ $(M + Na)^+$ 367.1781, found 367.1787 (–2.7 ppm error).

Lab book reference: HSK-2-117

6.4. X-ray Crystal Structure Data Data

X-ray crystal structure data for pyrimidine methanesulfonamide **133**

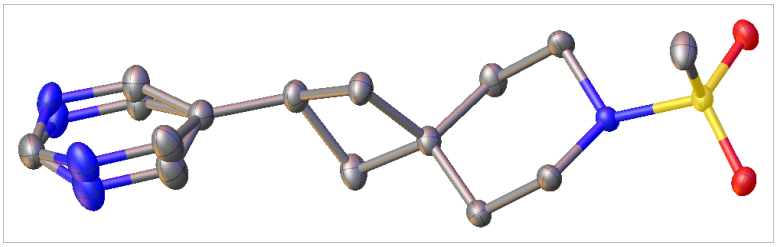

Table 6.1 - Crystal data and structure refinement for paob22006

Identification code	**paob22006**
Empirical formula	C 13 H 19 N 3 O 2 S
Formula weight	281.37
Temperature/K	110.00(10)
Crystal system	monoclinic
Space group	P2 1 /n
a/Å	6.03968(11)
b/Å	27.4177(5)
c/Å	8.52436(15)
α/°	90
β/°	98.9134(18)
γ/°	90
Volume/Å 3	1394.54(4)
Z	4
ρ calc g/cm 3	1.340
μ/mm 1	2.088
F(000)	600.0
Crystal size/mm 3	0.238 × 0.199 × 0.141
Radiation	Cu Kα (λ = 1.54184)
2Θ range for data collection/°	10.99 to 134.052
Index ranges	-7 ≤ h ≤ 6, -32 ≤ k ≤ 32, -10 ≤ l ≤ 9
Reflections collected	4914
Independent reflections	2494 [R int = 0.0186, R sigma = 0.0255]
Data/restraints/parameters	2494/5/250
Goodness-of-fit on F 2	1.059
Final R indexes [I>=2σ (I)]	R 1 = 0.0302, wR 2 = 0.0758
Final R indexes [all data]	R 1 = 0.0339, wR 2 = 0.0782
Largest diff. peak/hole / e Å -3	0.27/-0.29

Data collected, solved and refined by Adrian C Whitwood

7. Abbreviations

(±)-BINAP	(±)-2,2′-Bis(diphenylphosphino)-1,1′-binaphthalene
2-D	Two-dimensional
3-D	Three-dimensional
μM	Micromolar
δ	Chemical shift
Ac	Acetyl
ADME	Absorption, distribution, metabolism and excretion
AEA	endocannabinoid anandamide
aq.	Aqueous
Ar	Aryl
Ar_F	4-$(CF_3)C_6F_4$
ART	Amino radical transfer
ATAD2	ATPase Family AAA Domain Containing 2
ATP	Adenosine triphosphate
ATR	Attenuated total reflection
BMIDA	N-methyliminodiacetyl boronate
Boc	*tert*-Butoxycarbonyl
bpy	2,2′-Bipyridine
Br	Broad
BRD4	Bromodomain-containing protein 4
Calcd	calculated
CataCXium A	Di(1-adamantyl)-*n*-butylphosphine
CDK2	Cyclin-dependent kinase 2
CFL	Compact fluorescent bulbs
cLogP	Partition coefficient
cm	centimetre
cm^{-1}	Wavelength
CPME	Cyclopentyl methyl ether
CNS	Central nervous system
d	Doublet
Da	Daltons
DCE	1,2-Dichloroethane

DEPT	Distortionless Enhancement by Polarization Transfer
dF(CF_3)ppy	5-(trifluoromethyl)pyridine
DMA	Dimethylacetamide
DMAP	Dimethylaminopyridine
DME or dme	1,2-Dimethoxyethane
DMF	Dimethylformamide
DMSO	Dimethylsulfoxide
d_6-DMSO	Deuterated dimethylsulfoxide
dppbz	1,2-Bis(diphenylphosphino)benzene
dppf	1,1′-Ferrocenediyl-bis(diphenylphosphine)
dppp	1,3-Bis(diphenylphosphino)propane
dr	Diastereomeric ratio
dtbbpy	4,4′-Di-*tert*-butyl-2,2′-dipyridyl
ee	Enantiomeric excess
ESI	Electronspray ionisation
Et	Ethyl
eq	Equivalents
FAAH	fatty acid amide hydrolase
FBDD	Fragment-based drug discovery
FDA	Food and drug administration
FT-IR	Fourier Transform Infrared Spectroscopy
g	Gram(s)
h	Hour(s)
HSQC	Heteronuclear Single Quantum Coherence
HTS	High throughput screening
HRMS	High resolution mass spectroscopy
hν	light
Hz	Hertz
i-Pr	Isopropyl
IC_{50}	Half-maximal inhibitory concentration
IR	Infra-red
J	Coupling constant in Hz
JAK3	Janus Kinase 3

KHMDS	Potassium bis(trimethylsilyl)amide
LED	Light-emitting diode
LiHMDS	Lithium bis(trimethylsilyl)amide
Lit.	literature
L_n	Ligand(s)
m	Multiplet
M	Molar
M^+	Molecular ion
MAGL	monoacylglycerol lipase
Me	Methyl
mg	Milligrams
MHz	Mega Hertz
MIDA	N-methyliminodiacetic acid
min	Minute
mL	Millilitre
mM	Millimolar
mmol	Millimole
mol	Mole
mp	Melting point
Ms	Mesyl
MS	Mass spectrometry
MTBE	Methyl tert-butyl ether
MW	Molecular weight
m/z	Mass to charge ratio
N	Normality
NaHMDS	Sodium bis(trimethylsilyl)amide
NHC	*N*-heterocyclic carbene
nm	nanometres
nM	nanomolar
NMR	Nuclear magnetic resonance
p-Ts	Para-tosyl
pin	pinacol
PCy_3	Tricyclohexylphosphine

Ph	Phenyl
ppm	Parts per million
PTFE	Polytetrafluoroethylene
Py	Pyridine
Q	Quartet
R	Alkyl or aryl group
R_F	Retention factor
Ro3	Rule of three
Ro5	Rule of five
rpm	Revolutions per minute
rt	Room temperature
RuPhos	2-Dicyclohexylphosphino-2′,6′-diisopropoxybiphenyl
s	Singlet
SET	Single-electron transfer
SMCC	Suzuki-Miyaura cross-coupling
SPhos	2-Dicyclohexylphosphino-2′,6′-dimethoxybiphenyl
t	Triplet
t-Bu	*tert*-Butyl
T3P	Propanephosphonic acid anhydride
Tf	Triflate
TFA	Trifluoroacetic acid
THF	Tetrahydrofuran
TLC	Thin layer chromatography
Ts	Tosyl
UV	Ultraviolet
W	Watt
Xantphos	4,5-Bis(diphenylphosphino)-9,9-dimethylxanthene

8. References

1 D. A. Erlanson, S. W. Fesik, R. E. Hubbard, W. Jahnke and H. Jhoti, *Nat. Rev. Drug Discov.*, 2016, **15**, 605–619.

2 C. W. Murray and D. C. Rees, *Nat. Chem.*, 2009, **1**, 187–192.

3 M. Congreve, G. Chessari, D. Tisi and A. J. Woodhead, *J. Med. Chem.*, 2008, **51**, 3661–3680.

4 H. Jhoti, G. Williams, D. C. Rees and C. W. Murray, *Nat. Rev. Drug Discov.*, 2013, **12**, 644–645.

5 V. Velvadapu, B. T. Farmer and A. B. Reitz, in *The Practice of Medicinal Chemistry (Fourth Edition)*, ed. C. G. Wermuth, D. Aldous, P. Raboisson and D. Rognan, Academic Press, San Diego, 2015, pp. 161–180.

6 D. A. Erlanson, *Top. Curr. Chem.*, 2012, **317**, 1–32.

7 A. Ciulli and C. Abell, *Curr. Opin. Biotechnol.*, 2007, **18**, 489–496.

8 D. E. Scott, A. G. Coyne, S. A. Hudson and C. Abell, *Biochemistry*, 2012, **51**, 4990–5003.

9 M. Baker, *Nat. Rev. Drug Discov.*, 2013, **12**, 5–7.

10 C. W. Murray, M. L. Verdonk and D. C. Rees, *Trends Pharmacol. Sci.*, 2012, **33**, 224–232.

11 R. E. Hubbard and J. B. Murray, in *Methods in Enzymology*, ed. L. C. Kuo, Academic Press, 2011, vol. 493, pp. 509–531.

12 P. J. Hajduk and J. Greer, *Nat. Rev. Drug Discov.*, 2007, **6**, 211–219.

13 S. Bartoli, C. I. Fincham and D. Fattori, *Drug Discov. Today Technol.*, 2006, **3**, 425–431.

14 E. R. Zartler and M. J. Shapiro, *Curr. Opin. Chem. Biol.*, 2005, **9**, 366–370.

15 D. C. Rees, M. Congreve, C. W. Murray and R. Carr, *Nat. Rev. Drug Discov.*, 2004, **3**, 660–672.

16 C. W. Murray and D. C. Rees, *Angew. Chem. Int. Ed Engl.*, 2016, **55**, 488–492.

17 A. Schuffenhauer, S. Ruedisser, A. L. Marzinzik, W. Jahnke, M. Blommers, P. Selzer and E. Jacoby, *Curr. Top. Med. Chem.*, 2005, **5**, 751–762.

18 M. Congreve, R. Carr, C. Murray and H. Jhoti, *Drug Discov. Today*, 2003, 8, 876–877.

19 C. A. Lipinski, F. Lombardo, B. W. Dominy and P. J. Feeney, *Adv. Drug Deliv. Rev.*, 1997, **23**, 3–25.

20 D. J. Wood, J. D. Lopez-Fernandez, L. E. Knight, I. Al-Khawaldeh, C. Gai, S. Lin, M. P. Martin, D. C. Miller, C. Cano, J. A. Endicott, I. R. Hardcastle, M. E. M. Noble and M. J. Waring, *J. Med. Chem.*, 2019, **62**, 3741–3752.

21 G. Davison, M. P. Martin, S. Turberville, S. Dormen, R. Heath, A. B. Heptinstall, M. Lawson, D. C. Miller, Y. M. Ng, J. N. Sanderson, I. Hope, D. J. Wood, C. Cano, J. A. Endicott, I. R. Hardcastle, M. E. M. Noble and M. J. Waring, *J. Med. Chem.*, 2022, **65**, 15416–15432.

22 D. Erlanson, Practical Fragments, https://practicalfragments.blogspot.com/2022/11/fragments-in-clinic-2022-edition.html, (accessed December 6, 2022).

23 J. Schoepfer, W. Jahnke, G. Berellini, S. Buonamici, S. Cotesta, S. W. Cowan-Jacob, S. Dodd, P. Drueckes, D. Fabbro, T. Gabriel, J.-M. Groell, R. M. Grotzfeld, A. Q. Hassan, C. Henry, V. Iyer, D. Jones, F. Lombardo, A. Loo, P. W. Manley, X. Pellé, G. Rummel, B. Salem, M. Warmuth, A. A. Wylie, T. Zoller, A. L. Marzinzik and P. Furet, *J. Med. Chem.*, 2018, **61**, 8120–8135.

24 C. W. Murray, D. R. Newell and P. Angibaud, *Medchemcomm*, 2019, **10**, 1509–1511.

25 B. Benner, L. Good, D. Quiroga, T. E. Schultz, M. Kassem, W. E. Carson, M. A. Cherian, S. Sardesai and R. Wesolowski, *Drug Des. Devel. Ther.*, 2020, **14**, 1693–1704.

26 D. S. Hong, M. G. Fakih, J. H. Strickler, J. Desai, G. A. Durm, G. I. Shapiro, G. S. Falchook, T. J. Price, A. Sacher, C. S. Denlinger, Y.-J. Bang, G. K. Dy, J. C. Krauss, Y. Kuboki, J. C. Kuo, A. L. Coveler, K. Park, T. W. Kim, F. Barlesi, P. N. Munster, S. S. Ramalingam, T. F. Burns, F. Meric-Bernstam, H. Henary, J. Ngang, G. Ngarmchamnanrith, J. Kim, B. E. Houk, J. Canon, J. R. Lipford, G. Friberg, P. Lito, R. Govindan and B. T. Li, *N. Engl. J. Med.*, 2020, **383**, 1207–1217.

27 A. Kim and M. S. Cohen, *Expert Opin. Drug Discov.*, 2016, **11**, 907–916.

28 W. J. Fairbrother, J. D. Leverson, D. Sampath and A. J. Souers, *Successful Drug Discovery*, 2019, 225–245.

29 G. Bollag, P. Hirth, J. Tsai, J. Zhang, P. N. Ibrahim, H. Cho, W. Spevak, C. Zhang, Y. Zhang, G. Habets, E. A. Burton, B. Wong, G. Tsang, B. L. West, B. Powell, R. Shellooe, A. Marimuthu, H. Nguyen, K. Y. J. Zhang, D. R. Artis, J. Schlessinger, F. Su, B. Higgins, R. Iyer, K. D'Andrea, A. Koehler, M. Stumm, P. S. Lin, R. J. Lee, J. Grippo, I. Puzanov, K. B. Kim, A. Ribas, G. A. McArthur, J. A. Sosman, P.

B. Chapman, K. T. Flaherty, X. Xu, K. L. Nathanson and K. Nolop, *Nature*, 2010, **467**, 596–599.

30 T. Staton, Roche melanoma drug wins early FDA nod, https://www.fiercepharma.com/pharma/roche-melanoma-drug-wins-early-fda-nod, (accessed December 6, 2022).

31 J. J. Luke and F. S. Hodi, *Clin. Cancer Res.*, 2012, **18**, 9–14.

32 J. Tsai, J. T. Lee, W. Wang, J. Zhang, H. Cho, S. Mamo, R. Bremer, S. Gillette, J. Kong, N. K. Haass, K. Sproesser, L. Li, K. S. M. Smalley, D. Fong, Y.-L. Zhu, A. Marimuthu, H. Nguyen, B. Lam, J. Liu, I. Cheung, J. Rice, Y. Suzuki, C. Luu, C. Settachatgul, R. Shellooe, J. Cantwell, S.-H. Kim, J. Schlessinger, K. Y. J. Zhang, B. L. West, B. Powell, G. Habets, C. Zhang, P. N. Ibrahim, P. Hirth, D. R. Artis, M. Herlyn and G. Bollag, *Proc. Natl. Acad. Sci. U. S. A.*, 2008, **105**, 3041–3046.

33 F. Lovering, J. Bikker and C. Humblet, *J. Med. Chem.*, 2009, **52**, 6752–6756.

34 G. Li Petri, M. V. Raimondi, V. Spanò, R. Holl, P. Barraja and A. Montalbano, *Top. Curr. Chem.*, 2021, **379**, 34.

35 N. Jeelan Basha, S. M. Basavarajaiah and K. Shyamsunder, *Mol. Divers.*, 2022, **26**, 2915–2937.

36 R. Vardanyan, *Piperidine-Based Drug Discovery*, Elsevier, 2017.

37 M. M. Abdelshaheed, I. M. Fawzy, H. I. El-Subbagh and K. M. Youssef, *Future J. Pharm. Sci.*, 2021, **7**, 188.

38 Z. Časar, *Synthesis* , 2020, **52**, 1315–1345.

39 M.-R. Sun, H.-L. Li, M.-Y. Ba, W. Cheng, H.-L. Zhu and Y.-T. Duan, *Mini Rev. Med. Chem.*, 2021, **21**, 150–170.

40 T. T. Talele, *J. Med. Chem.*, 2016, **59**, 8712–8756.

41 B. E. Uno, E. P. Gillis and M. D. Burke, *Tetrahedron*, 2009, **65**, 3130–3138.

42 F. W. Goldberg, J. G. Kettle, T. Kogej, M. W. D. Perry and N. P. Tomkinson, *Drug Discov. Today*, 2015, **20**, 11–17.

43 H. Klein, PhD Thesis, University of York, 2020

44 S. Yao, *Unpublished Results.*

45 J. Donald, *Unpublished Results.*

46 G. Lauri and P. A. Bartlett, *J. Comput. Aided Mol. Des.*, 1994, **8**, 51–66.

47 O. O. Grygorenko, P. Babenko, D. M. Volochnyuk, O. Raievskyi and I. V. Komarov, *RSC Adv.*, 2016, **6**, 17595–17605.

48 J.-B. Telliez, M. E. Dowty, L. Wang, J. Jussif, T. Lin, L. Li, E. Moy, P. Balbo, W. Li, Y. Zhao, K. Crouse, C. Dickinson, P. Symanowicz, M. Hegen, M. E. Banker, F. Vincent, R. Unwalla, S. Liang, A. M. Gilbert, M. F. Brown, M. Hayward, J. Montgomery, X. Yang, J. Bauman, J. I. Trujillo, A. Casimiro-Garcia, F. F. Vajdos, L. Leung, K. F. Geoghegan, A. Quazi, D. Xuan, L. Jones, E. Hett, K. Wright, J. D. Clark and A. Thorarensen, *ACS Chem. Biol.*, 2016, **11**, 3442–3451.

49 H. A. Ramírez-Marín and A. Tosti, *Drug Des. Devel. Ther.*, 2022, **16**, 363–374.

50 S. Yao, A. R, Gomez Angel, P. O'Brien and S. C. C. Lucas, *Unpublished results*.

51 E. M. Carreira and T. C. Fessard, *Chem. Rev.*, 2014, **114**, 8257–8322.

52 J. D. Dunitz and V. Schomaker, *J. Chem. Phys.*, 1952, **20**, 1703–1707.

53 Y. Zheng, C. M. Tice and S. B. Singh, *Bioorg. Med. Chem. Lett.*, 2014, **24**, 3673–3682.

54 D. S. Wishart, Y. D. Feunang, A. C. Guo, E. J. Lo, A. Marcu, J. R. Grant, T. Sajed, D. Johnson, C. Li, Z. Sayeeda, N. Assempour, I. Iynkkaran, Y. Liu, A. Maciejewski, N. Gale, A. Wilson, L. Chin, R. Cummings, D. Le, A. Pon, C. Knox and M. Wilson, *Nucleic Acids Res.*, 2018, **46**, D1074–D1082.

55 E. Vitaku, D. T. Smith and J. T. Njardarson, *J. Med. Chem*., 2014, **57**, 10257–10274

56 J. A. Burkhard, B. Wagner, H. Fischer, F. Schuler, K. Müller and E. M. Carreira, *Angew. Chem. Int. Ed Engl.*, 2010, **49**, 3524–3527.

57 Y.-J. Zheng and C. M. Tice, *Expert Opin. Drug Discov.*, 2016, **11**, 831–834.

58 A. A. Kirichok, I. Shton, M. Kliachyna, I. Pishel and P. K. Mykhailiuk, *Angew. Chem. Weinheim Bergstr. Ger.*, 2017, **129**, 8991–8995.

59 G. Müller, T. Berkenbosch, J. C. J. Benningshof, D. Stumpfe and J. Bajorath, *Chemistry*, 2017, **23**, 703–710.

60 K. Hiesinger, D. Dar'in, E. Proschak and M. Krasavin, *J. Med. Chem.*, 2021, **64**, 150–183.

61 G. A. Molander and N. Ellis, *Acc. Chem. Res.*, 2007, **40**, 275–286.

62 S. Darses and J.-P. Genet, *Chem. Rev.*, 2008, **108**, 288–325.

63 M. J. Meyers, S. A. Long, M. J. Pelc, J. L. Wang, S. J. Bowen, M. C. Walker, B. A. Schweitzer, H. M. Madsen, R. E. Tenbrink, J. McDonald, S. E. Smith, S. Foltin, D. Beidler and A. Thorarensen, *Bioorg. Med. Chem. Lett.*, 2011, **21**, 6538–6544.

64 K. Ahn, M. K. McKinney and B. F. Cravatt, *Chem. Rev.*, 2008, **108**, 1687–1707.

65 M. J. Meyers, S. A. Long, M. J. Pelc, J. L. Wang, S. J. Bowen, B. A. Schweitzer, M. V. Wilcox, J. McDonald, S. E. Smith, S. Foltin, J. Rumsey, Y.-S. Yang, M. C. Walker, S. Kamtekar, D. Beidler and A. Thorarensen, *Bioorg. Med. Chem. Lett.*, 2011, **21**, 6545–6553.

66 L. Nóvoa, L. Trulli, A. Parra and M. Tortosa, *Angew. Chem. Int. Ed Engl.*, 2021, **60**, 11763–11768.

67 L. Nóvoa, L. Trulli, I. Fernández, A. Parra and M. Tortosa, *Org. Lett.*, 2021, **23**, 7434–7438.

68 G. M. Bures, S. N. Haydar, T. Heckrodt, M. Walker, M. Zhong, WO2021216661A1, 2021; Assembly Biosciences, Inc.

69 A. Bonet, C. Pubill-Ulldemolins, C. Bo, H. Gulyás and E. Fernández, *Angew. Chem. Int. Ed Engl.*, 2011, **50**, 7158–7161.

70 D. G. Brown, P. R. Bernstein, A. Griffin, S. Wesolowski, D. Labrecque, M. C. Tremblay, M. Sylvester, R. Mauger, P. D. Edwards, S. R. Throner, J. J. Folmer, J. Cacciola, C. Scott, L. A. Lazor, M. Pourashraf, V. Santhakumar, W. M. Potts, S. Sydserff, P. Giguère, C. Lévesque, M. Dasser and T. Groblewski, *J. Med. Chem.*, 2014, **57**, 733–758.

71 T. Kaneko, R. S. J. Clark, O. H. I. Norihito, F. Ozaki, T. Kawahara, A. Kamada, K. Okano, H. Yokohama, M. Ohkuro, K. Muramoto, O. Takenaka and S. Kobayashi, *Chem. Pharm. Bull.*, 2004, **52**, 675–687.

72 M. Tissot, N. Body, S. Petit, J. Claessens, C. Genicot and P. Pasau, *Org. Lett.*, 2018, **20**, 8022–8025.

73 H. Guenther and G. Jikeli, *Chem. Rev.*, 1977, **77**, 599–637.

74 J. Clayden, N. Greeves and S. Warren, *Organic Chemistry*, Oxford University Press, Oxford, 2012.

75 D. Hemming, R. Fritzemeier, S. A. Westcott, W. L. Santos and P. G. Steel, *Chem. Soc. Rev.*, 2018, **47**, 7477–7494.

76 A. R. Gomez-Angel, J. R. Donald, J. D. Firth, C. De Fusco, R. Ian Storer, D. J. Cox and P. O'Brien, *Tetrahedron*, 2021, **83**, 131961.

77 D. L. Comins and A. Dehghani, *Tetrahedron Lett.*, 1992, **33**, 6299–6302.

78 T. Ishiyama, M. Murata and N. Miyaura, *J. Org. Chem.*, 1995, **60**, 7508–7510.

79 E. Hupe, I. Marek and P. Knochel, *Org. Lett.*, 2002, **4**, 2861–2863.

80 D. N. Primer, I. Karakaya, J. C. Tellis and G. A. Molander, *J. Am. Chem. Soc.*, 2015, **137**, 2195–2198.

81 J. P. Phelan, R. J. Wiles, S. B. Lang, C. B. Kelly and G. A. Molander, *Chem. Sci.*, 2018, **9**, 3215–3220.

82 K. Nguyen, H. A. Clement, L. Bernier, J. W. Coe, W. Farrell, C. J. Helal, M. R. Reese, N. W. Sach, J. C. Lee and D. G. Hall, *ACS Catal.*, 2021, **11**, 404–413.

83 D. N. Primer and G. A. Molander, *J. Am. Chem. Soc.*, 2017, **139**, 9847–9850.

84 S. O. Scholz, J. B. Kidd, L. Capaldo, N. E. Flikweert, R. M. Littlefield and T. P. Yoon, *Org. Lett.*, 2021, **23**, 3496–3501.

85 N. Borlinghaus, B. Schönfeld, S. Heitz, J. Klee, S. Vukelić, W. M. Braje and A. Jolit, *J. Org. Chem.*, 2021, **86**, 16535–16547.

86 T. J. DeLano, U. K. Bandarage, N. Palaychuk, J. Green and M. J. Boyd, *J. Org. Chem.*, 2016, **81**, 12525–12531.

87 E. Speckmeier and T. C. Maier, *J. Am. Chem. Soc.*, 2022, **144**, 9997–10005.

88 J. Dong, F. Yue, H. Song, Y. Liu and Q. Wang, *Chem. Commun.* , 2020, **56**, 12652–12655.

89 F. Minisci, E. Vismara and F. Fontana, *Heterocycles*, 1989, **28**, 489.

90 N. E. Behnke, Z. S. Sales, M. Li and A. T. Herrmann, *J. Org. Chem.*, 2021, **86**, 12945–12955.

91 Z. Dong and D. W. C. MacMillan, *Nature*, 2021, **598**, 451–456.

92 S. Kotha, K. Lahiri and D. Kashinath, *Tetrahedron*, 2002, **58**, 9633–9695.

93 F.-S. Han, *Chem. Soc. Rev.*, 2013, **42**, 5270–5298.

94 M. C. D'Alterio, È. Casals-Cruañas, N. V. Tzouras, G. Talarico, S. P. Nolan and A. Poater, *Chemistry*, 2021, **27**, 13481–13493.

95 A. J. J. Lennox and G. C. Lloyd-Jones, *Chem. Soc. Rev.*, 2014, **43**, 412–443.

96 *J. Organomet. Chem.*, 2002, **653**, 54–57.

97 A. J. J. Lennox and G. C. Lloyd-Jones, *Angew. Chem. Int. Ed Engl.*, 2013, **52**, 7362–7370.

98 A. A. Thomas and S. E. Denmark, *Science*, 2016, **352**, 329–332.

99 B. P. Carrow and J. F. Hartwig, *J. Am. Chem. Soc.*, 2011, **133**, 2116–2119.

100 A. A. Thomas, H. Wang, A. F. Zahrt and S. E. Denmark, *J. Am. Chem. Soc.*, 2017, **139**, 3805–3821.

101 A. Suzuki, *Heterocycles*, 2010, **80**, 15–43

102 J. El-Maiss, T. Mohy El Dine, C.-S. Lu, I. Karamé, A. Kanj, K. Polychronopoulou and J. Shaya, *Catalysts*, 2020, **10**, 296.

103 A. J. J. Lennox and G. C. Lloyd-Jones, *Isr. J. Chem.*, 2010, **50**, 664–674.

104 D. M. Knapp, E. P. Gillis and M. D. Burke, *J. Am. Chem. Soc.*, 2009, **131**, 6961–6963.

105 G. A. Molander and P. E. Gormisky, *J. Org. Chem.*, 2008, **73**, 7481–7485.

106 L. Li, S. Zhao, A. Joshi-Pangu, M. Diane and M. R. Biscoe, *J. Am. Chem. Soc.*, 2014, **136**, 14027–14030.

107 J. He, H. Jiang, R. Takise, R.-Y. Zhu, G. Chen, H.-X. Dai, T. G. M. Dhar, J. Shi, H. Zhang, P. T. W. Cheng and J.-Q. Yu, *Angew. Chem. Int. Ed Engl.*, 2016, **55**, 785–789.

108 D. L. Sandrock, L. Jean-Gérard, C.-Y. Chen, S. D. Dreher and G. A. Molander, *J. Am. Chem. Soc.*, 2010, **132**, 17108–17110.

109 J. He, Q. Shao, Q. Wu and J.-Q. Yu, *J. Am. Chem. Soc.*, 2017, **139**, 3344–3347.

110 T. Awano, T. Ohmura and M. Suginome, *J. Am. Chem. Soc.*, 2011, **133**, 20738–20741.

111 J. C. H. Lee, R. McDonald and D. G. Hall, *Nat. Chem.*, 2011, **3**, 894–899.

112 G. A. Molander and S. R. Wisniewski, *Adv. Synth. Catal.* 2013, **355**, 3037–3057

113 G. L. Hoang and J. M. Takacs, *Chem. Sci.*, 2017, **8**, 4511–4516.

114 S. N. Mlynarski, C. H. Schuster and J. P. Morken, *Nature*, 2014, **505**, 386–390.

115 W. Butler, *Unpublished Results.*

116 L. Tomczyk, *Unpublished Results.*

117 G. Yunhang, X. Hai, W. Zhiwei, S. Hanzi, WO2019210828A1, 2019; BeiGene, Ltd.

118 M. A. Brodney, C. R. Butler, L. A. McAllister, C. J. Helal, S. V. O'Neil, P. R. Verhoest, US2018208607A1, 2018; Pfizer Inc.

119 S. A. Long, M. J. Meyers; M. J. Pelc, B. A. Schweitzer, A. Thorarensen, J. L. Wang, US2010113465A1, 2010; Pfizer Inc.

120 M. W. Matthew, M. Zablocki, S. Mente, C. Dinsmore, W. Zhongguo, Z. Xiaozhang, EP3636637A1, 2020; Forma Therapeutics, Inc.

121 J. Alcazar, C. B. Berry, P. Garcia-Reynaga, A. V. Samant, J. A. Vega-Ramiro, M. K. Ameriks, WO2021191390A1, 2021; Janssen Pharmaceutica NV

122 P. V. Fish, N. S. Barta, D. L. F. Gray, T. Ryckmans, A. Stobie, F. Wakenhut and G. A. Whitlock, *Bioorg. Med. Chem. Lett.*, 2008, **18**, 4355–4359.

123 J. D. Firth and P. O'Brien, *Unpublished Results.*

124 P. Chen, C. G. Caldwell, W. Ashton, J. K. Wu, H. He, K. A. Lyons, N. A. Thornberry and A. E. Weber, *Bioorg. Med. Chem. Lett.*, 2011, **21**, 1880–1886.

125 M. N. Greco, M. J. Hawkins, E. T. Powell, H. R. Almond Jr, T. W. Corcoran, L. de Garavilla, J. A. Kauffman, R. Recacha, D. Chattopadhyay, P. Andrade-Gordon and B. E. Maryanoff, *J. Am. Chem. Soc.*, 2002, **124**, 3810–3811.

126 L.-X. Wang, M. Tang, T. Suzuki, K. Kitajima, Y. Inoue, S. Inoue, J.-Q. Fan and Y. C. Lee, *J. Am. Chem. Soc.*, 1997, **119**, 11137–11146.

127 K. L. Granberg, Z.-Q. Yuan, B. Lindmark, K. Edman, J. Kajanus, A. Hogner, M. Malmgren, G. O'Mahony, A. Nordqvist, J. Lindberg, S. Tångefjord, M. Kossenjans, C. Löfberg, J. Brånalt, D. Liu, N. Selmi, G. Nikitidis, P. Nordberg, A. Hayen, A. Aagaard, E. Hansson, M. Hermansson, I. Ivarsson, R. Jansson-Löfmark, U. Karlsson, U. Johansson, L. William-Olsson, J. Hartleib-Geschwindner and K. Bamberg, *J. Med. Chem.*, 2019, **62**, 1385–1406.

128 A. Gomez-Angel, *Unpublished Results.*

129 T. Kaneko, R. S. J. Clark, N. Ohi, F. Ozaki, T. Kawahara, A. Kamada, K. Okano, H. Yokohama, M. Ohkuro, K. Muramoto and Others, *Chem. Pharm. Bull.*, 2004, **52**, 675–687.

130 M. Presset, N. Fleury-Brégeot, D. Oehlrich, F. Rombouts and G. A. Molander, *J. Org. Chem.*, 2013, **78**, 4615–4619.

131 J.-J. Dai, W.-M. Zhang, Y.-J. Shu, Y.-Y. Sun, J. Xu, Y.-S. Feng and H.-J. Xu, *Chem. Commun.* , 2016, **52**, 6793–6796.

132 M. Amatore and C. Gosmini, *Chemistry*, 2010, **16**, 5848–5852.

133 P. Klumphu and B. H. Lipshutz, *J. Org. Chem.*, 2014, **79**, 888–900.

134 C. Reichardt, A.-R. Ferwanah and K.-Y. Yun, *Justus Liebigs Ann. Chem.*, 1984, **1984**, 649–679.

135 Q.-H. Xu, L.-P. Wei and B. Xiao, *Angew. Chem. Int. Ed Engl.*, 2022, **61**, e202115592.

136 J. Choi, G. Laudadio, E. Godineau and P. S. Baran, *J. Am. Chem. Soc.*, 2021, **143**, 11927–11933.

137 S. Biswas, B. Qu, J.-N. Desrosiers, Y. Choi, N. Haddad, N. K. Yee, J. J. Song and C. H. Senanayake, *J. Org. Chem.*, 2020, **85**, 8214–8220.

138 X. Zhang and D. W. C. MacMillan, *J. Am. Chem. Soc.*, 2016, **138**, 13862–13865.

139 Z. Zhang, B. Górski and D. Leonori, *J. Am. Chem. Soc.*, 2022, **144**, 1986–1992.

9. Appendix: NMR Spectra

400 MHz ^{1}H NMR spectrum; 100.6 MHz ^{13}C NMR spectrum; $CDCl_3$ of cyclobutanone **30**

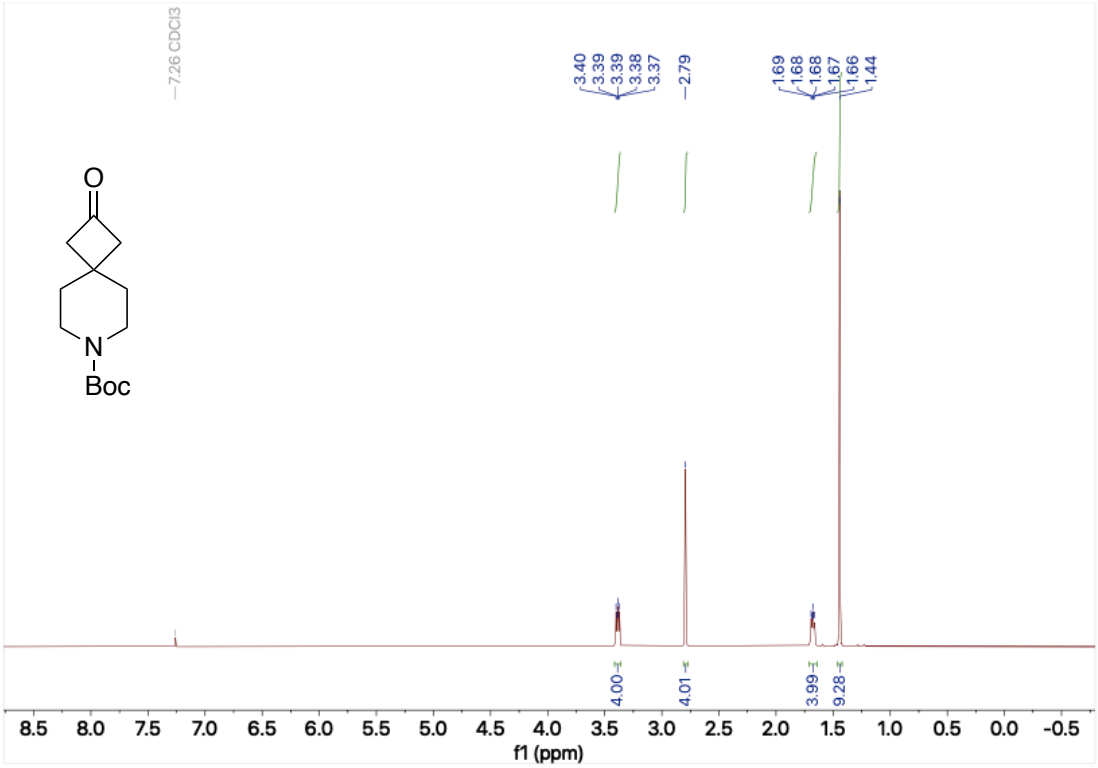

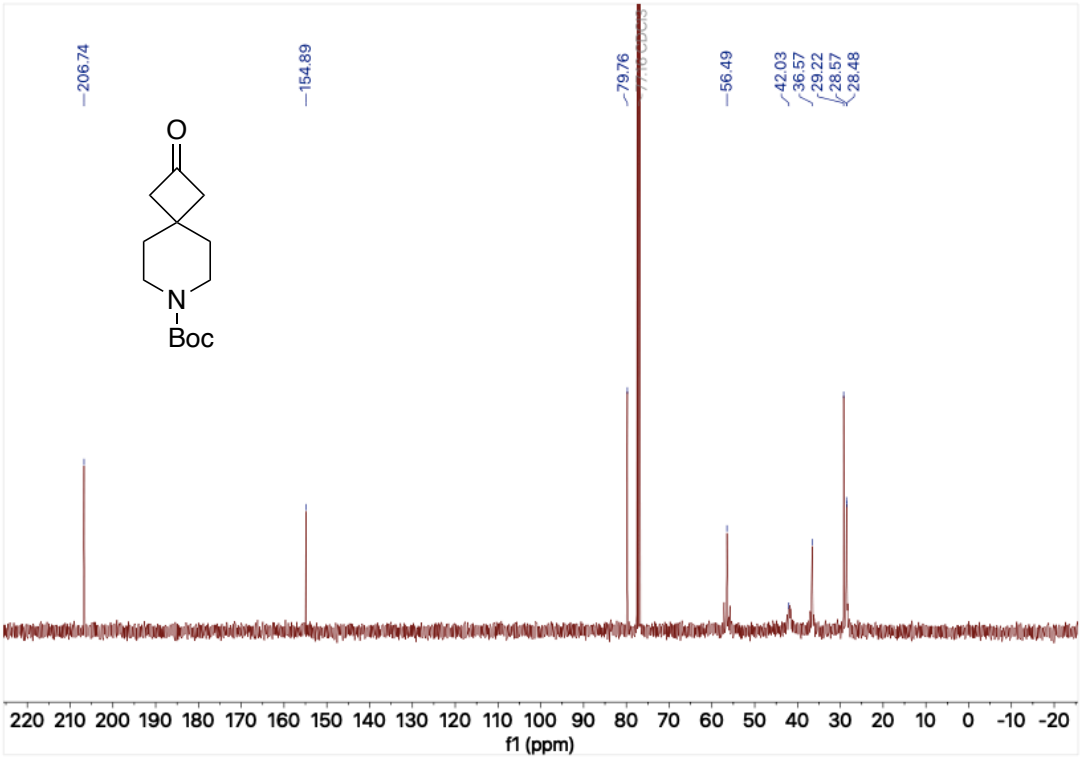

400 MHz ^{1}H NMR spectrum; 100.6 MHz ^{13}C NMR spectrum; $CDCl_3$ of cyclobutyl tosylate **40**

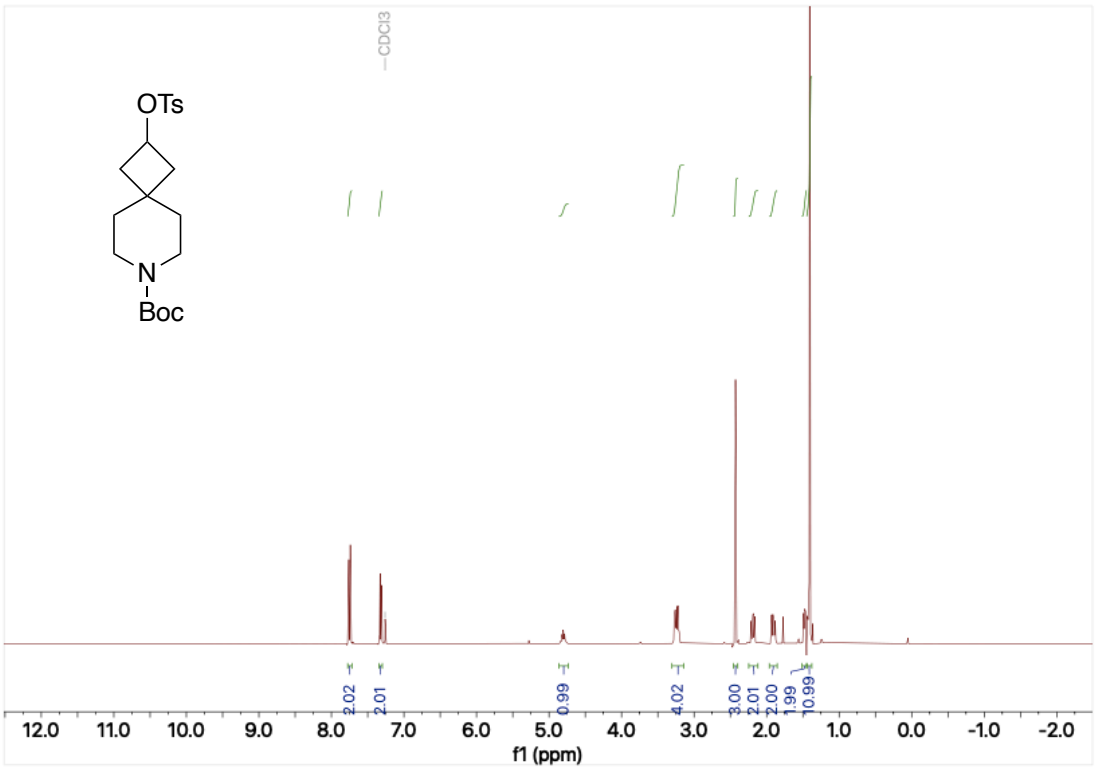

B

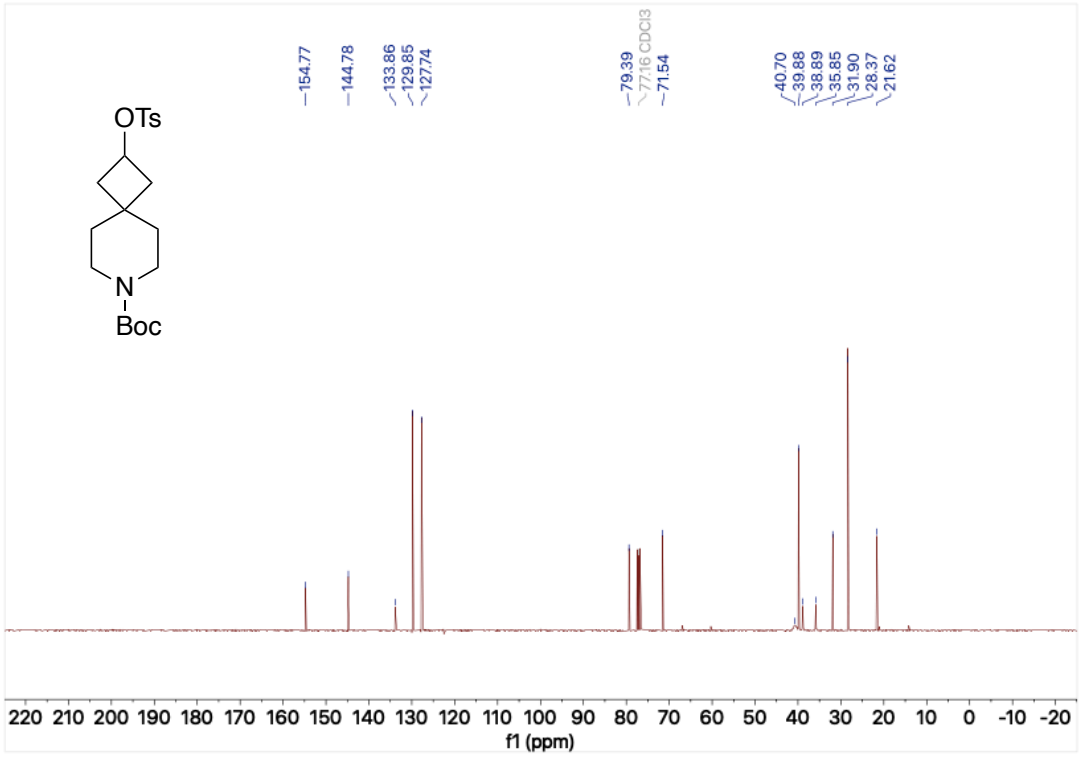
OTs
N
Boc
154.77
144.78
133.86
129.85
127.74
79.39
77.16 CDCl3
71.54
40.70
39.88
38.89
35.85
31.90
28.37
21.62
220 210 200 190 180 170 160 150 140 130 120 110 100 90 80 70 60 50 40 30 20 10 0 -10 -20
f1 (ppm)

C

400 MHz ^{1}H NMR spectrum; 100.6 MHz ^{13}C NMR spectrum; $CDCl_3$ of cyclobutene **29**

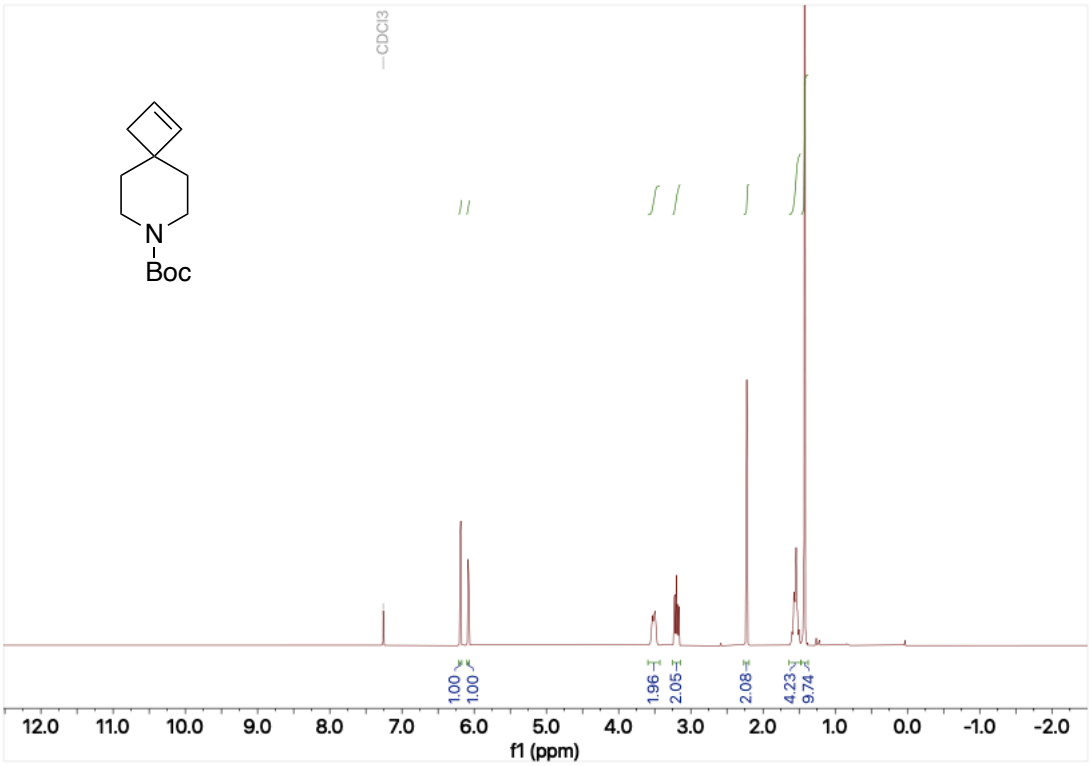

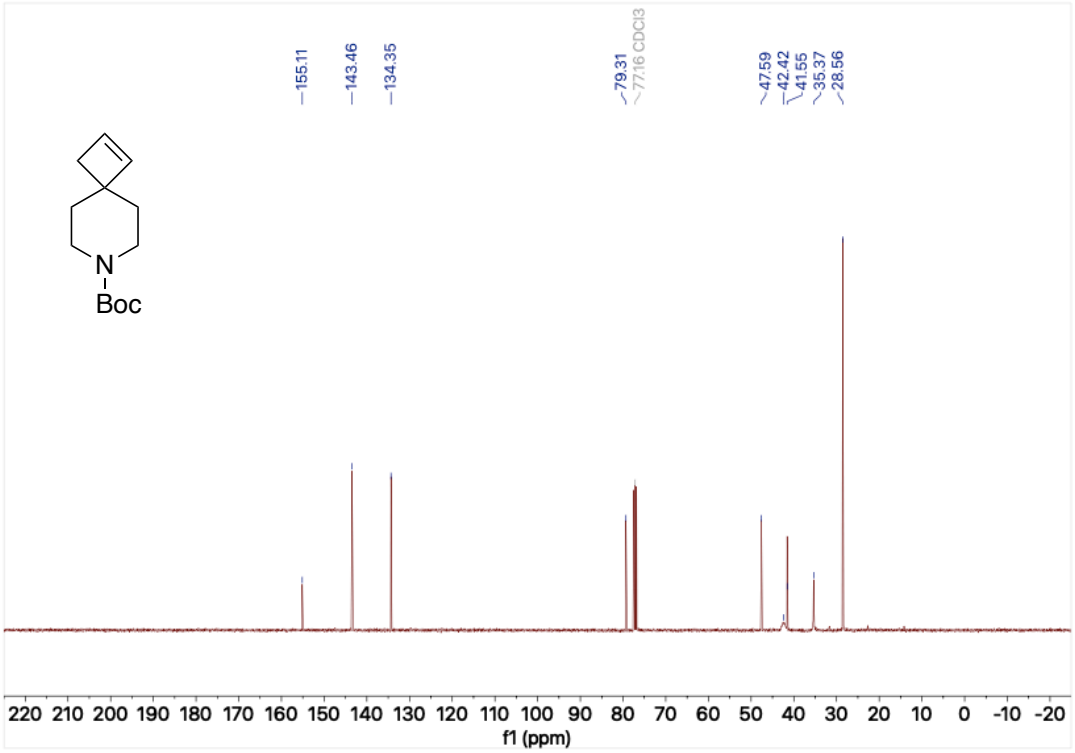

D

400 MHz ^{1}H NMR spectrum; 100.6 MHz ^{13}C NMR spectrum; 128 MHz ^{11}B NMR spectrum; $CDCl_3$ of cyclobutyl Bpin **32**

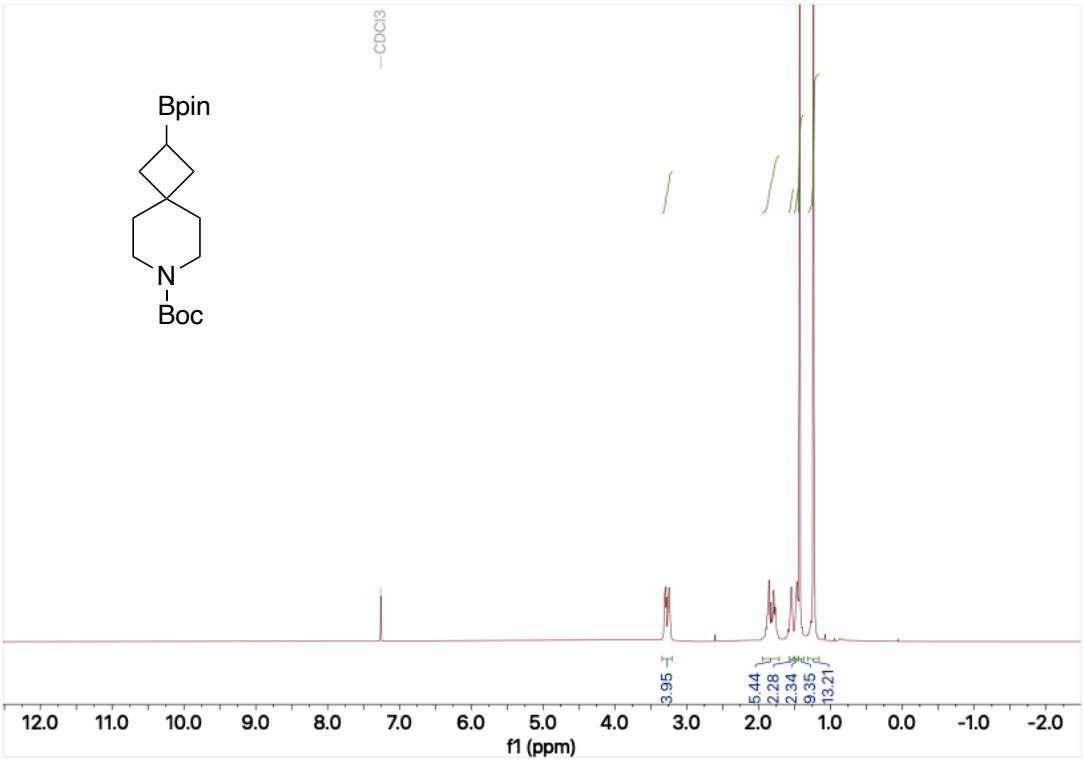

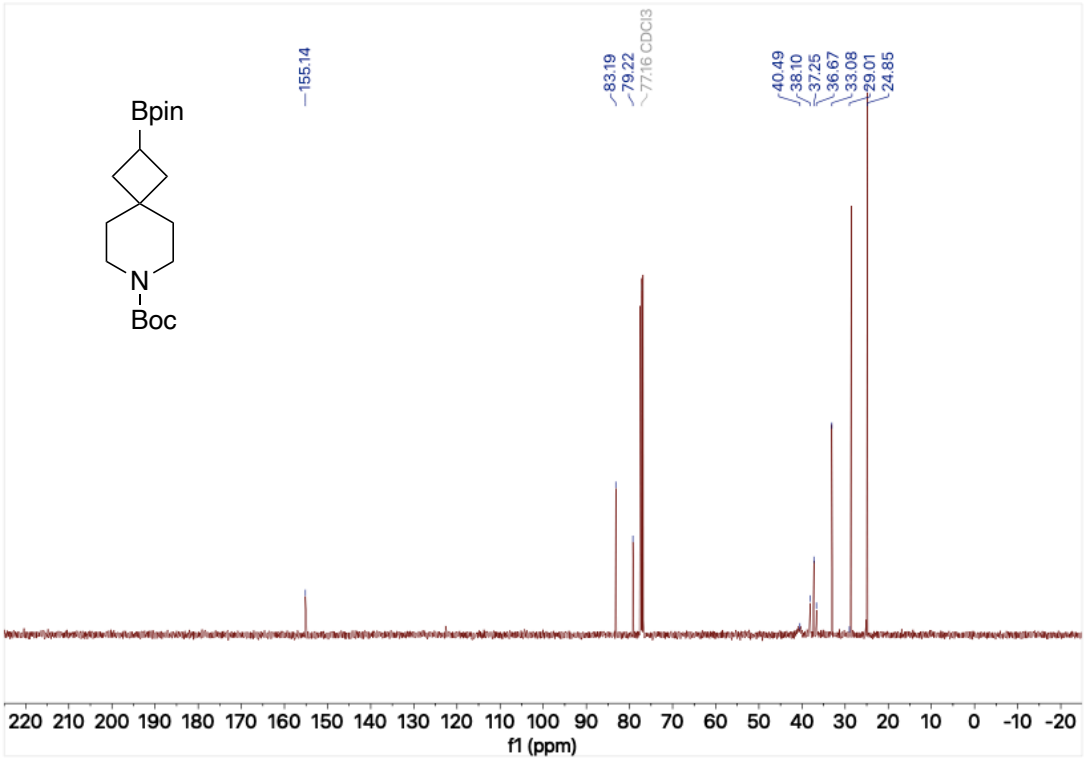

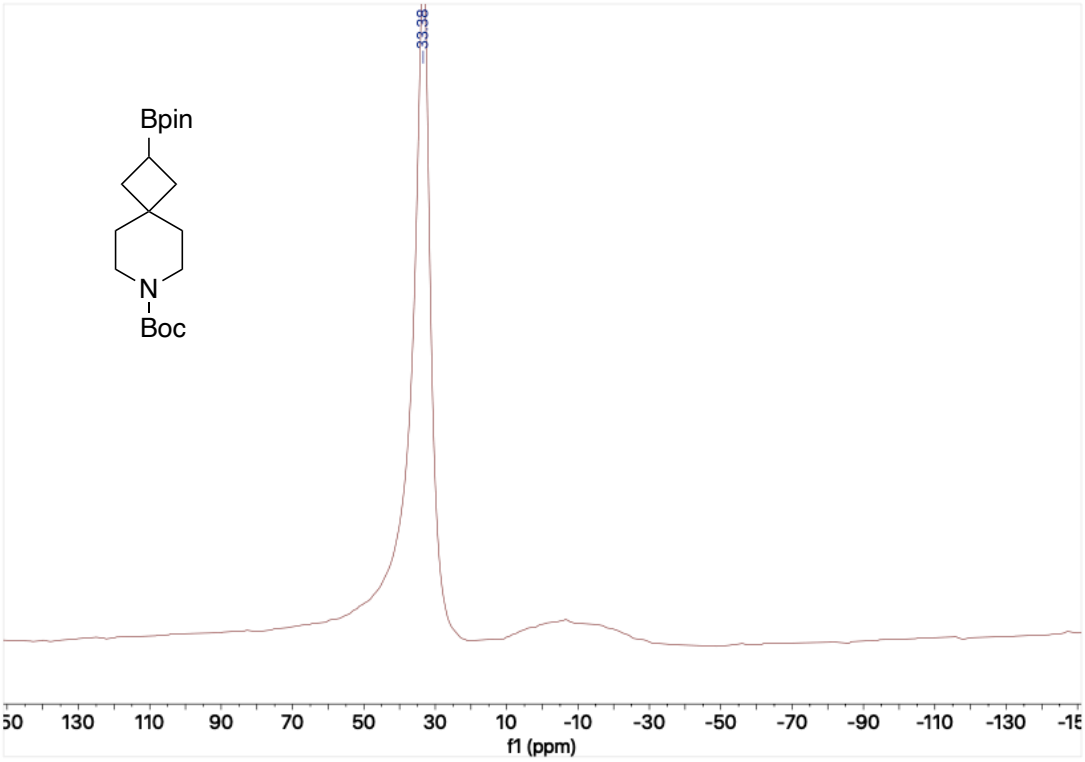
33.38
Bpin
N
Boc
50
130
110
90
70
50
30
10
-10
-30
-50
-70
-90
-110
-130
f1 (ppm)

F

400 MHz ^{1}H NMR spectrum; 100.6 MHz ^{13}C NMR spectrum; 376 MHz ^{19}F NMR spectrum; 128 MHz ^{11}B NMR spectrum; d_6-DMSO of cyclobutyl trifluoroborate salt **25**

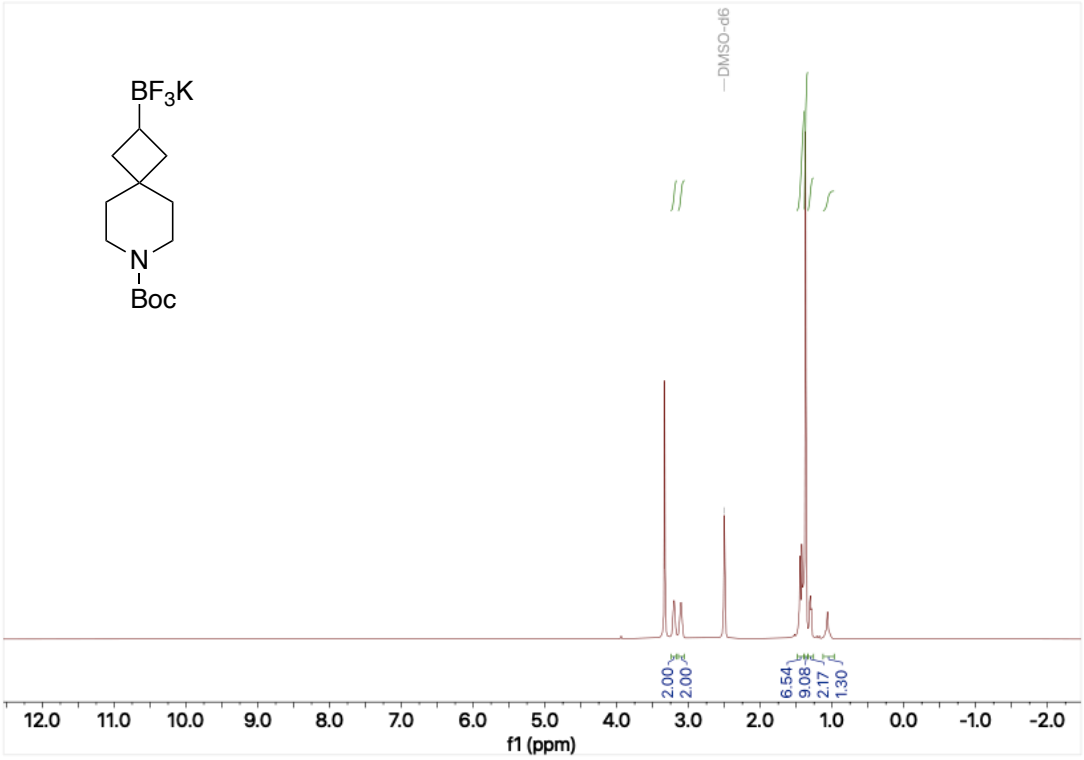

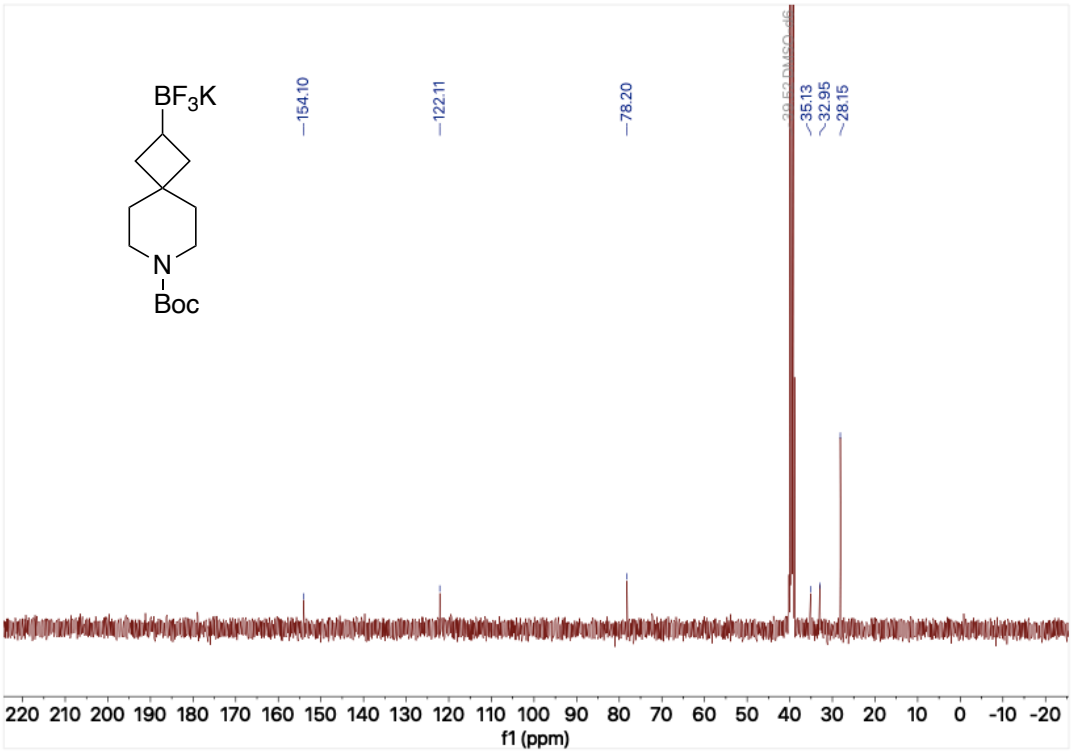

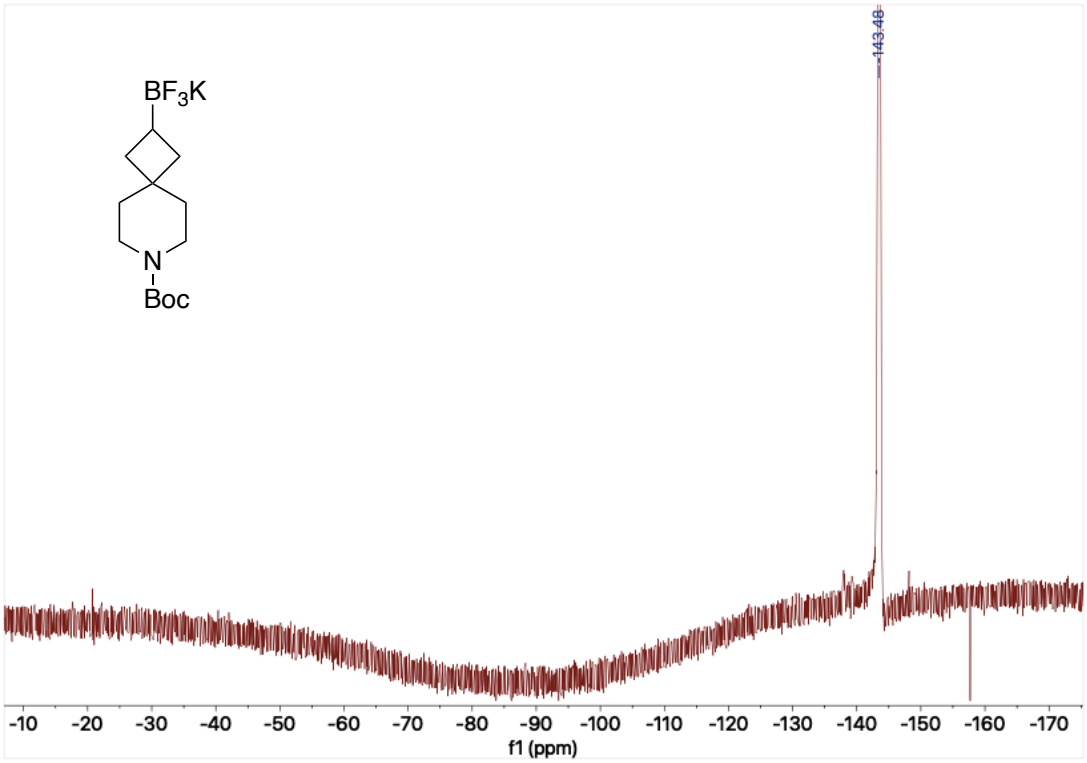
BF3K
N
Boc
143.48
-10 -20 -30 -40 -50 -60 -70 -80 -90 -100 -110 -120 -130 -140 -150 -160 -170
f1 (ppm)

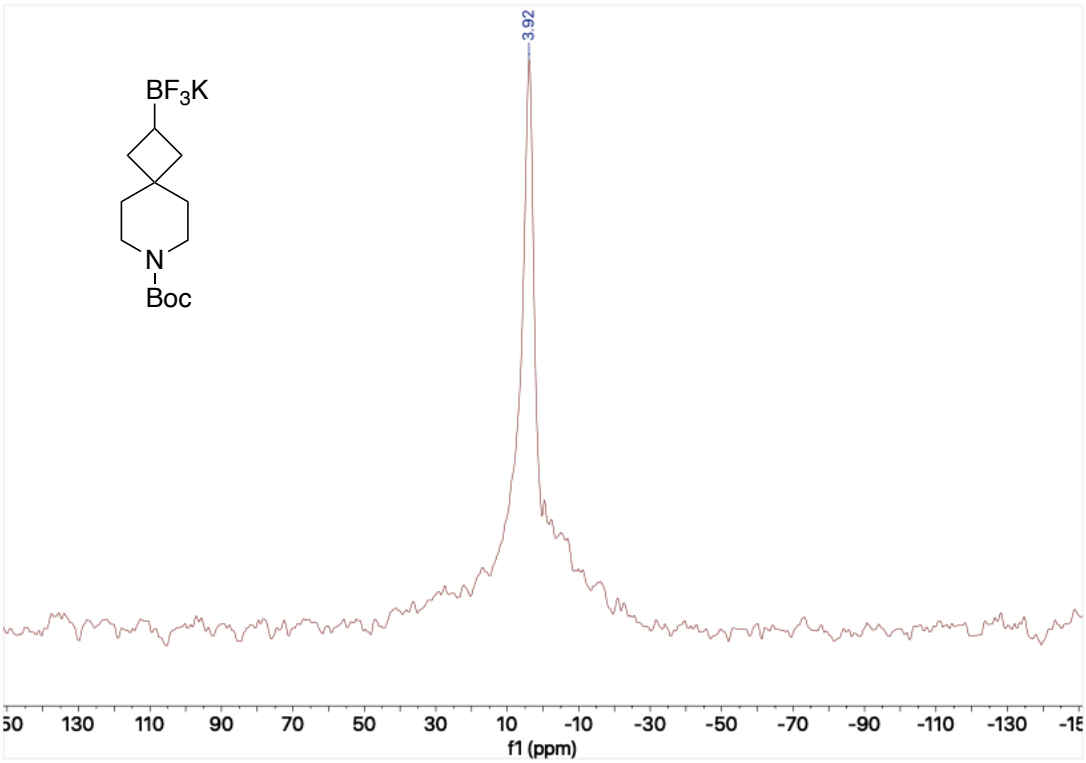
BF3K
N
Boc
3.92
50 130 110 90 70 50 30 10 -10 -30 -50 -70 -90 -110 -130
f1 (ppm)

H

400 MHz ^{1}H NMR spectrum; 100.6 MHz ^{13}C NMR spectrum; 376 MHz ^{19}F NMR spectrum; 128 MHz ^{11}B NMR spectrum; d_6-DMSO of *N*-Boc piperidinyl trifluoroborate salt **52**

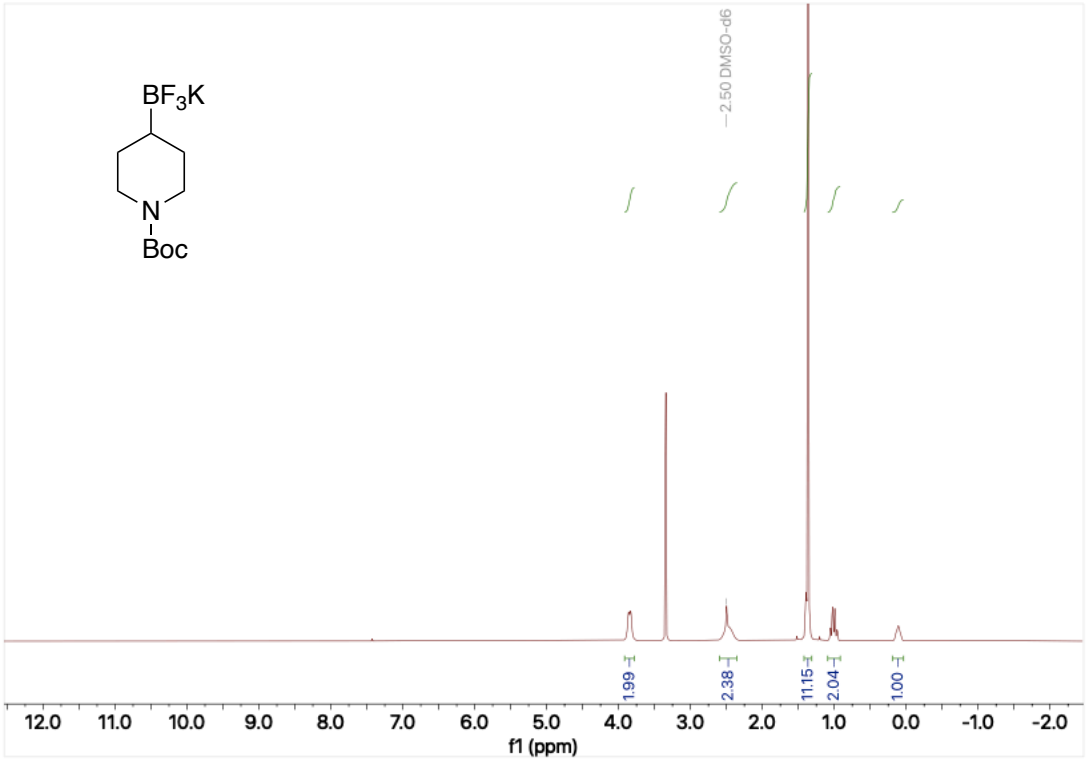

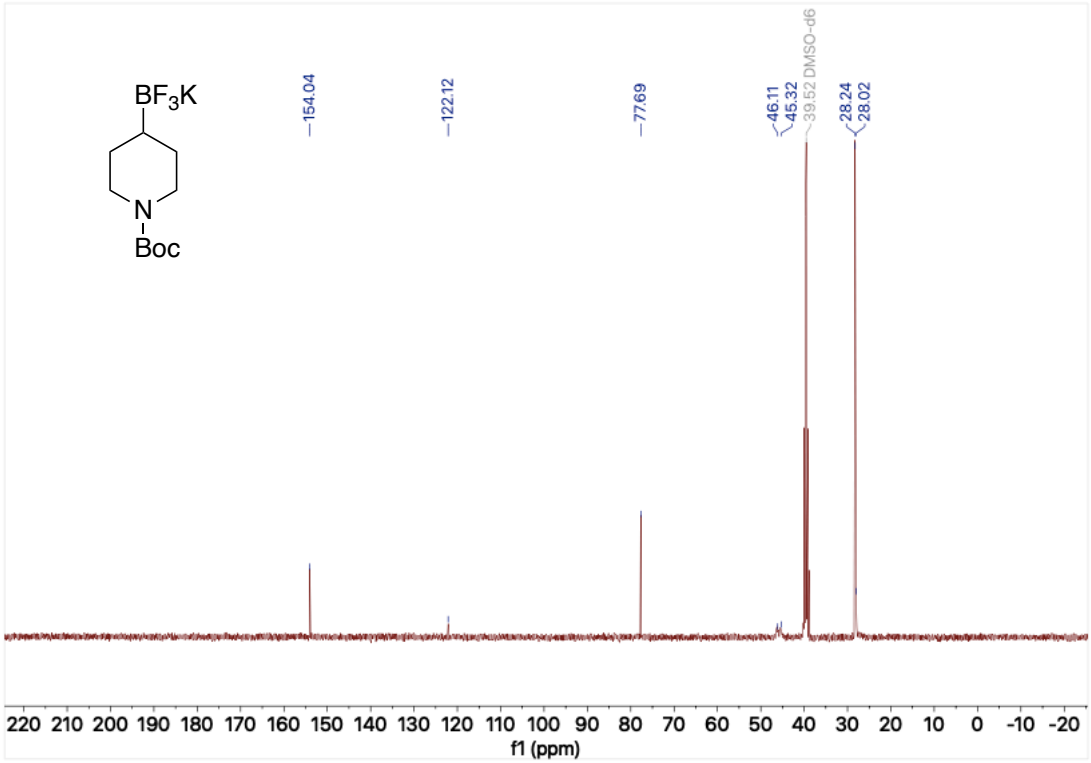

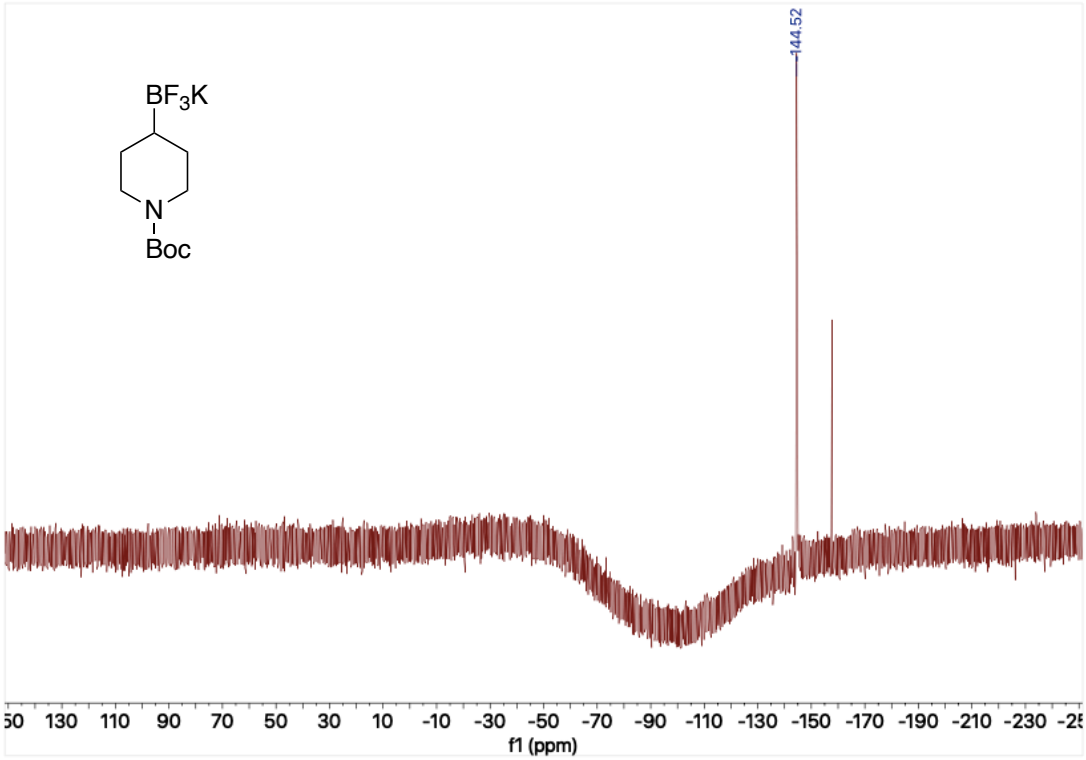
144.52
BF3K
N
Boc
50 130 110 90 70 50 30 10 -10 -30 -50 -70 -90 -110 -130 -150 -170 -190 -210 -230 -25
f1 (ppm)

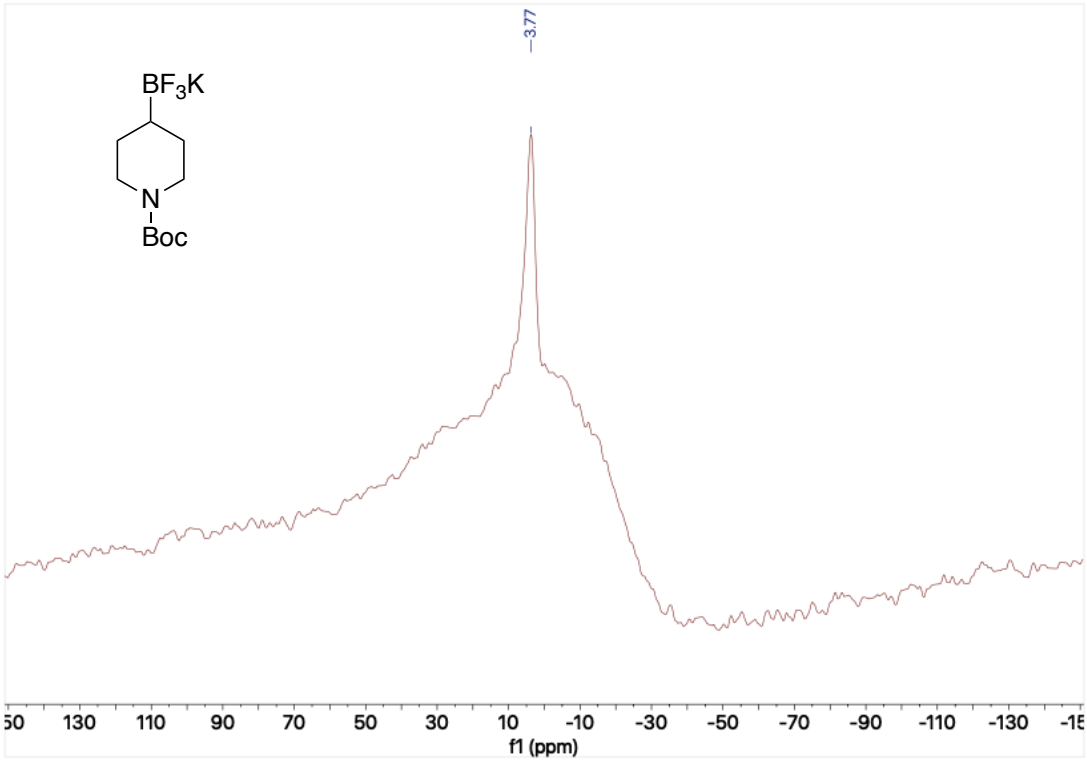
3.77
BF3K
N
Boc
50 130 110 90 70 50 30 10 -10 -30 -50 -70 -90 -110 -130 -15
f1 (ppm)

J

400 MHz ^{1}H NMR spectrum; 100.6 MHz ^{13}C NMR spectrum; 375 MHz ^{19}F NMR spectrum; $CDCl_3$ of cyclobutyl enol triflate **31**

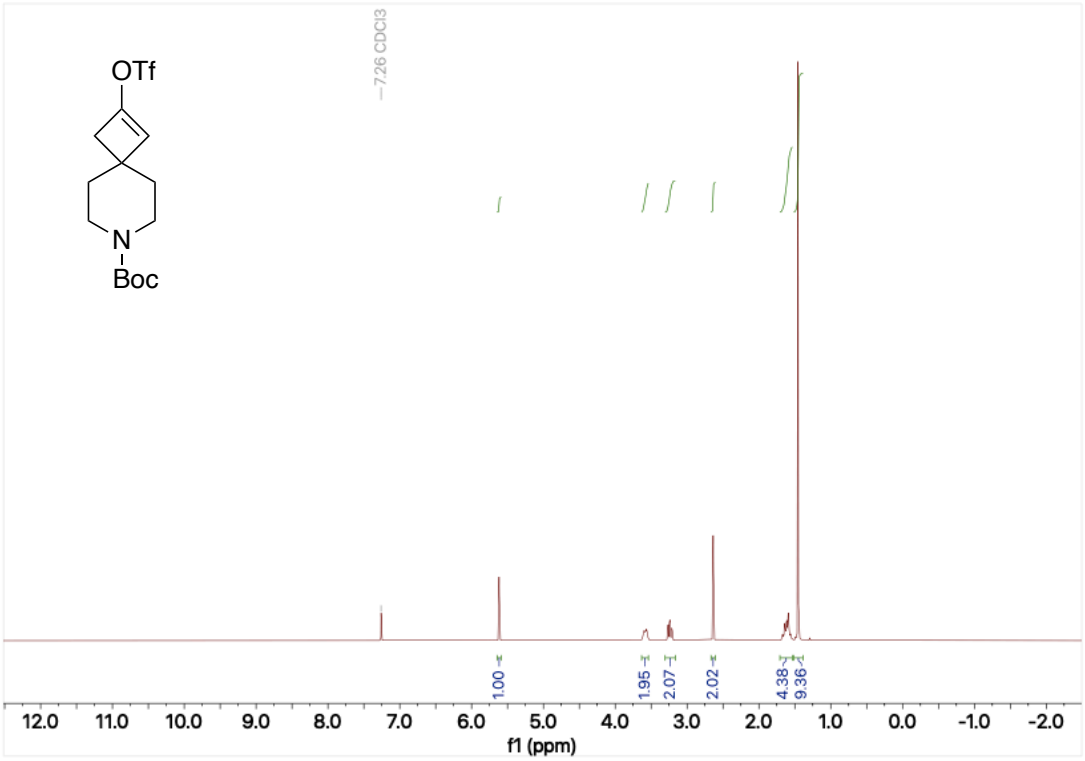

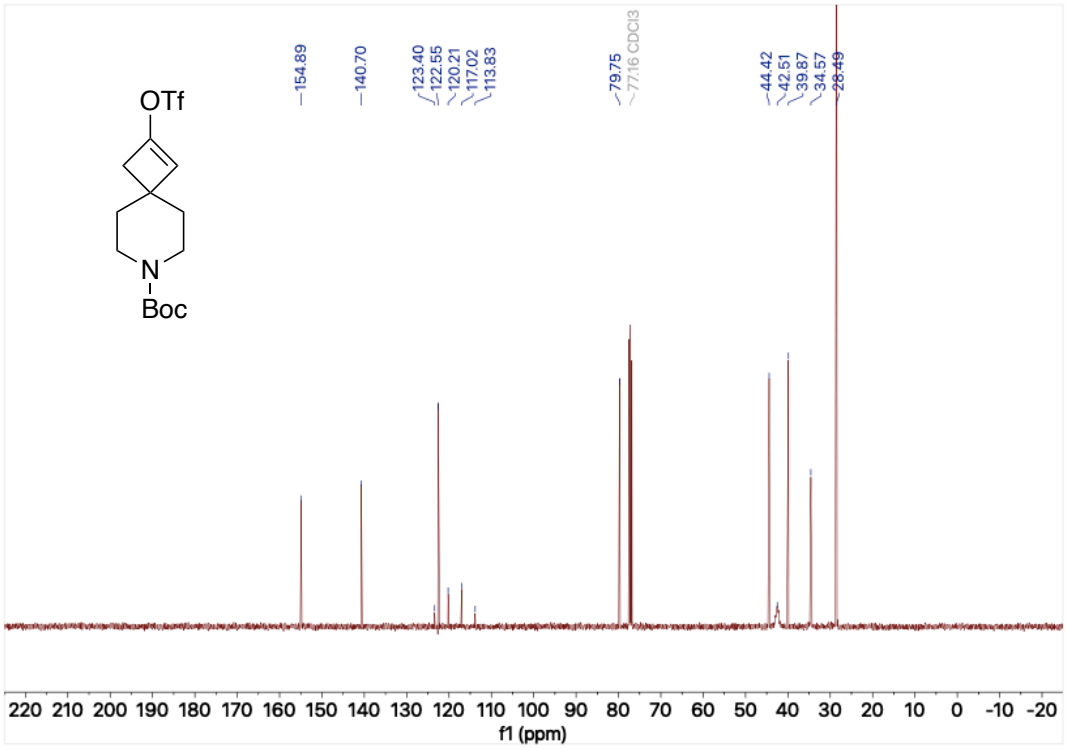

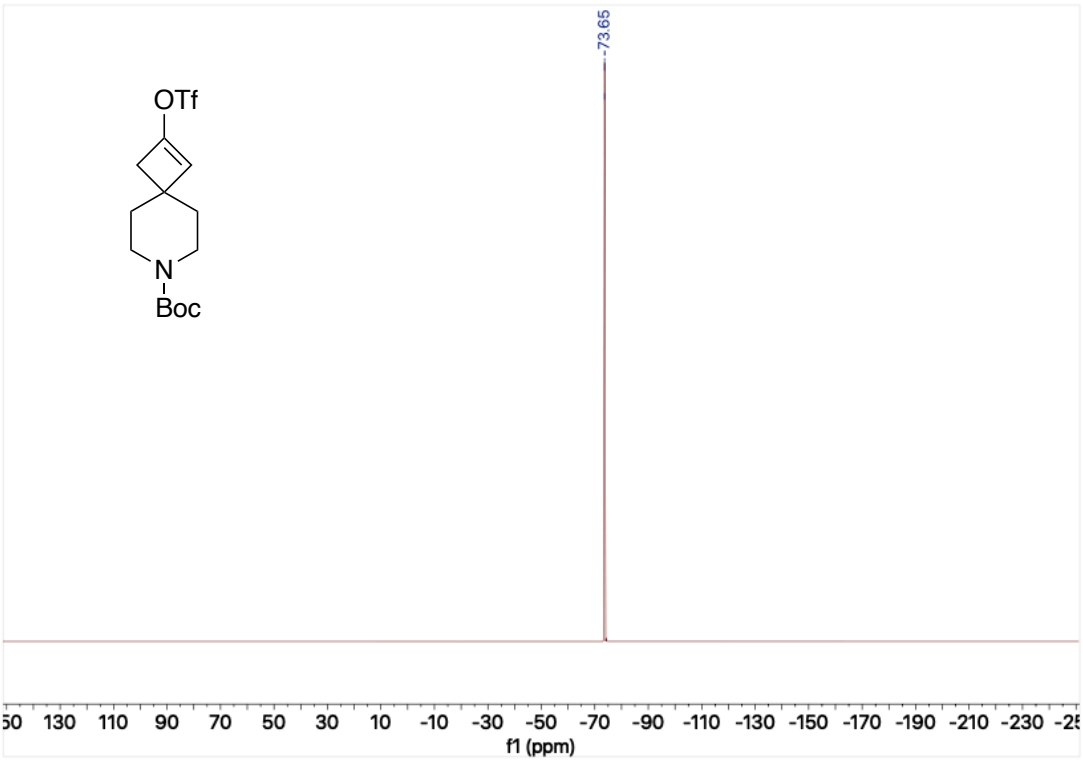
OTf
N
Boc
-73.65
50 130 110 90 70 50 30 10 -10 -30 -50 -70 -90 -110 -130 -150 -170 -190 -210 -230 -25
f1 (ppm)

L

400 MHz ^{1}H NMR spectrum; 100.6 MHz ^{13}C NMR spectrum; 128 MHz ^{11}B NMR spectrum; $CDCl_3$ of cyclobutyl vinyl Bpin **34**

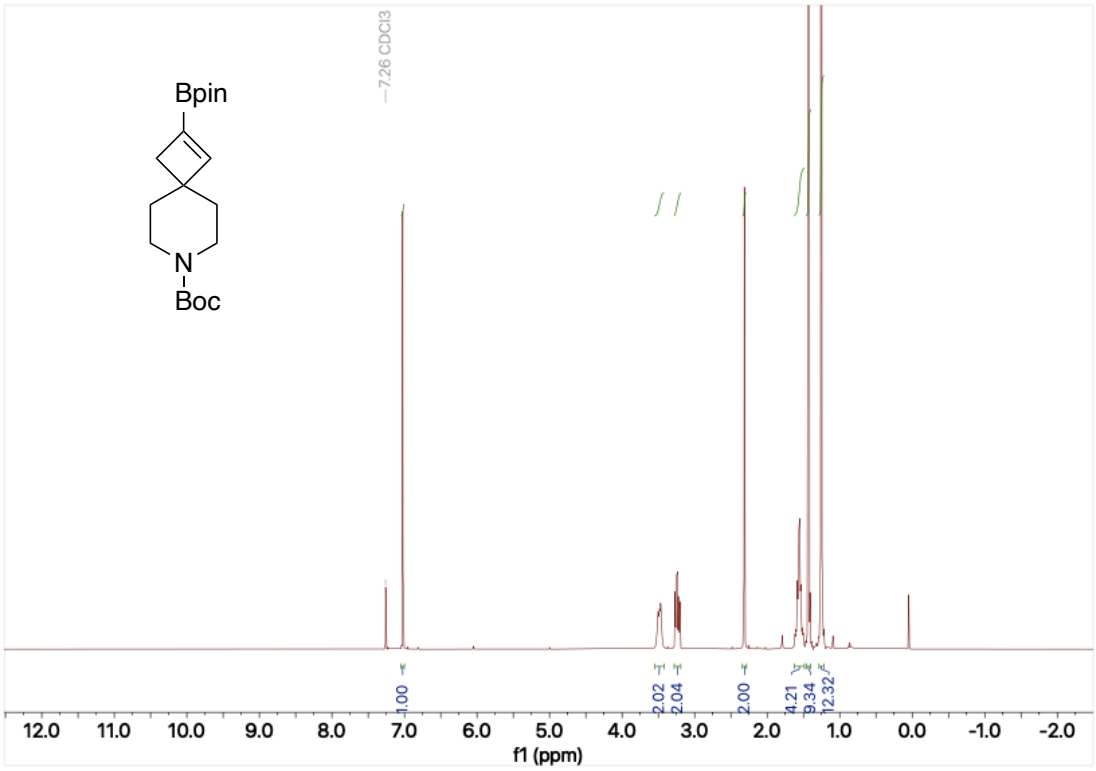

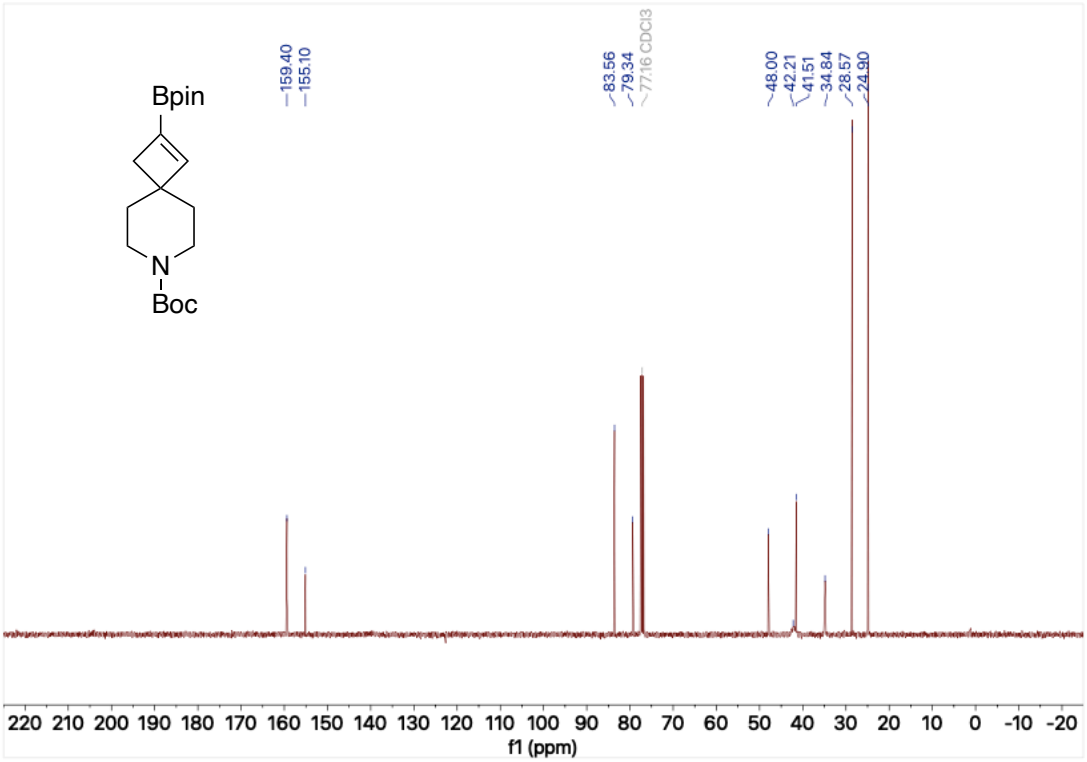

M

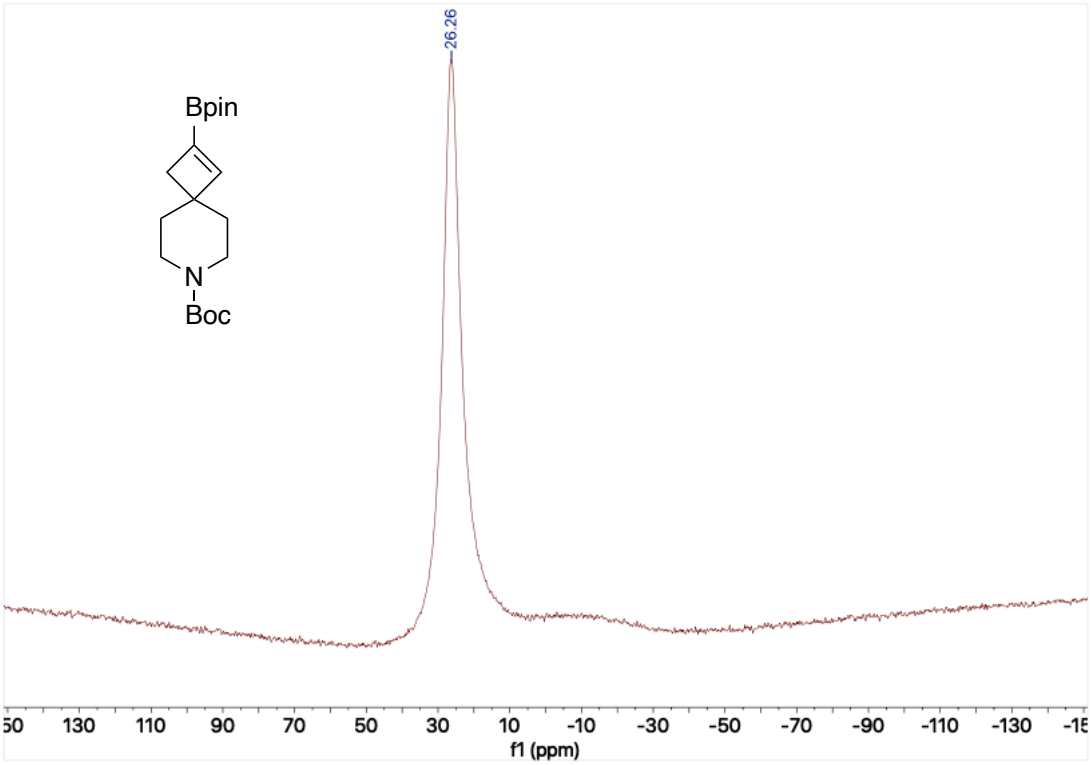
26.26
Bpin
N
Boc
50
130
110
90
70
50
30
10
-10
-30
-50
-70
-90
-110
-130
f1 (ppm)

N

400 MHz ^{1}H NMR spectrum; 100.6 MHz ^{13}C NMR spectrum; $CDCl_3$ of cyclobutanol **50**

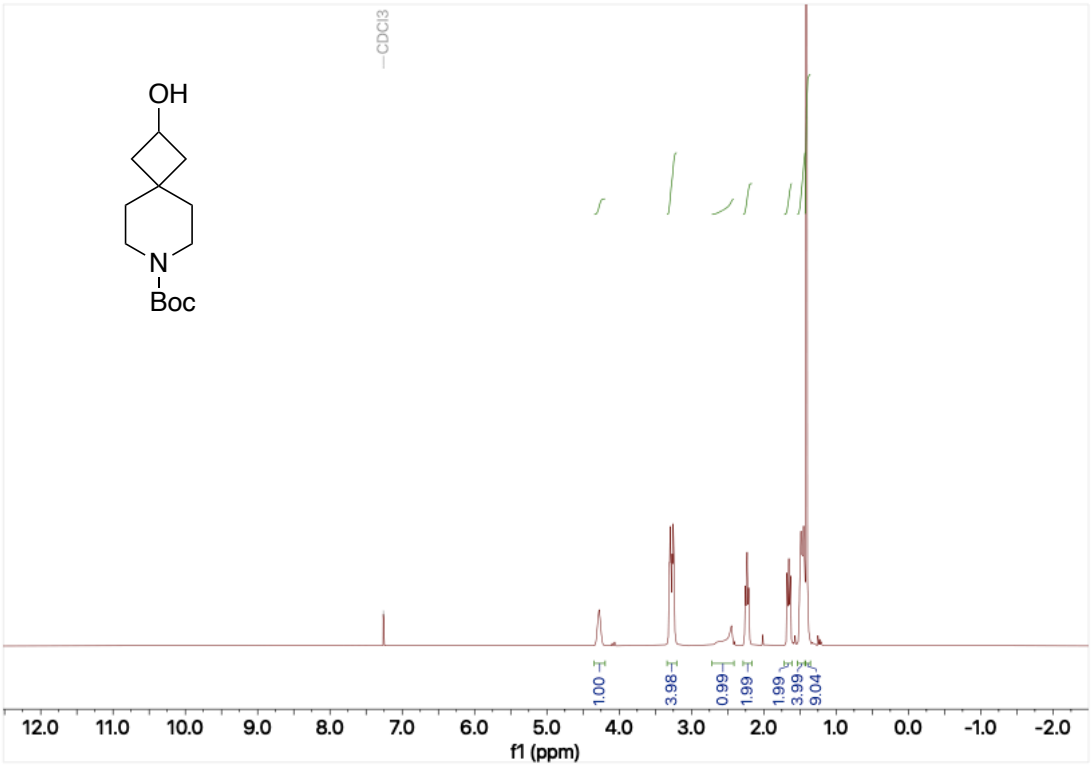

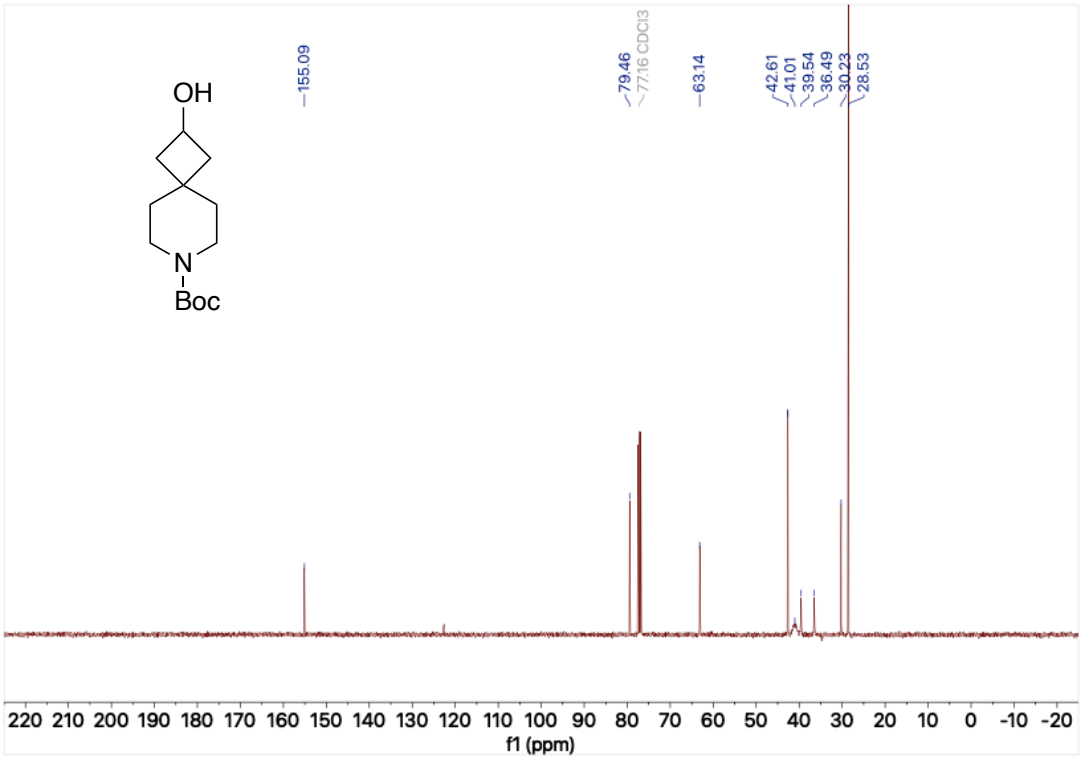

O

400 MHz ^{1}H NMR spectrum; 100.6 MHz ^{13}C NMR spectrum; $CDCl_3$ of ethyl ester phenyl cyclohexane **123**

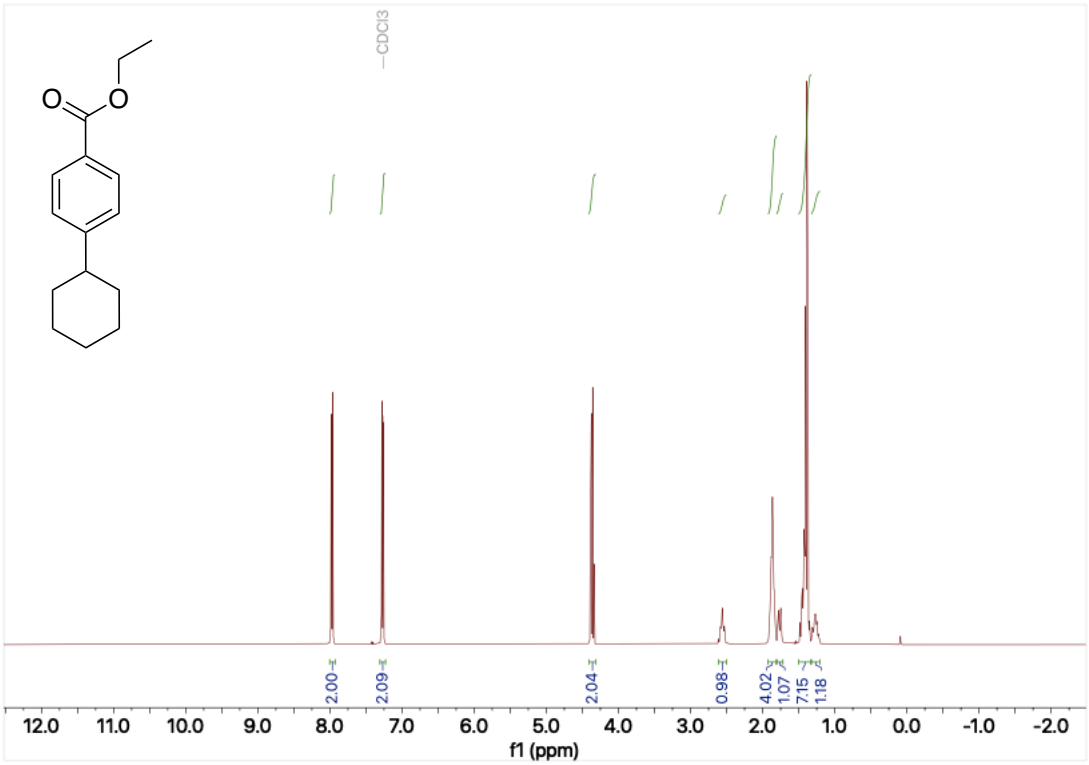

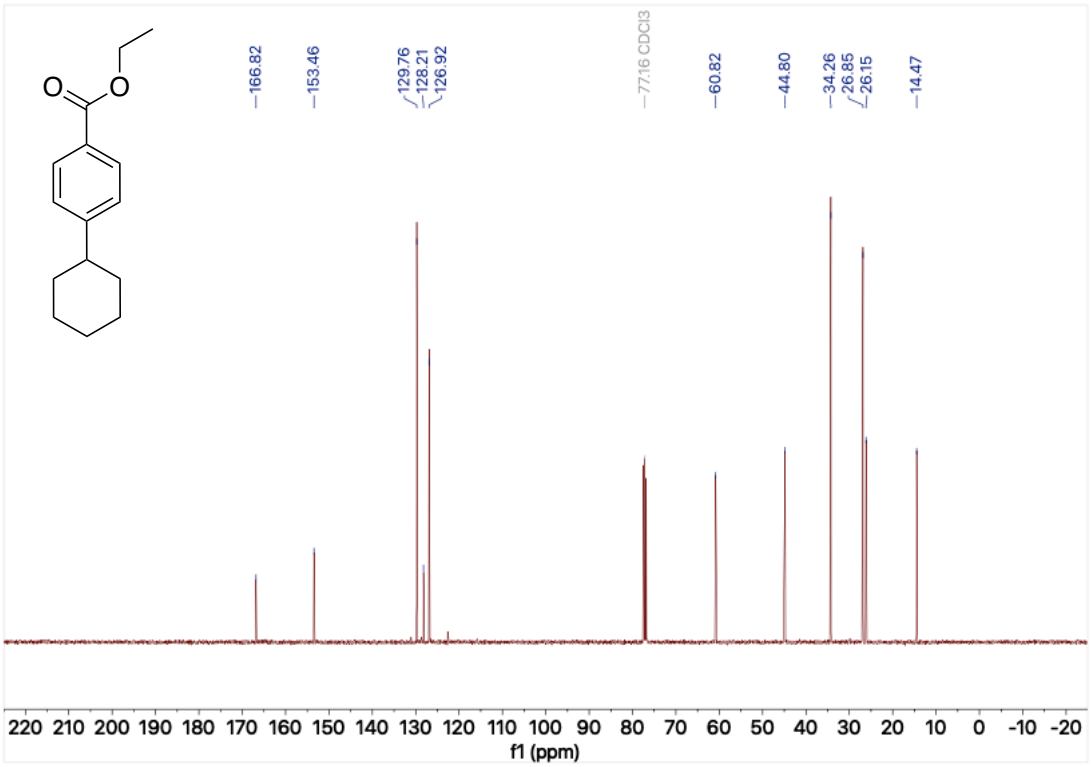

P

400 MHz ^{1}H NMR spectrum; 100.6 MHz ^{13}C NMR spectrum; $CDCl_3$ of pyrimidine cyclohexane **126**

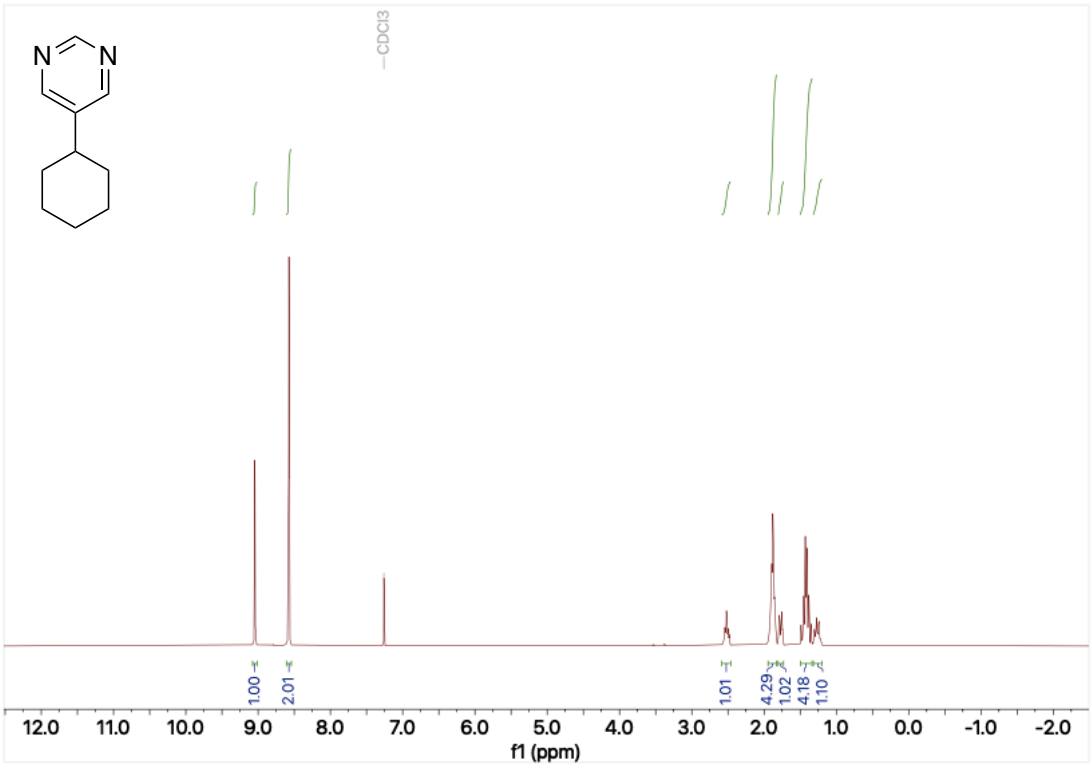

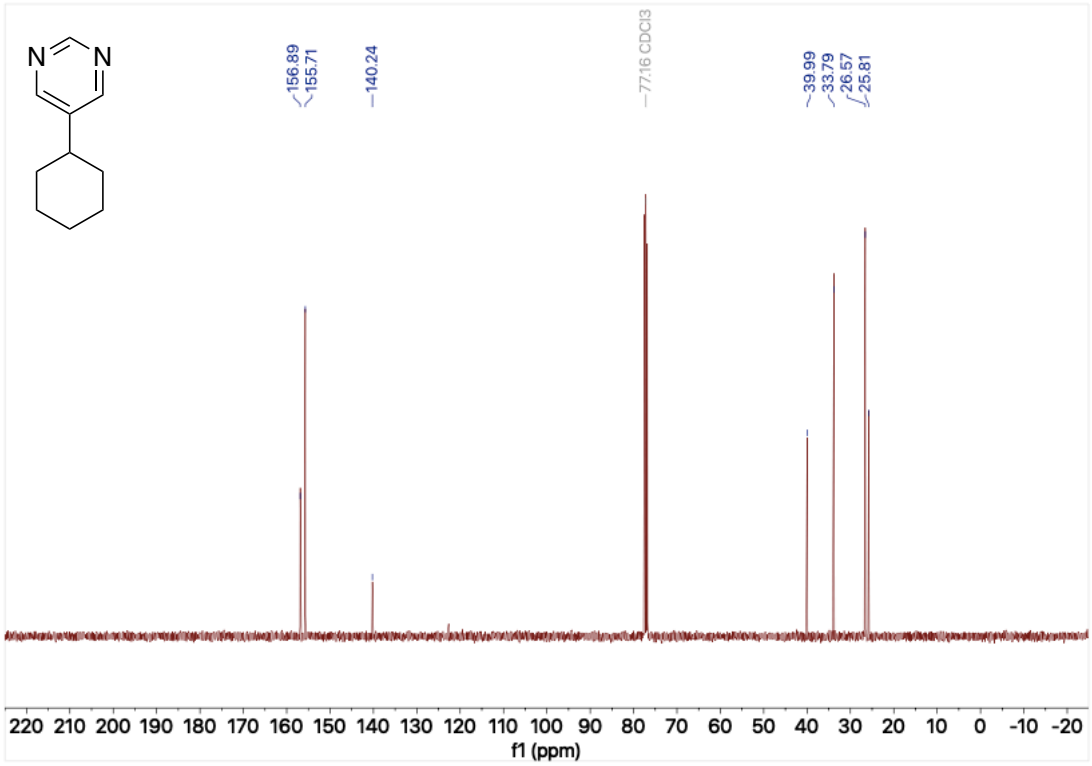

Q

400 MHz ^{1}H NMR spectrum; 100.6 MHz ^{13}C NMR spectrum; 375 MHz ^{19}F NMR spectrum; $CDCl_3$ of fluoropyridine cyclohexane **127**

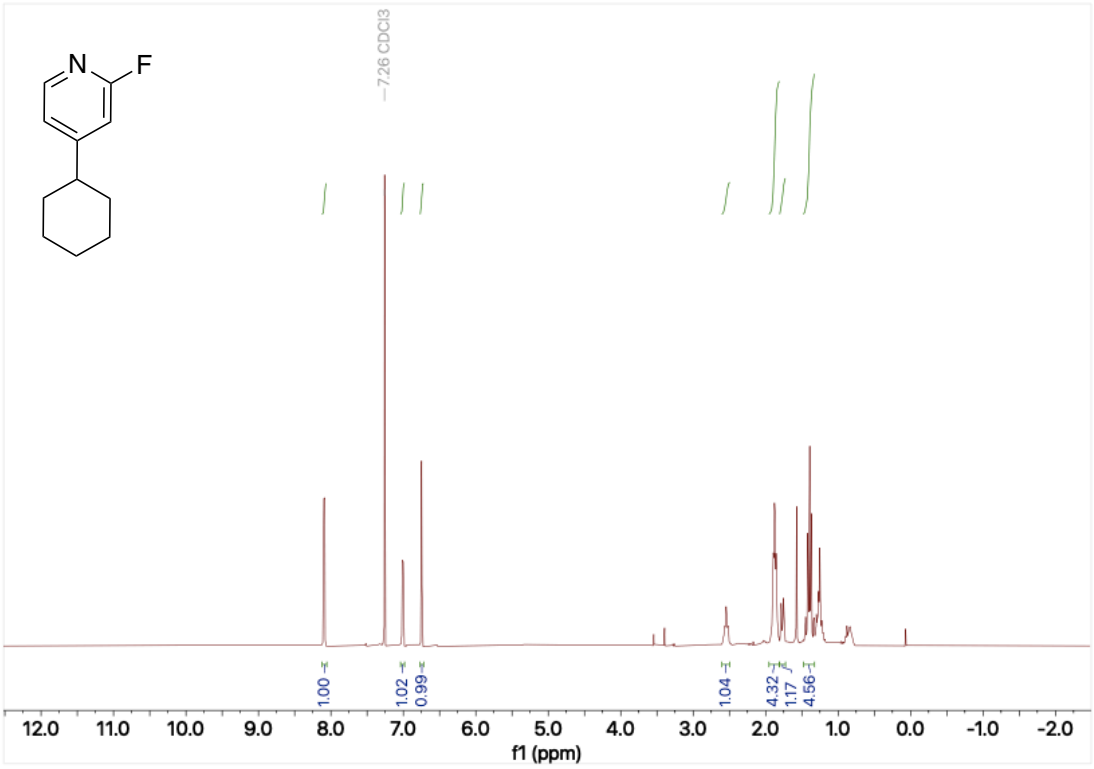

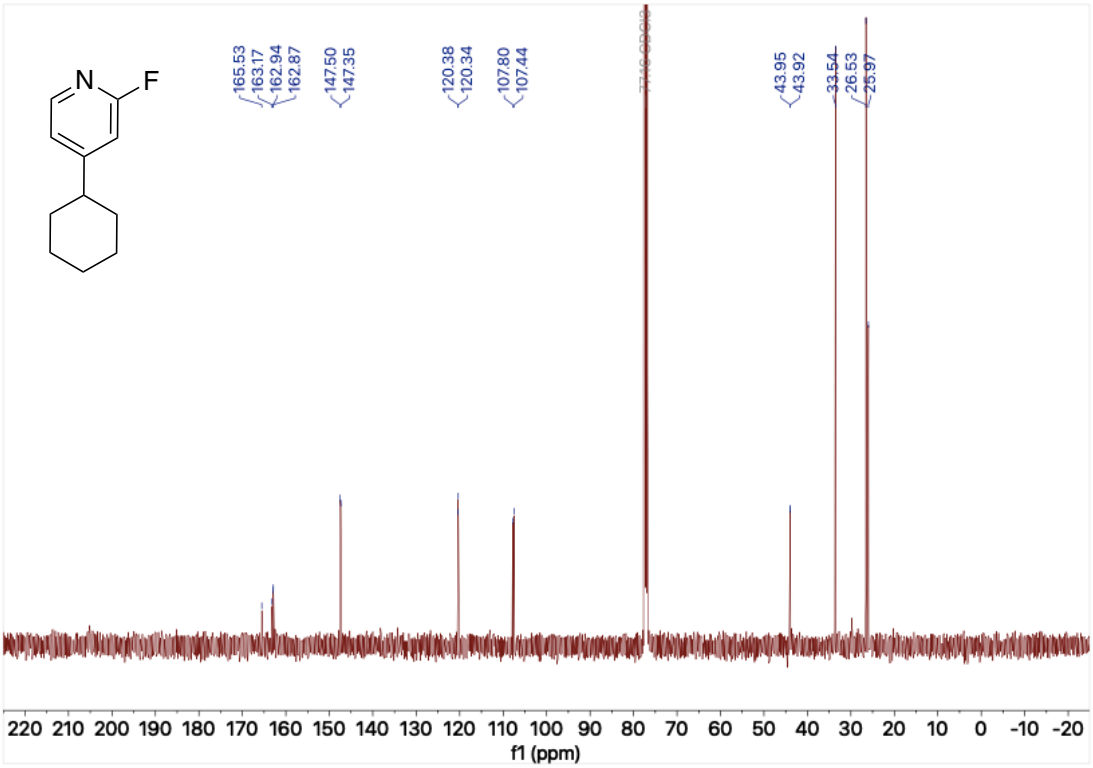

R

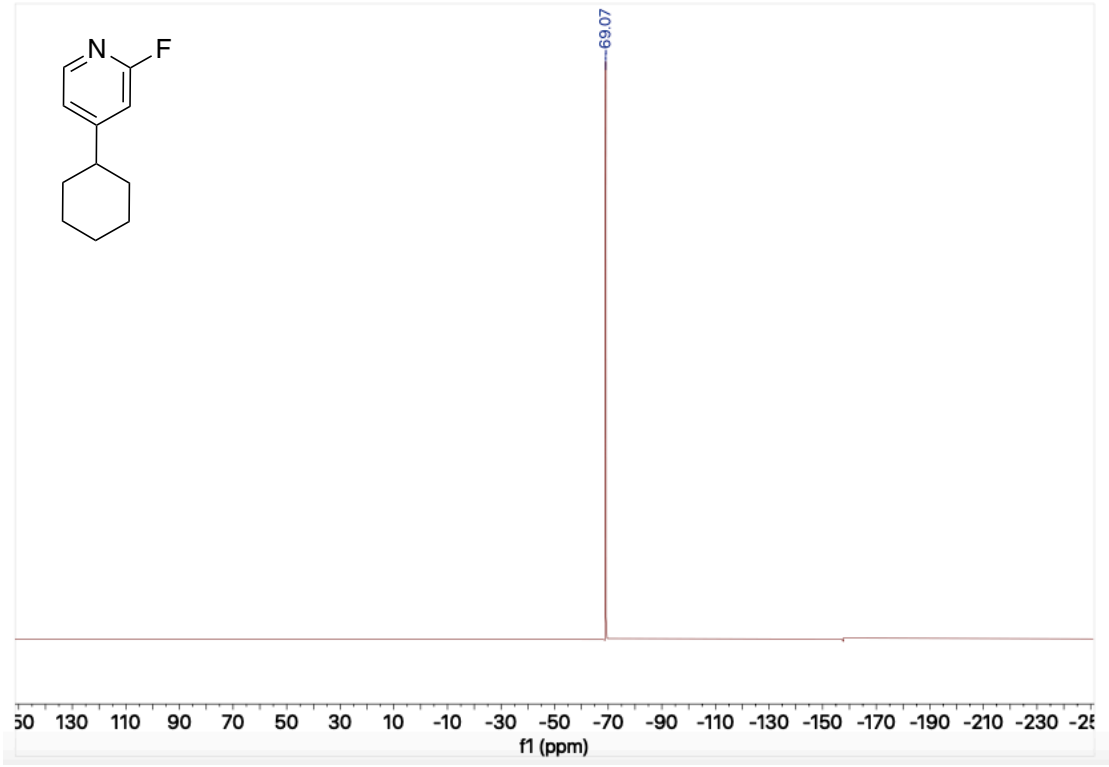
N
F
-69.07
50 130 110 90 70 50 30 10 -10 -30 -50 -70 -90 -110 -130 -150 -170 -190 -210 -230 -25
f1 (ppm)

400 MHz ^{1}H NMR spectrum; 100.6 MHz ^{13}C NMR spectrum; $CDCl_3$ of ethyl ester phenyl *N*-Boc piperidine **129**

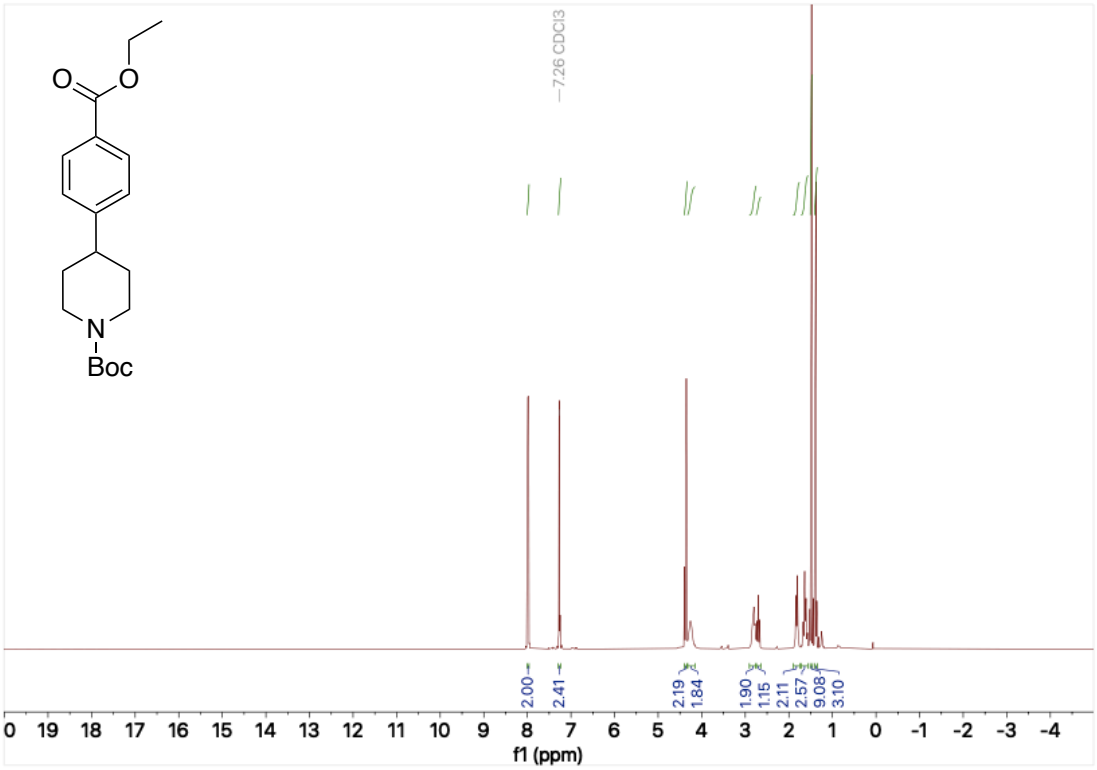

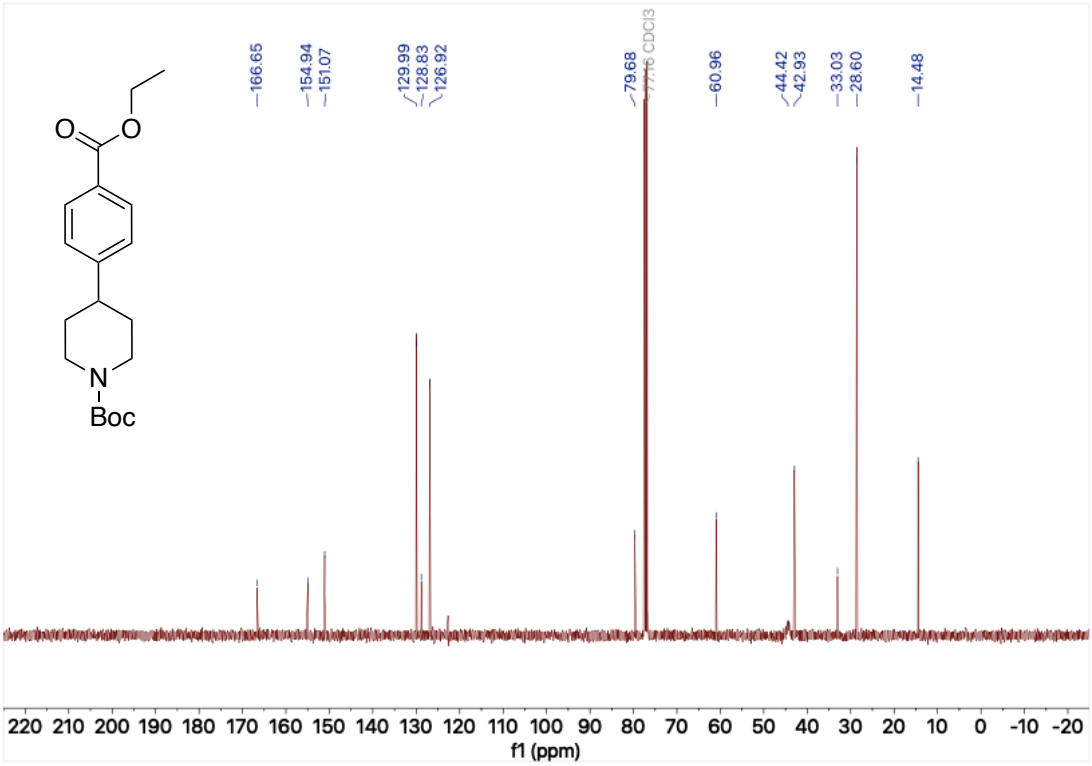

T

400 MHz ^{1}H NMR spectrum; 100.6 MHz ^{13}C NMR spectrum; 375 MHz ^{19}F spectrum; $CDCl_3$ of fluoropyridine *N*-Boc piperidine **131**

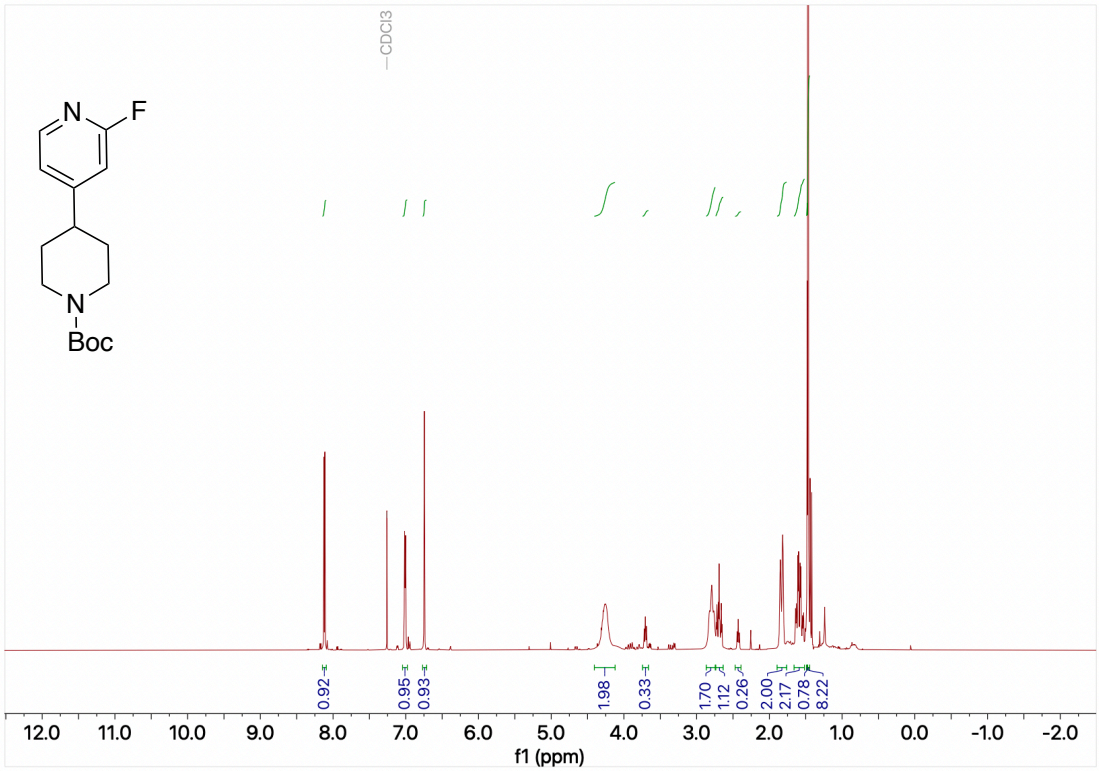

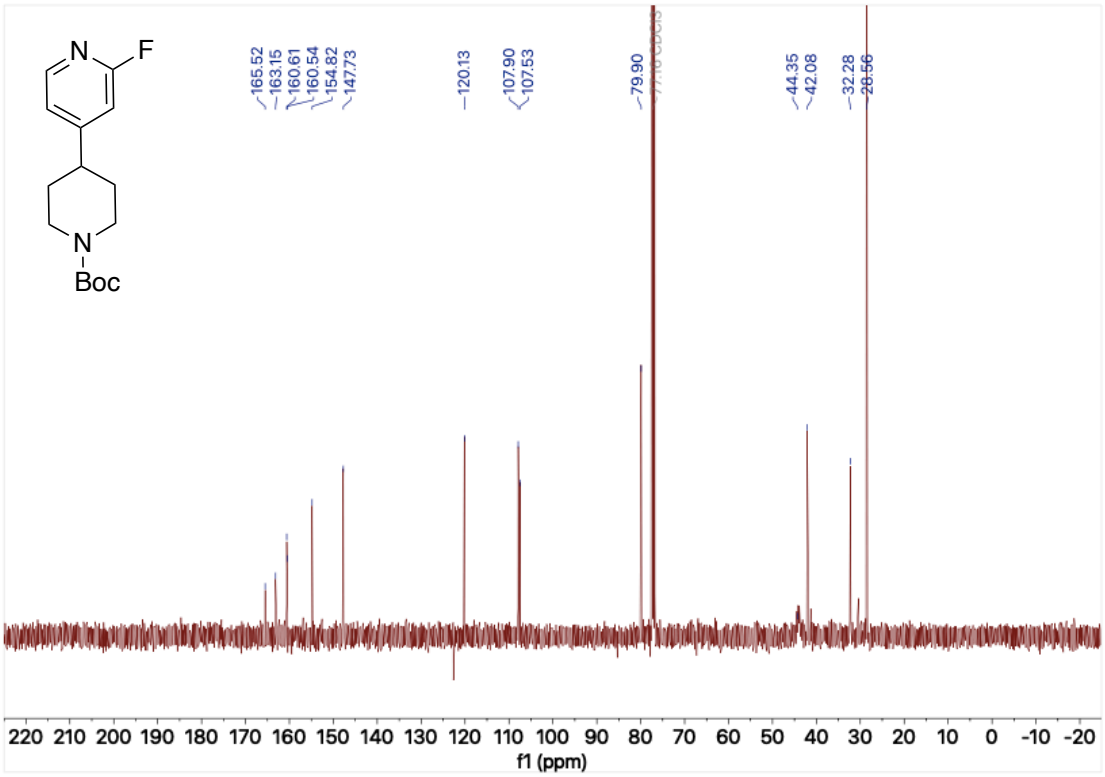

U

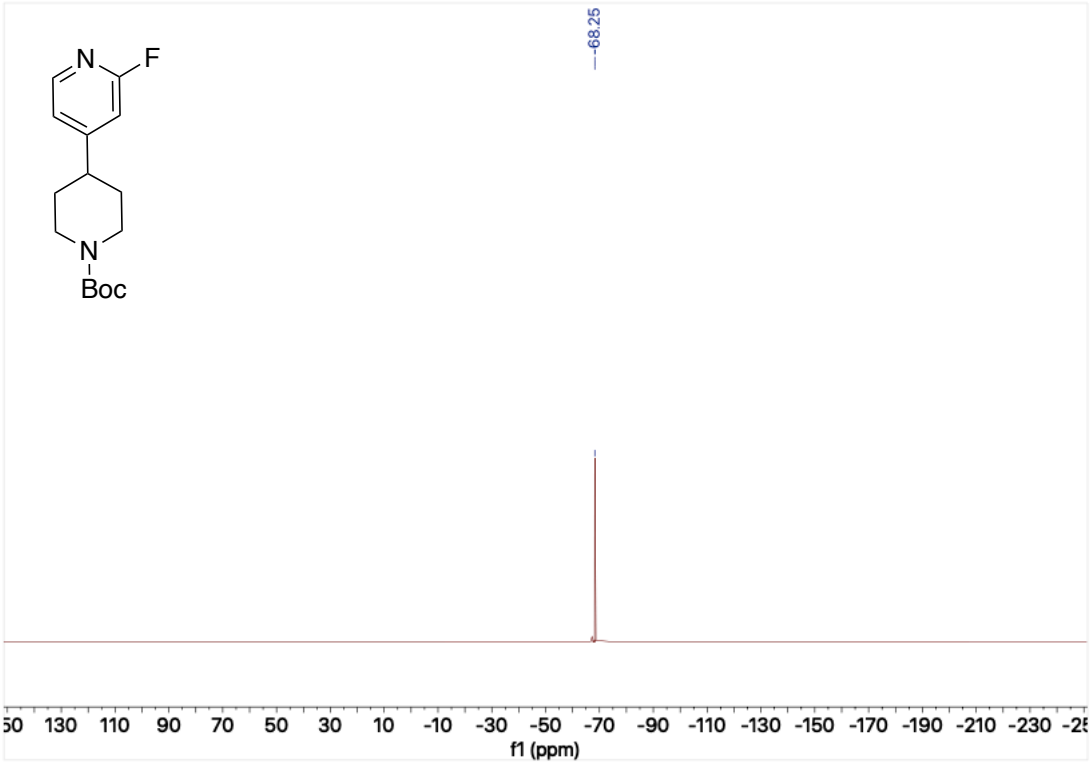
N
F
N
Boc
-68.25
50 130 110 90 70 50 30 10 -10 -30 -50 -70 -90 -110 -130 -150 -170 -190 -210 -230 -25
f1 (ppm)

400 MHz ^{1}H NMR spectrum; 100.6 MHz ^{13}C NMR spectrum; $CDCl_3$ of ethyl ester phenyl cyclobutane **132**

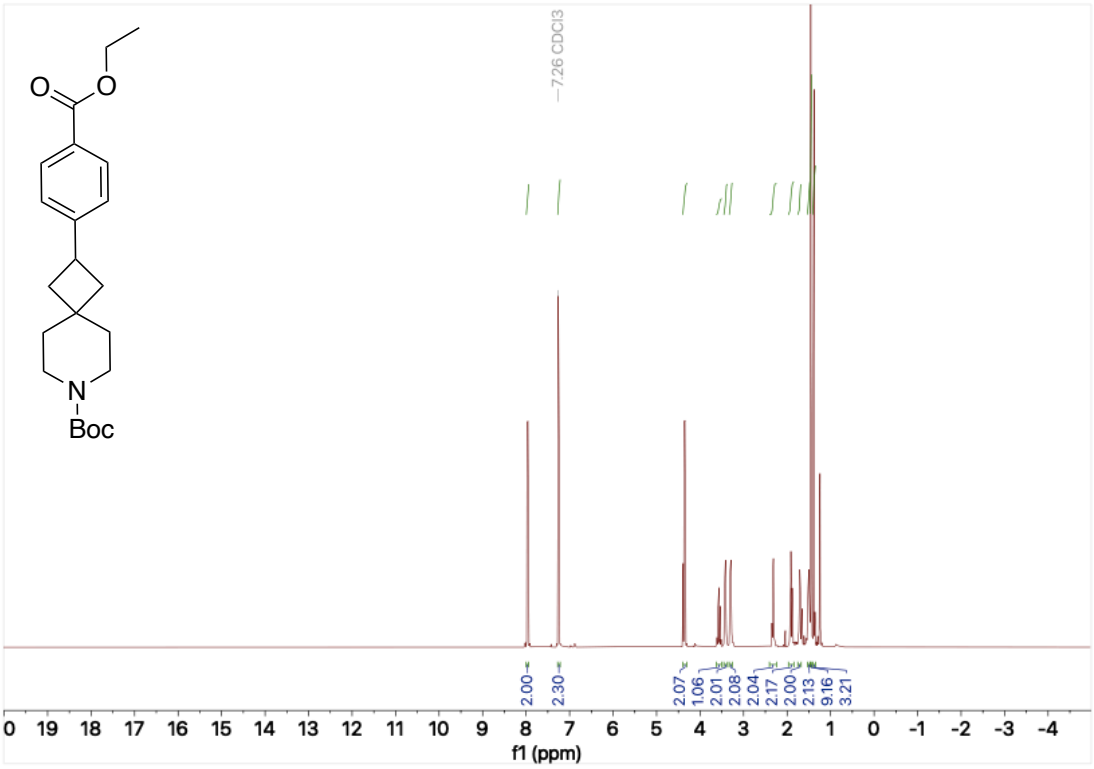

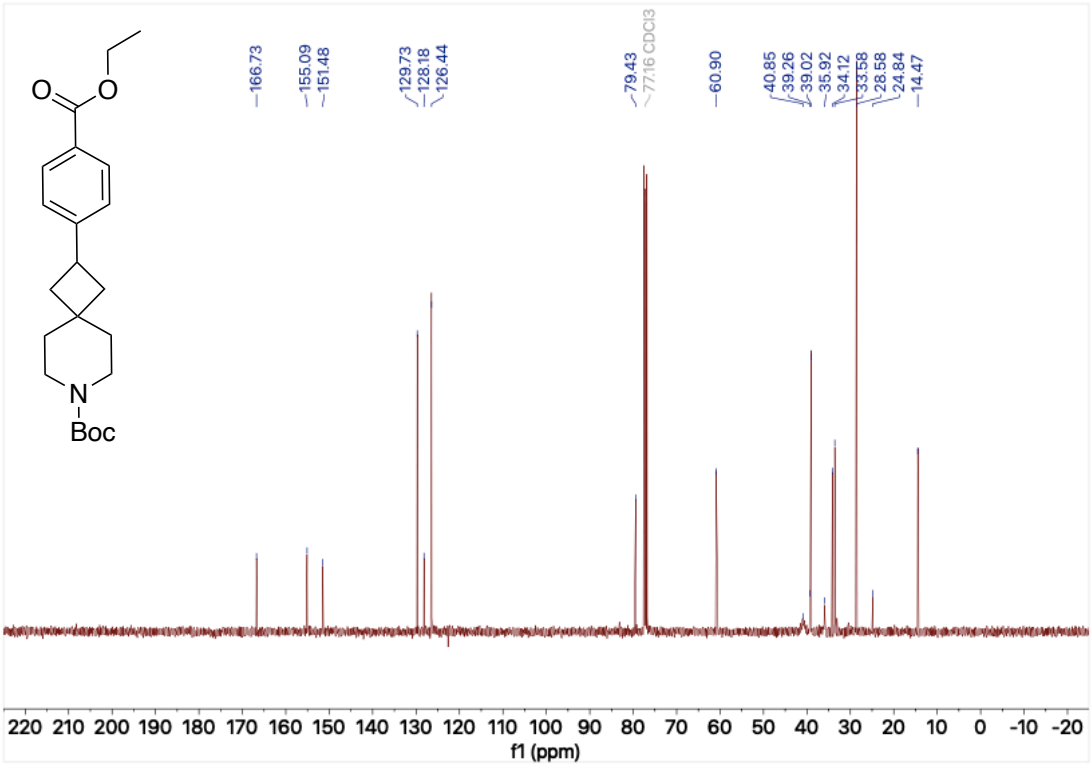

W

400 MHz ^{1}H NMR spectrum; 100.6 MHz ^{13}C NMR spectrum; $CDCl_3$ of sulfamoylphenyl cyclobutane **137**

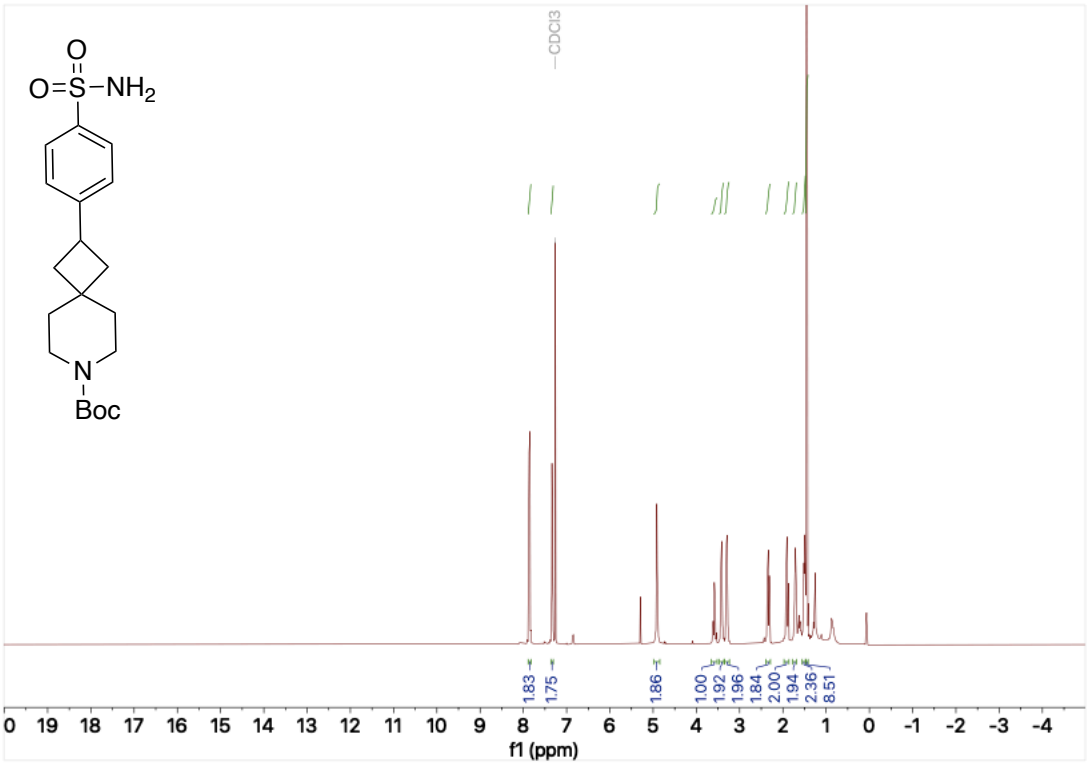

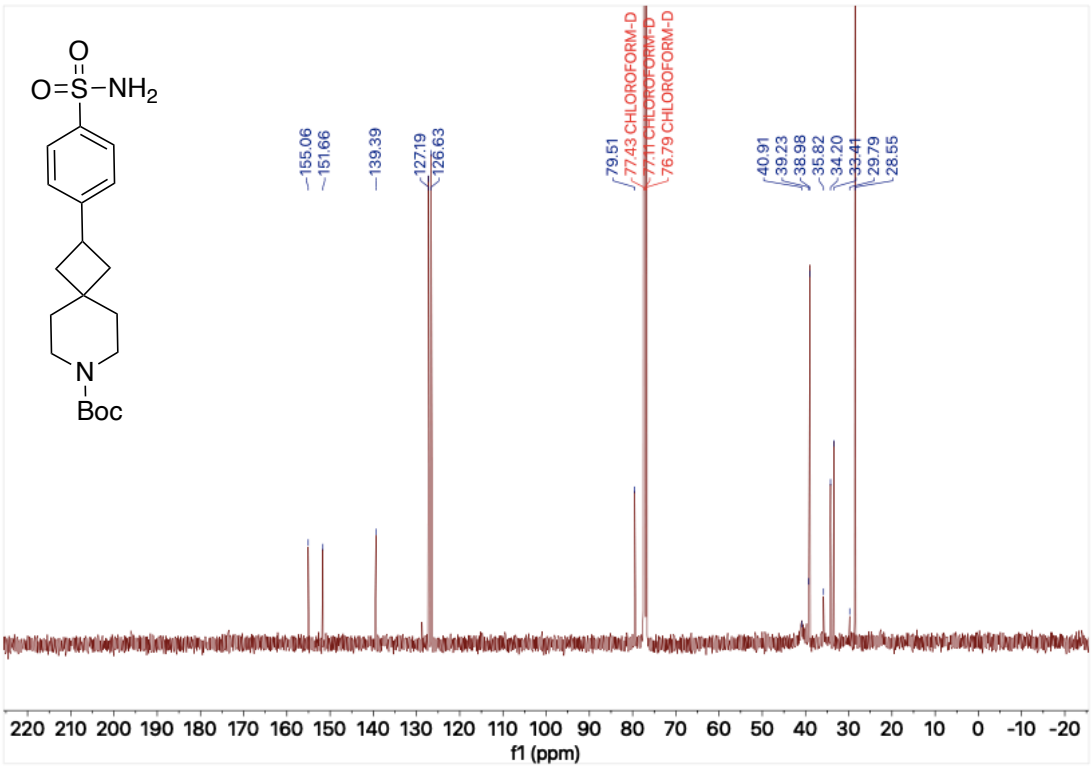

400 MHz ^{1}H NMR spectrum; 100.6 MHz ^{13}C NMR spectrum; $CDCl_3$ of pyrimidine cyclobutane **133**

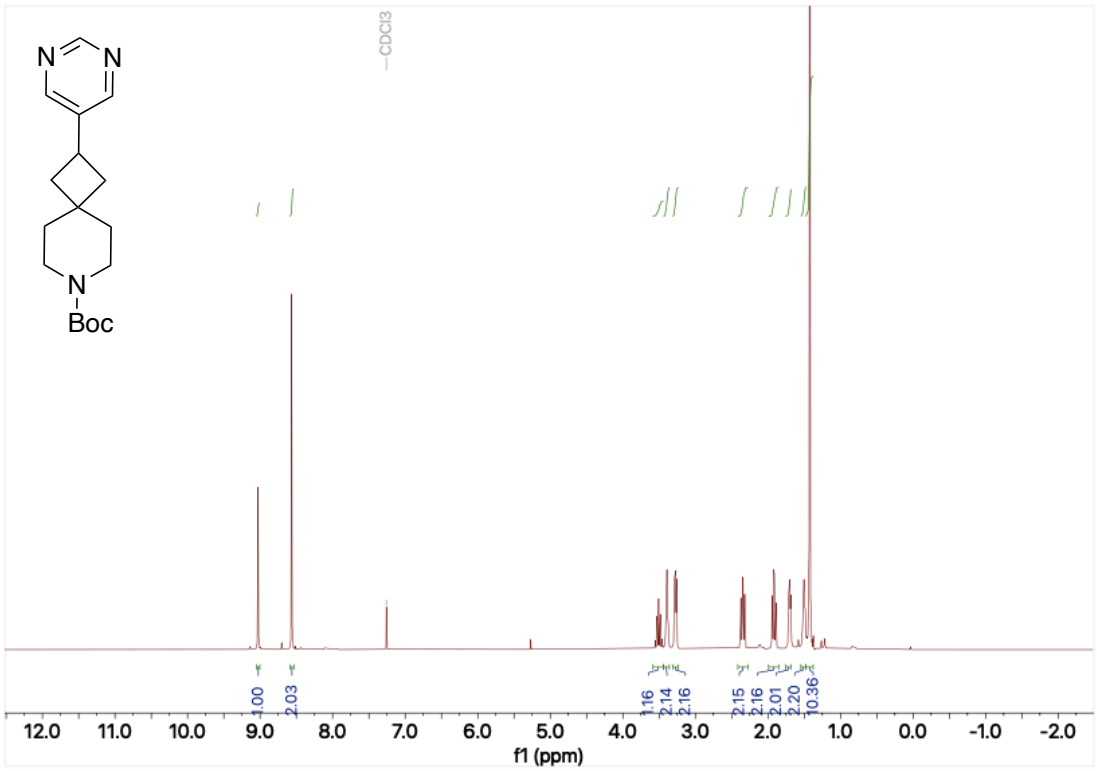

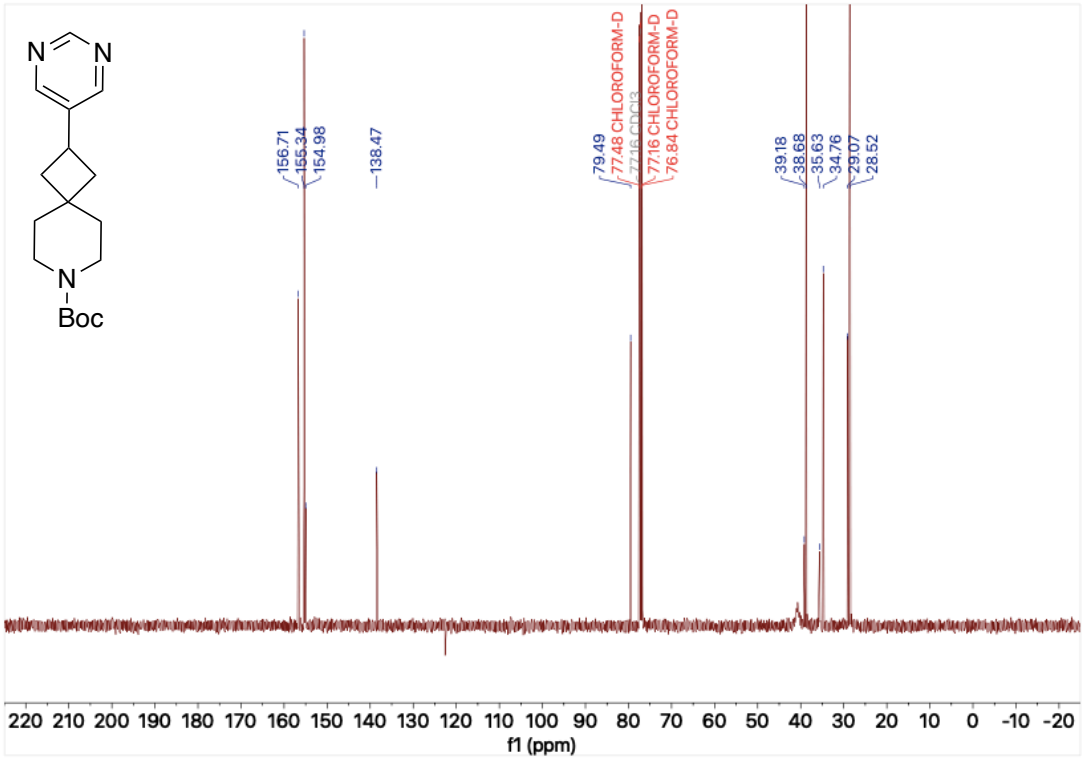

Y

400 MHz ^{1}H NMR spectrum; 100.6 MHz ^{13}C NMR spectrum; $CDCl_3$ of methanesulfonylphenyl cyclobutane **136**

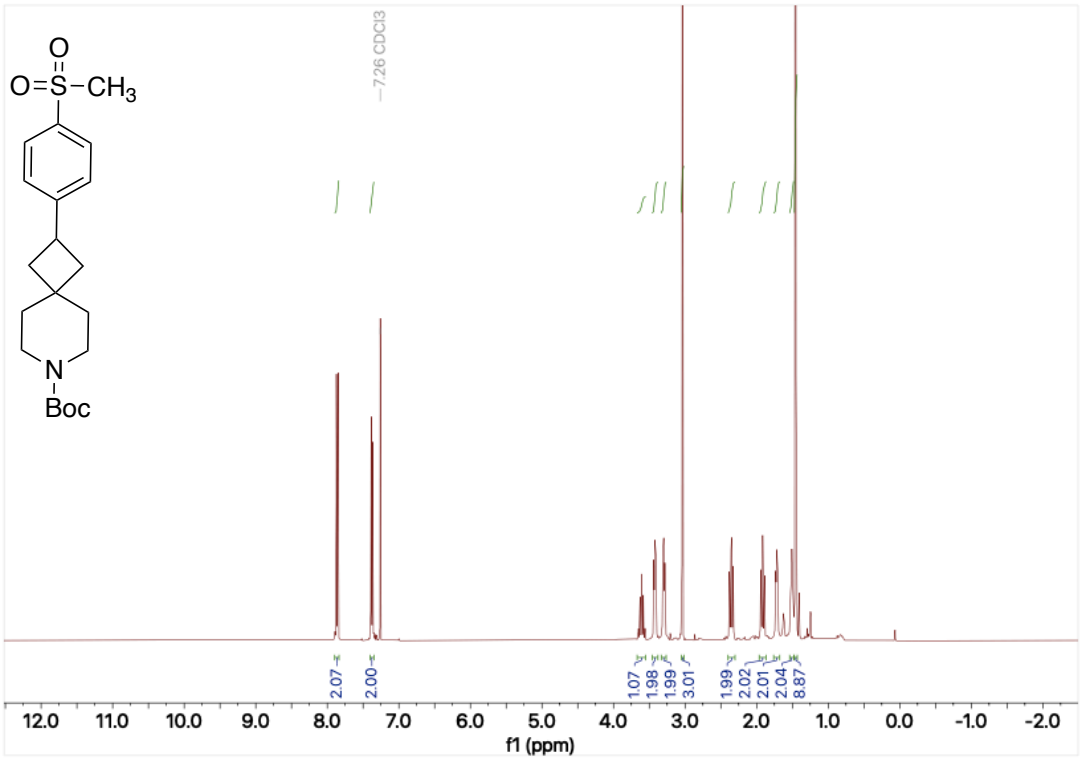

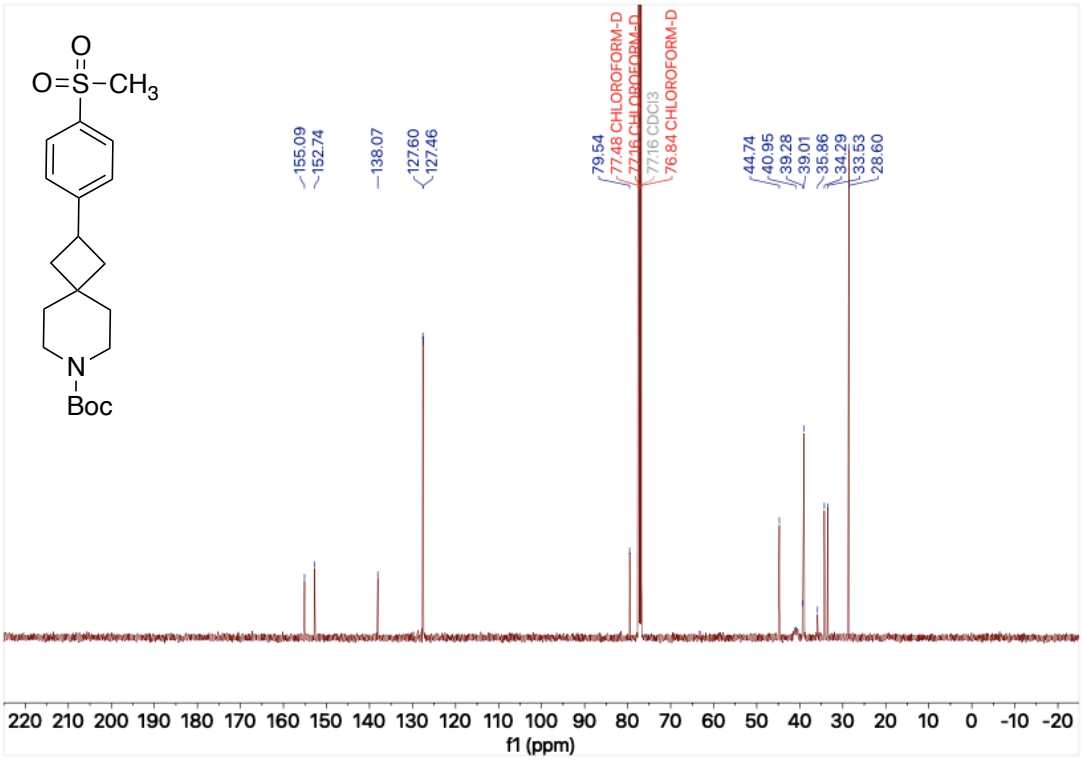

Z

400 MHz ^{1}H NMR spectrum; 100.6 MHz ^{13}C NMR spectrum; $CDCl_3$ of acetanilide cyclobutane **135**

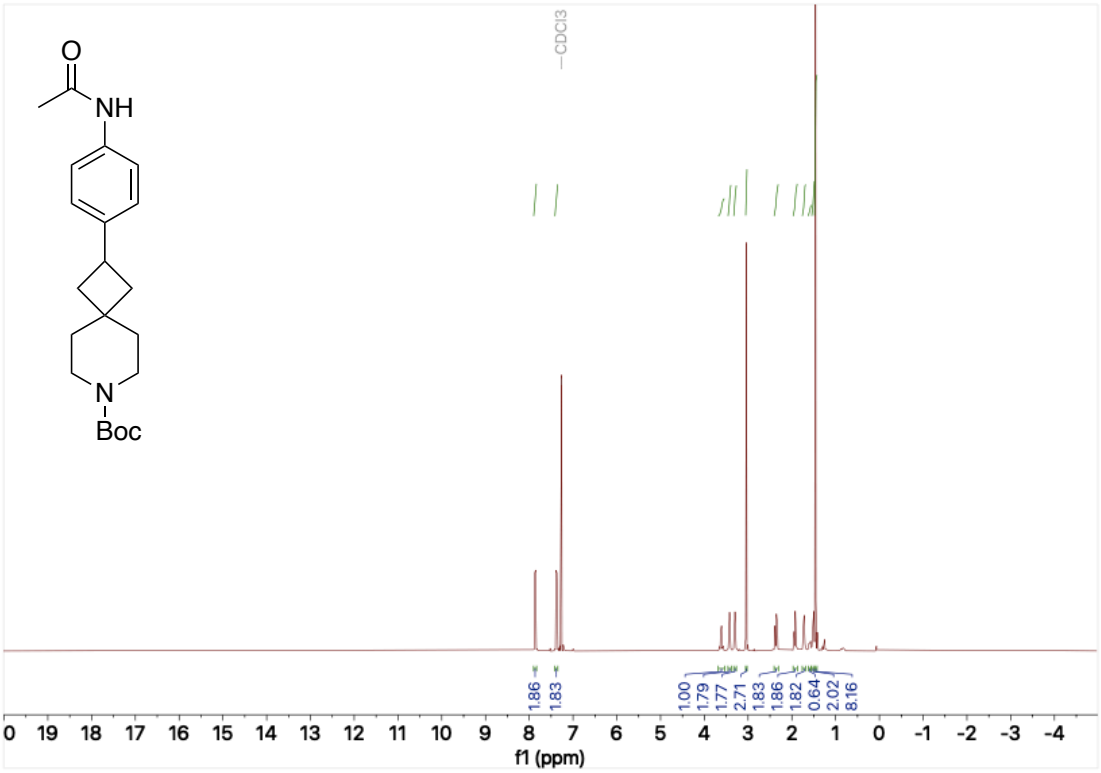

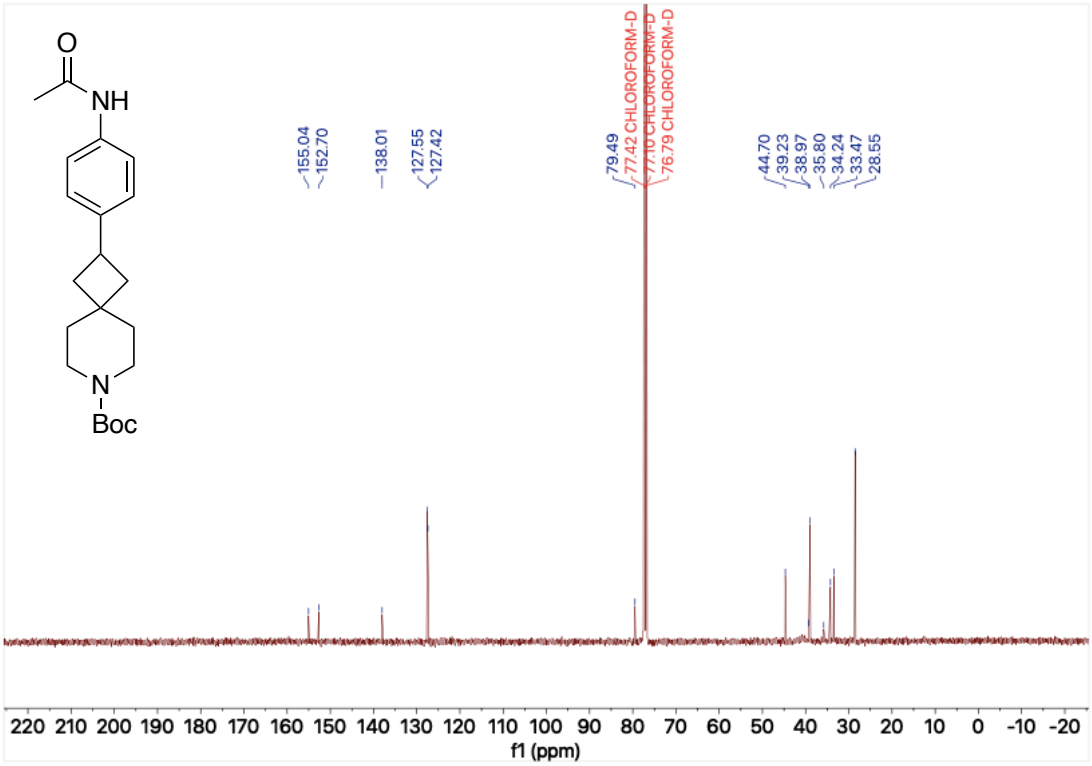

400 MHz ^{1}H NMR spectrum; 100.6 MHz ^{13}C NMR spectrum; $CDCl_3$ of methoxypyridine cyclobutane **134**

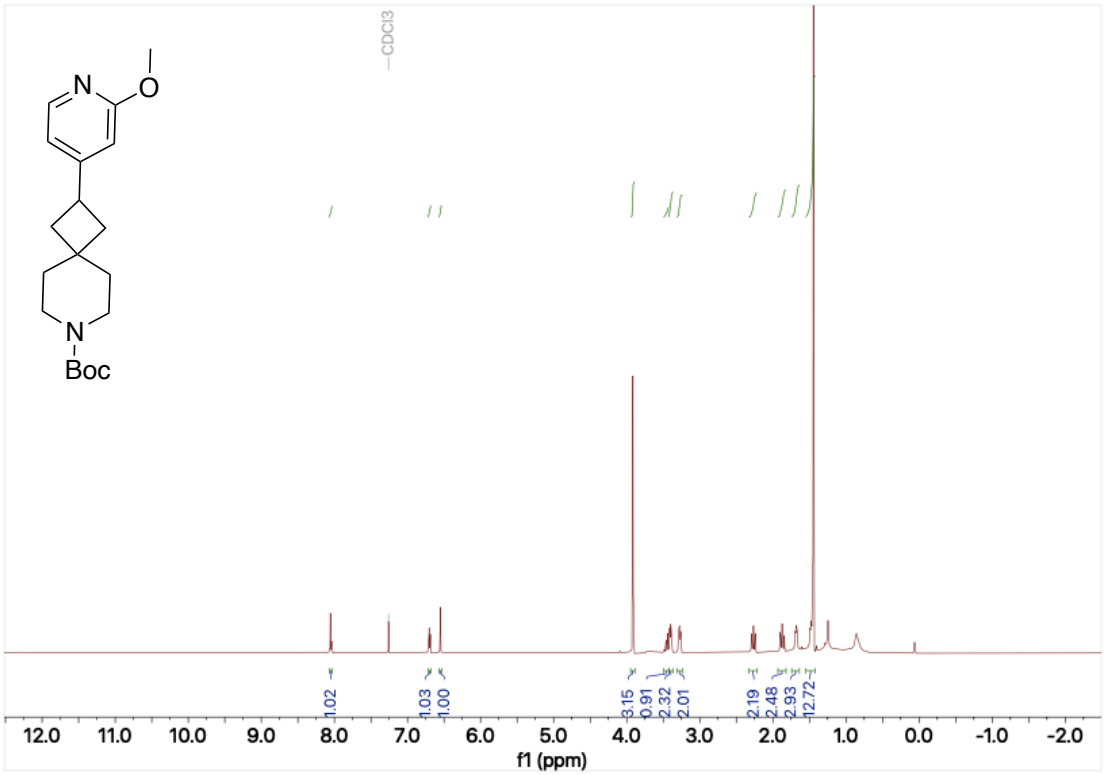

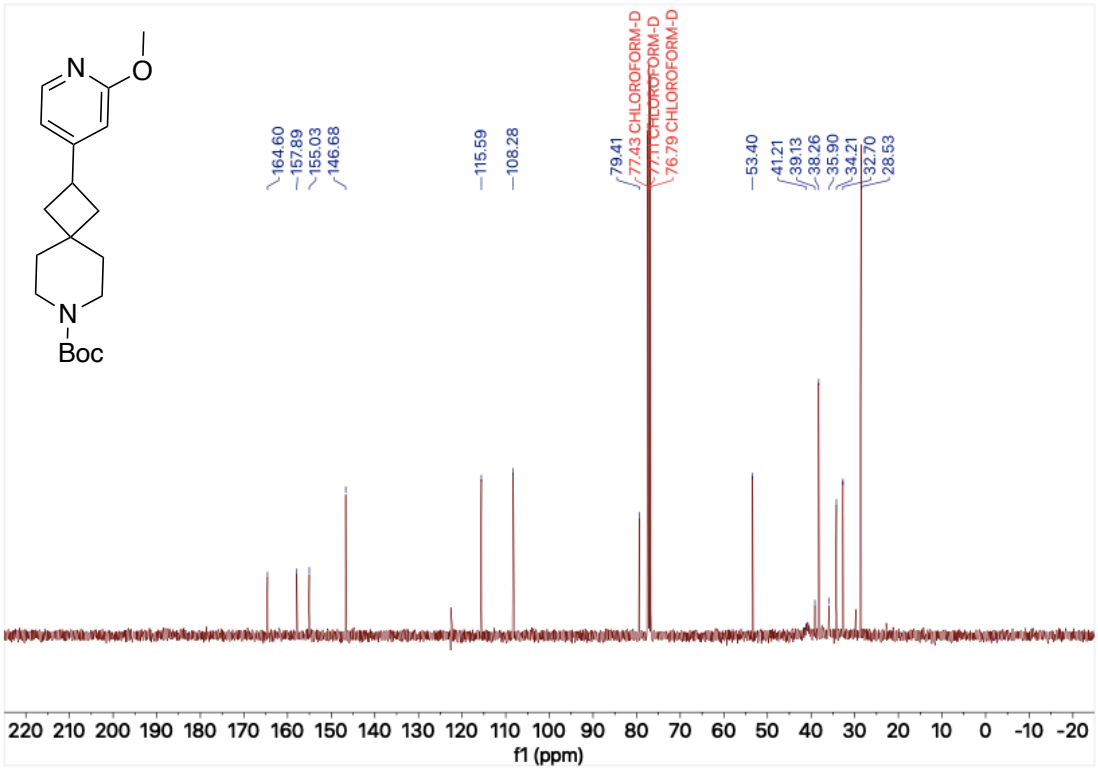

BB

400 MHz ^{1}H NMR spectrum; 100.6 MHz ^{13}C NMR spectrum; $CDCl_3$ of phenyl cyclobutane **149**

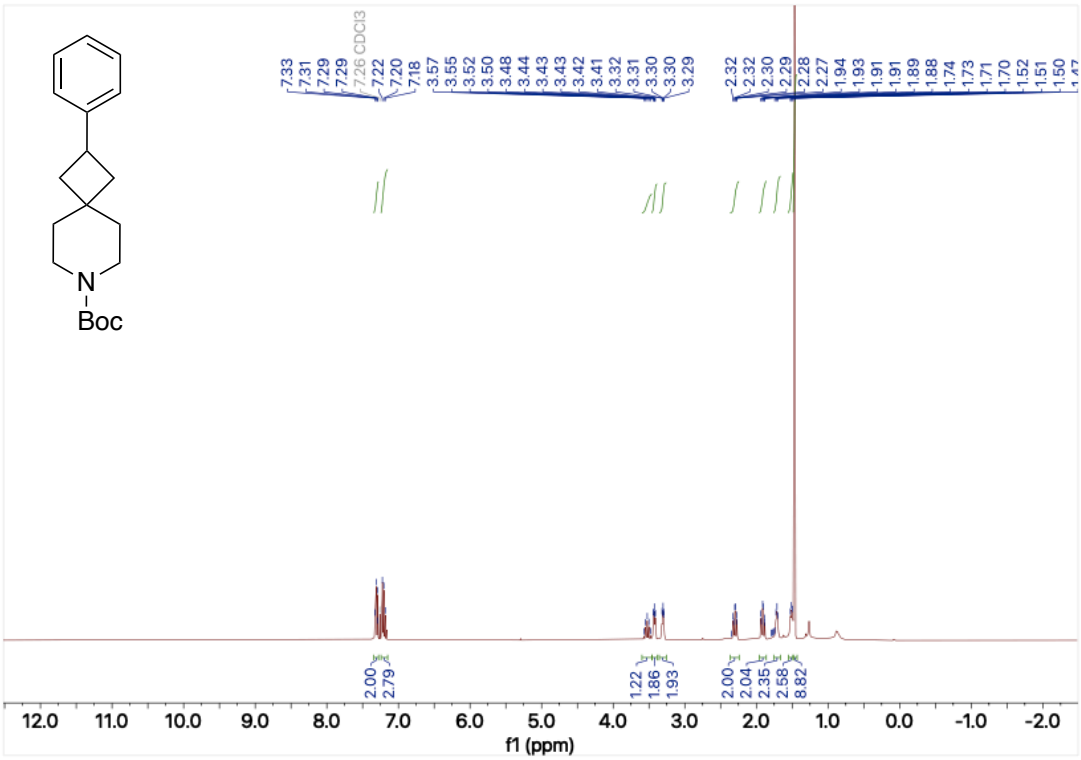

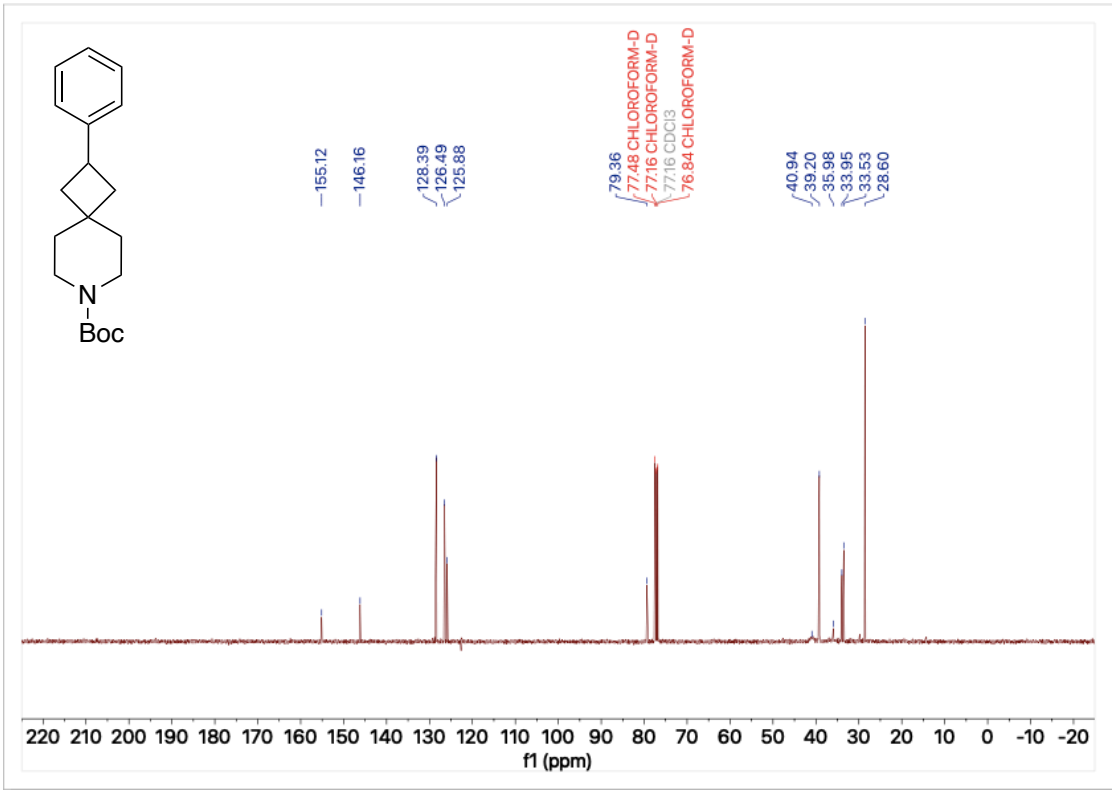

CC

400 MHz ^{1}H NMR spectrum; 100.6 MHz ^{13}C NMR spectrum; $CDCl_3$ of *N*-methanesulfonamide pyrimidine cyclobutane **159**

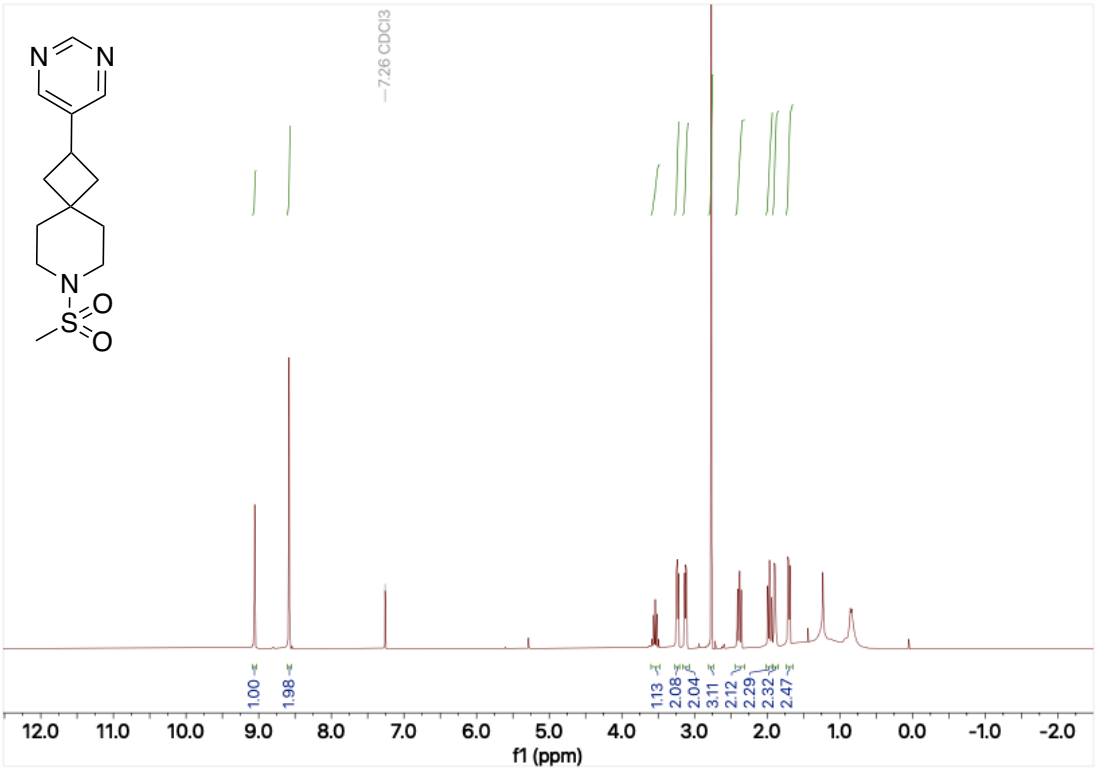

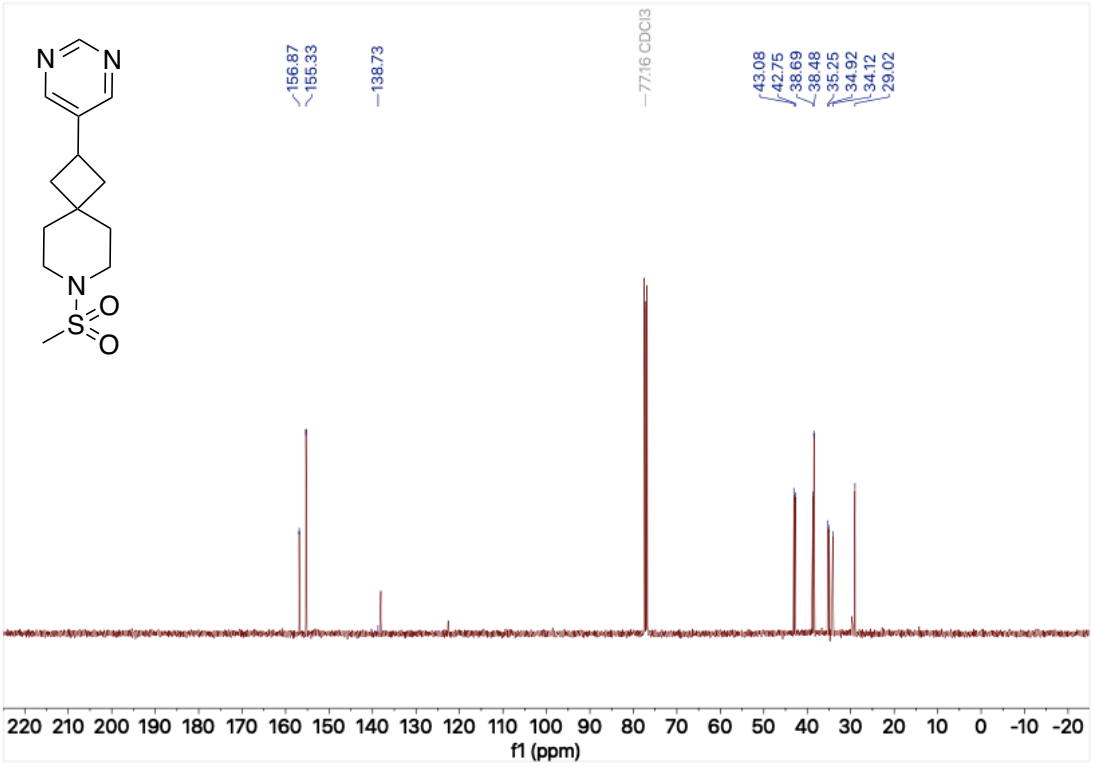

DD

400 MHz ^{1}H NMR spectrum; 100.6 MHz ^{13}C NMR spectrum; $CDCl_3$ of *N*-dimethyloxazolylsulfonyl ethyl ester phenyl cyclobutane **160**

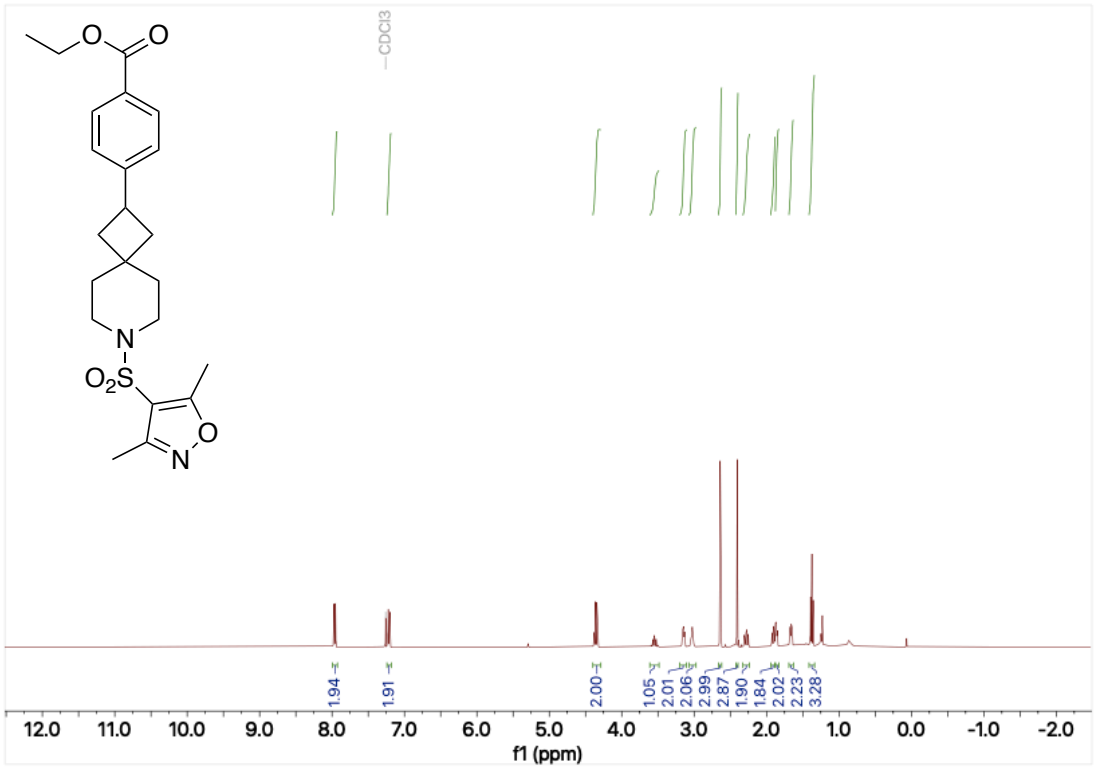

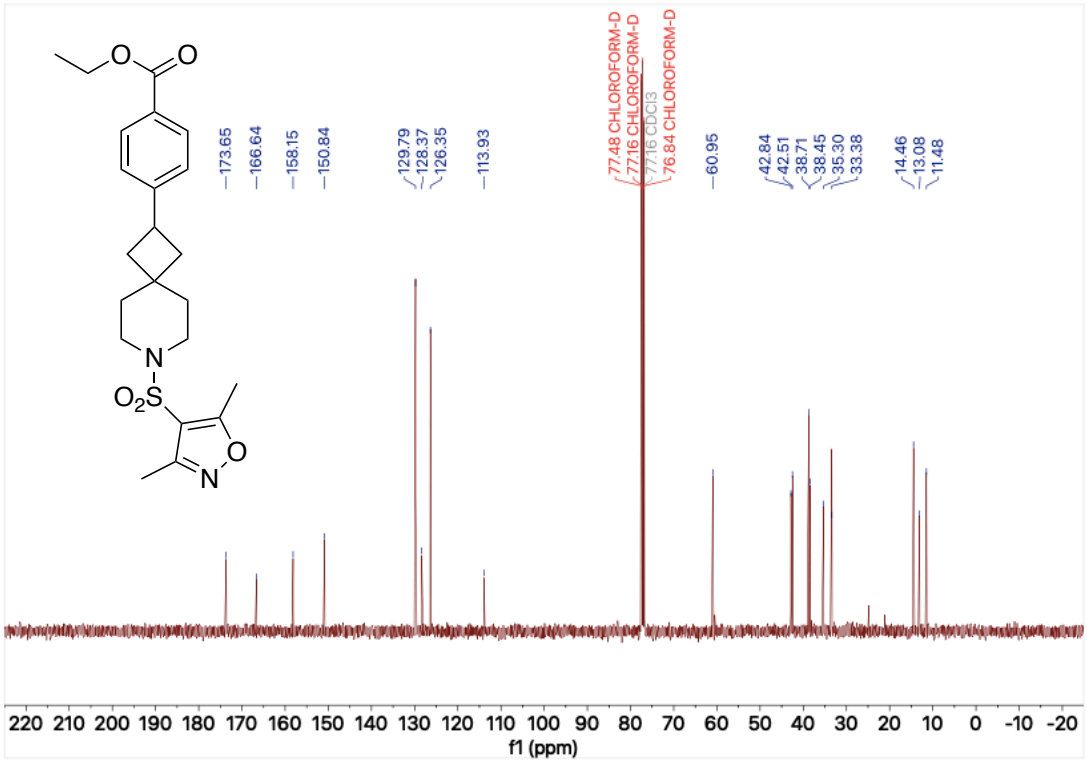

EE

400 MHz ^{1}H NMR spectrum; 100.6 MHz ^{13}C NMR spectrum; $CDCl_3$ of *N*-benzamide acetanilide cyclobutane **161**

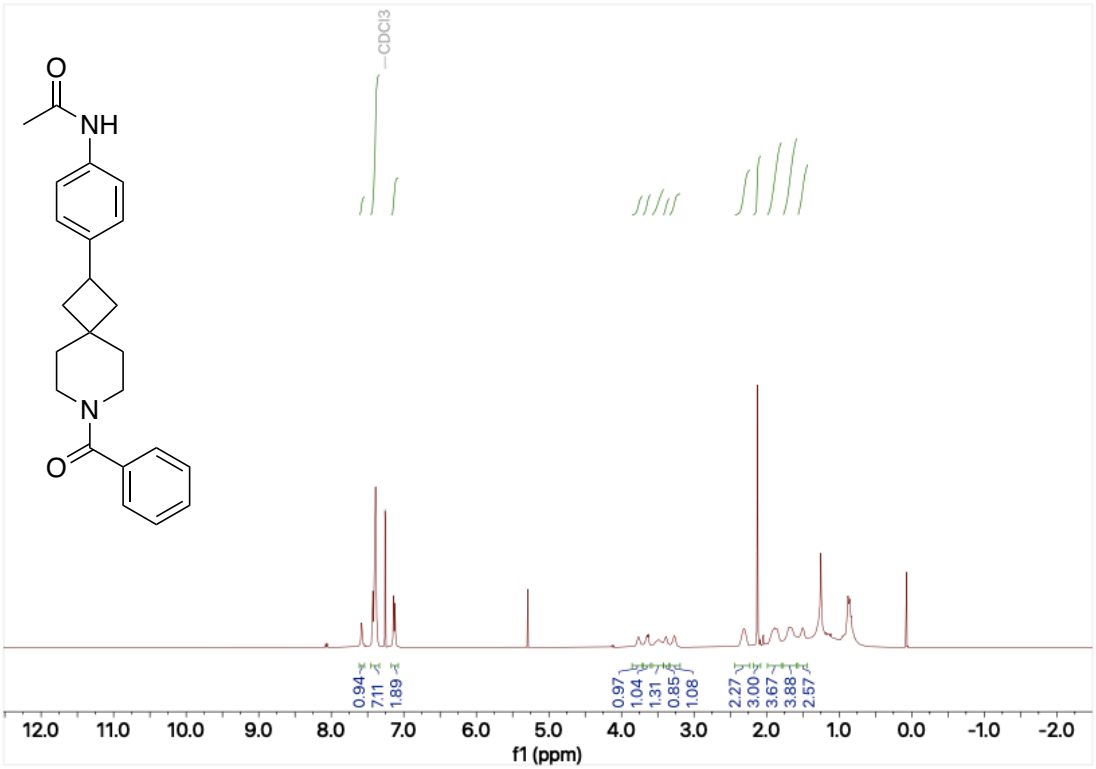

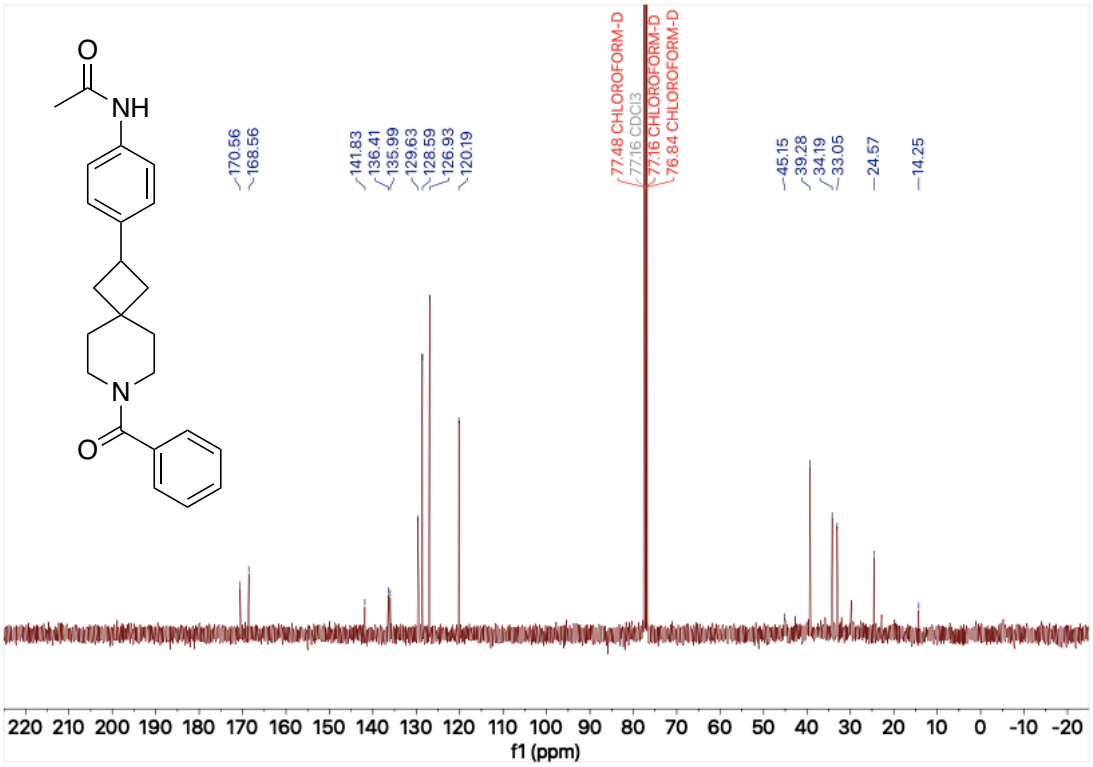

FF

400 MHz ^{1}H NMR spectrum; 100.6 MHz ^{13}C NMR spectrum; $CDCl_3$ of *N*-acetamide methoxypyridine cyclobutane **162**

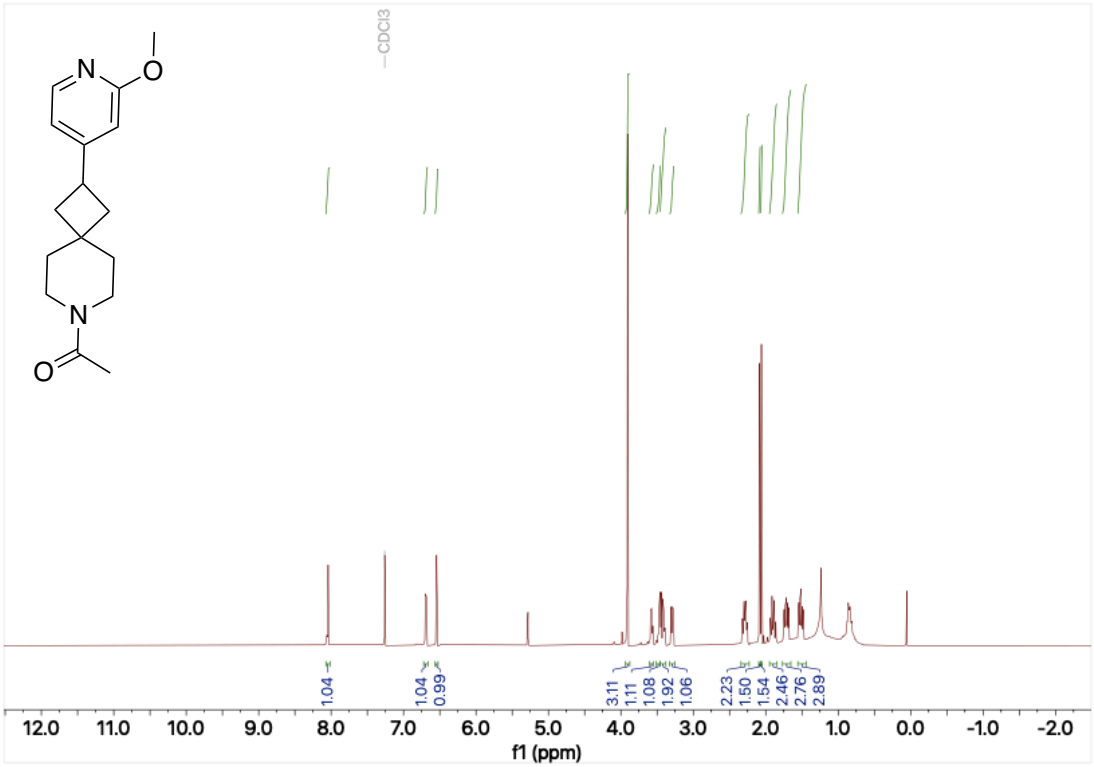

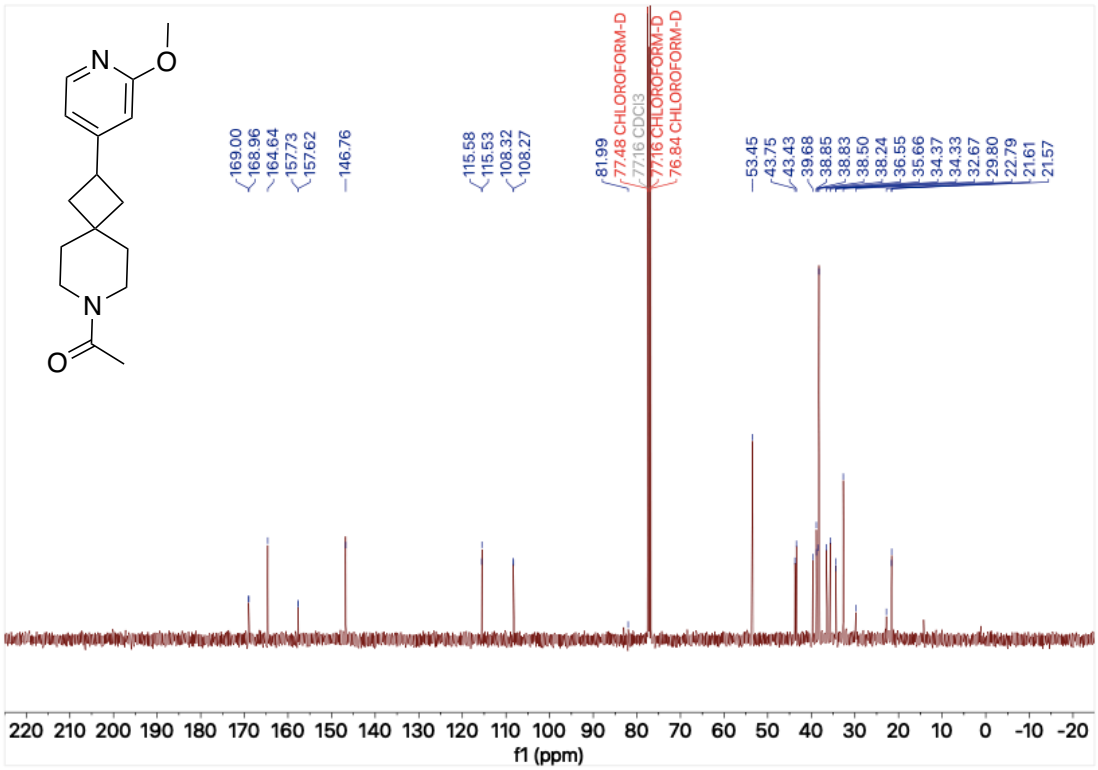

GG

400 MHz ^{1}H NMR spectrum; 100.6 MHz ^{13}C NMR spectrum; $CDCl_3$ of *N*-indoleamide phenyl cyclobutane **163**

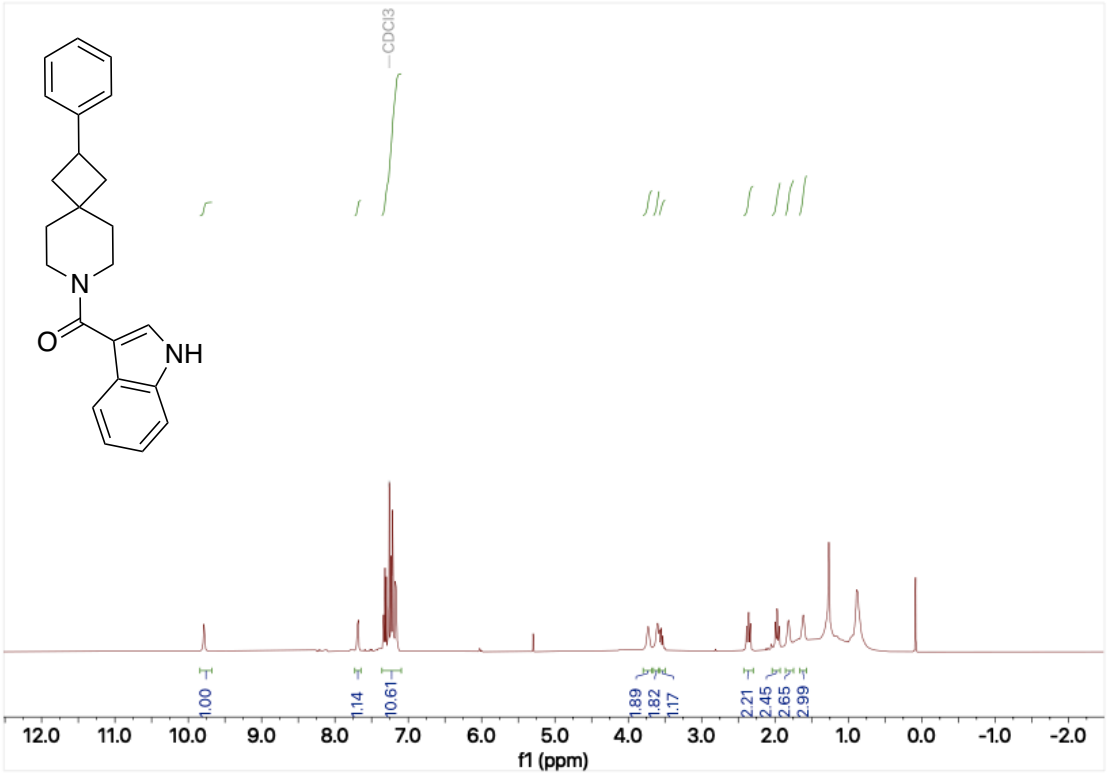

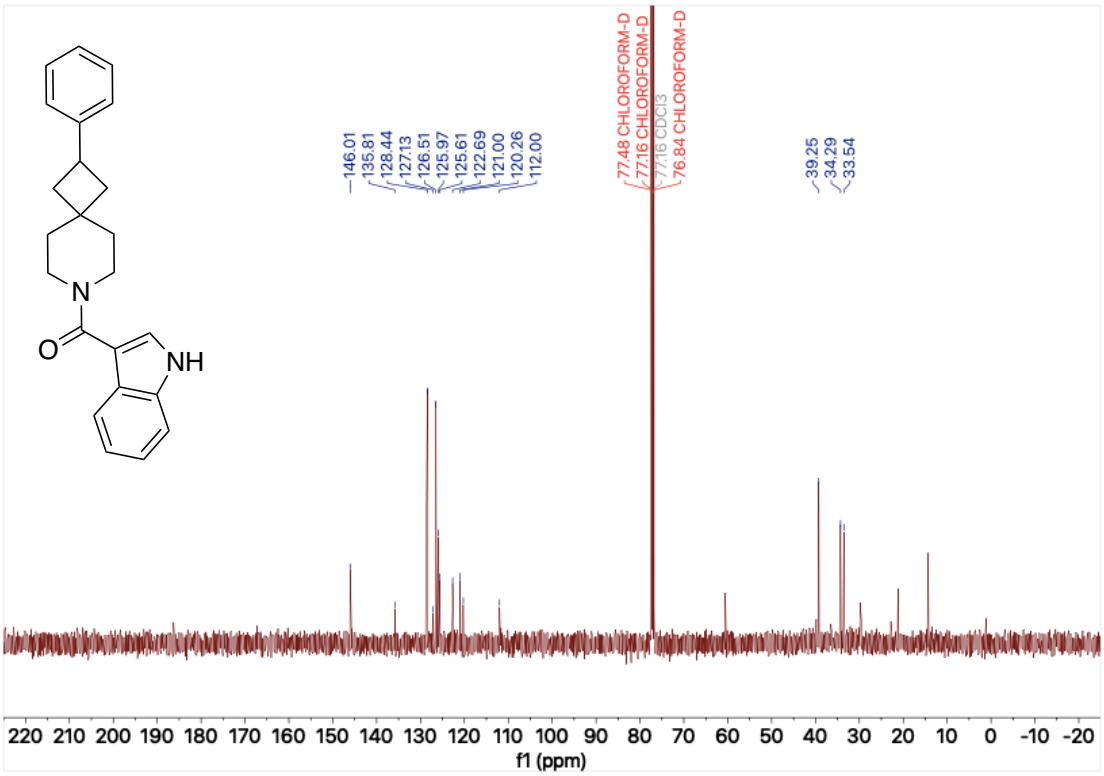

HH